

State of California
The Resources Agency
Department of Water Resources
Office of State Water Project Planning

METHODOLOGY FOR FLOW AND SALINITY ESTIMATES IN THE SACRAMENTO-SAN JOAQUIN DELTA AND SUISUN MARSH



**TWENTY-SECOND ANNUAL PROGRESS REPORT TO THE
STATE WATER RESOURCES CONTROL BOARD**
In Accordance with Water Right Decision 1485, Order 9

August 2001

Gray Davis
Governor
State of California

Mary D. Nichols
Secretary for Resources
The Resources Agency

Thomas M. Hannigan
Director
Department of Water Resources

FOREWORD

This is the twenty-second annual progress report of the California Department of Water Resources' San Francisco Bay-Delta Evaluation Program, which is carried out by the Delta Modeling Section.

It documents progress in the development and enhancement of the Delta Modeling Section's computer models and reports the latest findings of studies conducted as part of the program. This report was compiled by Michael Mierzwa under the direction of Paul Hutton, program manager for the Bay-Delta Evaluation Program.

On-line versions of previous annual progress reports are available at:

<http://modeling.water.ca.gov/branch/reports.html>

For more information contact:

Paul Hutton
hutton@water.ca.gov
(916) 653-6501

-or-

Michael Mierzwa
mmierzwa@water.ca.gov
(916) 653-9794

TABLE OF CONTENTS

	FOREWORD	iii
1	INTRODUCTION	1-1
2	DSM2 CALIBRATION AND VALIDATION	2-1
2.1	Introduction	2-1
2.2	Choice of Model Grid	2-1
2.3	DSM2-HYDRO Calibration	2-2
2.4	DSM2-QUAL Calibration	2-3
2.5	DSM2 Validation	2-5
2.6	General Comments on DSM2 Calibration / Validation	2-6
2.7	Conclusion.....	2-7
2.8	References.....	2-7
3	SIMULATION OF HISTORICAL DOC AND UVA CONDITIONS IN THE DELTA	3-1
3.1	Introduction	3-1
3.2	Study Assumptions	3-1
3.2.1	Model Version	3-1
3.2.2	Simulation Constituents and Period.....	3-1
3.2.3	Hydrodynamics, Hydrology, and Operations	3-2
3.2.4	Boundary Water Quality	3-2
3.2.5	Delta Islands Diversions and Returns.....	3-2
3.3	Validation Results.....	3-3
3.4	Future Directions	3-21
3.5	References.....	3-21
4	VALIDATION OF DISPERSION USING THE PARTICLE TRACKING MODEL IN THE SACRAMENTO-SAN JOAQUIN DELTA	4-1
4.1	Introduction	4-1
4.2	PTM Model	4-4
4.2.1	PTM Introduction.....	4-4
4.2.2	PTM Theory	4-4
4.2.3	Longitudinal Dispersion.....	4-5
4.3	Data.....	4-8
4.3.1	ADCP	4-8
4.3.2	Tracer	4-11
4.4	Modeling Results	4-15
4.4.1	Profile Comparisons.....	4-15
4.4.2	Longitudinal Dispersion.....	4-18
4.5	DSM2 Results	4-23
4.5.1	Hydrodynamics	4-23
4.5.2	PTM – Tracer Comparisons.....	4-26
4.5.3	No Dispersion.....	4-29
4.5.4	No Vertical Shear	4-30
4.5.5	No Transverse Shear	4-31
4.6	Conclusions.....	4-32
4.7	Future Directions	4-33

4.8	References.....	4-34
5	DSM2 SAN JOAQUIN RIVER BOUNDARY EXTENSION	5-1
5.1	Introduction	5-1
5.2	Description	5-1
5.3	Model Geometry Development	5-2
5.4	Geometry Refinement.....	5-4
5.5	Historical Study Development	5-6
5.5.1	Development of Boundary Conditions	5-6
5.5.2	Calibration Procedure	5-15
5.5.3	Pre-Calibration Results	5-16
5.5.4	Current Calibration Results	5-24
5.5.5	Discussion	5-30
5.5.6	Conclusions.....	5-31
5.6	Future Directions	5-31
5.7	References.....	5-32
6	DISSOLVED OXYGEN AND TEMPERATURE MODELING USING DSM2	6-1
6.1	Introduction	6-1
6.2	Model Input	6-1
6.3	Calibration	6-3
6.4	Validation	6-6
6.5	Conclusions.....	6-10
6.6	References.....	6-10
7	INTEGRATION OF CALSIM AND ARTIFICIAL NEURAL NETWORKS MODELS FOR SACRAMENTO-SAN JOAQUIN DELTA FLOW-SALINITY RELATIONSHIPS.....	7-1
7.1	Introduction	7-1
7.2	Background	7-1
7.3	Implementation of Artificial Neural Networks in CALSIM.....	7-2
7.3.1	Flow-Salinity Relationship	7-2
7.3.2	Operational Constraints	7-4
7.3.3	Modeled Locations	7-6
7.3.4	Partial Month Standards.....	7-6
7.4	Limitations	7-7
7.5	Recommendations	7-8
7.6	References.....	7-8
8	AN INITIAL ASSESSMENT OF DELTA CARRIAGE WATER REQUIREMENTS USING A NEW CALSIM FLOW-SALINITY ROUTINE	8-1
8.1	Introduction	8-1
8.2	Background	8-2
8.2.1	Carriage Water Definitions.....	8-2
8.2.2	Previous Efforts to Model Delta Flow-Salinity Relationships	8-2
8.3	A New CALSIM Routine to Estimate Delta Flow-Salinity Relationships	8-3
8.3.1	Formulation and Implementation	8-3
8.3.2	Validation	8-5
8.3.3	Impact on CALSIM Water Supply Estimates	8-8
8.4	Methodology for Estimating Carriage Water Requirements.....	8-10

8.4.1	Study Assumptions	8-10
8.4.2	Study Mechanics.....	8-10
8.5	Results	8-11
8.6	Discussion	8-19
8.6.1	Significance of Results.....	8-19
8.6.2	Using DSM2 to Quantify Carriage Water Costs.....	8-19
8.6.3	Negotiations with BDMF.....	8-20
8.6.4	Future Refinements.....	8-20
8.7	References	8-20
9	USE OF REPEATING TIDES IN PLANNING RUNS	9-1
9.1	Introduction	9-1
9.2	Design Repeating Tide	9-1
9.3	Results	9-2
9.4	Recommendations	9-4
10	PLANNING TIDE AT THE MARTINEZ BOUNDARY.....	10-1
10.1	Introduction	10-1
10.2	Available Data.....	10-1
10.3	Tidal Composition.....	10-2
10.4	Astronomical Estimation.....	10-3
10.5	Residual Tide.....	10-3
10.6	Reconstruction.....	10-4
10.7	Implementation and Discussion.....	10-4
10.8	References.....	10-5
11	IMPROVING ESTIMATES OF SALINITY AT THE MARTINEZ BOUNDARY.....	11-1
11.1	Introduction	11-1
11.2	G-model Basics	11-2
11.3	Tidal Model	11-4
11.4	Mathematical Formulation	11-7
11.5	Estimation.....	11-10
11.6	Validation and Discussion	11-14
11.7	References.....	11-17
12	DSM2 REAL-TIME FORECASTING SYSTEM	12-1
12.1	Introduction	12-1
12.2	Background	12-2
12.3	Real-Time Modeling Forecast Processes.....	12-4
12.3.1	Raw Data	12-4
12.3.2	Pre-processing	12-5
12.3.3	Running DSM2.....	12-13
12.3.4	Post-processing	12-13
12.3.5	On-line Output.....	12-15
12.4	Running Alternative Scenarios.....	12-21
12.5	Conclusions.....	12-23
12.6	Future Directions	12-24
12.7	References.....	12-25

LIST OF TABLES

Table 3-1:	Summary of Study Assumptions.....	3-1
Table 3-2:	Data Availability at DSM2 Output Locations.....	3-6
Table 4-1:	Location and Dates of Collected ADCP Data.....	4-8
Table 4-2:	PTM Velocity Profile Coefficients.....	4-26
Table 5-1:	Summary of Data Sources for DSM2 Boundary Conditions.....	5-7
Table 5-2:	Description of Current DSM2 Tributary Boundary Conditions.....	5-8
Table 8-1:	Carriage Water Requirements for a 30-TAF Transfer by Month and Water Year Type (values in percent of transfer).....	8-11
Table 8-2:	Carriage Water Requirements for a 60-TAF Transfer by Month and Water Year Type (values in percent of transfer).....	8-11
Table 8-3:	Required Sacramento Flow for September Water Transfers (60 TAF) Over the 73-year Hydrologic Sequence.....	8-16
Table 11-1:	Coefficient Estimates, Standard Error, and Z-Scores (GEE).....	11-12
Table 12-1:	Standard IEP DSS Hydrodynamic DSM2 Real-Time Inputs.....	12-6
Table 12-2:	Standard IEP DSS Water Quality DSM2 Real-Time Boundary Inputs.....	12-7
Table 12-3:	Standard IEP DSS Water Quality DSM2 Real-Time Initial Condition Inputs.....	12-7

LIST OF FIGURES

Figure 2-1a:	Error Index Calculations for Field / Model Stage Data Comparisons	2-2
Figure 2-1b:	Error Index Equations for Field / Model Stage Data Comparisons.....	2-3
Figure 2-2:	San Joaquin River EC at Jersey Point.....	2-5
Figure 2-3:	Net Delta Outflow for 1992.....	2-7
Figure 3-1:	Monthly Delta Inflow DOC Boundary Conditions	3-3
Figure 3-2:	Monthly Delta Inflow UVA Boundary Conditions.....	3-3
Figure 3-3:	Monthly Agricultural Return Flow DOC Concentrations.....	3-4
Figure 3-4:	DSM2 Output Locations	3-5
Figure 3-5:	Dissolved Organic Carbon at Banks Pumping Plant, Clifton Court Forebay, and Contra Costa Pumping Plant #1	3-7
Figure 3-6:	Dissolved Organic Carbon at Tracy Pumping Plant, False River at Webb Tract, and Grant Line Canal.....	3-8
Figure 3-7:	Dissolved Organic Carbon at Mallard Island, Middle River at Highway 4, and Middle River at Bacon Island	3-9
Figure 3-8:	Dissolved Organic Carbon at North Canal, North Victoria Canal and Woodward Island, and Old River Near DMC	3-10
Figure 3-9:	Dissolved Organic Carbon at Old River at Rock Slough, Sandmound Slough, and Santa Fe Railroad at Bacon Island.....	3-11
Figure 3-10:	Dissolved Organic Carbon at Jersey Point, Los Vaqueros Reservoir Intake on Old River, and North Bay Aqueduct Intake	3-12
Figure 3-11:	Dissolved Organic Carbon at the Mokelumne River, Rio Vista, and the Middle River at Mowry Bridge	3-13
Figure 3-12:	Ultraviolet Absorbance at Banks Pumping Plant, Clifton Court Forebay, and Contra Costa Pumping Plant #1	3-14
Figure 3-13:	Ultraviolet Absorbance at Tracy Pumping Plant, False River at Webb Tract, and Grant Line Canal.....	3-15
Figure 3-14:	Ultraviolet Absorbance at Mallard Island, Middle River at Highway 4, and Middle River at Bacon Island	3-16
Figure 3-15:	Ultraviolet Absorbance at North Canal, North Victoria Canal and Woodward Island, and Old River Near DMC	3-17
Figure 3-16:	Ultraviolet Absorbance at Old River at Rock Slough, Sandmound Slough, and Santa Fe Railroad at Bacon Island	3-18
Figure 3-17:	Ultraviolet Absorbance at Jersey Point, Los Vaqueros Reservoir Intake on Old River, and North Bay Aqueduct Intake.....	3-19
Figure 3-18:	Ultraviolet Absorbance at the Mokelumne River, Rio Vista, and Middle River at Mowry Bridge.....	3-20
Figure 4-1:	DSM2 Schematic of the Sacramento – San Joaquin Delta	4-2
Figure 4-2:	Major Sacramento – San Joaquin Delta Boundary Flows	4-3
Figure 4-3:	Transverse Velocity Profiles	4-6
Figure 4-4:	Vertical Velocity Profiles	4-7
Figure 4-5:	Historical Flow at Turner Cut	4-9
Figure 4-6:	Turner Cut ADCP Profile Data (1:30 PM, April 9, 1997).....	4-9
Figure 4-7:	Historical Flow for SJR between Turner and Columbia Cuts	4-10
Figure 4-8:	SJR between Turner and Columbia Cuts ADCP Profile Data (10:30 PM, April 4, 1997).....	4-10
Figure 4-9:	Location of Tracer Study Data Collection Sites	4-11
Figure 4-10:	Tracer Concentration at Stockton UVM Site.....	4-12
Figure 4-11:	Measured Flow at Stockton UVM Site	4-12
Figure 4-12:	Tracer Concentration at Turner Cut.....	4-13
Figure 4-13:	Measured Flow at Turner Cut	4-13
Figure 4-14:	Tracer Concentration at San Joaquin River near Mandeville Ranch.....	4-13

Figure 4-15:	Tracer Concentration at Middle River near Columbia Cut.....	4-14
Figure 4-16:	Measured Flow at Middle River near Columbia Cut	4-14
Figure 4-17:	Tracer Concentration at Grantline Canal near Tracy Blvd. Bridge	4-14
Figure 4-18:	Measured Stage at Grantline Canal near Tracy Blvd. Bridge.....	4-15
Figure 4-19:	Turner Cut Flow	4-16
Figure 4-20:	Turner Cut Profile – ADCP Comparison (1:30 PM, April 9, 1997).....	4-16
Figure 4-21:	SJR between Columbia and Turner Cuts Flow.....	4-17
Figure 4-22:	SJR between Columbia and Turner Cuts Profile – ADCP Comparison (10:30 PM, April 4, 1997)	4-17
Figure 4-23:	Velocity Profile Differences for a Single Long Channel	4-19
Figure 4-24:	Variance of Longitudinal Displacement for Original Profiles.....	4-20
Figure 4-25:	Effective Longitudinal Dispersion for Original Profiles.....	4-20
Figure 4-26:	Variance of Longitudinal Displacement for Modified Profiles	4-21
Figure 4-27:	Effective Longitudinal Dispersion for Modified Profiles.....	4-21
Figure 4-28:	Stage Boundary Condition for Long Channel	4-22
Figure 4-29:	Stage at Various Locations Influenced by Tidal Boundary Condition.....	4-22
Figure 4-30:	Particle Concentration for Long Channel with Tidal Boundary Condition.....	4-23
Figure 4-31:	Martinez Stage Boundary Condition	4-24
Figure 4-32:	DSM2 and Measured Flow at Turner Cut	4-24
Figure 4-33:	DSM2 and Measured Flow at Jersey Point	4-25
Figure 4-34:	DSM2 and Measured Flow at Old River near Bacon Island	4-25
Figure 4-35:	DSM2 and Measured Flow at Middle River South of Columbia Cut.....	4-25
Figure 4-36:	PTM and Tracer Comparison at Stockton UVM site.....	4-27
Figure 4-37:	PTM and Tracer Comparison at Turner Cut	4-27
Figure 4-38:	PTM and Tracer Comparison on SJR at Mandeville Reach.....	4-28
Figure 4-39:	PTM and Tracer Comparison on Middle River South of Columbia Cut.....	4-29
Figure 4-40:	PTM and Tracer Comparison with No Dispersion at Turner Cut.....	4-30
Figure 4-41:	PTM and Tracer Comparison with Uniform Vertical Velocity Profile at Turner Cut.....	4-31
Figure 4-42:	PTM and Tracer Comparison with Uniform Transverse Velocity Profile at Turner Cut.....	4-32
Figure 5-1:	San Joaquin River.....	5-3
Figure 5-2:	Stage-Area Relationship for Channels 619 to 624	5-5
Figure 5-3:	Bottom Elevation Transition for the Irregular Cross Sections from Channels 619 to 624.....	5-5
Figure 5-4:	Map of Gauging Stations	5-8
Figure 5-5:	Boundaries of Relevant Public Agencies.....	5-10
Figure 5-6:	DSM2 Pre-Calibration Results for Stage at NEW.....	5-17
Figure 5-7:	DSM2 Pre-Calibration Results for Stage at CLB	5-17
Figure 5-8:	DSM2 Pre-Calibration Results for Stage at SJP.....	5-18
Figure 5-9:	DSM2 Pre-Calibration Results for Stage at VER.....	5-19
Figure 5-10:	DSM2 Pre-Calibration Results for Flow at NEW.....	5-20
Figure 5-11:	DSM2 Pre-Calibration Results for Flow at CLB	5-20
Figure 5-12:	DSM2 Pre-Calibration Results for Flow at SJP	5-21
Figure 5-13:	DSM2 Pre-Calibration Results for Flow at VER.....	5-22
Figure 5-14:	Example of Flood Peak Phase Shift at VER.....	5-22
Figure 5-15:	DSM2 Pre-Calibration Results for Salinity at CLB	5-23
Figure 5-16:	DSM2 Pre-Calibration Results for Salinity at VER.....	5-24
Figure 5-17:	DSM2 Calibration Results for Stage at SJP	5-25
Figure 5-18:	DSM2 Calibration Results for Stage at VER.....	5-26
Figure 5-19:	Comparison of Pre-Calibration and Calibration Stage at SJP and VER.....	5-26
Figure 5-20:	DSM2 Calibration Results for Flow at SJP	5-27
Figure 5-21:	DSM2 Calibration Results for Flow at VER	5-27
Figure 5-22:	Comparison of Pre-Calibration and Calibration Flows at SJP and VER.....	5-28
Figure 5-23:	DSM2 Calibration Results for Salinity at VER	5-29

Figure 5-24:	Comparison of Pre-Calibration and Calibration Salinities at VER	5-29
Figure 6-1:	Interaction among Water Quality Constituents	6-2
Figure 6-2:	Temperature Calibration in the San Joaquin River at Rough and Ready Island near Stockton, 1998	6-4
Figure 6-3:	Dissolved Oxygen Calibration at Rough and Ready Island near Stockton, 1998	6-5
Figure 6-4:	Daily Averaged Dissolved Oxygen at Rough and Ready Island near Stockton, 1998	6-6
Figure 6-5:	Temperature Validation at Rough and Ready Island near Stockton, 1999	6-7
Figure 6-6:	Dissolved Oxygen Validation at Rough and Ready Island near Stockton, 1999	6-8
Figure 6-7:	Daily Averaged Dissolved Oxygen at Rough and Ready Island near Stockton, 1999	6-8
Figure 6-8:	Dissolved Oxygen in the San Joaquin River near Fourteen Mile Slough, 1999.	6-9
Figure 6-9:	Dissolved Oxygen in the San Joaquin River near Columbia Cut, 1999	6-9
Figure 7-1:	Salinity Surface Plot: Emmaton (Ex: October 1976) (uS/cm)	7-3
Figure 7-2:	Salinity Contour Plot: Emmaton (Ex: October 1976) (uS/cm).....	7-4
Figure 7-3:	Salinity Contour Plot with Linearization: Old River at Rock Slough (Ex: October 1976) (uS/cm)	7-4
Figure 7-4:	Exponential Averaging Function for Partial Month Salinity Standards	7-7
Figure 8-1:	CALSIM Linear Approximation of ANN Iso-Salinity Contours: Emmaton in October of 1976	8-4
Figure 8-2:	Full-Circle Analysis Schematic.....	8-5
Figure 8-3:	Full-Circle Analysis Time Series Results: Water Years 1976 – 1991	8-6
Figure 8-4:	Full-Circle Analysis Scatter Results: Water Years 1976 – 1991	8-7
Figure 8-5:	Impact of ANN Module on CALSIM Water Supply Estimates.....	8-8
Figure 8-6:	Time Series Comparison of DSM2 Predicted Water Quality from G-Model and ANN: Water Years 1976 – 1991	8-9
Figure 8-7:	Average Sacramento Flow Required for a 30-TAF Transfer by Month and Water Year Type	8-12
Figure 8-8:	Average Sacramento Flow Required for a 60-TAF Transfer by Month and Water Year Type	8-13
Figure 8-9:	Carriage Water Cost Comparison Between a 30-TAF and 60-TAF Transfer	8-15
Figure 8-10:	Distribution of Sacramento River Flow Required to Transfer 30-TAF by Month and Water Year Type	8-17
Figure 8-11:	Distribution of Sacramento River Flow Required to Transfer 60-TAF by Month and Water Year Type	8-18
Figure 9-1:	19-Year Mean Tide and Adjustment	9-2
Figure 9-2:	Comparison of EC for the Sacramento River at Emmaton	9-3
Figure 9-3:	Comparison of EC for the San Joaquin River at Jersey Point.....	9-3
Figure 9-4:	Comparison of EC for the Old River at Bacon Island	9-3
Figure 10-1:	Stage After Application of a Low Pass Tidal Filter	10-2
Figure 10-2:	Comparison of the Planning and Astronomical Residual Tides in 1993.....	10-5
Figure 11-1:	Advection of a Concentration Profile Back and Forth of an Observer	11-5
Figure 11-2:	Advection of a Changing Concentration Profile	11-6
Figure 11-3:	Comparing the Shape of the Stage and EC Tidal Fluctuation.....	11-6
Figure 11-4:	Models of Tidal Displacement. a) The Displacement Model as a Linear Filtration of Stage, b) The Displacement Model as Embedded in the Full Salinity Model.....	11-8
Figure 11-5:	Transfer Function Characteristics of the Filter Relating Concentration Profile Displacement $x'(t)$ to Water Surface Height. Estimate Using GEE with Robust Gamma Distribution and Log Link.....	11-13

Figure 11-6:	Transfer Function Characteristics of the Filter Relating Concentration Profile Displacement $x'(t)$ to Water Surface Height. Estimate Using GLM with Robust Gamma Distribution and Log Link.....	11-13
Figure 11-7:	Validation Estimates for the Years 1993 – 1994.....	11-15
Figure 11-8:	Model Performance Over a Two-Week Period	11-15
Figure 11-9:	Comparing Low-Passed Martinez Stage (Filling and Draining) to Low-Passed Squared Tide (a Measure of Tidal Energy).....	11-17
Figure 12-1:	Flow Chart of Numerical Modeling Forecast System.....	12-4
Figure 12-2:	VPlotter DSS Data Retrieval GUI.....	12-5
Figure 12-3:	Retrieving Multiple Time Series for Same Location.....	12-6
Figure 12-4:	Martinez Stage Verification	12-8
Figure 12-5:	Example of Filling In Historical Flow Data (Without Tidal Influence)	12-9
Figure 12-6:	Example of Filling In Historical Flow Data (With Tidal Influence)	12-9
Figure 12-7:	MS Access Forecast Form.....	12-11
Figure 12-8:	Martinez EC Verification	12-12
Figure 12-9:	Filling in Rim Boundary EC	12-12
Figure 12-10:	Comparison of Modeled Flow versus Observed Flow at Freeport	12-14
Figure 12-11:	Comparison of Modeled Stage versus Observed Stage at Antioch	12-14
Figure 12-12:	DSM2 Real-Time Forecast Results Web Page	12-16
Figure 12-13:	Interactive Delta Map to View HYDRO and QUAL Forecast Results	12-17
Figure 12-14:	Viewing Forecast Input Results on Interactive Delta Map	12-18
Figure 12-15:	Selecting HYDRO and QUAL Results from Interactive Delta Map.....	12-18
Figure 12-16:	Static PTM Forecast Results	12-20
Figure 12-17:	PTM Dual Animator.....	12-21
Figure 12-18:	Comparing Scenarios When Using On-line Results	12-22

1 Introduction

Over the last eight years, the Delta Modeling Section has been developing and enhancing the Delta Simulation Model 2 (DSM2) and its support tools. The following are brief summaries of work that was conducted during the past year. The names of contributing authors are in parentheses.

Chapter 2 – DSM2 Calibration and Validation

Last year's annual progress report described the Section's participation in an Interagency Ecological Program project work team created for the recalibration of DSM2-HYDRO and QUAL with new geometry and flow data. Calibration and validation were completed and the Section began using the new calibrated version in January 2001. In general, the new version matches observed flow and water quality conditions much better than the 1997 version. Improvements in flow estimates around the Delta Cross Channel and Bacon Island are particularly noteworthy. The IEP project work team will undertake future calibration efforts as new data become available. These efforts will focus on issues that were not resolved in the most recent calibration work. (*Parviz Nader-Tehrani*)

Chapter 3 – Simulation of Historical DOC and UVA Conditions in the Delta

An *ad hoc* workgroup was assembled in late 1999 to assist CALFED's Drinking Water Constituents Workgroup in one of several tasks necessary to define baseline Delta water quality conditions. This *ad hoc* workgroup, which consisted of members of DWR's Delta Modeling Section and Municipal Water Quality Investigations Program, developed boundary conditions from available grab sample data to validate DSM2's capability to simulate organic constituents transport. For the validation period of March 1991 to December 1997, DSM2 does a satisfactory job simulating the distribution of dissolved organic carbon and ultraviolet absorbance and in representing observed seasonal peaks and trends. DSM2 is being used by the Section to evaluate DOC transport in support of the Integrated Storage Investigation (ISI) In-Delta Storage Project Feasibility Study. (*Ganesh Pandey*)

Chapter 4 – Validation of Dispersion Using the Particle Tracking Model in the Sacramento-San Joaquin Delta

This chapter is a condensed version of Ryan Wilbur's M.S. Thesis and covers the validation of dispersion using the DSM2 Particle Tracking Model (PTM). A complete copy of his thesis is on file with University of California, Davis. PTM results are compared with ADCP velocity profiles collected between 1997 and 1999 and tracer dye observations from a spring 1997 field study. This validation was done prior to the release of the latest DSM2 calibrated version described in Chapter 2. (*Ryan Wilbur*)

Chapter 5 – DSM2 San Joaquin River Boundary Extension

Last year's progress report described the Section's initial efforts to extend the DSM2 San Joaquin River (SJR) boundary upstream of Vernalis. This chapter summarizes work that was conducted over the past year to calibrate and validate the model extension. The simulation period of May 1997 to September 1999 was selected for initial calibration and validation in consideration of available stage, flow and salinity data. While DSM2 results generally showed good trending with field observations, it was clear that some significant sources of flow and salinity were not being modeled. To compensate for this apparent input data gap, constant base flows were added upstream of Patterson and Vernalis. These "add-water" flows were assigned a salinity signature with the temporal variability of an agriculture return and a magnitude reflecting a high-salinity groundwater and agriculture tail-water mixture. Historical data are being collected to conduct a longer-term simulation to test the robustness of the assumed "add-water" flows and salinity signature. The model extension will be used to evaluate Delta Mendota Canal re-circulation alternatives. CALFED funding has been secured to develop a "stand-alone" version of the upper SJR model in support of the San Joaquin River Total Maximum Daily Load (TMDL) stakeholder process. *(Thomas Pate)*

Chapter 6 – Dissolved Oxygen and Temperature Modeling Using DSM2

The Section has been reporting progress in dissolved oxygen and temperature modeling in its annual reports since 1994. This chapter summarizes a recent DSM2 dissolved oxygen and temperature calibration in the vicinity of Stockton on the San Joaquin River. The process of calibrating a numerical model to predict dissolved oxygen concentrations is highly data intensive. Based primarily on data availability, the periods of August to October 1998 and July to September 1999 were chosen for calibration and validation, respectively. DSM2 is now considered adequate for dissolved oxygen planning studies in the vicinity of Stockton, in view of significant data limitations. CALFED funding has been secured to conduct dissolved oxygen planning studies and to calibrate the DSM2 upper SJR extension for dissolved oxygen and temperature; these projects will be conducted in collaboration with an outside party in support of the San Joaquin River TMDL stakeholder process. *(Hari Rajbhandari)*

Chapter 7 – Integration of CALSIM and Artificial Neural Networks Models for Sacramento-San Joaquin Delta Flow-Salinity Relationships

Chapter 7 describes work conducted by the Office of State Water Project Planning Hydrology and Operations Section to integrate an Artificial Neural Network (ANN) representation of DSM2 into the statewide planning model CALSIM. The ANN will be used to model flow-salinity relationships within CALSIM II. Chapter 8 describes an application of the ANN to estimate Delta carriage water requirements. The Section has been reporting ANN development progress in its annual reports since 1995. *(Ryan Wilbur and Armin Munevar)*

Chapter 8 – An Initial Assessment of Delta Carriage Water Requirements Using a New CALSIM Flow-Salinity Routine

This chapter presents a new approach to estimating carriage water requirements in the Delta; the approach utilizes the ANN implementation discussed in Chapter 7. Water supply impacts of the ANN routine are compared with the previous G-model Delta formulation utilized by DWRSIM and CALSIM I. This chapter, which is the first to quantify Delta carriage water costs over a long-term hydrologic sequence, supports DWR's typical carriage water assessments of 10 to 30%. Carriage water costs are shown to be sensitive to water year type, particularly costs associated with meeting salinity standards. Report findings have been shared with the Bay Delta Modeling Forum Carriage Water Review Team, in support of the State Water Resources Control Board's Phase 8 Water Rights Hearing. The review team intends to reach a settlement regarding the calculation of carriage water among interested parties. Carriage water estimates will be updated as new information and model enhancements become available. In particular, carriage water estimates will be updated to include input from the BDMF Carriage Water Review Team and to reflect progress in baseline modeling of CVPIA b(2) and EWA operations. *(Paul Hutton and Sanjaya Seneviratne)*

Chapter 9 – Use of Repeating Tides in Planning Runs

This chapter summarizes the development of a new repeating tide for DSM2 planning studies. DSM2 requires that tidal (i.e. stage) values be specified at its downstream Martinez boundary. DSM2 simulations that utilize this new “design-repeating tide” provide salinity results more representative of a non-repeating tide than simulations that utilize the higher energy “19-year mean tide.” *(Parviz Nader-Tehrani)*

Chapter 10 – Planning Tide at the Martinez Boundary

DSM2 planning studies have traditionally relied on DWRSIM (and later CALSIM) monthly varying hydrology and operations as input boundary conditions. Repeating tides have been computationally advantageous when used by DSM2 in concert with monthly varying hydrology. However, CALSIM is presently being restructured to compute daily varying Delta hydrology and operations in support of the ISI In-Delta Storage Program Feasibility Study, and DSM2 is being restructured to accept these new boundary conditions. By moving from a monthly to a daily hydrology, repeating tides will lose their computational advantages over non-repeating tides. Chapter 10 summarizes the development of a non-repeating tide for DSM2 planning studies. This new planning tide, developed from data collected at Martinez and San Francisco between 1968 and 1999, has two components: (1) an astronomical tide that includes accurate harmonic components and spring-neap variation, and (2) a residual tide to estimate long-period fluctuations due to barometric changes and nonlinear interactions. *(Eli Ateljevich)*

Chapter 11 – Improving Estimates of Salinity at the Martinez Boundary

This chapter introduces an improved method of salinity estimation at Martinez, the downstream tidal boundary in DSM2. Development of a better boundary salinity estimator was motivated by the need for better absolute accuracy in the DSM2 real-time forecasting system (see Chapter 12) and by the re-structuring of DSM2 planning studies to include non-repeating tides (see Chapter 10). The method, designed to accommodate both real-time and planning applications, is based on the G-model with modifications to derive tidal (15-minute) salinity estimates. Model coefficients were calibrated for the period August 20, 1991 to September 5, 1992. The model provides a satisfactory validation of observed data over a period spanning the two calendar years 1993 and 1994. (*Eli Ateljevich*)

Chapter 12 – DSM2 Real-Time Forecasting System

Chapter 12 summarizes work conducted by the Section, in collaboration with other DWR staff, to develop and use DSM2 as an operations decision support tool. This DSM2 Real-Time Forecasting System combines real-time field data with operational forecasts of the inflows, exports, and barrier configurations in the Delta through a series of pre-processing tools and scripts. These new real-time tools have reduced the time necessary to run DSM2-HYDRO, QUAL, and PTM. These tools also make it much easier to create alternative scenarios, thus encouraging DSM2 users to explore several “what if” questions while evaluating an operational forecast. The emphasis of this development effort has been to create easy-to-view model results in a timely fashion, while ensuring quality control. (*Michael Mierzwa*)

Methodology for Flow and Salinity Estimates in the Sacramento-San Joaquin Delta and Suisun Marsh

**22nd Annual Progress Report
August 2001**

Chapter 2: DSM2 Calibration and Validation

Author: Parviz Nader-Tehrani

2 DSM2 Calibration and Validation

2.1 Introduction

DSM2-HYDRO (HYDRO) and DSM2-QUAL (QUAL) were originally calibrated and validated in 1997 (see the Eighteenth Annual Progress Report, June 1997). Since then, a great amount of new bathymetry, flow, and water quality data have become available. A project work team (PWT) was formed with representatives from various agencies under IEP (Interagency Ecological Program). Members included representatives from the following agencies:

- ❑ DWR
- ❑ USGS
- ❑ USBR
- ❑ Contra Costa Water District (CCWD)
- ❑ Metropolitan Water District (MWD)
- ❑ Stanford University

Chris Enright (DWR, Environmental Services Office) was the chair of this PWT. The team was given the task of calibrating and validating HYDRO and QUAL. It was decided that the calibration/validation of DSM2 be an open process. All the results were posted on a public web-site during each iteration of the calibration. Conference calls made it easier for the PWT to frequently discuss these public results and agree upon what changes to make for the next iteration of the calibration.

Comparison of model-predicted values and field data was done both in an instantaneous and tidally averaged sense. The comparison of instantaneous data shows the model's capability to predict the tidal amplitude and phase. The comparison of the tidally averaged data demonstrates the long-term effects. It is also useful for evaluating flow splits at key locations in the Delta.

All the activities with regards to the calibration can be found at the IEP web-site at:

<http://www.iep.water.ca.gov/dsm2pwt/dsm2pwt.html>

2.2 Choice of Model Grid

Staff from DWR ESO (Environmental Services Office) had made several changes to the DSM1 grid. Most of the changes were in the Suisun Marsh area. IEP-PWT decided to adapt ESO's version of its grid map for the DSM2 calibration/validation effort. For a more in-depth explanation of the differences between the two grids, refer to the Twenty-First Annual Progress Report (pg. 10-2).

2.3 DSM2-HYDRO Calibration

HYDRO was calibrated using data from four different time-periods:

- 1- May 1988
- 2- April 1997
- 3- April 1998
- 4- Sept.-Oct. 1998

For HYDRO, the Manning's n parameter was chosen as the calibration parameter. The Manning's n set corresponding to the 1997 calibrated version was used as the initial set. With each subsequent run, these values were modified with the hope of achieving a better match. Phase and tidal amplitude error indexes were introduced to quantify the goodness of fit for stage. The magnitude of the error indexes was calculated for each period separately, and values were written directly on the figures. The presence of these indexes directly on the plot made it a lot easier to improve the fit. See Figure 2-1a and 2-1b for an explanation of these error indexes.

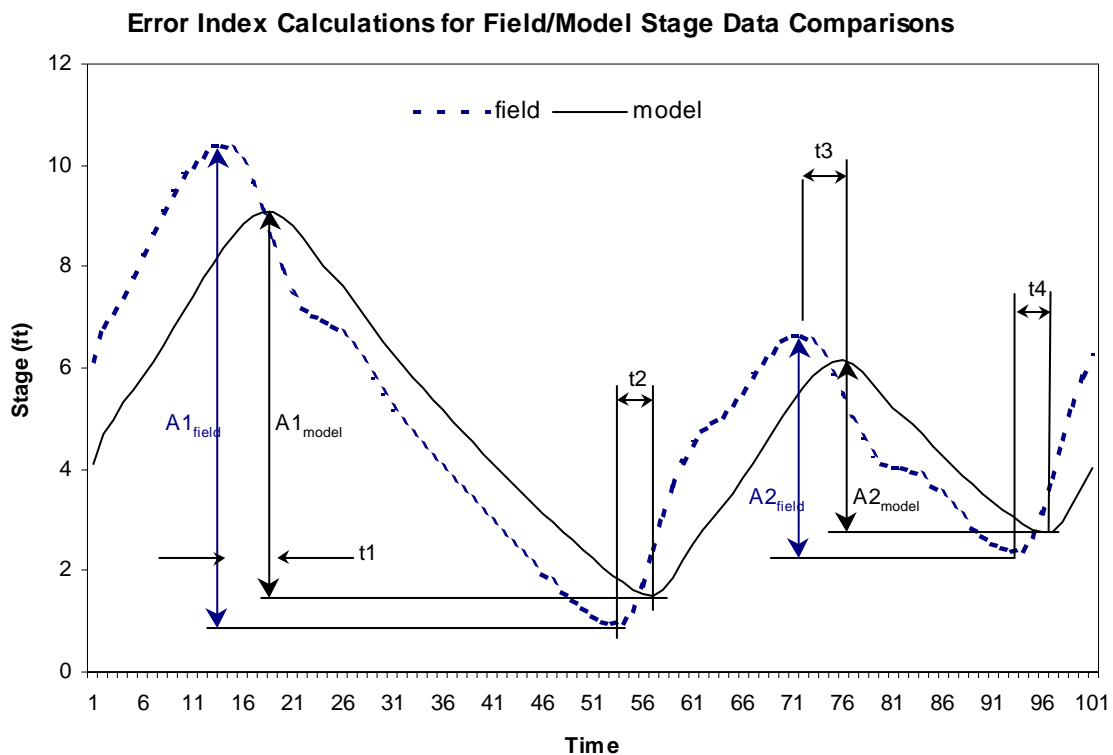


Figure 2-1a: Error Index Calculations for Field / Model Stage Data Comparisons.

<u>Error Index Equations:</u>		
rms error =	$\frac{[\text{sum}(\text{model}-\text{field})^{**2}]^{**.5}}{n^{**.5}}$	
amp error = (feet)	$\frac{\text{dif1}+\text{dif2}}{2}$	where: dif1 = A1model - A1field dif2 = A2model - A2field
ph error = (minutes)	$\frac{(\text{t1}+\text{t2}+\text{t3}+\text{t4})}{4}$	where: t1 = time of model peak1 - time of field peak2 t2 = time of model peak2 - time of field peak2 t3 = time of model peak3 - time of field peak3 t4 = time of model peak4 - time of field peak4

Figure 2-1b: Error Index Equations for Field / Model Stage Data Comparisons.

A total of 56 iterations were completed. In the final version, the Delta was divided into 59 regions, each containing one or more channels. Each group was assigned a single Manning’s n value. Overall, model predictions for the final iteration of the calibration are noticeably closer to the field data than the 1997 version. This is especially true for the flow data. This is clearly important, since one expects that an improvement in flow predictions would naturally follow with improvements in water quality predictions. For a direct comparison of the results corresponding to the final iteration of the calibration with the 1997 version, the reader is referred to:

<http://iep.water.ca.gov/dsm2pwt/calibrate/Run56vsRun1/index.html>

2.4 DSM2-QUAL Calibration

Unlike HYDRO, QUAL was calibrated in one continuous interval. In general, QUAL needs about two to six months to ‘warm-up’. In other words, the model results are affected by the initial conditions (initial water quality in all the channels) during that time span. HYDRO’s predictions, on the other hand, are only affected by the initial conditions for about two days. This renders QUAL calibration for short periods impractical.

QUAL was calibrated using electric conductivity (EC) data. This was primarily due to the fact that EC data is in plentiful supply. The assumption was that EC behaves like a conservative substance. Ideally, one would prefer to calibrate using chloride data, which is believed to be truly conservative. However, chloride data are only available on a limited basis. Regression equations have been developed to convert EC to chloride, but these equations have their own errors. A recent investigation (literature search and data analysis) conducted by the Delta Modeling Section concluded that EC values of up to about 3,000 umhos/cm can be considered as conservative. EC values of 15,000 umhos/cm or higher are clearly in the non-conservative range. The Delta Modeling Section plans to revisit the QUAL calibration using ‘Practical Salinity’. More explanation will be provided in the next annual report.

Meanwhile, the recent calibrated model is suitable for use with EC, but not for predicting other minerals, simply because the calibrated parameters are selected based on EC predictions. Use of the model for predicting organic constituents is also appropriate, since the ocean is not a major source of organics. See Chapter 3 for information about the validation of DSM2-Qual for DOC and UVA.

The choice of time period for QUAL calibration is also an important one. Periods with high flows with little salinity intrusion are not really suitable. Most suitable periods are dry periods, during which highly saline water from the ocean enters the Delta and blends in with the water that is from 100 to 300 times less saline. During dry periods, a small change in flow regime can potentially lead to noticeable changes in water quality. If the model predictions are close to field data for various dry periods, that would increase the level of confidence in the model. The IEP-PWT selected the 3-year period from October 1991 to September 1994. This period contains four sub-periods when high-salinity intrusions were recorded.

Dispersion factors were considered to be the calibration parameter. The Delta was divided into 22 regions, each containing many channels. Adjustments of the dispersion factors started from Martinez (the downstream boundary). The dispersion factors for regions further upstream were modified with each iteration. After 16 iterations, the IEP-PWT decided that the objective was met and calibration considered complete. The reader is referred to:

<http://wwwdelmod.water.ca.gov/studies/calibration/base-hydro-56/run16cv15a/index.html>

for a clickable map showing a comparison of the model results versus the field data. Overall, there is a good agreement. Salt intrusion into the Delta is captured fairly well. However, in the San Joaquin River between Antioch and Jersey Point and continuing up the Old River to Bacon Island, the model seems to over-predict the high peak of salt intrusion. This is especially evident in the summer of 1992. For an example, see Figure 2-2. For additional comments on the QUAL calibration, please refer to Sec. 2.6.

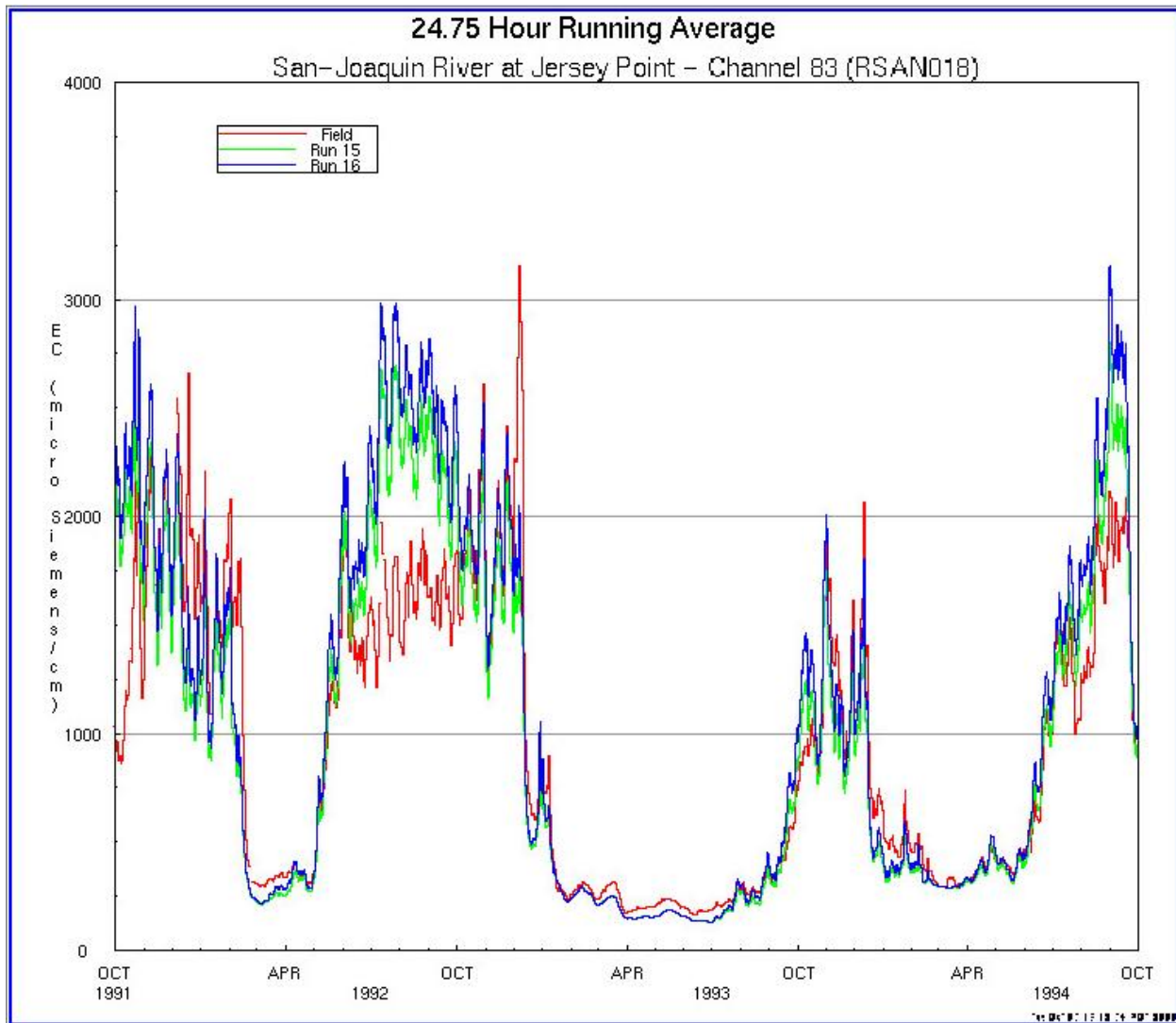


Figure 2-2: San Joaquin River EC at Jersey Point.

2.5 DSM2 Validation

Once the calibration parameters were selected, these parameters were kept constant. The validation period selected was from early 1990 to September 1999. The reader is referred to:

<http://wwdelmod.water.ca.gov/studies/validation/>

for a clickable map pointing to all validation plots. There, the reader will find a three-way comparison of model predictions (flow, stage, and EC) for the new calibrated version (referred to as the new grid), the 1997 calibrated version (referred to as the old grid), and the observed data. These comparisons are available as 14-day moving averages, tidal day averages, and instantaneous plots. Overall, the results for the new calibrated model are in much better agreement with observed data.

2.6 General Comments on DSM2 Calibration/Validation

With HYDRO, flow predictions improved the most. This is especially true for Cross-Delta Flow (sum of flow going through Delta Cross Channel and Georgiana Slough), flow at Old River at Bacon Island, and Middle River at Bacon Island. During the course of calibration, it was discovered that the datum position for measuring the stage for many locations was questionable. This made it difficult to compare stage in an absolute sense. So the IEP-PWT decided to check stage amplitude and phase, and not rely on stage data in an absolute sense. Stage predictions also improved somewhat. The biggest improvement came in South Delta (Grant Line Canal and Old River near DMC), and North Delta (Sacramento River above Delta Cross Channel and below Georgiana Slough).

With QUAL, the validation period actually contained the calibration period. So to check the validation, one should look for the comparison of model output, either prior to October 1991, or beyond September 1994. Comparison of model results clearly shows a much better match for almost all locations with the new validated model. Surprisingly, in the reach from Antioch to Old River at Holland's Tract, model results show a better match during the validation period than during the calibration period.

The IEP-PWT looked for reasons for the EC over-predictions in the San Joaquin River during the calibration period. The IEP-PWT believes that inaccuracies in the channel depletion estimates are one possible cause of the over-predictions. Channel depletions are estimated by the Delta Island Consumptive Use (DICU) model. DICU computes channel depletions based on water needs of the plants, and assumes diversion water is in plentiful supply. As an example, according to DICU, Delta channel depletions for July 1992 were around 4200 cfs. When one computes the Net Delta Outflow (NDO) using this estimate, NDO values that approach 1000 cfs are observed (see Figure 2-3). Under such hydrologic conditions, a great amount of salinity intrusion is expected. This is clearly reflected in the model results. Yet, there is no trace of huge salinity intrusion in the field data. In fact, the field data show the peak salinity intrusion in 1992 to have occurred from October through December, with EC values about double those for the summer (as an example, see EC data for Jersey Point). This is an inconsistency since the computed NDO was, in fact, higher in October through December 1992 than in summer. The IEP-PWT performed a sensitivity test (run 17 versus run 16) with channel depletion values adjusted for 1992. This was done by decreasing the irrigation water demands for June through September by around 500 cfs. That, in turn, increased the water demands in October through November due to a lower stored soil moisture. The result is a predicted salinity that is noticeably closer to the field data. Channel depletion estimates can easily be off by 500 cfs or more. The IEP-PWT decided to concentrate on improving QUAL's performance during the next phase of calibration. Overall, the IEP-PWT does not feel that the mismatch from 1992 through 1994 in the San Joaquin River can be resolved without adjusting the flow field (i.e. NDO).

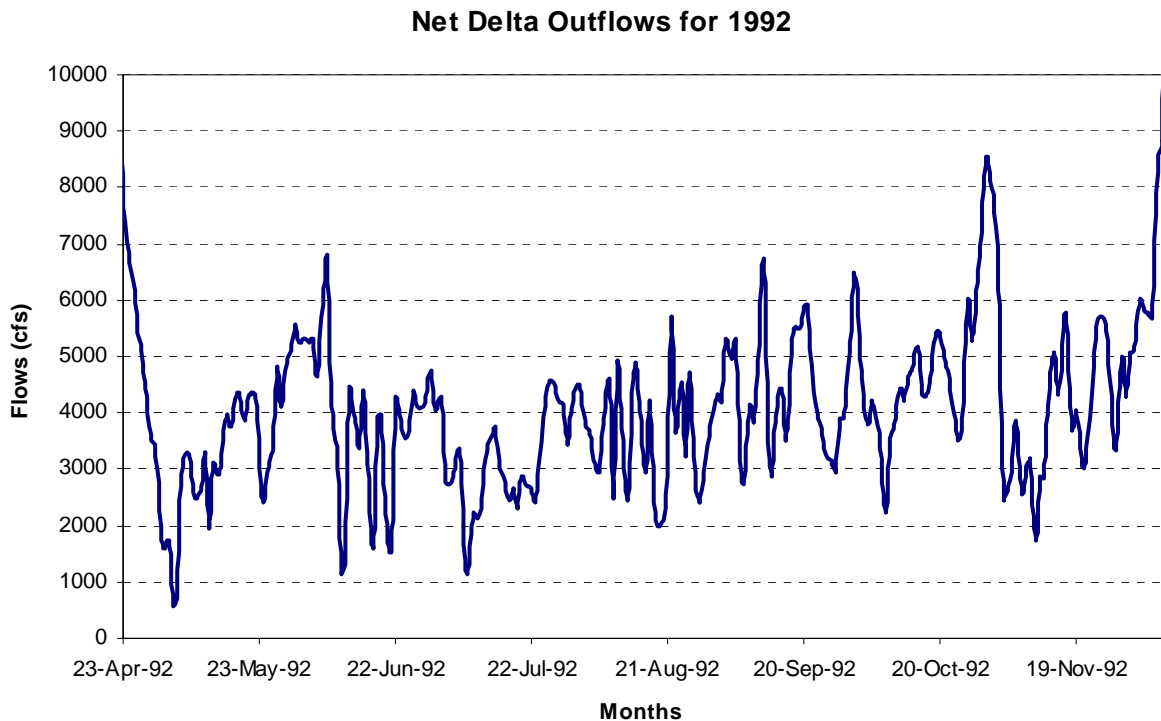


Figure 2-3: Net Delta Outflow for 1992.

2.7 Conclusion

Overall, model predictions using the most recent calibration seem to capture field conditions much better than the 1997 version. Since January 1, 2001, the Delta Modeling Section has officially started using the new calibrated version. It is, however, expected that there will be future calibration efforts when significant new bathymetry, flow, stage, and water quality data become available. The IEP-PWT also plans to look for ways to clarify some of the unresolved issues (such as DICU estimates).

Refer to Chapter 3 for work done in simulation of other water quality constituents such as DOC and UVA. For additional work done in dissolved oxygen and water temperature calibration, refer to Chapter 6.

2.8 References

- California Department of Water Resources. (1997). *Methodology for Flow and Salinity Estimates in the Sacramento-San Joaquin Delta and Suisun Marsh. 18th Annual Progress Report to the State Water Resources Control Board.* Sacramento, CA.
- Nader-Tehrani, P. and B. Shrestha. (2000). "Chapter 10: DSM2 Recalibration." *Methodology for Flow and Salinity Estimates in the Sacramento-San Joaquin Delta and Suisun Marsh. 21st Annual Progress Report to the State Water Resources Control Board.* Sacramento, CA.

Methodology for Flow and Salinity Estimates in the Sacramento-San Joaquin Delta and Suisun Marsh

**22nd Annual Progress Report
August 2001**

Chapter 3: Simulation of Historical DOC and UVA Conditions in the Delta

Author: Ganesh Pandey

3 Simulation of Historical DOC and UVA Conditions in the Delta

3.1 Introduction

The purpose of this study is to validate DSM2 transport of disinfection by-product (DBP) precursor surrogates in the Delta. The study was conducted by an *ad hoc* workgroup that included staff from the Department’s Municipal Water Quality Investigations (MWQI) Program as well as from the Delta Modeling Section. This *ad hoc* workgroup was assembled in late 1999 to assist CALFED’s Drinking Water Constituents Workgroup in defining baseline Delta water quality conditions.

DSM2 is currently being used by the Section to evaluate transport of dissolved organic carbon (DOC) and ultraviolet absorbance at 254 nm (UVA) – two widely accepted DBP precursor surrogates – in support of the Integrated Storage Investigation (ISI) In-Delta Storage Project Feasibility Study. Model-derived DOC and UVA values are being used to compute carbon loading and DBP formation at the urban intakes under base and plan conditions.

3.2 Study Assumptions

The assumptions used in the DSM2 validation study are shown in Table 3-1 and discussed below.

Table 3-1: Summary of Study Assumptions

Delta inflow and export/diversion rates	Daily average IEP data
Martinez stage	15-minute IEP data
Delta island diversion and return flows	Monthly DICU data
Delta inflow water quality	Monthly grab sample MWQI data
Martinez water quality	Monthly grab sample MWQI data at Mallard Island
Delta island return flow water quality	Monthly aggregated MWQI data

3.2.1 Model Version

This study was conducted with the current version of DSM2, which was recently calibrated in collaboration with the DSM2 IEP Project Work Team (see Chapter 2). Flow, stage, and electrical conductivity (EC) data were used to calibrate DSM2. DOC and UVA data were not used in model calibration.

3.2.2 Simulation Constituents and Period

This study evaluated the transport of two drinking water quality constituents: DOC and UVA. Both constituents were modeled as conservative tracers. The simulation covered the period October 1, 1990 through December 31, 1997. This simulation period includes a five-month “warm up” period that allows for adequate mixing of the initial boundary conditions within

DSM2. The simulation period was selected based on availability of grab sample data to run the model and validate results.

3.2.3 Hydrodynamics, Hydrology, and Operations

DSM2 hydrodynamics, hydrology, and operations were generally specified with a daily time step. The IEP database was the primary source of historical information for Delta inflow, Delta export and diversion rates, stage at the downstream boundary, and gate operations. Stage at the DSM2 downstream boundary (Martinez) was specified with a 15-minute time step. The IEP database contains data collected by various state and federal agencies, and can be downloaded via Internet at <http://www.iep.water.ca.gov/dss/>.

3.2.4 Boundary Water Quality

DOC and UVA boundary conditions were developed by MWQI Program staff from grab sample data on a monthly time step (Agee 2000). A simple interpolation scheme was used to complete each time series. Field observations suggest that DOC and UVA values can vary considerably during a month at the model boundary locations, particularly during high precipitation runoff periods in the winter. But due to a lack of continuous monitoring, a smaller time interval was not justified.

DOC and UVA boundary conditions for the Sacramento and San Joaquin rivers are shown in Figures 3-1 and 3-2. Sacramento River DOC and UVA ranged from 1.5-5.6 mg/l and 0.01-0.17 cm^{-1} over the simulation period, respectively. San Joaquin River DOC and UVA ranged from 2.2-11.4 mg/l and 0.05-0.44 cm^{-1} over the simulation period, respectively. The East Side Streams' water quality boundary conditions (not shown in the figures) were based on data collected at the American River Water Treatment Plant intake that serves the City of Sacramento. This site was selected for its low DOC characteristics, as little data have been collected on the Cosumnes or Mokelumne rivers. DOC ranged from 1.1-4.3 mg/l during the simulation period, and UVA ranged from 0.01-0.15 cm^{-1} . The Yolo Bypass, also specified as a DSM2 boundary but not shown in the figures below, was assumed to have the same water quality as the Sacramento River under high-flow conditions (> 50 cfs). Under low-flow conditions, Yolo Bypass water quality was assumed to be characteristic of low-DOC agricultural drainage (see Section 3.2.5). The downstream water quality boundary at Martinez was based on data collected at Mallard Island. Mallard Island DOC and UVA ranged from 1.6-7.0 mg/l and 0.05-0.21 cm^{-1} over the simulation period, respectively. Previous DSM2 simulations have shown that Delta organic concentrations are insensitive to Martinez water quality boundary conditions (Hutton and Chung 1992).

3.2.5 Delta Islands Diversions and Returns

Delta island diversion and return flow volumes were not measured in the field but were estimated with the DWR's Delta Island Consumptive Use (DICU) model (California Department of Water Resources 1995a). The DICU model computes diversion and return volumes on a monthly time step and allows for annual variability in response to changes in Delta land use, precipitation and pan evaporation. Return water quality estimates were based on MWQI measurements. Due to a lack of comprehensive monitoring of over 200 agricultural drains in the Delta, return water quality data were compiled using a simplified aggregation technique (Jung 2000). In his report, Jung segregated the Delta into three DOC subregions:

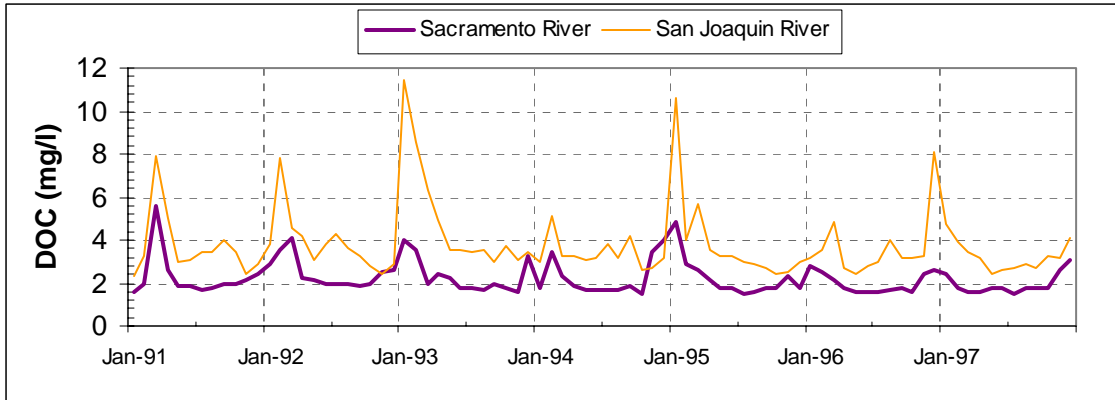


Figure 3-1: Monthly Delta Inflow DOC Boundary Conditions.

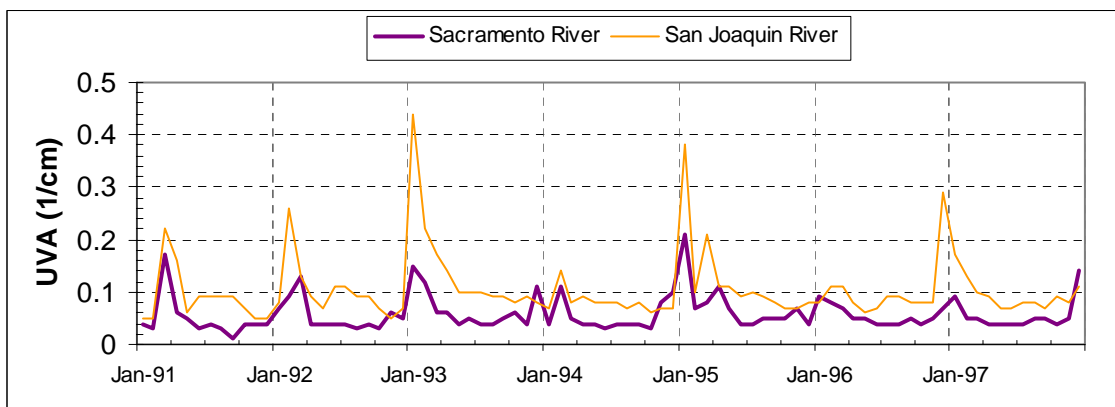


Figure 3-2: Monthly Delta Inflow UVA Boundary Conditions.

high-, mid- and low-DOC. Representative monthly average DOC and UVA values were developed for each subregion. UVA values were assumed as a linear function of DOC concentrations in all Delta island return flows:

$$\text{UVA (1/cm)} = 0.024 + 0.044 \text{ DOC (mg/l)} \quad [\text{Eqn. 3.1}]$$

DOC and UVA values were assumed to vary by month but not by year. Monthly DOC concentrations from the three sub-regions are displayed in Figure 3-3.

3.3 Validation Results

Selection of model validation locations was based upon the availability of grab sample data during the 82-month validation period (March 1, 1991 through December 31, 1997). Geographic coverage for the DSM2 validation is reasonably broad; refer to Figure 3-4. The relatively dense coverage along Old and Middle rivers coincides with key locations at or near drinking water diversions and storage diversions being considered by the ISI In-Delta Storage Project.

Data availability at the DSM2 output locations are summarized in Table 3-2. Output locations include reservoirs, nodes and channels. Channel locations are designated “U”, “M” and “D” to

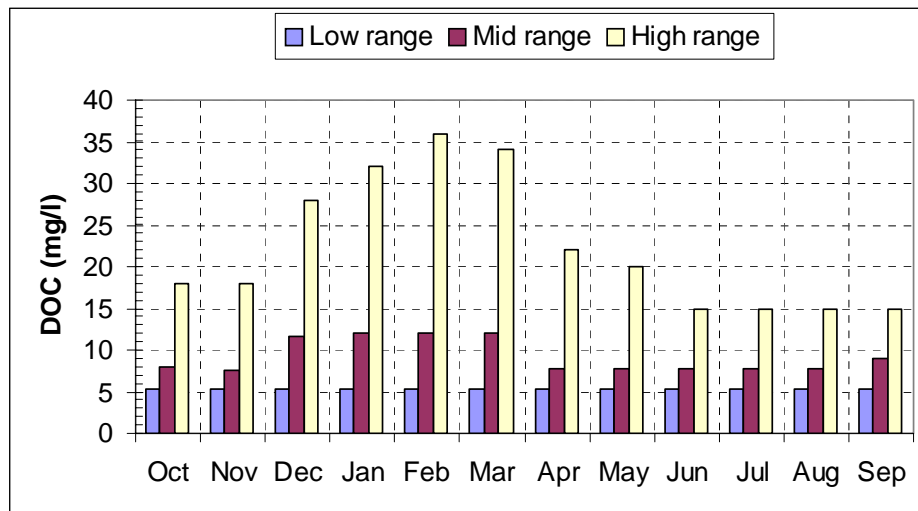


Figure 3-3: Monthly Agricultural Return Flow DOC Concentrations.

represent the upstream, longitudinal midpoint and downstream ends of a channel, respectively. Channel locations are also designated with a numerical value; these values represent the distance (measured in feet) from the upstream node.

Limited grab sample DOC and UVA data allowed for only a crude evaluation of the model's time series output. Figures 3-5 through 3-11 compare field data to predicted monthly average, minimum, and maximum DOC values. Figures 3-12 through 3-18 compare field data to predicted monthly average, minimum, and maximum UVA values.

The predicted minimum and maximum values represent the lowest and highest instantaneous (hourly) values for each month. Together, the minimum and maximum values bound the predicted monthly average values. Large differences in the minimum and maximum values occur in regions with high tidal variation or locations where the input parameters are subject to large fluctuations. Comparison of grab sample data with an envelope of minimum and maximum values is appropriate because grab samples are collected during different times on the tidal cycle.

Three significant results and conclusions from the model validation are as follows:

- Overall, DSM2 does a satisfactory job simulating the distribution of organics in the Delta region where data are available. The model captures the observed distribution of lower organic concentrations in the western and central Delta and higher organic concentrations in the southern Delta. The model also preserves trends in the observed time series. In particular, the effect of seasonality is well represented. Therefore, DSM2 is an appropriate tool for evaluating In-Delta Storage alternatives.

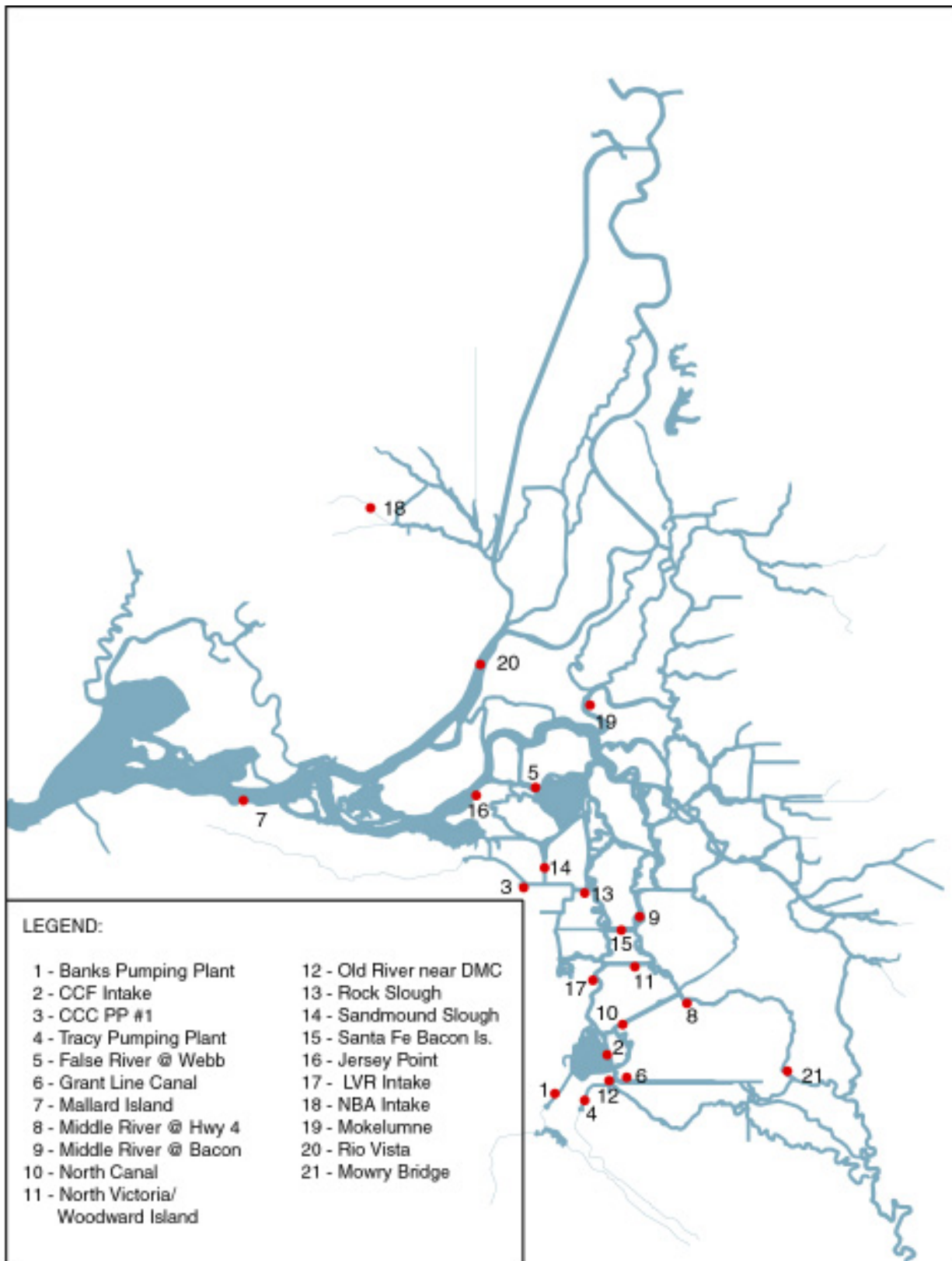


Figure 3-4: DSM2 Output Locations.

Table 3-2: Data Availability at DSM2 Output Locations.

Field Data Station	Abbreviation	Figures	Data Points	DSM2 Output Location
1- Banks Pumping Plant Headworks	Banks Pumping Plant	3-5; 3-12	181	Clifton Ct. Res.
2- Clifton Court Forebay Intake ¹	CCF Intake	3-5; 3-12	111	Node 72
3- Contra Costa Canal Pumping Plant #1	CCC PP #1	3-5; 3-12	80	Node 206
4- Delta Mendota Canal Intake	Tracy Pumping Plant	3-6; 3-13	134	Node 181
5- False River @ Southern Tip of Webb Tract	False R. @ Webb	3-6; 3-13	56	Ch 278 (U)
6- Grant Line Canal near Old River	Grant Line Canal	3-6; 3-13	56	Ch 213 (D)
7- Mallard Island	Mallard Island	3-7; 3-14	131	Ch 437 (M)
8- Middle River @ Highway 4	Middle River @ Hwy 4	3-7; 3-14	97	Ch 134 (D)
9- Middle River @ Bacon Island Bridge	Middle River @ Bacon	3-7; 3-14	91	Ch 148 (D)
10- North Canal near Old River	North Canal	3-8; 3-15	57	Ch 230 (D)
11- N. Victoria / Woodward Island near Old R.	NVICWOOD	3-8; 3-15	58	Ch 234 (U)
12- Old River near DMC Intake ²	Old R near DMC	3-8; 3-15	111	Ch 81 (D)
13- Old River @ Rock Slough ³	Rock Slough	3-9; 3-16	250	Ch 106 (2875)
14- Sandmound Slough	Sandmound Slough	3-9; 3-16	63	Ch 261 (D)
15- Santa Fe Railroad @ Bacon Island	Santa Fe Bacon	3-9; 3-16	58	Ch 258 (M)
16- San Joaquin River @ Jersey Point	Jersey Point	3-10; 3-17	63	Ch 83 (D)
17- Los Vaqueros Reservoir Intake	LVR Intake	3-10; 3-17	103	Node 80
18- NBA Intake @ Barker Slough	NBA Intake	3-10; 3-17	156	Node 273
19- Mokelumne River @ Georgiana Slough	Mokelumne	3-11; 3-18	18	Ch 374 (4627)
20- Sacramento River @ Rio Vista	Rio Vista	3-11; 3-18	72	Ch 430 (8731)
21- Middle River @ Mowry Bridge	Mowry Bridge	3-11; 3-18	17	Ch 126 (4044)

(1) includes data collected at West Canal near Clifton Court Forebay Intake

(2) includes data from a similarly located MWQI stations

(3) includes data from two similarly located MWQI stations (Old River @ Bacon Island and Station 04b)

- DSM2 results are less than satisfactory at the NBA Aqueduct intake at Barker Slough, an important urban intake. This location is strongly influenced by local hydrology (that is not modeled in DSM2) and agricultural return flows (Hutton and Chung 1992); Barker Slough is less influenced by reservoir releases and south Delta pumping operations. The Section does not advocate the use of DSM2 to predict changes in water quality at this location.
- Observed data represent instantaneous values throughout the tidal cycle, while model predictions represent monthly averages. This discrepancy introduces some difficulty in validating the model's ability to capture winter peak DOC and UVA values. Most of the observed values fall within the simulation envelope defined by monthly minimum and maximum values. However, it is doubtful that differences between observed data and monthly average predictions are due entirely to tidal variation, particularly in winter months. Some of the differences likely result from the coarse definition of Delta inflow and agricultural return water quality conditions. Some of the differences may also result from the DICU model's limited ability to estimate agricultural return flows.

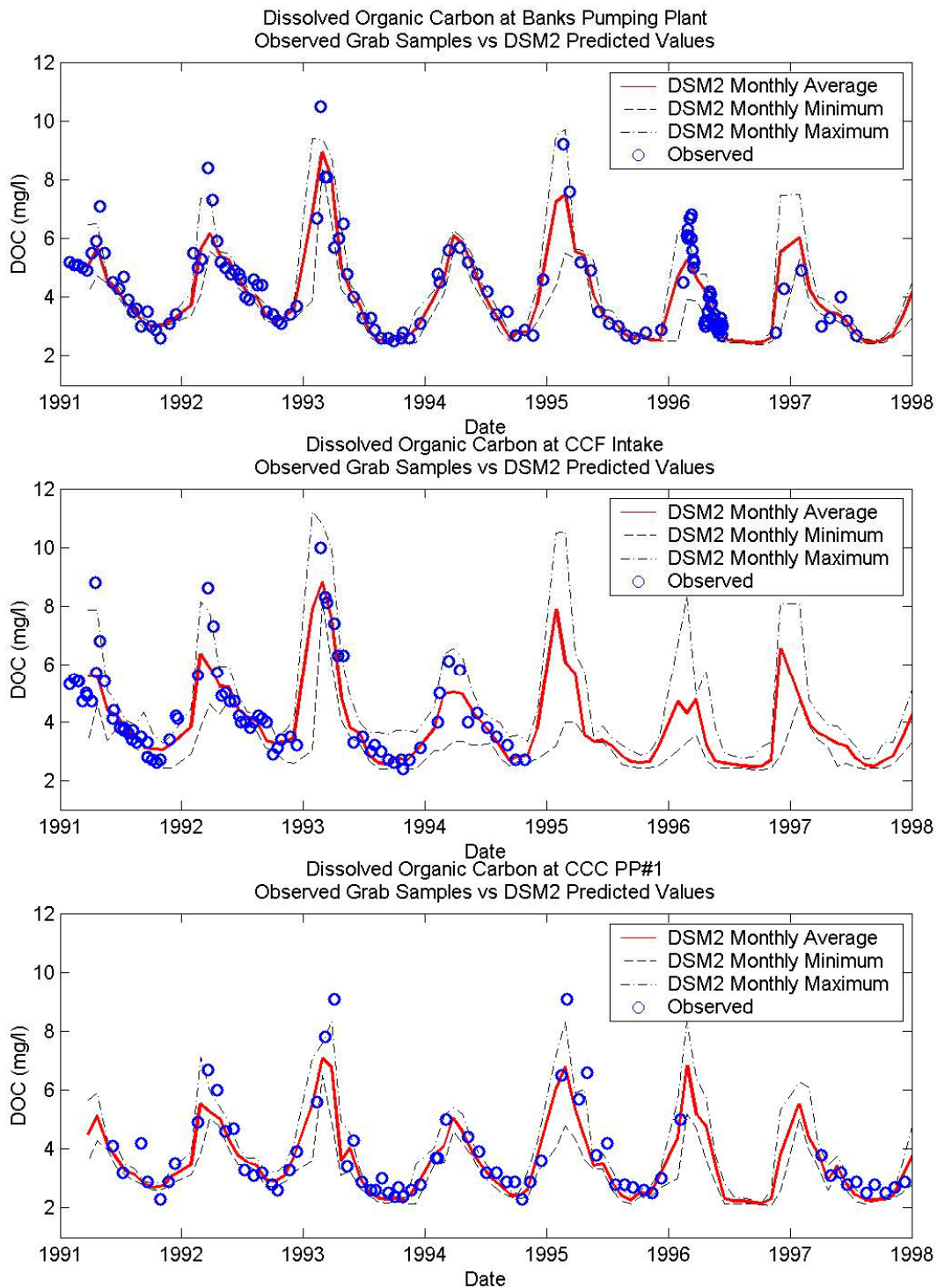


Figure 3-5: Dissolved Organic Carbon at Banks Pumping Plant, Clifton Court Forebay, and Contra Costa Pumping Plant #1.

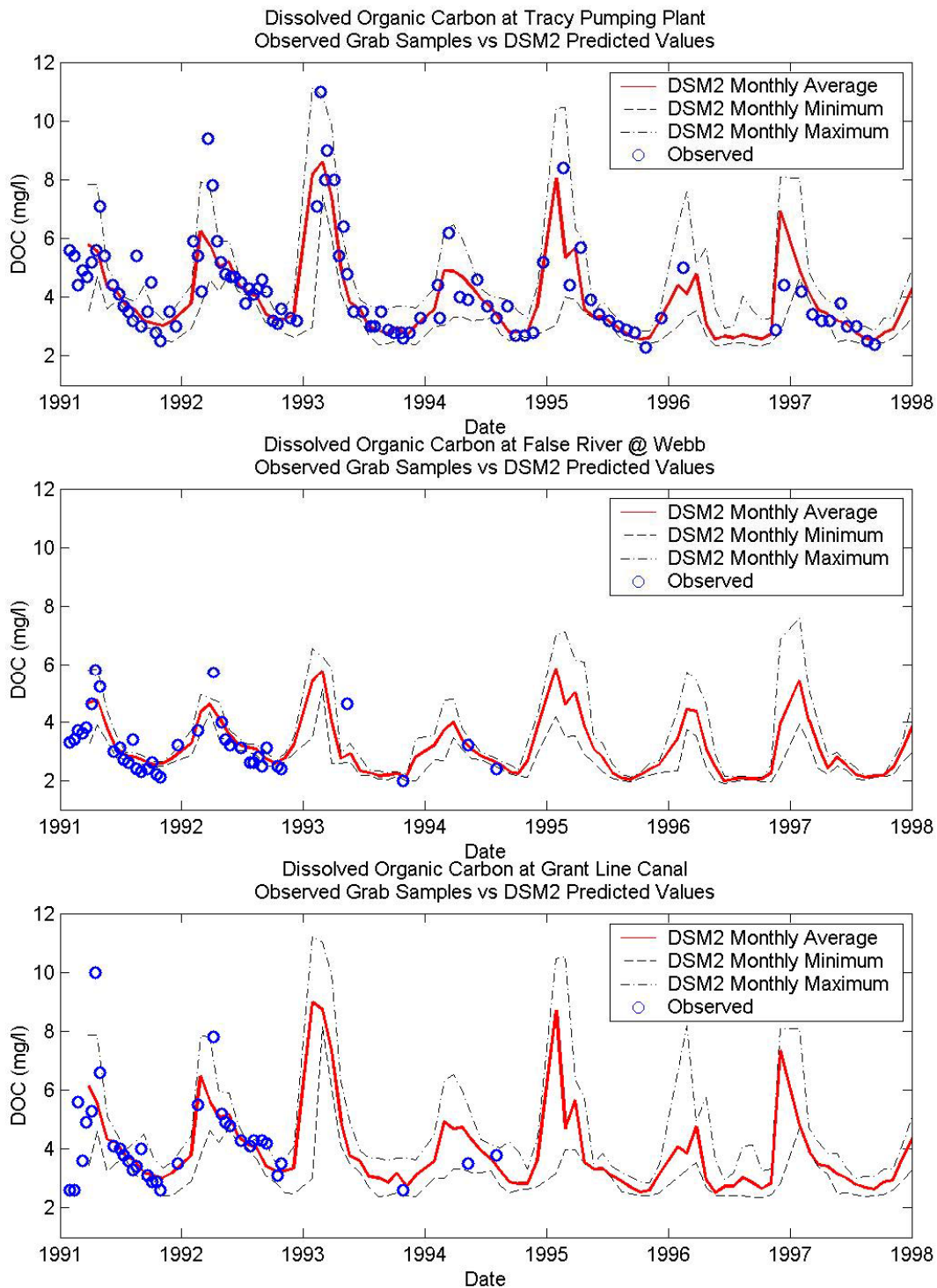


Figure 3-6: Dissolved Organic Carbon at Tracy Pumping Plant, False River at Webb Tract, and Grant Line Canal.

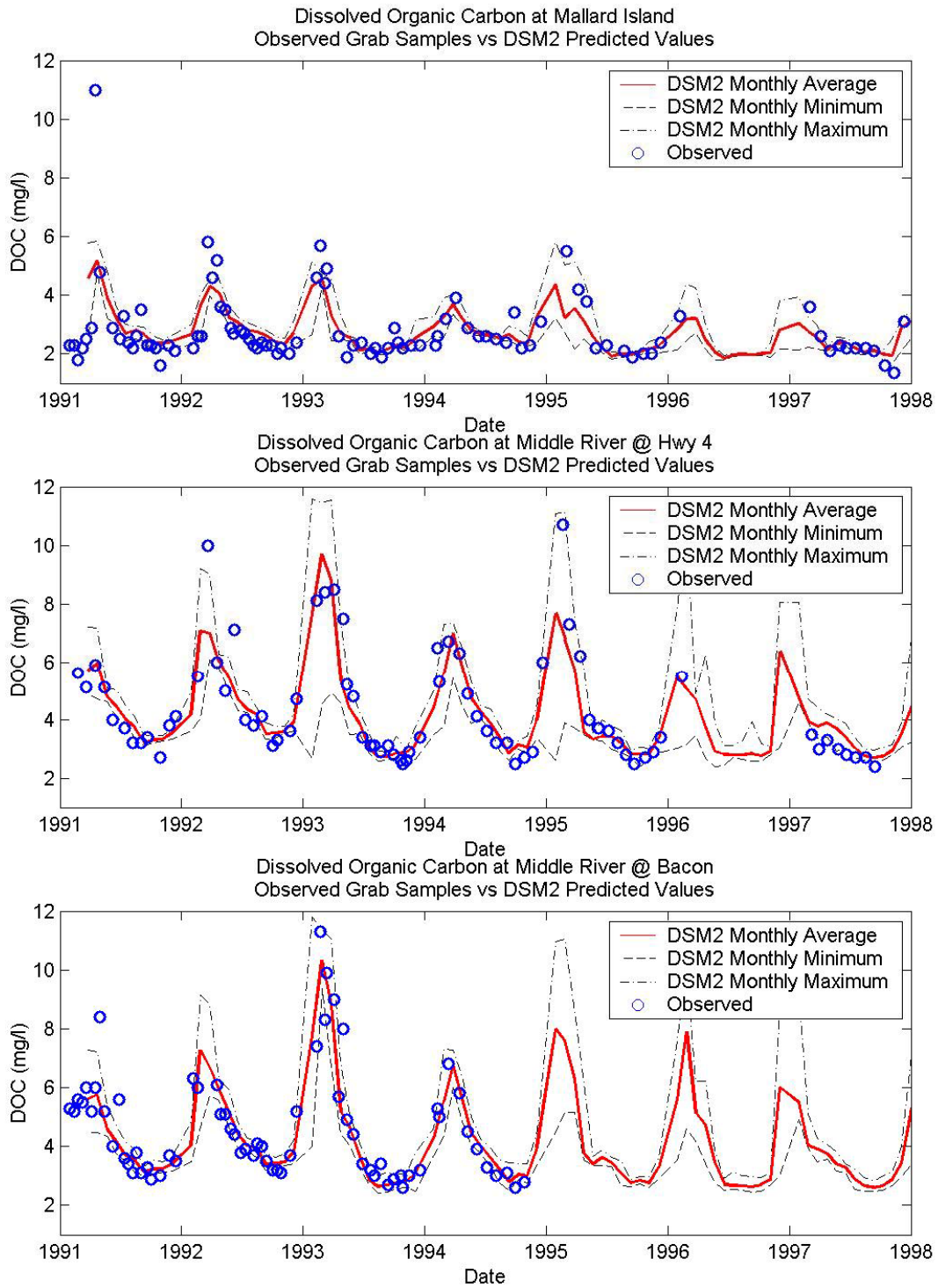


Figure 3-7: Dissolved Organic Carbon at Mallard Island, Middle River at Highway 4, and Middle River at Bacon Island.

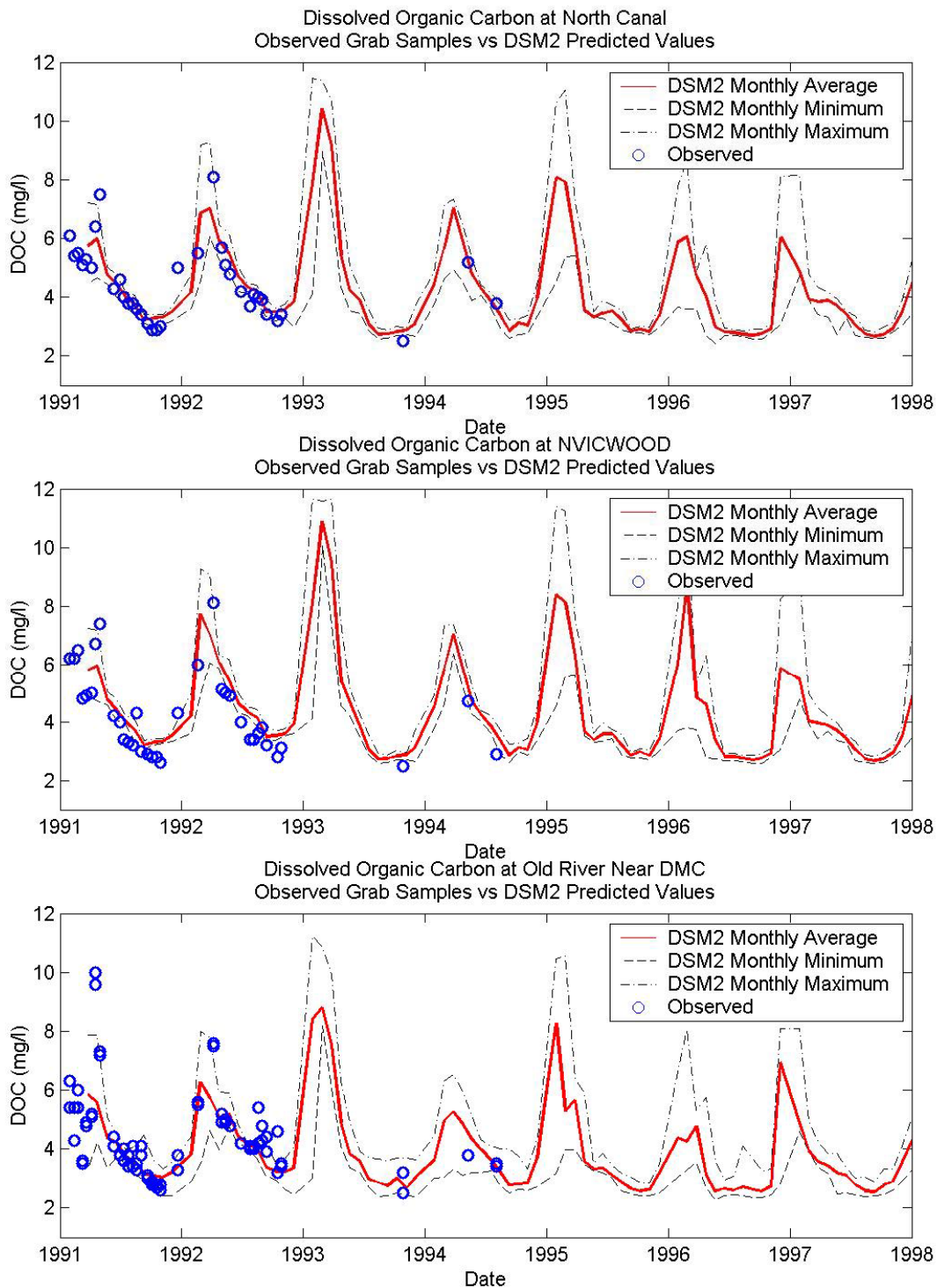


Figure 3-8: Dissolved Organic Carbon at North Canal, North Victoria Canal and Woodward Island, and Old River Near DMC.

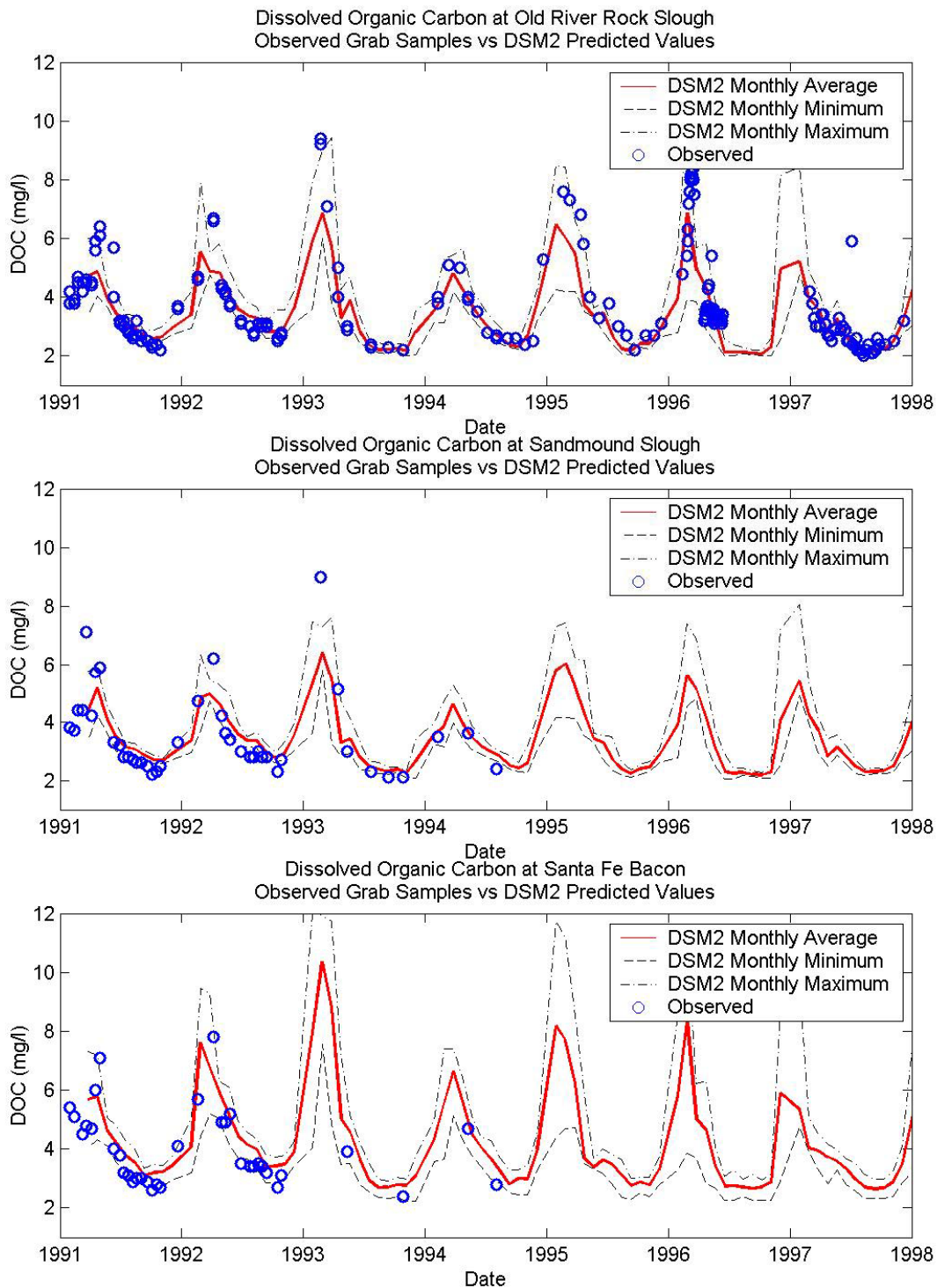


Figure 3-9: Dissolved Organic Carbon at Old River at Rock Slough, Sandmound Slough, and Santa Fe Railroad at Bacon Island.

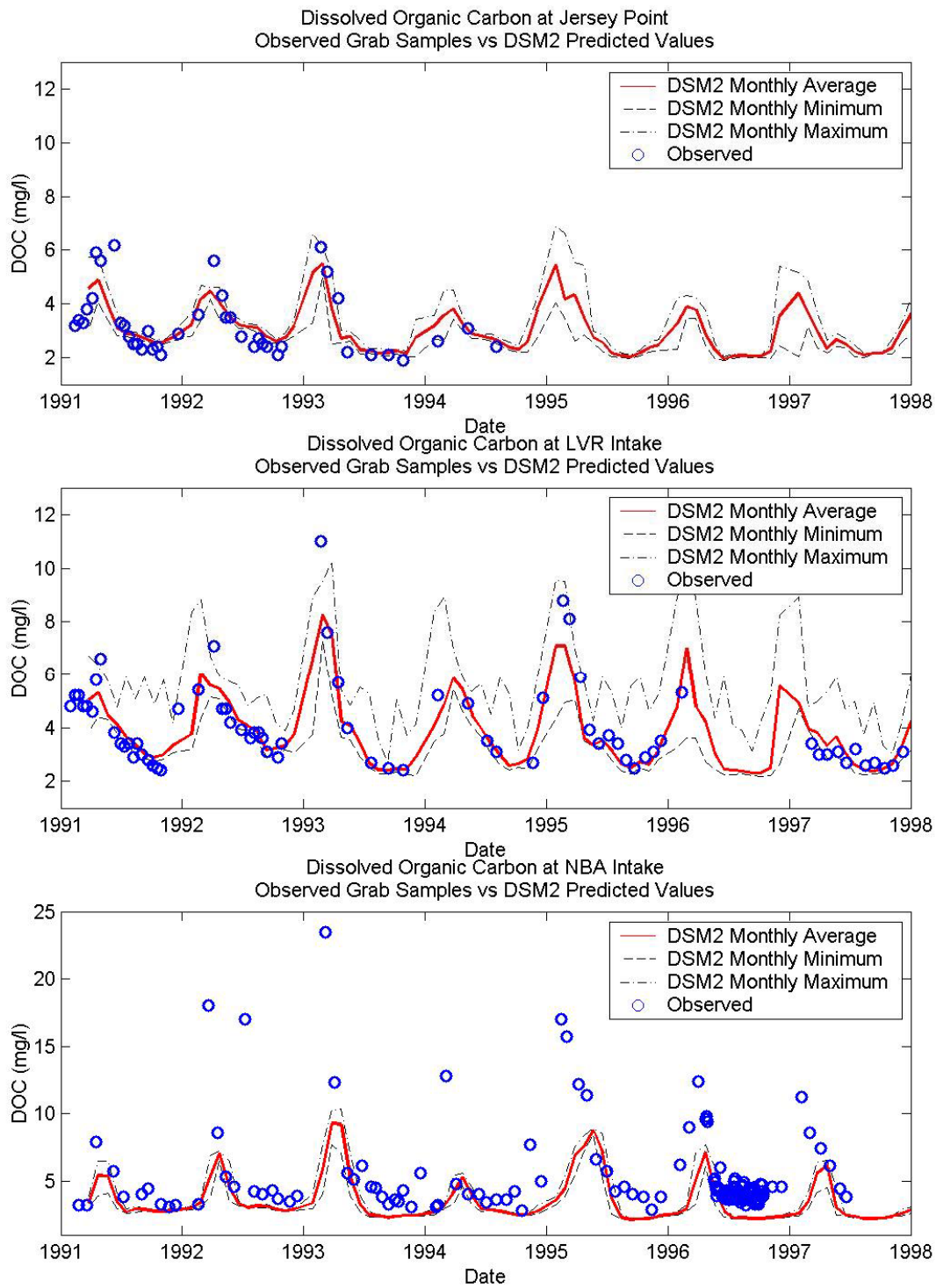


Figure 3-10: Dissolved Organic Carbon at Jersey Point, Los Vaqueros Reservoir Intake on Old River, and North Bay Aqueduct Intake.

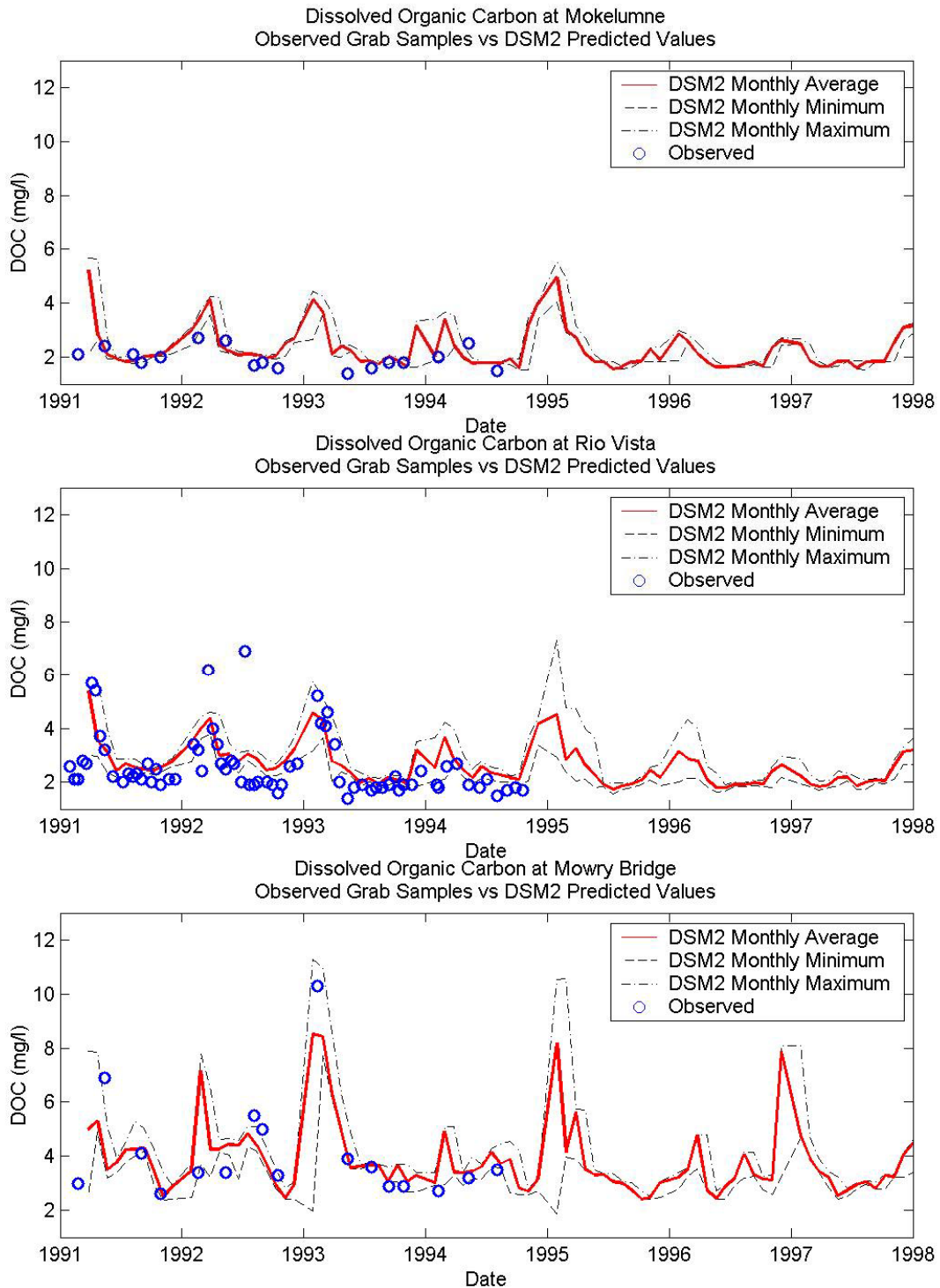


Figure 3-11: Dissolved Organic Carbon at the Mokelumne River, Rio Vista, and the Middle River at Mowry Bridge.

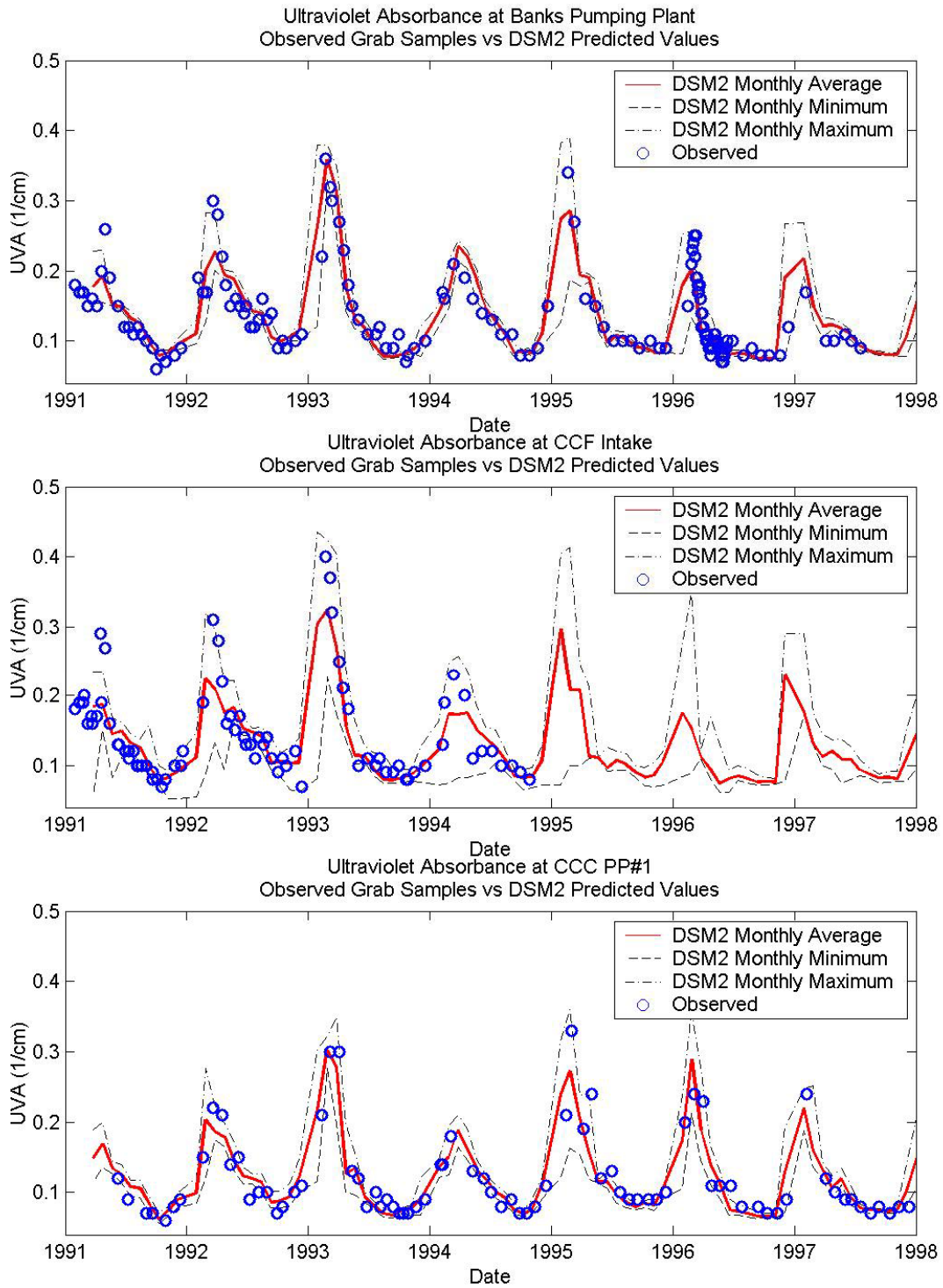


Figure 3-12: Ultraviolet Absorbance at Banks Pumping Plant, Clifton Court Forebay, and Contra Costa Pumping Plant #1.

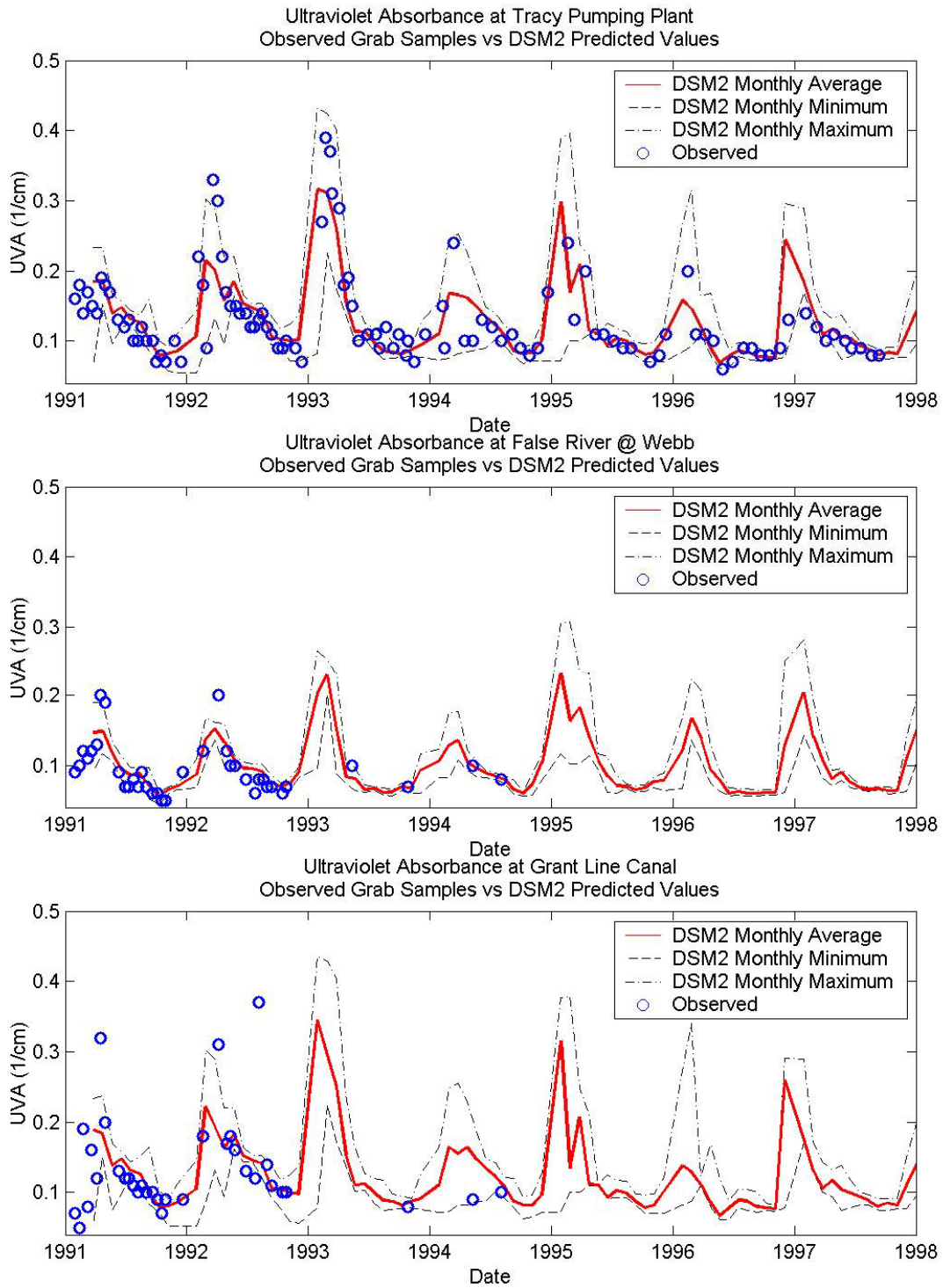


Figure 3-13: Ultraviolet Absorbance at Tracy Pumping Plant, False River at Webb Tract, and Grant Line Canal.

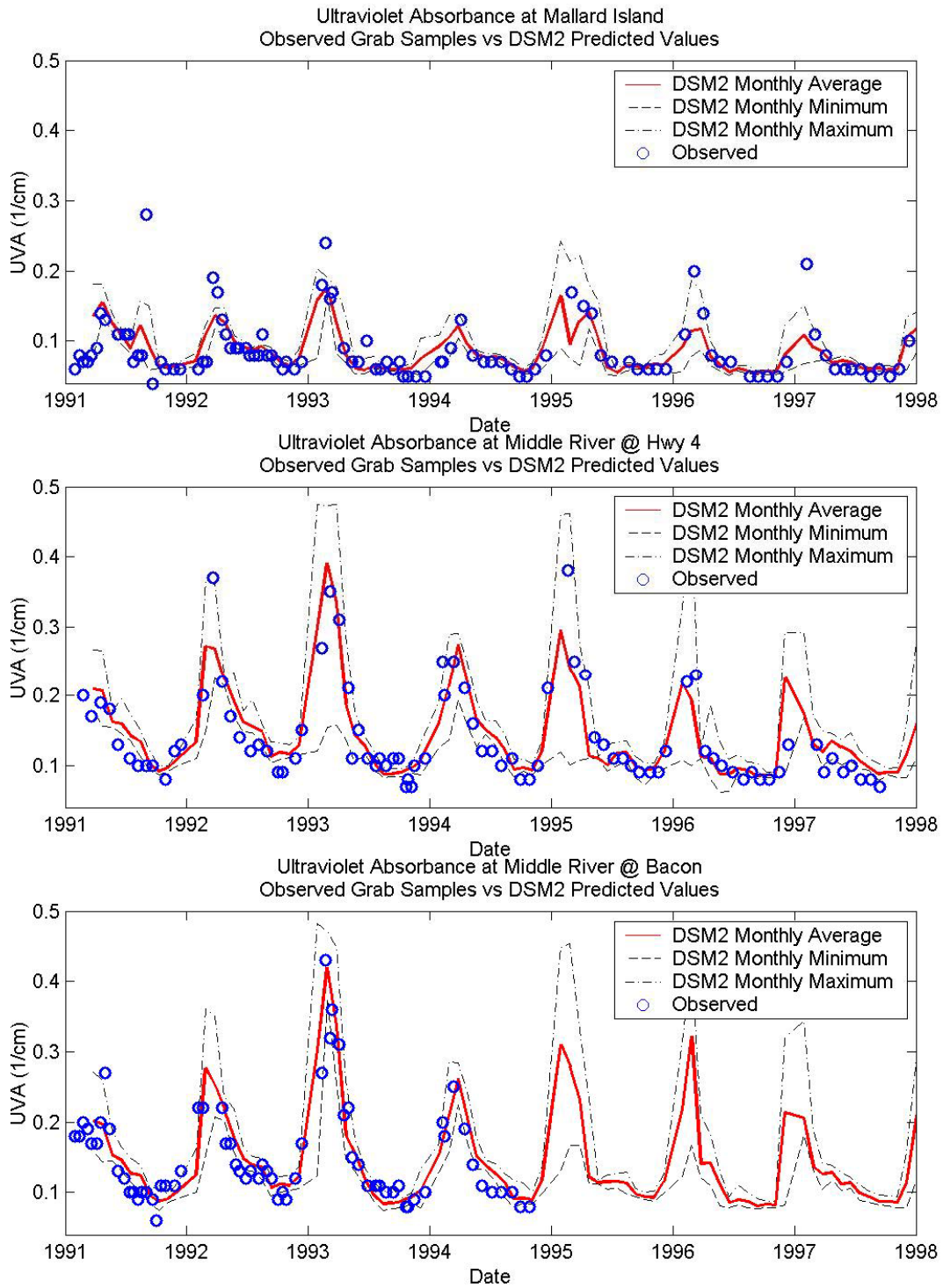


Figure 3-14: Ultraviolet Absorbance at Mallard Island, Middle River at Highway 4, and Middle River at Bacon Island.

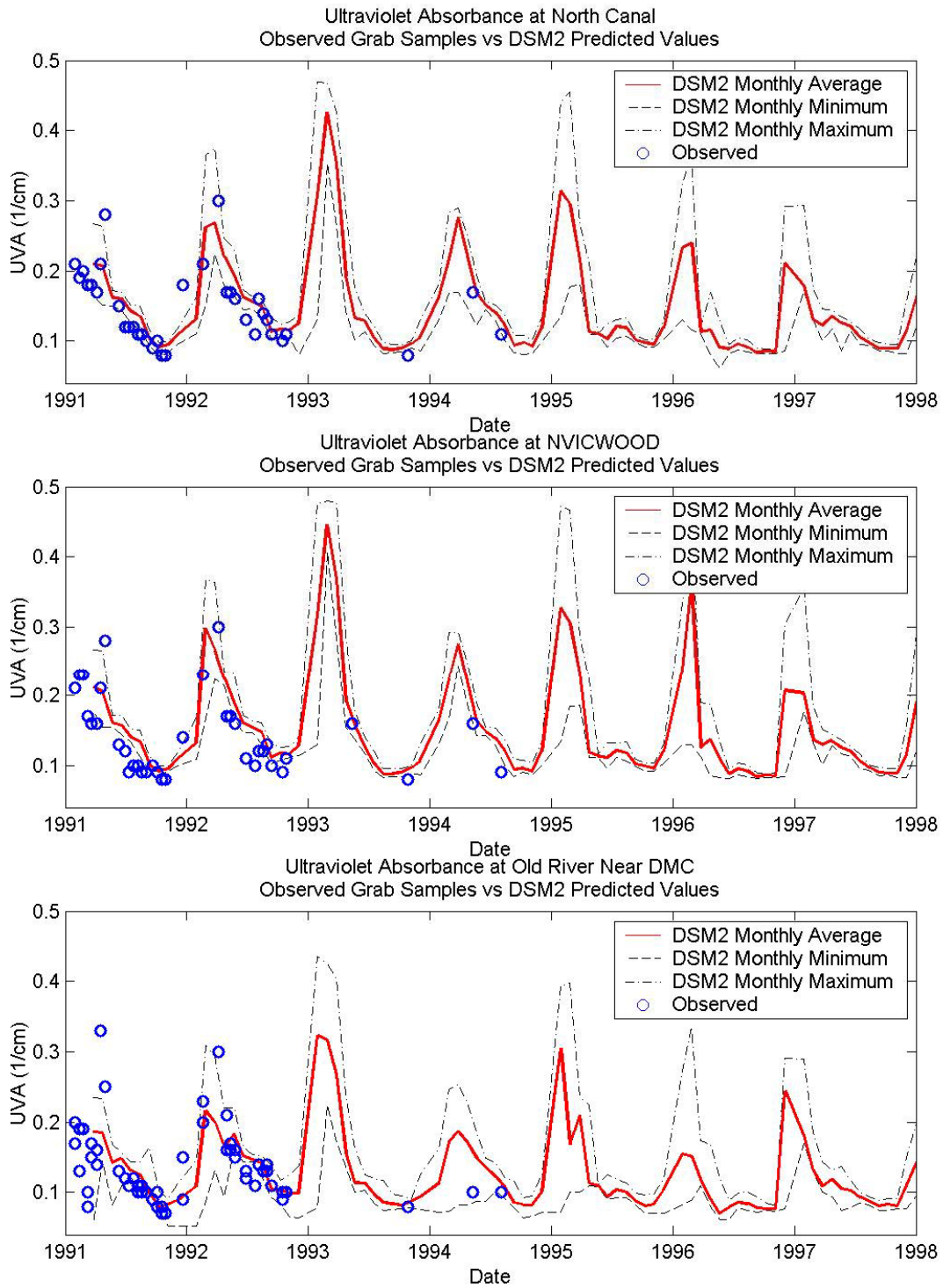


Figure 3-15: Ultraviolet Absorbance at North Canal, North Victoria Canal and Woodward Island, and Old River Near DMC.

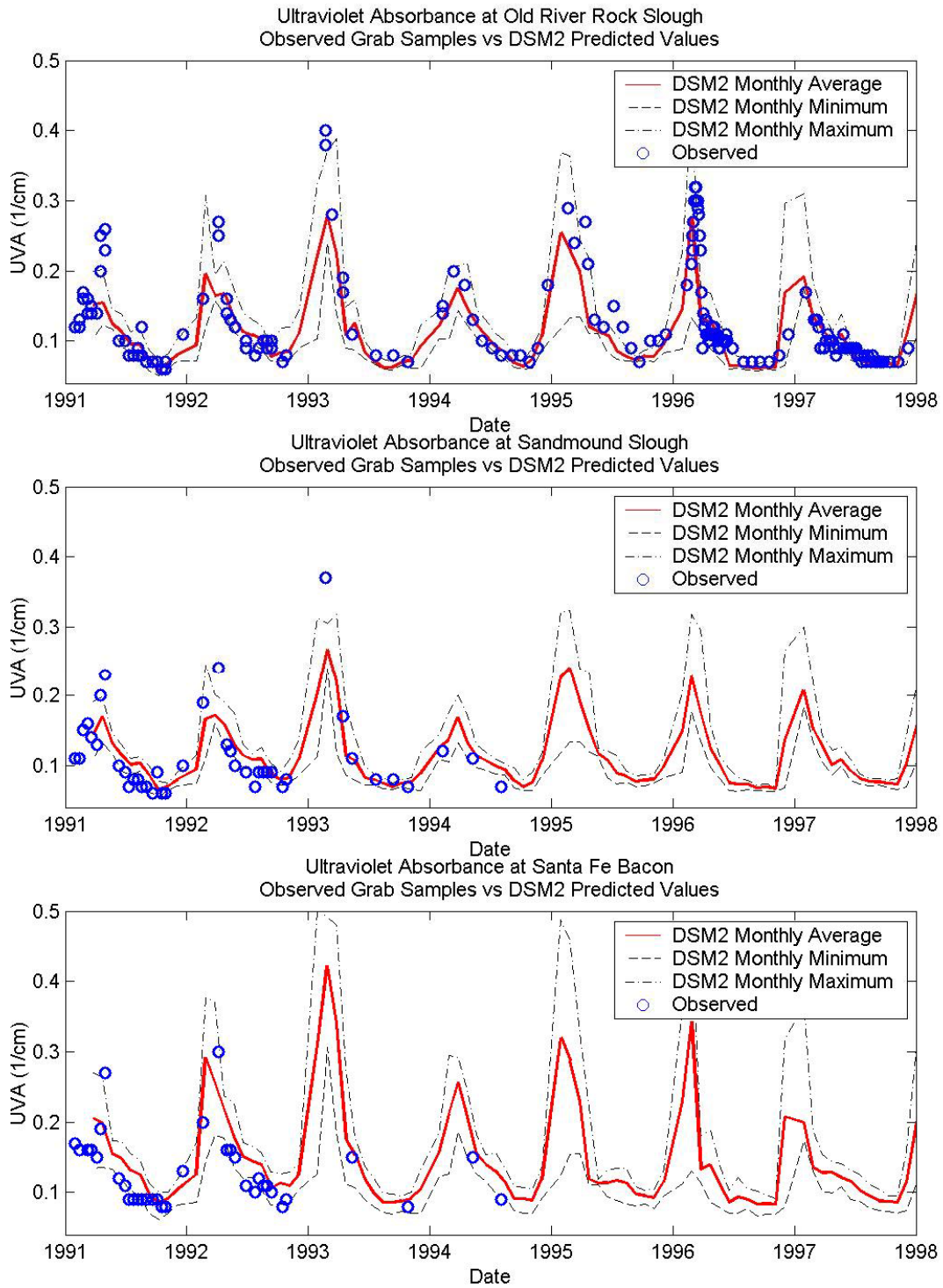


Figure 3-16: Ultraviolet Absorbance at Old River at Rock Slough, Sandmound Slough, and Santa Fe Railroad at Bacon Island.

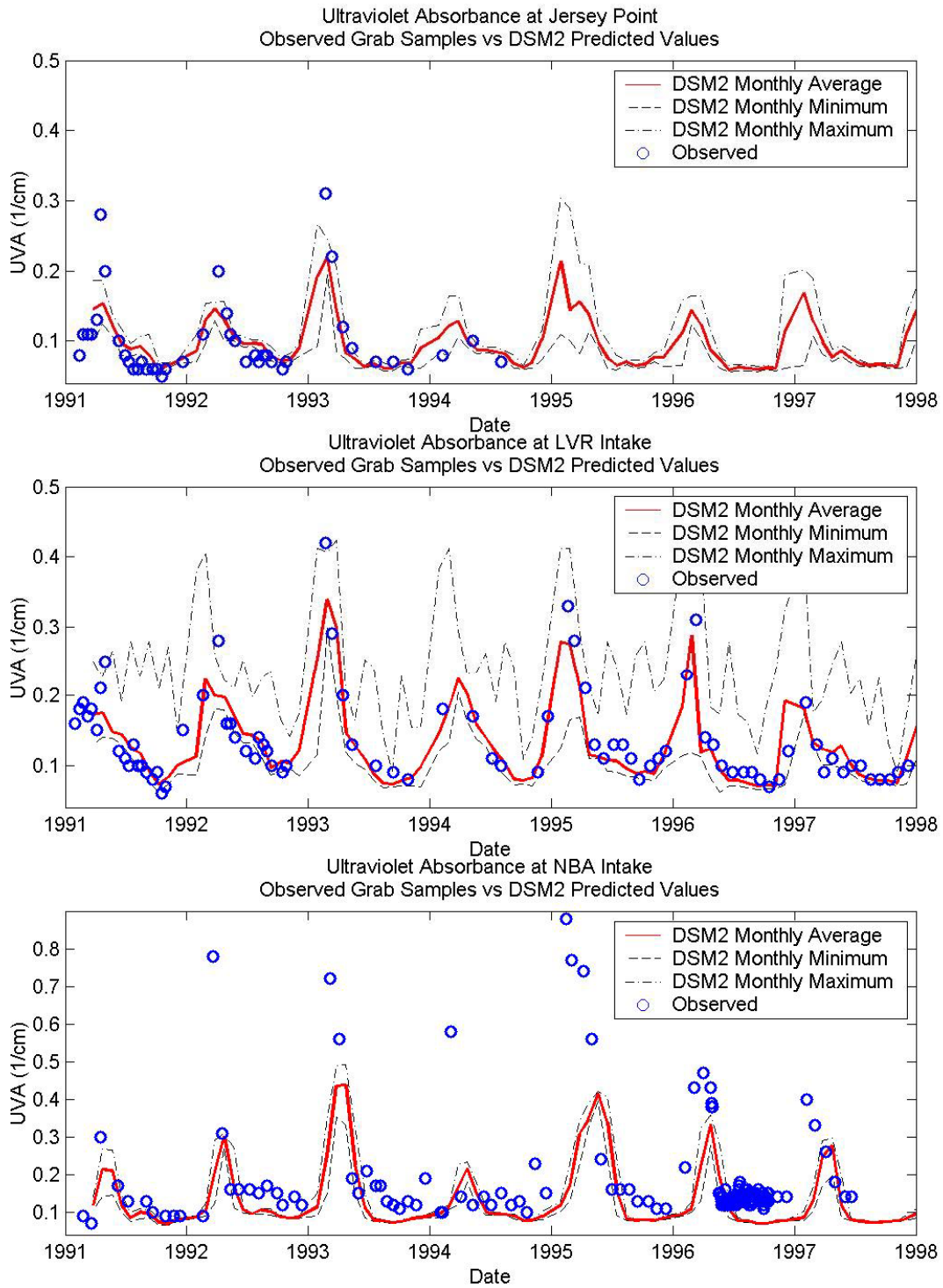


Figure 3-17: Ultraviolet Absorbance at Jersey Point, Los Vaqueros Reservoir Intake on Old River, and North Bay Aqueduct Intake.

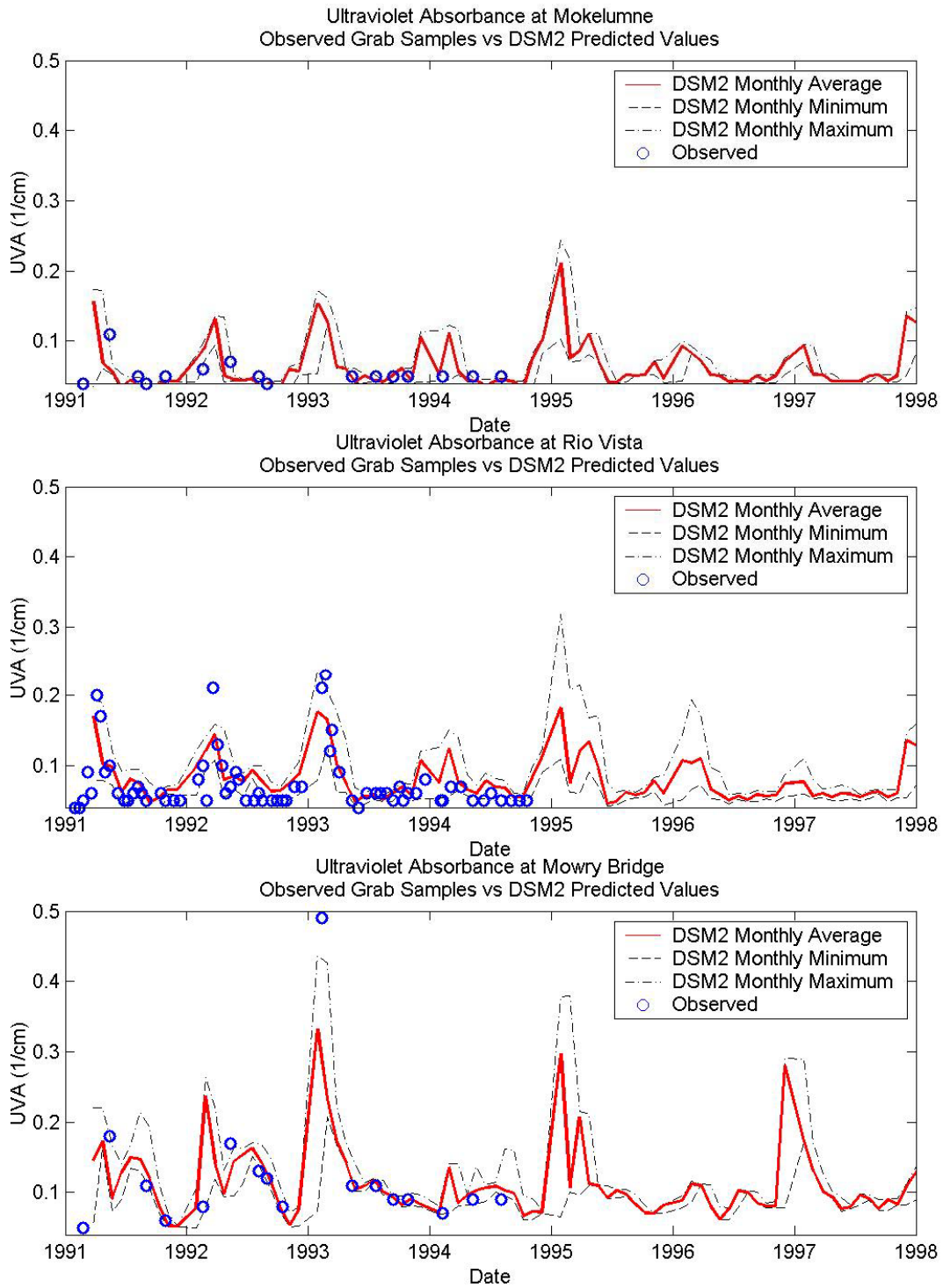


Figure 3-18: Ultraviolet Absorbance at the Mokelumne River, Rio Vista, and Middle River at Mowry Bridge.

3.4 Future Directions

- ❑ Model validation would likely be improved through a more refined specification of boundary conditions. Continuous monitoring of DOC and UVA at the Sacramento and San Joaquin river model boundaries may allow for these boundaries to be specified in daily time steps. Future DSM2 calibrations could also potentially improve results.
- ❑ Model validation would likely be improved through enhanced estimates of Delta island return flow and water quality. Assuming continued reliance on the DICU model to estimate return flows, compilation of historical land use during the simulation period would be a promising enhancement to the DSM2 validation.
- ❑ The sensitivity of model results to assumed boundary conditions should be explored. As a first step, a “fingerprint” analysis could be conducted to determine the relative impact of the Sacramento River, San Joaquin River, and agricultural return flows on urban intake water quality.
- ❑ Model results could be analyzed through statistical methods used by CALFED (Woodard 2000) to characterize Delta baseline water quality conditions, including frequency and seasonal analysis. Such an analysis should determine if the model provides a baseline characterization that is consistent with field observations.

3.5 References

- Agee, B. (2000). *Generation of Time Series Boundary Data for the Delta Simulation Model*. unpublished draft report, California Department of Water Resources, Division of Planning and Local Assistance. Sacramento, CA. April.
- California Department of Water Resources. (1995). *Representative Delta Island Return Flow Quality for DSM2*. Division of Planning. Sacramento, CA. May.
- Hutton, P.H. and F.I. Chung. (1992). “Simulating THM Formation Potential in the Sacramento Delta. Part II.” *Journal of Water Resources Planning and Management*. 118(5). American Society of Civil Engineers. pp. 530-42.
- Jung, Marvin. (2000). *Revision of Representative Delta Island Return Flow Quality for DSM2 and DICU Model Runs, Municipal Water Quality Investigation Program*. Prepared for the California Department of Water Resources – Division of Planning and Local Assistance, Sacramento, CA.
- Woodard, R. (2000). *Sources and Magnitudes of Water Quality Constituents of Concern in Drinking Water Supplies Taken From the Sacramento-San Joaquin Delta*. Prepared for the CALFED Bay-Delta Program, September.

Methodology for Flow and Salinity Estimates in the Sacramento-San Joaquin Delta and Suisun Marsh

**22nd Annual Progress Report
August 2001**

Chapter 4: Validation of Dispersion Using the Particle Tracking Model in the Sacramento-San Joaquin Delta

Author: Ryan Wilbur

4 Validation of Dispersion Using the Particle Tracking Model in the Sacramento-San Joaquin Delta

[Editor's Note: The following report is a condensed version of Ryan Wilbur's M.S. Thesis (2000). It has been reformatted to be consistent with this progress report. A complete copy of his thesis is on file with University of California, Davis. This validation did not use the DSM2 geometry that was discussed in Chapter 2 because the calibration was not yet finished.]

4.1 Introduction

The Particle Tracking Model (PTM) was developed by DWR's Delta Modeling Section. The purpose of the model is to simulate the transport and fate of individual, neutrally buoyant "particles" through the Sacramento – San Joaquin Delta.

The PTM model is a component of the Delta Modeling Section's DSM2. DSM2 simulates the hydrodynamic, water quality, and particle movement throughout the Sacramento – San Joaquin Delta in three models: HYDRO, QUAL, and PTM, respectively. Figure 4-1 shows the location of major cities on a schematic for the Delta region. Figure 4-2 shows significant inflows and outflows in the Delta. The Delta is the confluence of the Sacramento River, San Joaquin River, East Side Tributaries, and the open water of San Francisco Bay. The western boundary condition used by DSM2 is the stage at Martinez. The tidal motion influences the entire Delta. Flow reverses direction due to the tidal motion throughout most of the Delta.

The PTM model uses the hydrodynamics determined by HYDRO to extrapolate the average velocity in a channel to a pseudo 3-dimensional velocity cross-section. Assumed velocity profiles are used for this extrapolation. The velocity profiles assume the zero slip condition at the bottom and sides of the channel; while the fastest areas are the center of the transverse profile and the top of the water column. The selection of velocity profiles is equivalent to setting the longitudinal dispersion coefficient. In addition, movement due to mixing (in the transverse and vertical) is superimposed on the advective motion. Data collected by USGS are used to guide the selection of the velocity profiles. These new profiles are then compared to a tracer study to determine if the accuracy of the PTM is improved.

The PTM was originally developed in 1992 by Gilbert Bogle, a consultant working for Water Engineering and Modeling. Several modifications have been made by DWR and Bogle to this model to account for such particular phenomena as tidal effects and channel branches. The model was rewritten by Nicky Sandhu of DWR in Java and C++ to take advantage of object-oriented programming. Input-output was also updated to be consistent with the DSM2 model. Calibration of the advective characteristics was performed by Tara Smith of DWR. A limited investigation of dispersive characteristics of the Delta was performed by Bogle, but a full

calibration was not completed. The goal of this study: is to calibrate the dispersive characteristics of HYDRO-PTM.

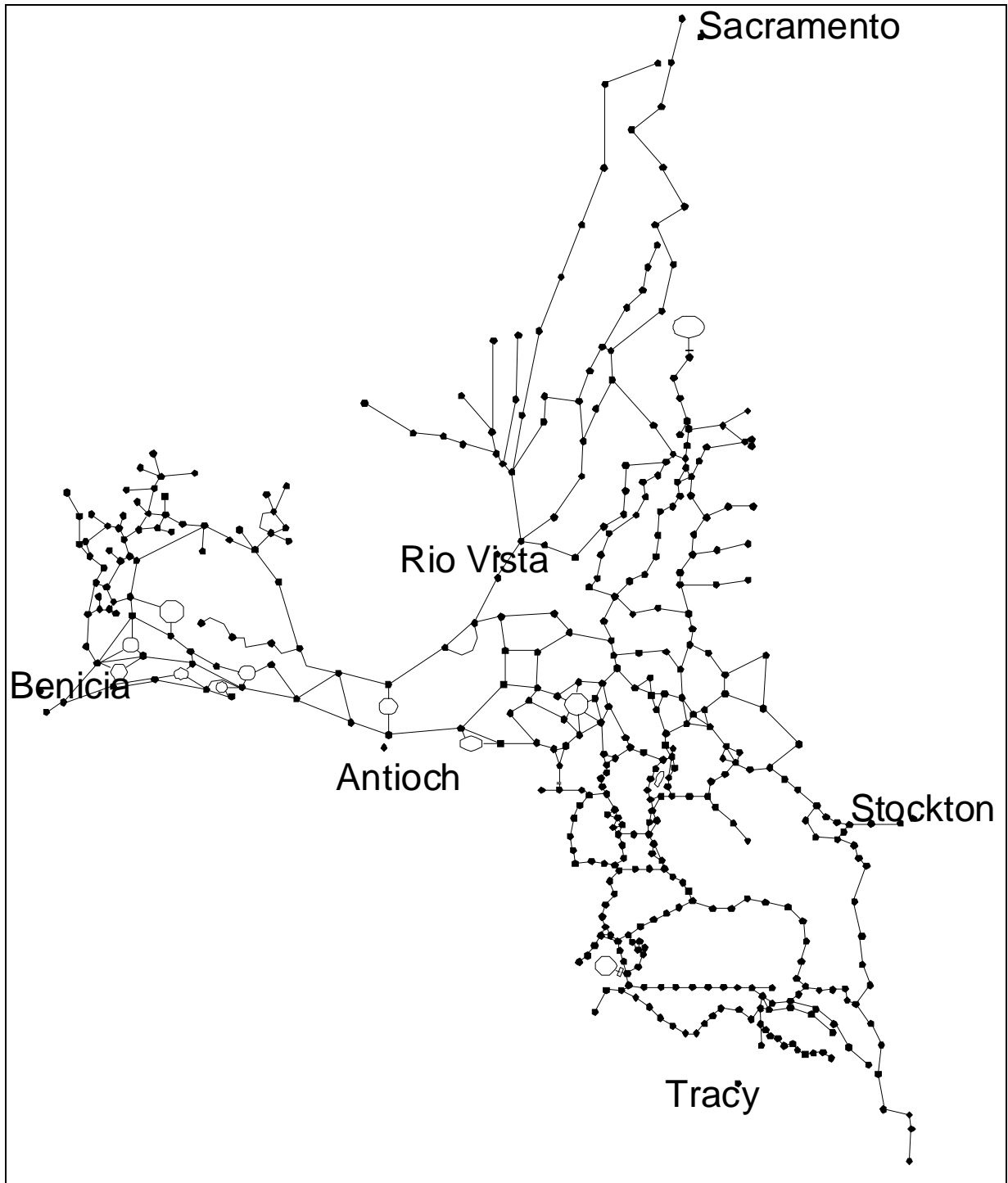


Figure 4-1: DSM2 Schematic of the Sacramento – San Joaquin Delta.

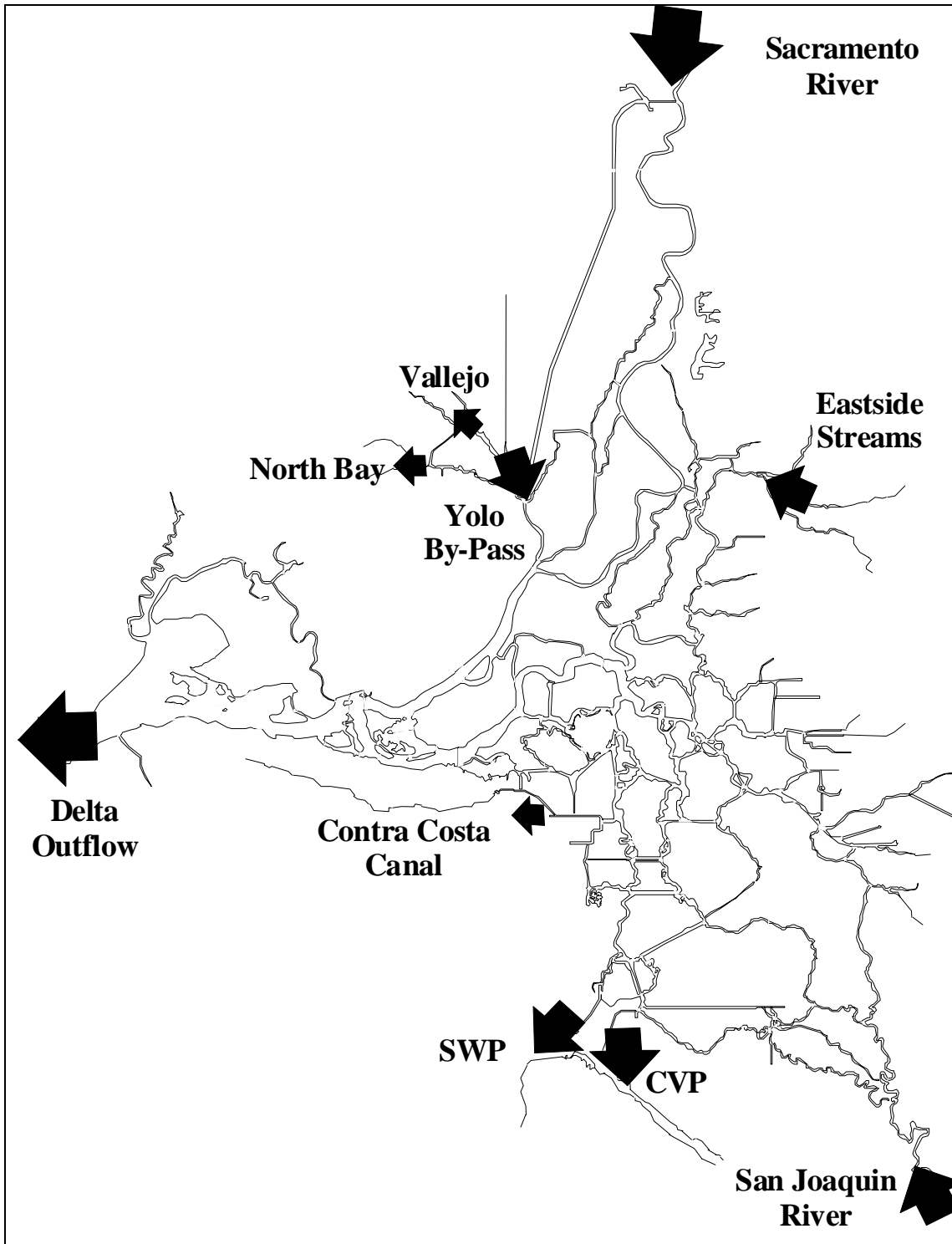


Figure 4-2: Major Sacramento – San Joaquin Delta Boundary Flows.

4.2 PTM Model

4.2.1 PTM Introduction

The DSM2 is the simulation model used by DWR's Delta Modeling Section. There are three components: HYDRO, QUAL, and PTM. HYDRO is a 1-dimensional, unsteady hydrodynamic model. HYDRO originated from the FourPt model developed by Lew Delong of USGS (DeLong 1995). It is a fully implicit unsteady flow model and is based on the 1-dimensional Saint Venant equations:

$$\frac{d}{dt}(\rho M_a A) + \frac{d}{dx}(\rho Q) - \rho_q q = 0 \quad [\text{Eqn. 4-1}]$$

$$\frac{d}{dt}(\rho M_q Q) + \frac{d}{dx} \left(\beta \rho \frac{Q^2}{A} + \rho g I_1 \right) + \rho g A (s_o + s_f) - \rho g I_2 = 0 \quad [\text{Eqn. 4-2}]$$

where t is time, ρ is density, A is a cross-sectional area, M_a is the area-weighted sinuosity coefficient, x is downstream distance, Q is the flow rate, q is the lateral inflow, ρ_q is the density of the lateral inflow, M_q is the flow-weighted sinuosity coefficient, β is the momentum coefficient, g is gravity, s_o is the channel bottom slope, s_f is the friction slope, and I_1 and I_2 are integrals for averaging the depth over the cross-section.

FourPt has been adapted for accommodating simulations in the Delta. These changes provide for inclusion of reservoirs, gates, and an entirely different input system. DSM2-HYDRO Version 6.1 and DSM2-PTM Version 1.10 were used for this thesis. Output from the HYDRO component is used by the other two modules for determination of the velocity and stage conditions throughout the Delta. Thus, the water quality parameters determined by QUAL and the particle movement from PTM do not affect the hydrodynamics of the Delta system. The schematic representation of the Delta is represented in Figures 4-1 and 4-2. This representation of the Delta is modeled as a network of channel segments and open water areas. The HYDRO setup currently used is being updated by the Delta Modeling Section. This new calibrated Delta setup will improve on the current one with new geometric information. This is not available for implementation in this study due to time restraints. *[Editor's Note: Since the time of original writing, the Delta Modeling Section has adopted a new DSM2 geometry as was discussed in Chapter 2.]*

4.2.2 PTM Theory

The PTM simulates the movement of particles in a channel by imposing a velocity field and random mixing across the channel. The mean channel velocity is found by the DSM2-HYDRO model. The dispersive characteristics are determined by PTM. Velocity profiles are used to extrapolate the calculated 1-dimensional velocity into a more realistic representation of velocity. This simulation of shear flow dispersion, along with random mixing coefficients, simulates the particle movements.

4.2.3 Longitudinal Dispersion

Longitudinal dispersion in the PTM is simulated by extrapolating the mean channel velocity from DSM2-HYDRO into a pseudo 3-dimensional velocity cross-section. This representation allows the simulation of shear flow dispersion in which a particle traveling in the center of the channel (or the top of the water column) will be subjected to a higher velocity than if it were at the sides of the channel (or at the bottom of the water column). This formulation does not directly use a longitudinal dispersion coefficient typically found in the literature. Instead, this is represented in the PTM as the standard deviation or variance of the distance of all the particles from the center of mass of the particles.

The transverse velocity profile is represented by a fourth order polynomial of the form developed by Bogle (1997):

$$F_T = A + B\left(\frac{2y}{W}\right)^2 + C\left(\frac{2y}{W}\right)^4 \quad [\text{Eqn. 4-3}]$$

where A, B, and C are constants, y is the depth of water, and w is the width of the rectangular channel. The three constants must be restricted such that the velocity at the sides of the channel is zero and to maintain a constant mean velocity. This is accomplished by satisfying the two equations:

$$A + B + C = 0 \quad [\text{Eqn. 4-4}]$$

$$A + \frac{B}{3} + \frac{C}{5} = 1 \quad [\text{Eqn. 4-5}]$$

When one constant value is selected, the other two are determined through solution of these two equations. Thus, selection of one constant determines the value of the others. Figure 4-3 shows the transverse velocity profile with various coefficients determined by A. The current transverse profile used by PTM is A = 1.62, B = -2.22, C = 0.6. Selection of this profile was achieved by matching the dispersion generated by these profiles to the dispersion predicted by the longitudinal dispersion coefficient equation, as is shown below in Equation 4-6 (Wilbur 2000). Higher A values yield stronger peak velocity, while lower A values yield a flatter profile.

$$K = \frac{0.11\bar{u}W^2}{d} \quad [\text{Eqn. 4-6}]$$

where W is width, d is depth, and \bar{u} is average velocity. Inclusion of the uncertainty over the transverse mixing coefficient results in a range of coefficient values of 0.06 and 0.229.

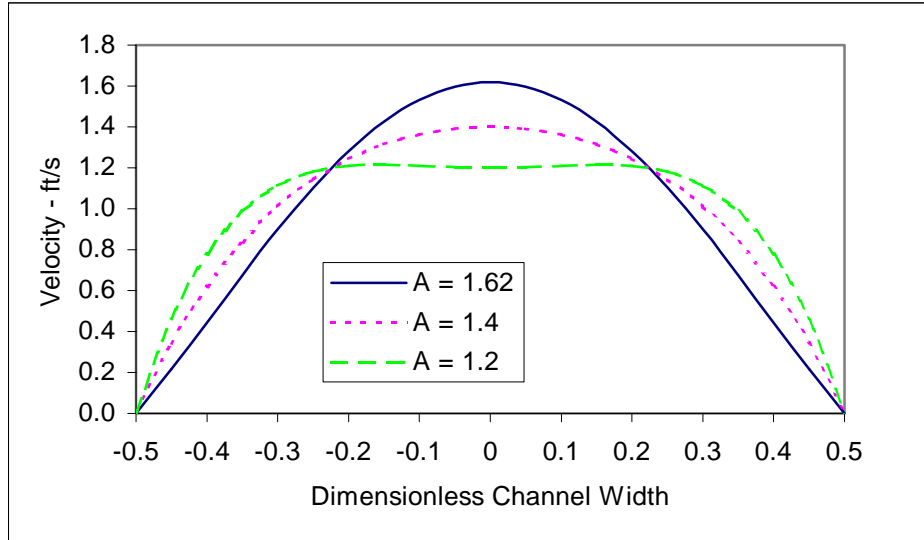


Figure 4-3: Transverse Velocity Profiles.

The vertical velocity profile is represented as the von Karman logarithmic equation:

$$F_v = 1 + \frac{0.1}{k} \left[1 + \log \left(\frac{z}{d} \right) \right] \quad [\text{Eqn. 4-7}]$$

where k is the von Karman constant, z is vertical position in the water column, and d is the depth of water. Inclusion of a shape factor s , multiplying the von Karman constant, allows the modification of the shear induced by the velocity profile:

$$F_v = 1 + \frac{0.1}{s k} \left[1 + \log \left(\frac{z}{d} \right) \right] \quad [\text{Eqn. 4-8}]$$

Changing the shape factor yields different peak velocities. Figure 4-4 shows various vertical velocity profiles with different shape factors. The current PTM model uses an s of 1.0. Increasing this constant reduces peak velocity.

One set of velocity profile coefficients is used for the entire Delta. The set does not change with time or location. The transverse and vertical velocity profiles are scaled by the mean velocity in each channel. This results in the velocity at any point in the channel cross-section represented in Equation 4-9:

$$V(y,z) = \underline{u} F_T F_V \quad [\text{Eqn. 4-9}]$$

Here, V is the velocity at any point in the cross section and \underline{u} is the mean velocity simulated by HYDRO. The profiles used in the initial model development were selected purely on a theoretical basis. The coefficients will be selected based on data presented later.

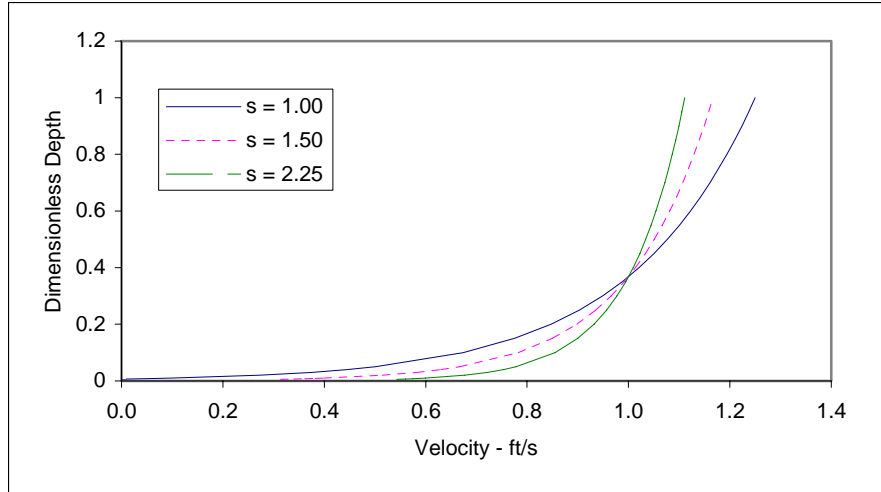


Figure 4-4: Vertical Velocity Profiles.

Comparison of the effective dispersion generated by selection of the velocity profiles to the theoretical longitudinal dispersion predicted by Equation 4-6 is performed by determining the simulated longitudinal dispersion. The variance of the longitudinal displacement of particles is found by:

$$\sigma^2 = \frac{1}{N} \left[\sum x_i^2 - \frac{(\sum x_i)^2}{N} \right] \quad [\text{Eqn. 4-10}]$$

Here, σ^2 is the variance, N is the number of particles, and x_i is the longitudinal location of particle i . The effective longitudinal dispersion is then found by:

$$K(t) = \frac{\sigma^2(t) - \sigma^2(t - dt)}{2 dt} \quad [\text{Eqn. 4-11}]$$

PTM determines the position of each simulated particle as the longitudinal distance from the beginning of each channel, the vertical distance from the bottom of the channel, and the transversal distance from the centerline of the channel. The output may be modified to allow the results to be compared to concentrations of dissolved substances, such as data from a tracer study. The number of particles in a channel segment is scaled by the volume of water in that segment. This may be represented as:

$$C = f \frac{(\# \text{ of particles})}{AL} \quad [\text{Eqn. 4-12}]$$

where A is the cross-sectional area, L is the length of the channel segment, and f is a scaling factor used to adjust to appropriate magnitude. The area changes with time as the stage and flow oscillate due to the hydrodynamics of the Delta.

4.3 Data

Two sets of data collected by USGS are used for this calibration study. These consist of channel cross-sectional velocity profiles and tracer (rhodamine WT) data.

4.3.1 ADCP

Acoustic Doppler Current Profiler (ADCP) data are used to measure the flow and velocity in the cross-section of a channel. The ADCP instrument is an advanced acoustic device that sends signals into the water column. These signals reflect off particles moving with the water and return to the instrument. The ADCP measures the change in frequency in the signal and determines particle velocity. The ADCP divides the depth of water into a series of vertical bins and returns each bin's average velocity. The depth of each bin is approximately 0.3 meters. A series of these depth readings is made as the boat carrying the ADCP travels across the channel. The speed of the boat is removed from the velocity by using "bottom tracking." This results in a cross-sectional view of the velocity field (RD Instruments 1996).

ADCP data were collected at 16 sites in the Delta over a period of 3 years starting in 1997. The typical collection pattern consists of between two and seven hours of cross-section transverses at one location. This enables the collection of data to include a portion of the tidal motion. One transverse takes between five and 15 minutes, depending on width of cross-section. Table 4-1 lists the locations and dates of this data.

Table 4-1: Location and Dates of Collected ADCP Data

Location	1997			1999					
	April	May	June	March	April	May	June	July	August
Connection Slough					x	x	x	x	
Dutch Slough below Jersey Island Road @ Jersey Point									x
False River					x	x	x	x	
Grantline Canal @ Tracy Road	x	x	x			x	x	x	
Middle River @ Middle River									x
Middle River South of Columbia Cut	x	x	x		x	x	x	x	
Old River @ Bacon Island									x
Old River @ Clifton Court Ferry	x	x	x						
Old River Near Webb Tract						x	x		
Sacramento River above Delta Cross Channel									x
San Joaquin River @ Jersey Point									x
San Joaquin River bet. Columbia & Turner Cuts	x	x	x						
San Joaquin River below Garwood Bridge @ Stockton				x					
Threemile Slough @ San Joaquin River						x			
Turner Cut	x	x	x		x	x			
Victoria Canal	x	x	x						

Figures 4-5 and 4-6 show the measured data for Turner Cut. Figure 4-6 shows the transverse and vertical velocity profiles measured on April 9, 1997 at 1:30 p.m. Figure 4-5 shows the tidal influence on the flow at this location. Averaging the velocity profile data allows the irregular data (due to turbulence) to be smoothed, as Figure 4-6 shows. The averaging was done as a running mean of 5 to 15 data points. The general trend of the velocity profiles does correlate with the vertical and transverse profiles assumed in the PTM model. Comparisons with the PTM profiles are presented in a later section.

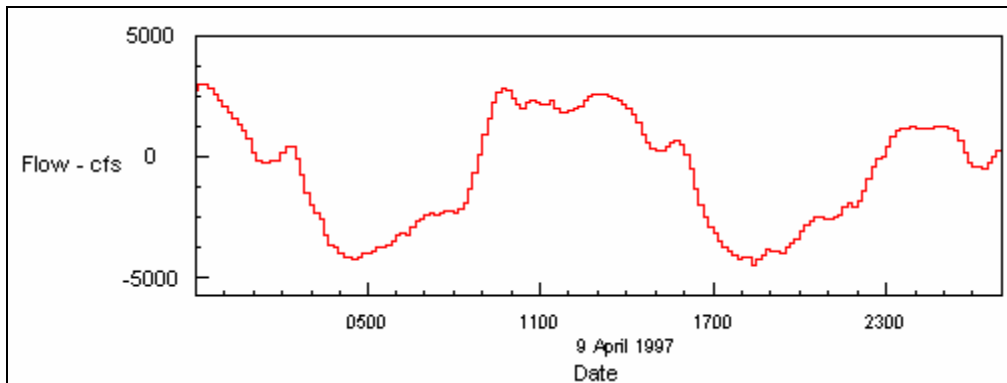


Figure 4-5: Historical Flow at Turner Cut.

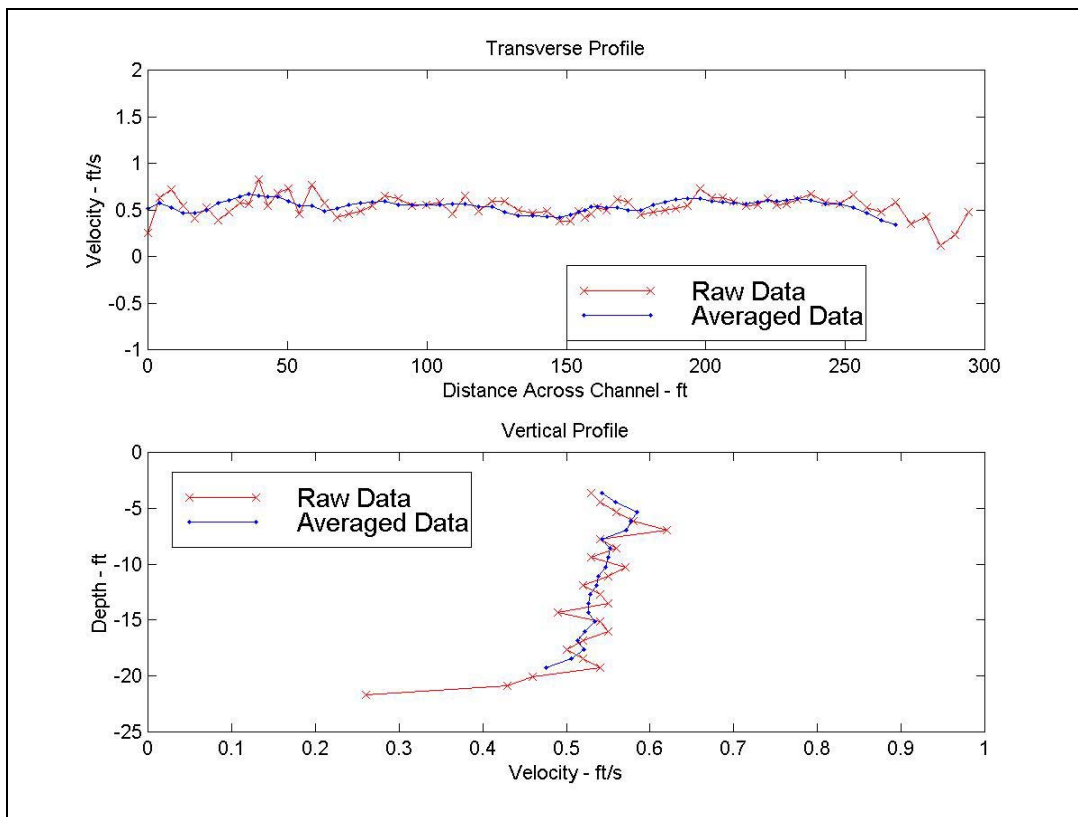


Figure 4-6: Turner Cut ADCP Profile Data (1:30 p.m., April 9, 1997).

Similar characteristics are found at the San Joaquin River between Columbia and Turner Cuts. Figures 4-7 and 4-8 show the flow and ADCP velocity profile data on April 4, 1997 at 10:30am.

Additional locations showing cross-sectional velocity magnitudes are shown in Wilbur (2000) for different stages in the tidal sequence. The stage data corresponding with these times are also provided. Inspection of these figures shows a great deal of heterogeneity in the channel cross-section and velocity magnitudes.

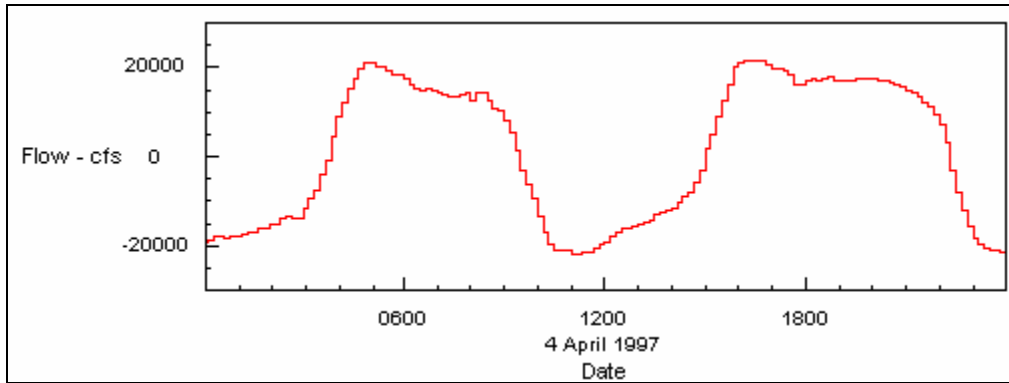


Figure 4-7: Historical Flow of SJR between Turner and Columbia Cuts.

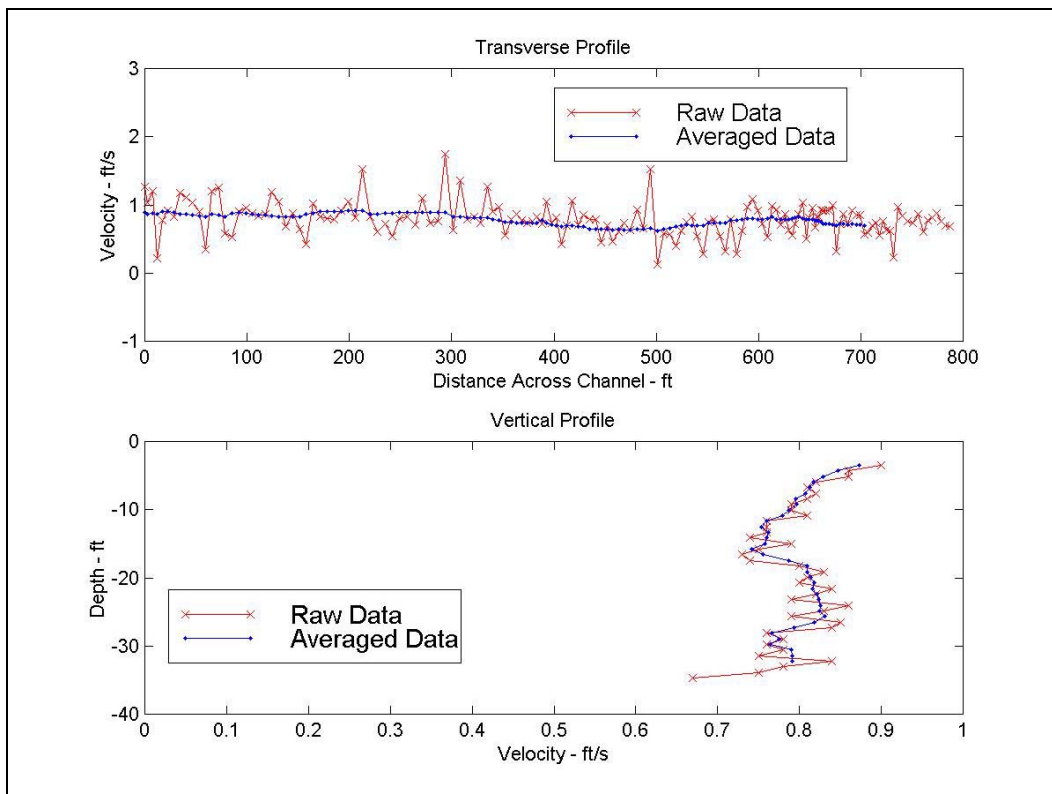


Figure 4-8: SJR between Turner and Columbia Cuts ADCP Profile Data (10:30 p.m., April 4, 1997).

4.3.2 Tracer

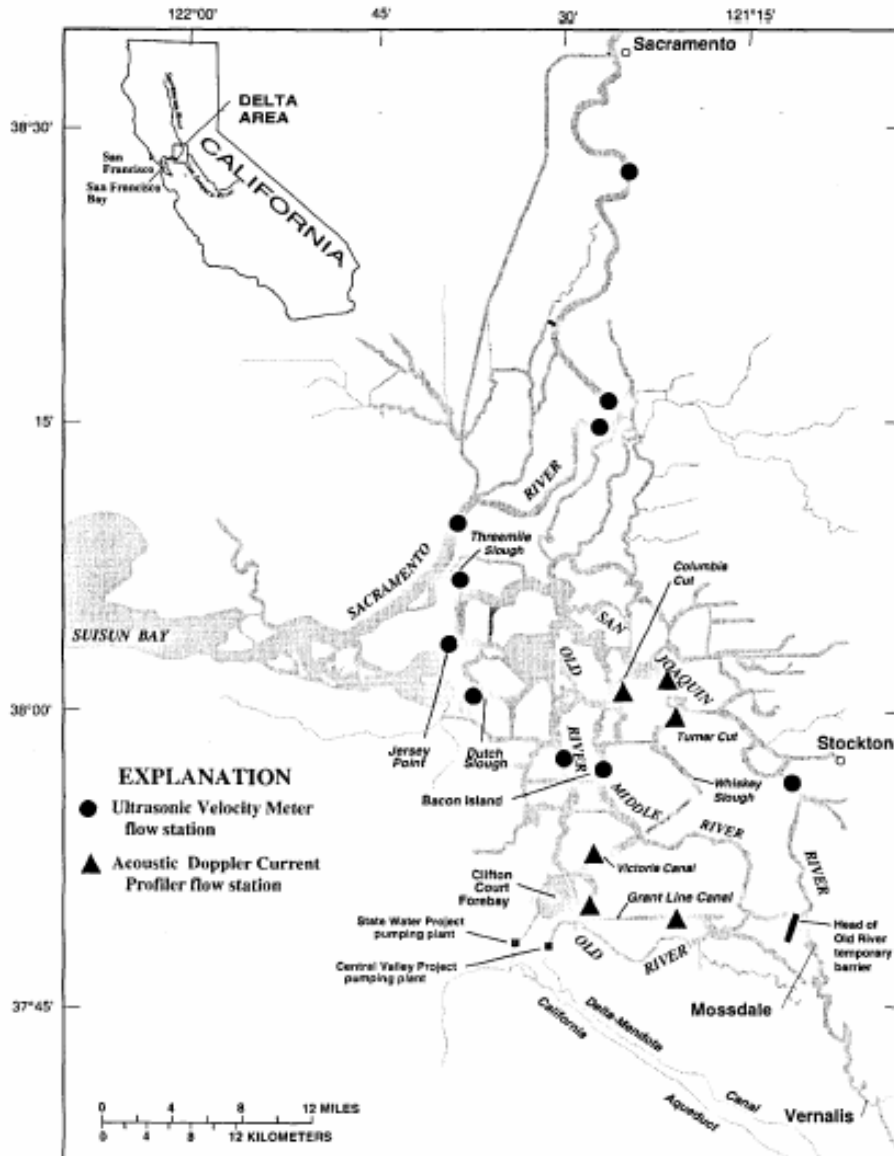


Figure 1. Locations of tidal-flow monitoring stations, Sacramento-San Joaquin Delta, California, UVM, ultrasonic velocity meter; ADCP, acoustic Doppler current profiler.

2 Measured Flow and Tracer-Dye Data Showing Anthropogenic Effects on the Hydrodynamics, south Sacramento-San Joaquin Delta

Figure 4-9: Location of Tracer Study Data Collection Sites.

The tracer study used in this project was conducted and presented by Oltmann (1998) and is summarized here. A Rhodamine WT tracer study was performed in April and May 1997 to track the movement of water into which tagged salmon smolts were released. The tracer was released at noon on April 28, 1997 near Mossdale on the San Joaquin River one hour prior to the release of 50,000 salmon smolts by the U.S. Fish and Wildlife Service and California Department of Fish and Game. Forty-eight liters of 20% Rhodamine WT were released over a 15- minute period. Nine automatic sampling measurement sites in the Delta were used to record the

concentration of the tracer. These took samples on an hourly basis and were retrieved and transported to a laboratory where a fluorometer was used to measure the tracer concentration. Figure 4-9 shows the locations of the tracer data collection sites. The locations are: Grantline Canal at Tracy Blvd bridge, Jersey Point, Middle River at Middle River, Middle River South of Columbia Cut, Old River at Bacon Island, Old River at Clifton Court Ferry, Turner Cut, San Joaquin River at Stockton UVM site, and San Joaquin River at Mandeville Ranch.

The tracer was released during the Vernalis Adaptive Management Plan's (VAMP) pulse-flow period on April 28, 1997. The flow on the San Joaquin River near Mossdale is shown in Figure 4-10. The tracer traveled from the release point to the Stockton UVM sampling site (about 13 miles) in about 10 hours (mean velocity of 1.9 ft/sec). Figure 4-11 shows the tracer concentration for the Stockton UVM site. This shows the peak concentration reached 10.5 ug/L and took about four hours to pass the site.

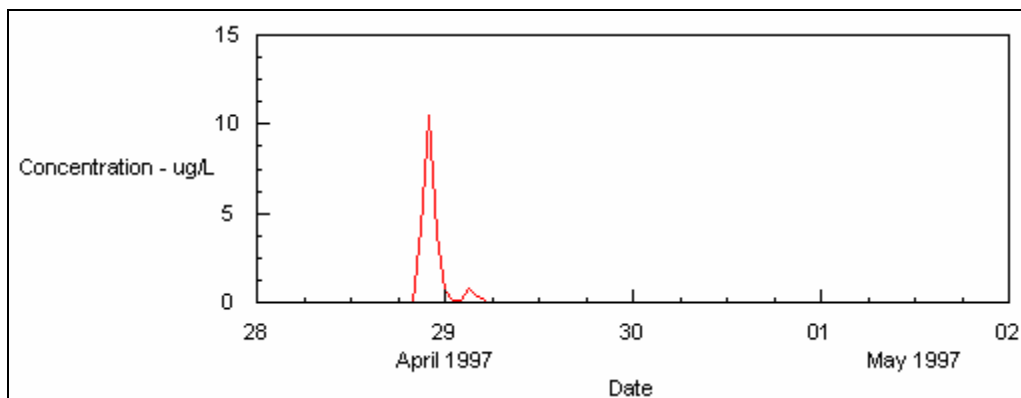


Figure 4-10: Tracer Concentration at Stockton UVM Site.

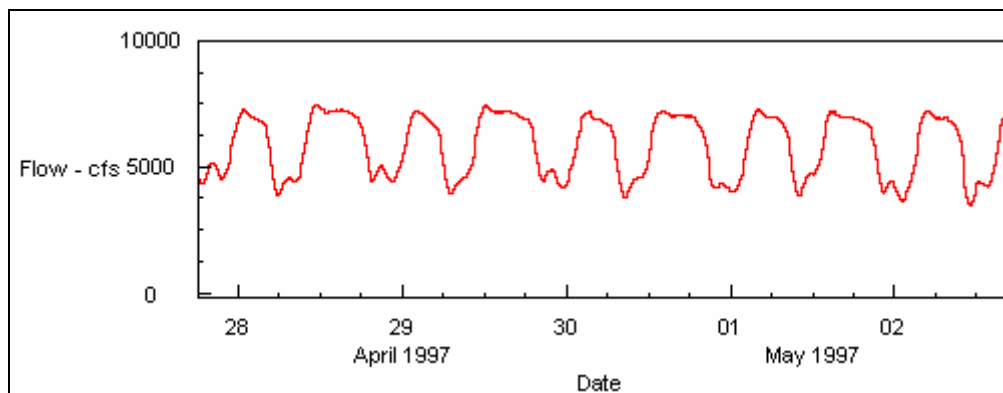


Figure 4-11: Measured Flow at Stockton UVM Site.

Turner Cut tracer concentration and flow are shown in Figures 4-12 and 4-13. Turner Cut is approximately 10 miles downstream from the Stockton UVM site. Travel time for the tracer to reach Turner Cut was about 25 hours (mean velocity 0.6 ft/sec). As Figure 4-13 shows, this portion of the Delta is influenced much more by tidal forces than the Stockton UVM site, resulting in the tracer taking more time to pass this site due to the reversing flow conditions. The peak concentration reached about 0.8 ug/L and the tracer took just over two days to pass the site.

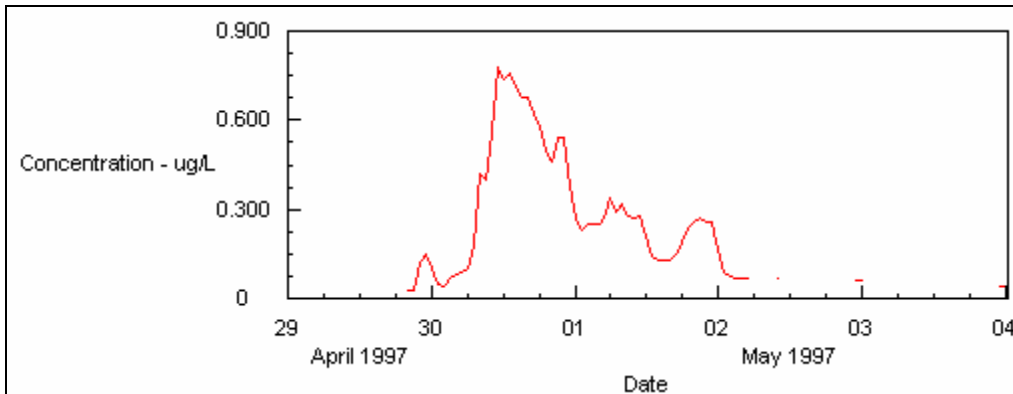


Figure 4-12: Tracer Concentration at Turner Cut.

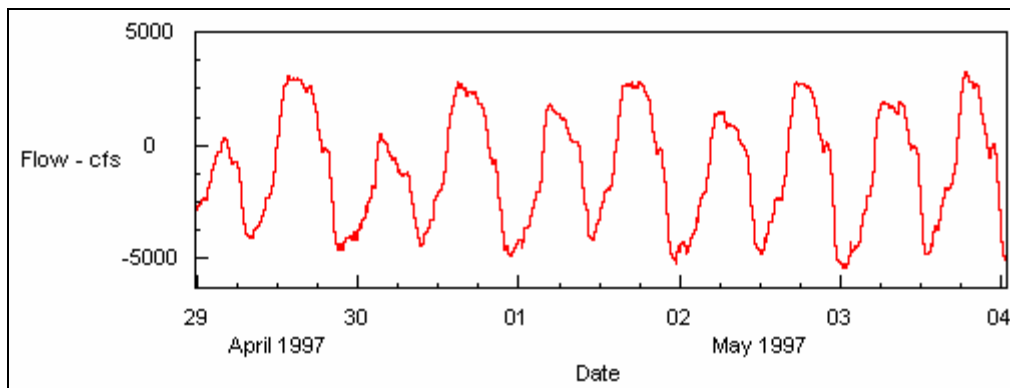


Figure 4-13: Measured Flow at Turner Cut.

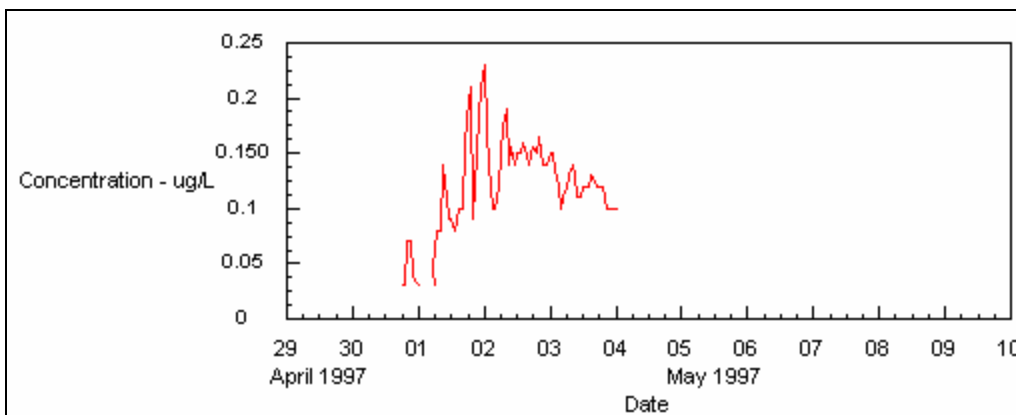


Figure 4-14: Tracer Concentration at San Joaquin River near Mandeville Ranch.

Figure 4-14 shows the tracer concentration at San Joaquin River near Mandeville Ranch. No measured flow data were available for this location. The peak concentration is reduced and the length of time passing the site is increased compared to the previous two locations. This is due to the increased mixing caused by tidal forces in the Delta. Similar results were found at Middle River South of Columbia Cut, shown in Figures 4-15 and 4-16.

Figures 4-17 and 4-18 show the tracer and measured stage at Grantline Canal near the Tracy Blvd Bridge. This shows some flow was able to pass through the barrier and culverts installed at

the head of Old River. The concentrations measured at Grantline are fairly small compared to the other locations.

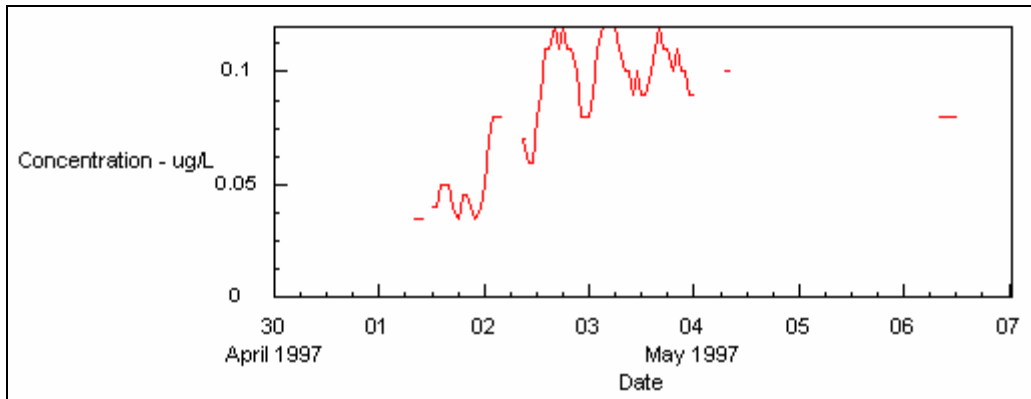


Figure 4-15: Tracer Concentration at Middle River near Columbia Cut.

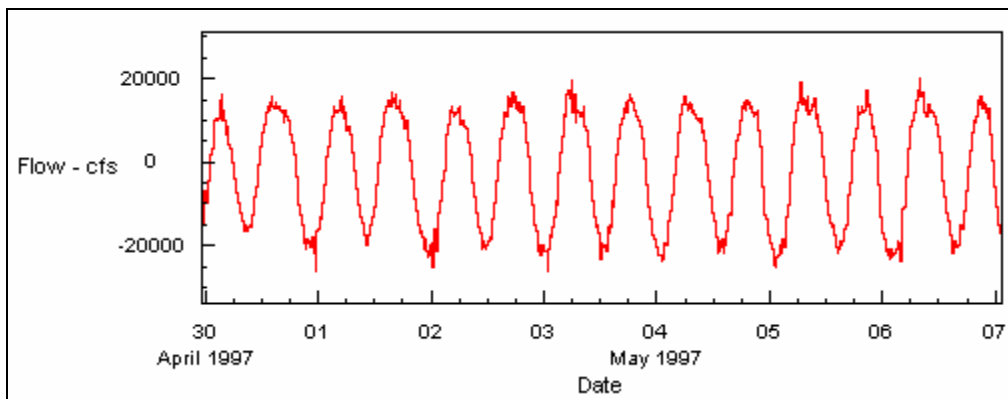


Figure 4-16: Measured Flow at Middle River near Columbia Cut.

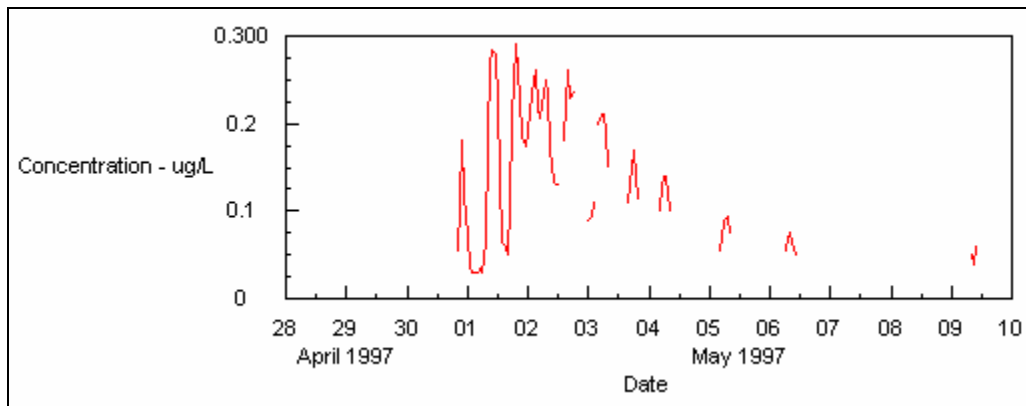


Figure 4-17: Tracer Concentration at Grantline Canal near Tracy Blvd. Bridge.

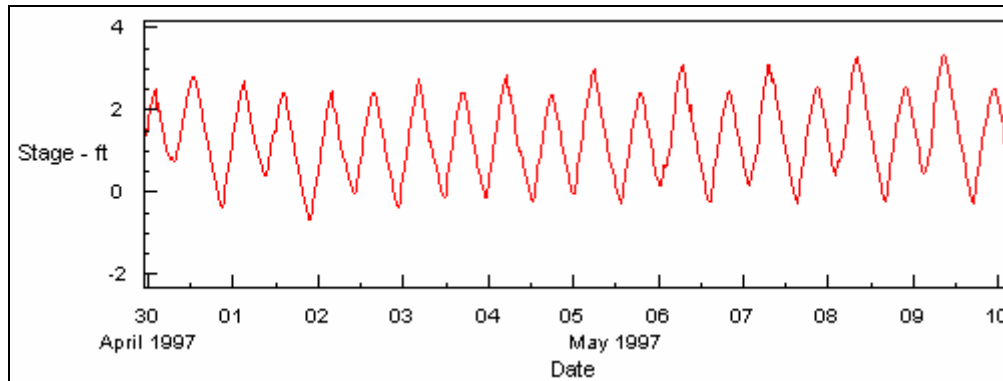


Figure 4-18: Measured Stage at Grantline Canal near Tracy Blvd. Bridge.

Other tracer sample recording locations experienced difficulties, making the data inapplicable for the purpose of this project. All collected at Old and Middle River UVM sites showed concentrations no higher than background concentrations (about 0.04 ug/L). The Old River UVM (near Clifton Court Forebay) measured the tracer arriving prior to the arrival at Grantline Canal – this shows something was interfering with the measurement. The Jersey Point station did not record any data.

4.4 Modeling Results

4.4.1 Profile Comparisons

Comparison of velocity profiles between the ADCP data and those used by the original PTM profiles show some inconsistencies. The profiles used by the PTM model have the same mean velocity, but consistently over-predict variation in peak velocity across the channel. This leads to the overestimation of shear flow dispersion calculated by PTM. Modification of the velocity profile coefficients yields an improved representation of the velocity fields.

Adjustments of the coefficients for the transverse and vertical velocity profiles make it possible to improve the representation of these idealized profiles to better approximate the profiles measured by the ADCP data. Figures 4-19 and 4-20 show the velocity data for Turner Cut. These now have additional information including the original and modified profiles. The modified profiles, obtained by inspection, were found to better represent the transverse and vertical velocities. Coefficients selected for the transverse profile are $A = 1.2$ and for the vertical profile the shape factor $s = 1.25$. Figures 4-21 and 4-22 show similar graphs for San Joaquin River between Columbia and Turner cuts.

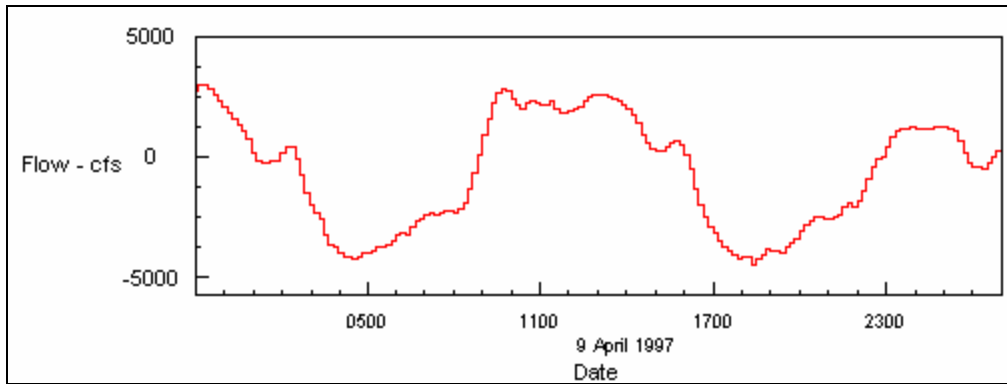


Figure 4-19: Turner Cut Flow.

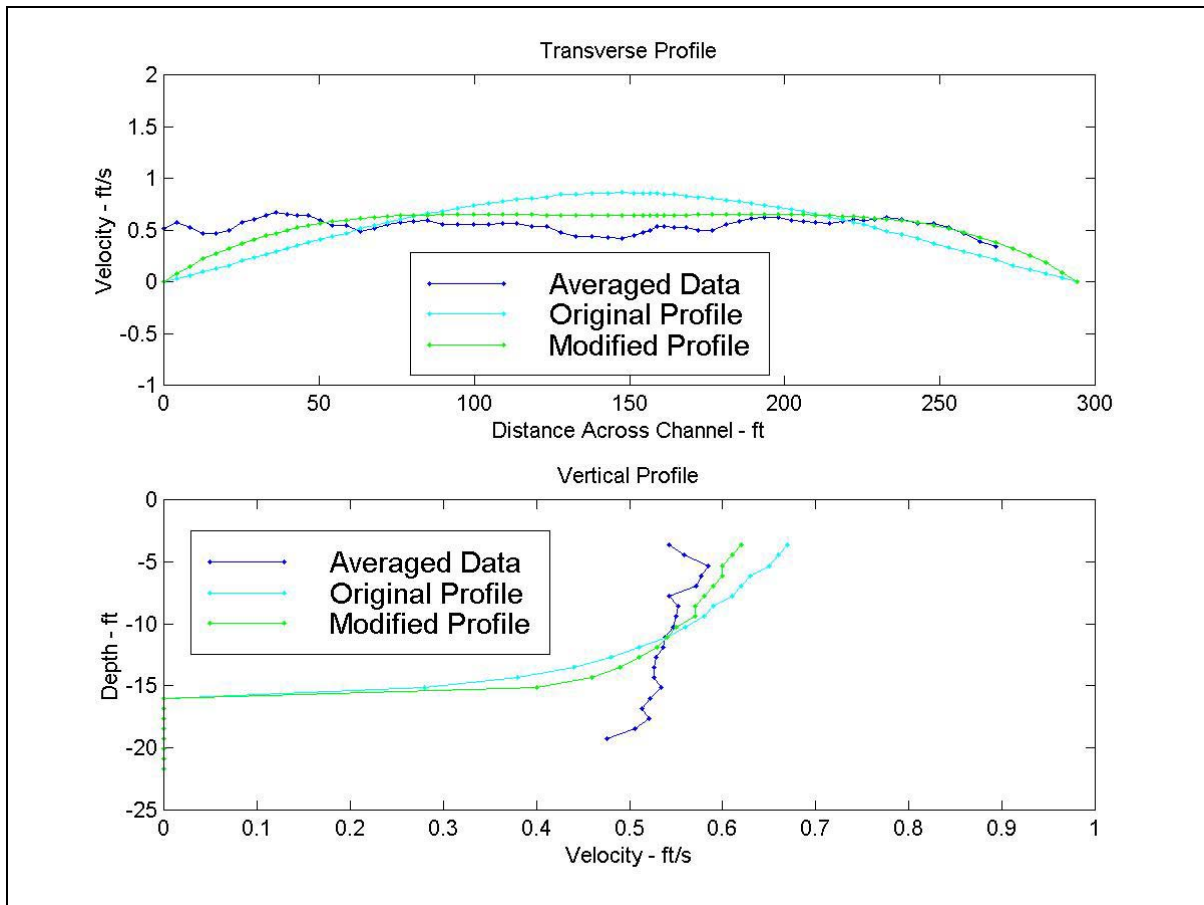


Figure 4-20: Turner Cut Profile – ADCP Comparison (1:30 p.m., April 9, 1997).

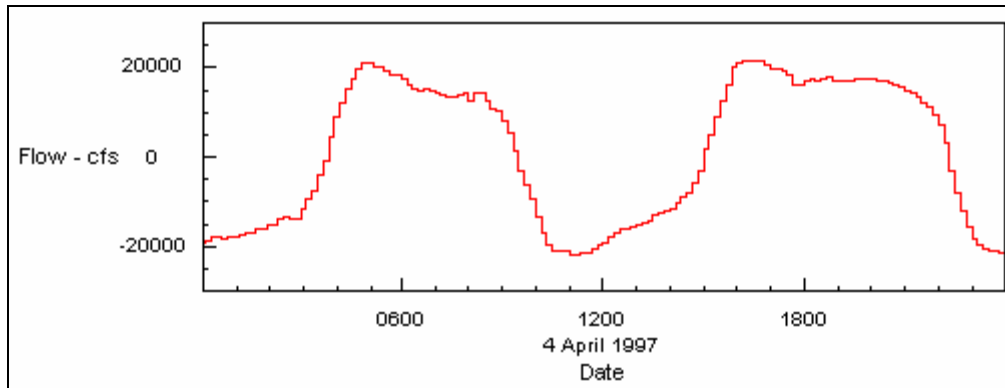


Figure 4-21: SJR between Columbia and Turner Cuts Flow.

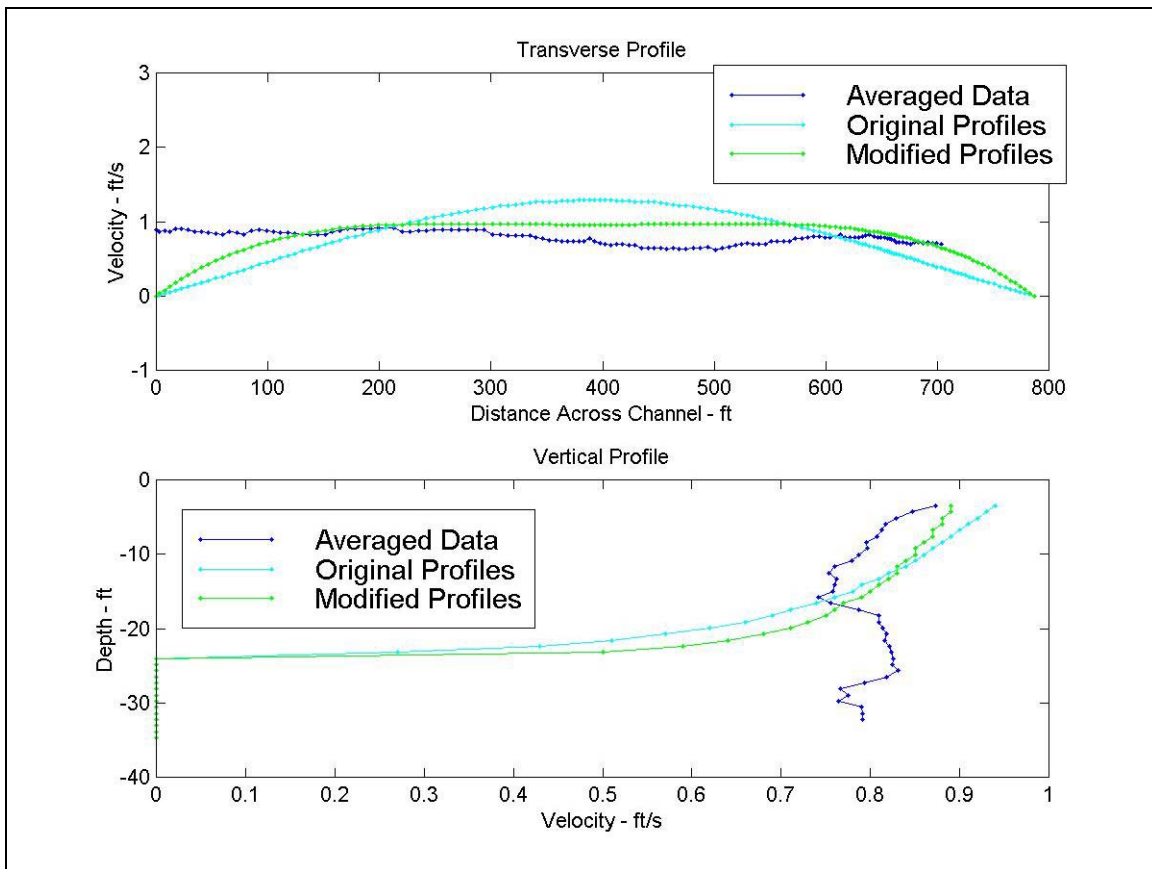


Figure 4-22: SJR between Columbia and Turner Cuts Profile – ADCP Comparison (10:30 p.m., April 4, 1997).

Additional figures presented by Wilbur (2000) show the comparisons between the ADCP data and the theoretical transverse and vertical velocity profiles for both the original and the modified profile coefficients. The vertical velocity profile shows more inconsistencies when compared to the ADCP data than the transverse profile. Several of the figures show that a uniform vertical velocity profile may better represent the observed data. In a later section, a uniform vertical velocity profile, as well as a uniform transverse velocity profile, will be compared to the modified velocity profiles shown in the figures.

4.4.2 Longitudinal Dispersion

A single hypothetical channel was represented in DSM2 in order to investigate the behavior of the Particle Tracking Model's implementation of longitudinal dispersion. Modification of the velocity profile coefficients controls the amount of dispersion superimposed on the advection of a mass of particles. Velocity profile coefficients used for this simulation were both the original ($A = 1.6$, $s = 1.0$) and the modified profiles ($A = 1.2$, $s = 1.25$). The channel has a width 500 feet, an average depth of 40 feet, and an average velocity of 1.6 ft/sec. Ten thousand particles were inserted instantaneously at the furthest upstream location.

Figure 4-23 shows the particle concentration for the original and modified velocity profiles. Three locations are shown (at 5, 20, and 35 miles downstream of the beginning of the channel), which demonstrate how, under steady flow conditions, the different dispersion scenarios transport the particles. The original profiles produce more dispersion. This is shown in the figure by the smaller peak concentration and the longer time it takes to pass a single site. The modified profiles, having less dispersion, have higher concentrations and behave more advectively.

Equation 4-6 may be used to predict theoretical longitudinal dispersion. The range of theoretical longitudinal dispersion for this channel is 165 to 4,900 ft^2/s as determined by the uncertainty of Equation 4-6. Figure 4-24 shows the variance for the longitudinal displacement of particles produced by the original velocity profiles. The linear nature, once dispersion has fully developed, reflects the steady state condition. Figure 4-25 shows the effective longitudinal dispersion coefficient based on the original profiles. The steady state range approaches 1,200 ft^2/s , which is in the range of theoretical dispersion in Equation 4-6. This figure shows the first 3 hours of simulation time. A period of about 2 hours is needed for the dispersion to fully develop. The fluctuations in the curve are due to the randomness of the random mixing coefficients.

Figures 4-26 and 4-27 show the variance of longitudinal displacement and the effective longitudinal dispersion coefficient using the modified velocity profiles. The steady-state value of dispersion for the modified profiles is about 300 ft^2/s , which is also in the range of theoretical longitudinal dispersion. The modified velocity profiles yield a smaller longitudinal dispersion coefficient. This value is still within the range of acceptable values, as compared to those from Fischer (1979).

Inclusion of a tidal influence at the downstream end of the channel allows for the investigation of how longitudinal dispersion behaves in the Delta. A repeating 25-hour oscillating stage was added to the downstream boundary condition. Figure 4-28 shows a segment of the historic tide used for this example. Predicting a longitudinal dispersion coefficient by Equation 4-6 in a tidally influenced system becomes difficult because a steady state condition never develops – the dispersion coefficient is always changing. Additionally, in real systems with many branches, such as the Delta, the mass of particles becomes separated into different channels as the tide forces the flow throughout the system. Each channel typically experiences different flow and tidal conditions at different times, producing different dispersion coefficients for each.

Figure 4-29 shows the tidal influence on the stage for different locations in the channel. The upper reaches (5 and 20 miles downstream) are slightly influenced while the lower reaches (34

and 45 miles downstream) are significantly affected by the tide. Figure 4-30 shows the particle concentration for three locations in the channel. The tide at the various locations has delayed the arrival time of the particle cloud by almost 12 hours and reduced the peak concentrations.

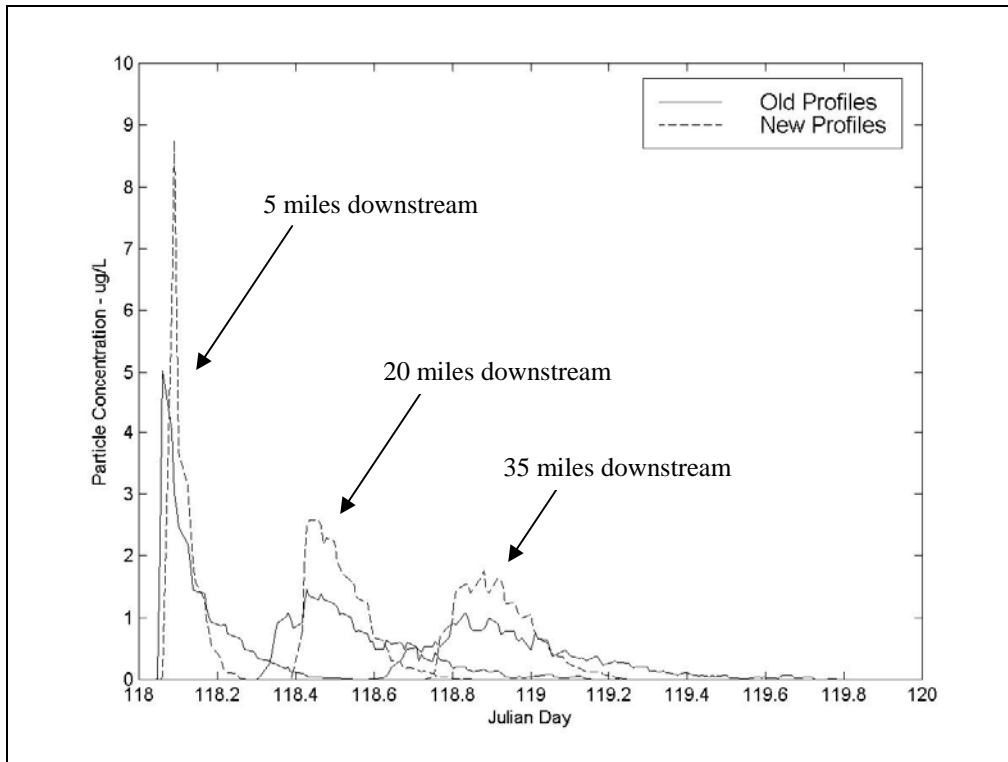


Figure 4-23: Velocity Profile Differences for a Single Long Channel.

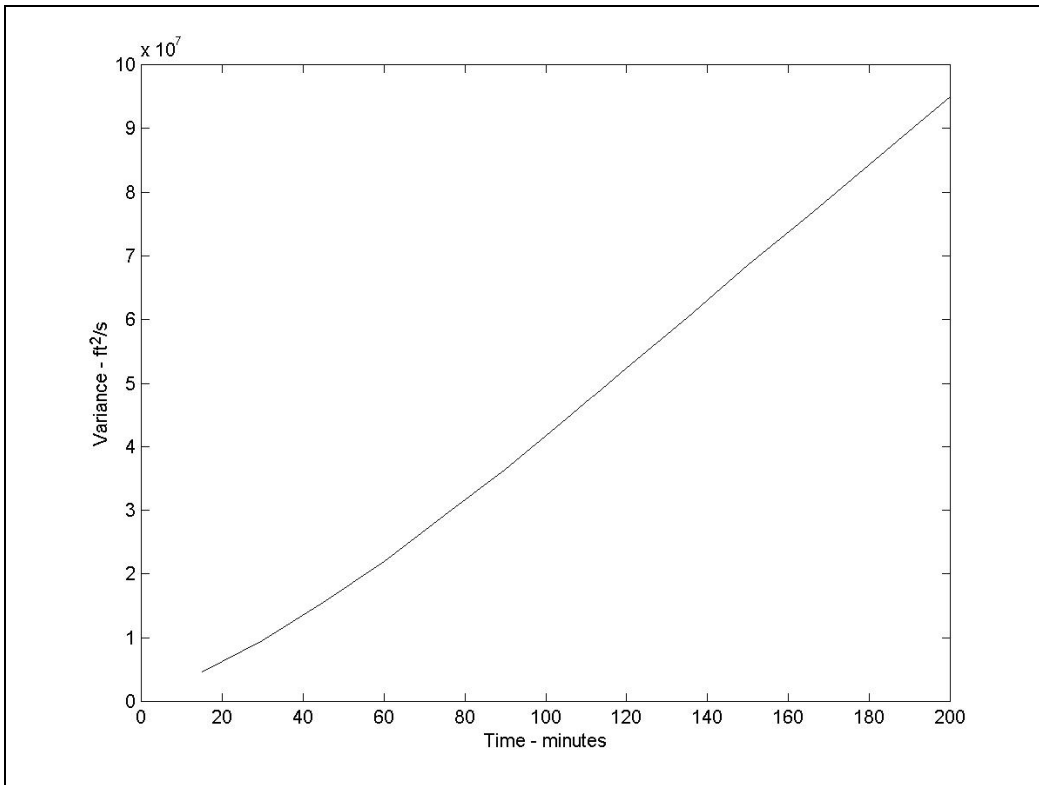


Figure 4-24: Variance of Longitudinal Displacement for Original Profiles.

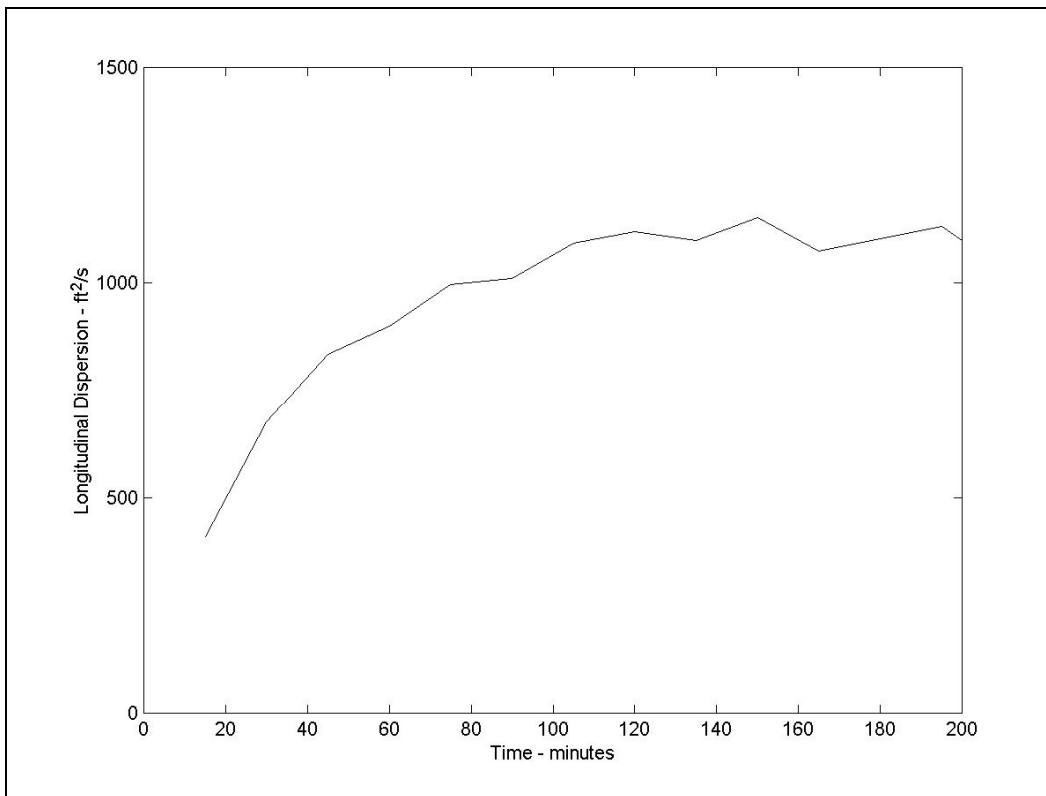


Figure 4-25: Effective Longitudinal Dispersion for Original Profiles.

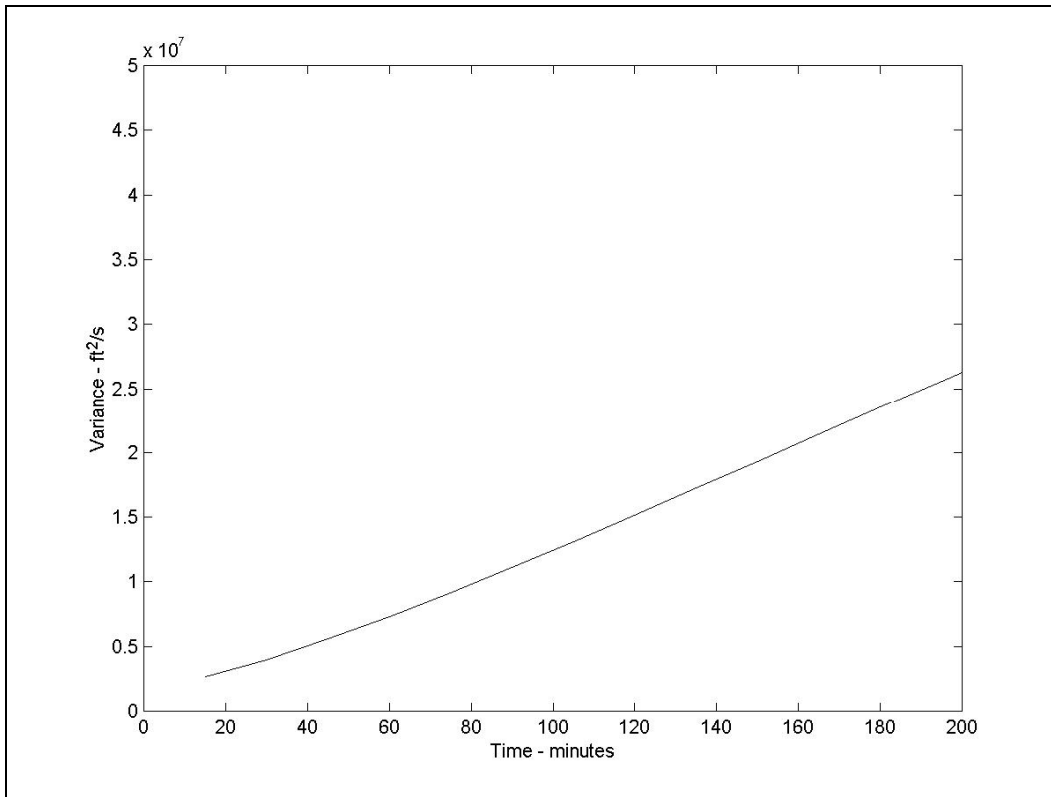


Figure 4-26: Variance of Longitudinal Displacement for Modified Profiles.

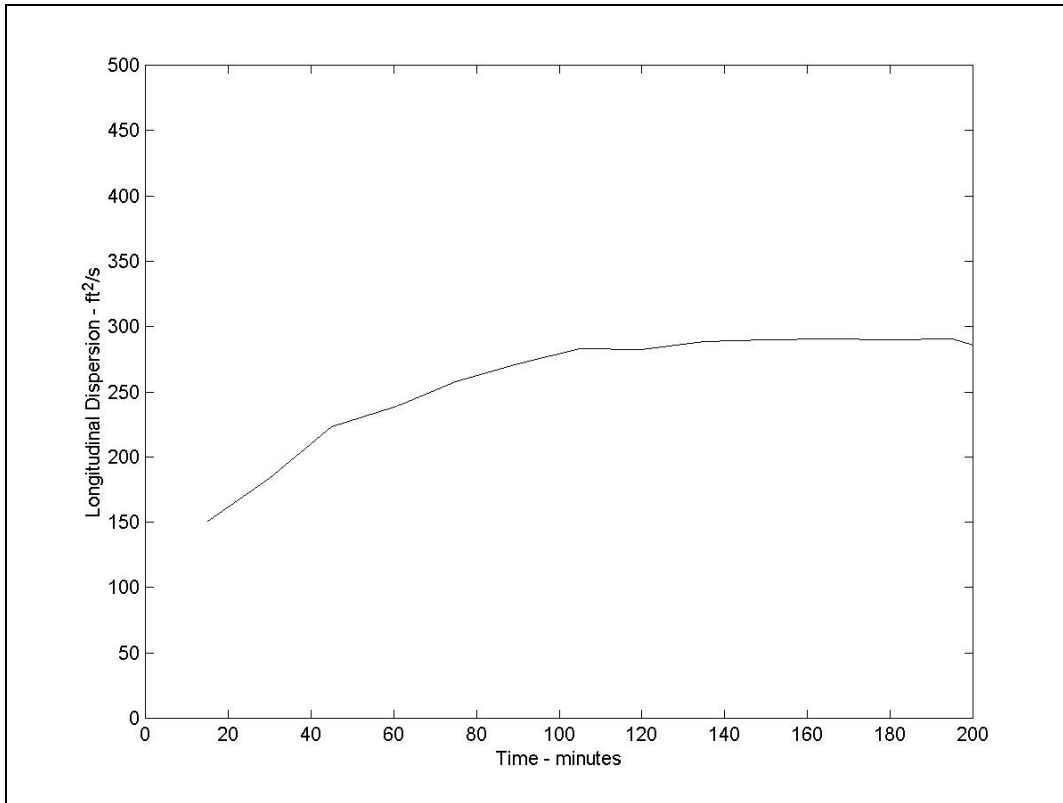


Figure 4-27: Effective Longitudinal Dispersion for Modified Profiles.

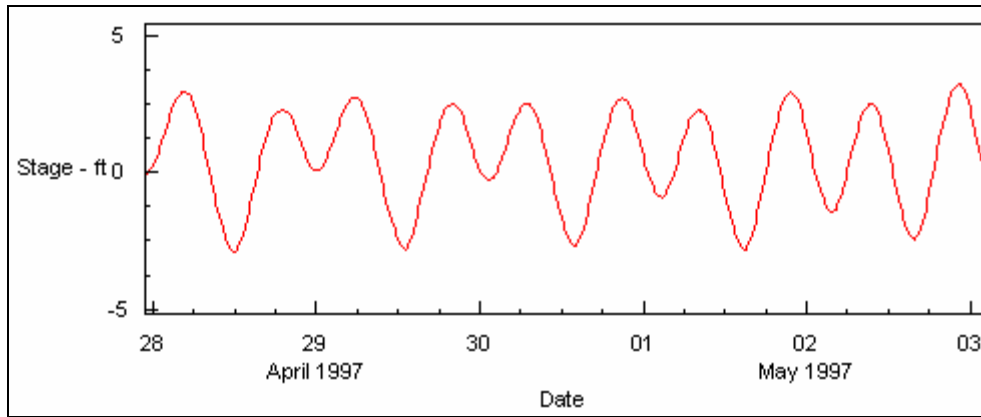


Figure 4-28: Stage Boundary Condition for Long Channel.

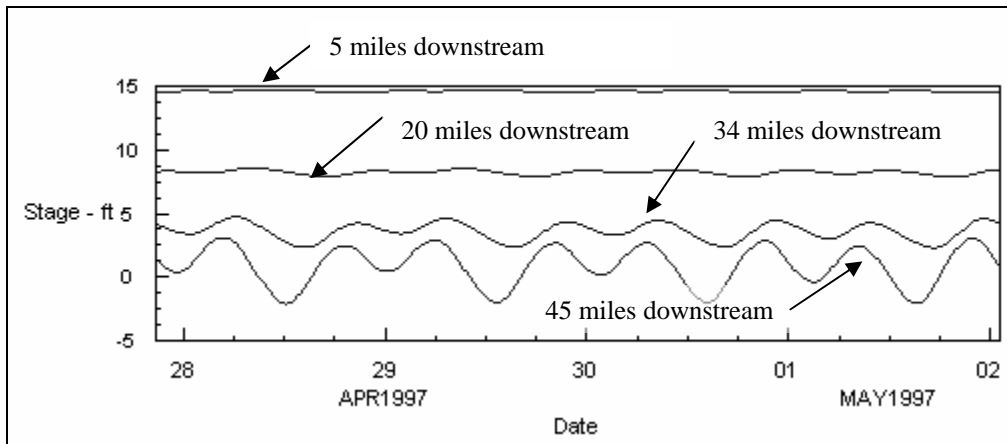


Figure 4-29: Stage at Various Locations influenced by Tidal Boundary Condition.

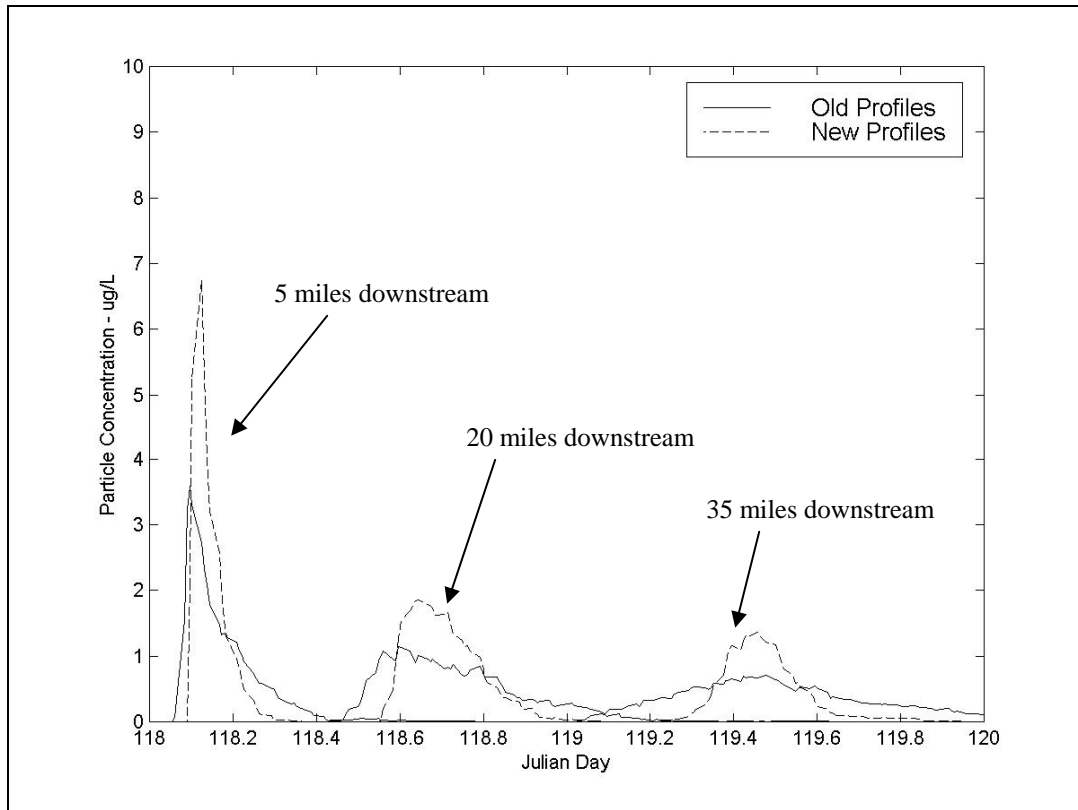


Figure 4-30: Particle Concentration for Long Channel with Tidal Boundary Condition.

4.5 DSM2 Results

[Editor’s Note: The results presented below were not based on the most recent geometry that is currently in use, because this new geometry had not been verified at the time of this study. The current DSM2 geometry is discussed in Chapter 2.]

4.5.1 Hydrodynamics

The hydrodynamics of the Delta are important for the PTM model to give accurate results. While the hydrodynamics are not the focus of this investigation, they are presented here for completeness.

The simulations use a historical real tide for the westernmost boundary at Martinez. The stage used as a boundary condition is shown in Figure 4-31 for the duration of the tracer study. There is a 25-hour repeating tide sequence. This includes a 12.5-hour period between each high tide (also for low tide).

Gate operations are accounted for in such places as the Delta Cross Channel and temporary barriers at the head of Old River. Documented gate installation and operations come from DWR (1998).

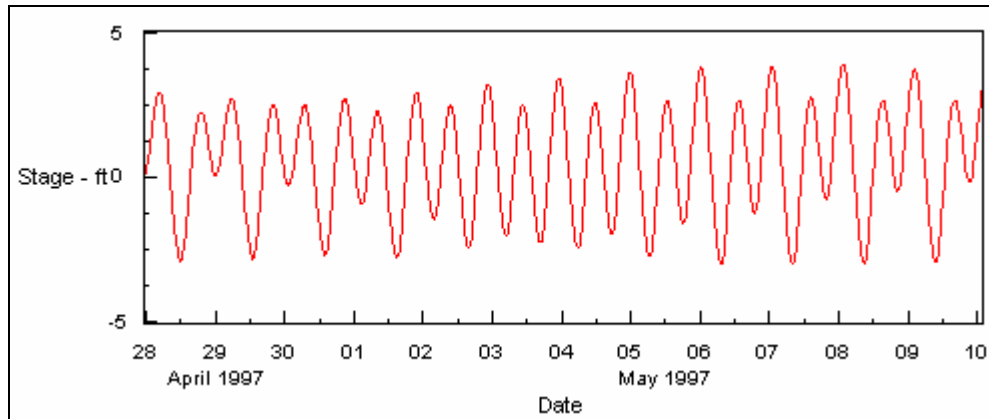


Figure 4-31: Martinez Stage Boundary Condition.

Stage and flow results are presented with historical data at various locations. Locations of interest for the tracer study are shown. Figures 4-32 – 4-35 show HYDRO simulation results with historical data for Turner Cut, Jersey Point, Old River near Bacon Island, and Middle River south of Columbia Cut.

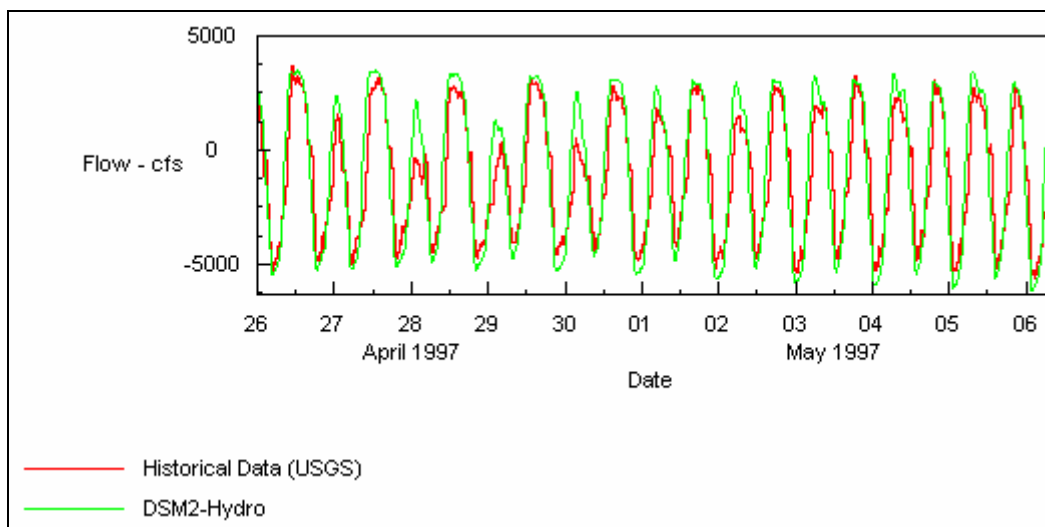


Figure 4-32: DSM2 and Measured Flow at Turner Cut.

Figure 4-32 shows the simulated flow at Turner Cut. HYDRO represents fairly well the measured flow. The extreme magnitudes on the tidal oscillation show the greatest amount of problems for this and other sites. The largest inconsistencies are about 600 cfs, while the majority of the time these measure less than 200 cfs.

Figure 4-33 shows the simulated and measured flow for Jersey Point. This also shows that the majority of the inaccuracies with HYDRO have to do with simulating the peak flows. Due to the magnitude of the flow at Jersey Point the small differences shown on the figure are approximately 2,000 cfs.

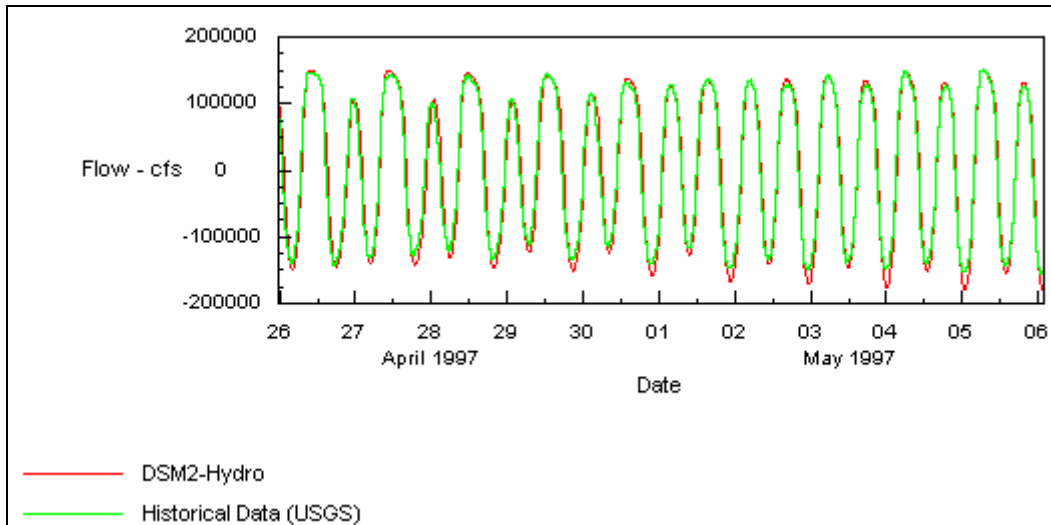


Figure 4-33: DSM2 and Measured Flow at Jersey Point.

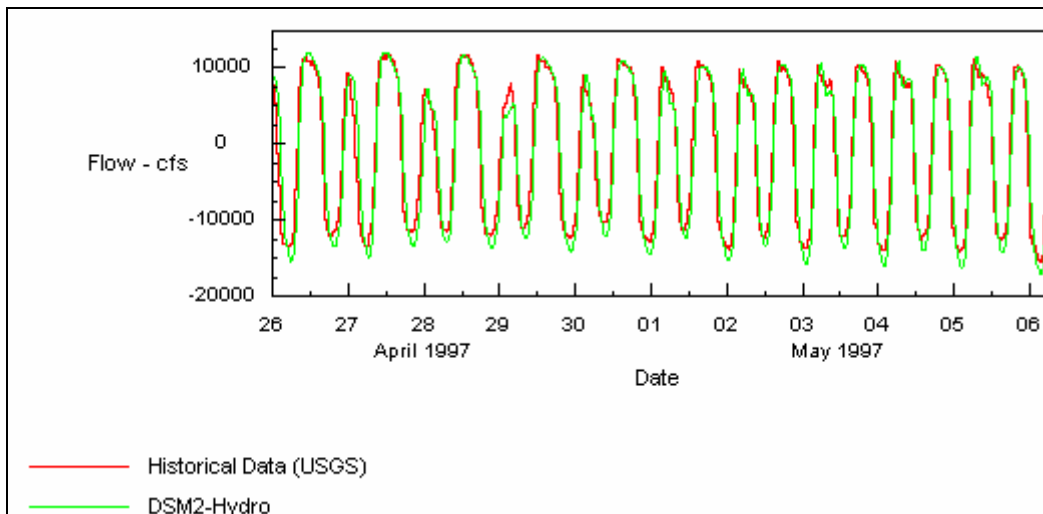


Figure 4-34: DSM2 and Measured Flow at Old River near Bacon Island.

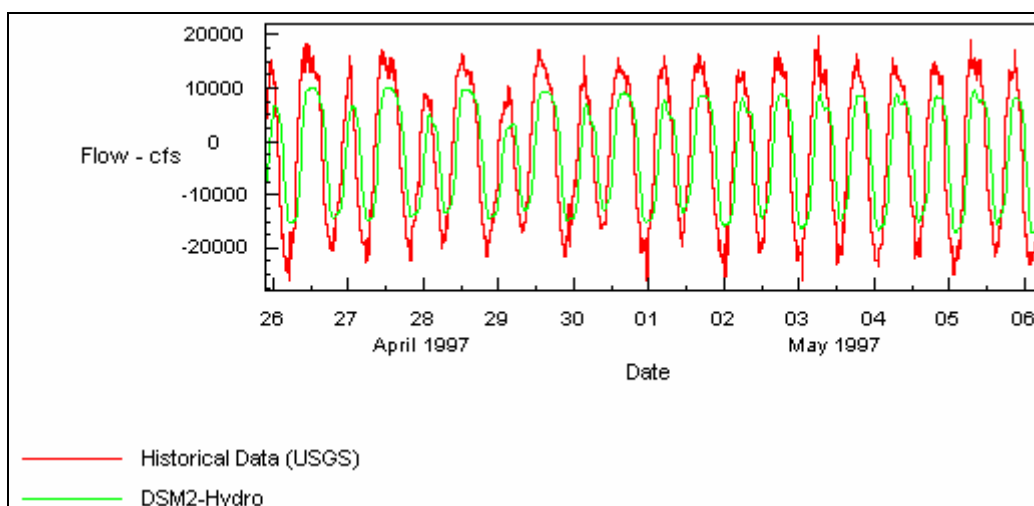


Figure 4-35: DSM2 and Measured Flow at Middle River South of Columbia Cut.

Flow at Old River near Bacon Island is shown in Figure 4-34. Similar results are found comparing the measured and simulated flow. Differences between the two are less than 1,000 cfs.

Simulated and measured flow for Middle River South of Columbia Cut shows a large amount of disagreement. Figure 4-35 shows differences of nearly 10,000 cfs. This mismatch is probably due to poor representation of the bathymetry.

4.5.2 PTM – Tracer Comparisons

The original velocity profiles are used in the first simulation to compare it to the collected tracer data. An additional simulation was performed with modified velocity profiles that more accurately represent the velocity profiles found in the ADCP data.

As discussed earlier, the concentrations for the tracer study are reliable at only a few sites. The PTM simulations and tracer data are compared at these locations only. Three locations in particular have high enough concentrations to be used in testing the PTM model. These are Turner Cut, Mandeville Ranch, the UVM site near Stockton, and Middle River south of Columbia Cut.

The PTM simulations compared here use the velocity profile coefficients listed in Table 4-2. The PTM results (position of each particle) are converted to a concentration through use of Equation 4-12. The factor used to scale the particles to micro-grams per liter is 318,000.

Table 4-2: PTM Velocity Profile Coefficients

	A	B	C	Shape Factor
Original Profile	1.62	-2.22	0.6	1.0
New Profile	1.2	0.3	-1.5	1.25

The first location, Stockton UVM, is shown in Figure 4-36. This figure shows the tracer data, and PTM simulation results with original and modified profile configurations. It appears the original profiles more accurately represent the tracer data. It should be kept in mind that the distance of the Stockton UVM site is close to the particle injection point. The modified profiles do not mix across the channel to simulate full mixing of particles.

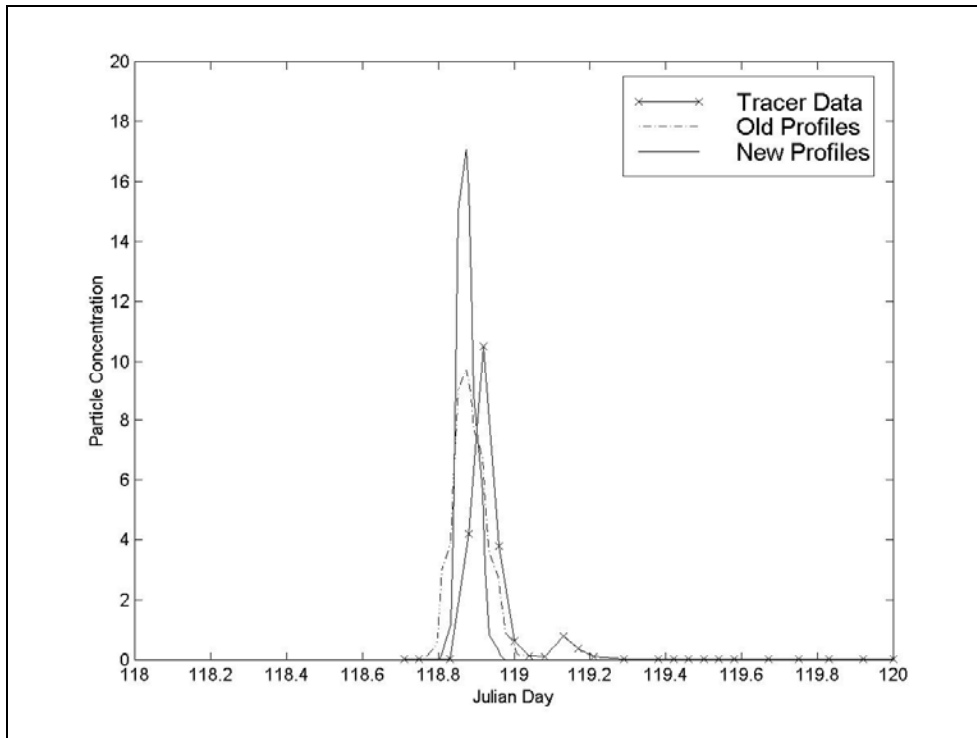


Figure 4-36: PTM and Tracer Comparison at Stockton UVM Site.

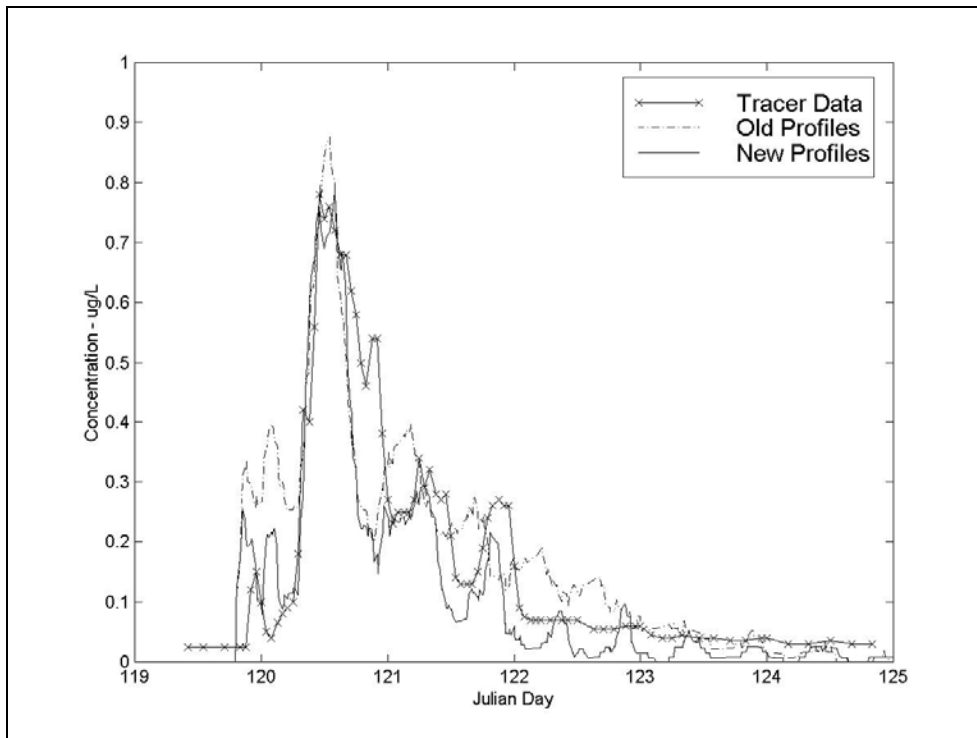


Figure 4-37: PTM and Tracer Comparison at Turner Cut.

Figure 4-37 shows the tracer data and PTM results for the Turner Cut location. This shows the clearest difference between the two sets of profiles in their effects on the particle dispersion.

While both profiles simulate the main peak concentration (at time 120.5) the new profiles better simulate the arrival of particles at the first (time 120), third (120.2), and fourth (120.9) peaks. The new profiles simulate a lower concentration at the first spike and arrives closer to the time the tracer data does. The original profiles do a poorer job at predicting the arrival time of these particles. Following the fourth concentration spike, both PTM profiles predict more oscillations in the concentration than exist in the data. This is possibly due to inaccuracies in the hydrodynamics or when recording of tracer at low concentrations close to background levels.

Figure 4-38 shows the same PTM – tracer comparisons at the San Joaquin River near Mandeville Tract. This location experiences much more oscillations, in both PTM and in the tracer data, than the other locations. Both profiles demonstrate they over-predict as well as under-predict concentrations at different times. Because of this, it is difficult to determine which one simulates the tracer data more accurately. The possible causes of these extreme oscillations include hydrodynamic problems and the method of converting the PTM output to concentrations.

Figure 4-39 shows different results for Middle River south of Columbia Cut. The PTM model does not simulate the tracer movement through this location very accurately. It is believed the problem is associated with the hydrodynamic model not properly simulating the flow (Figure 4-35).

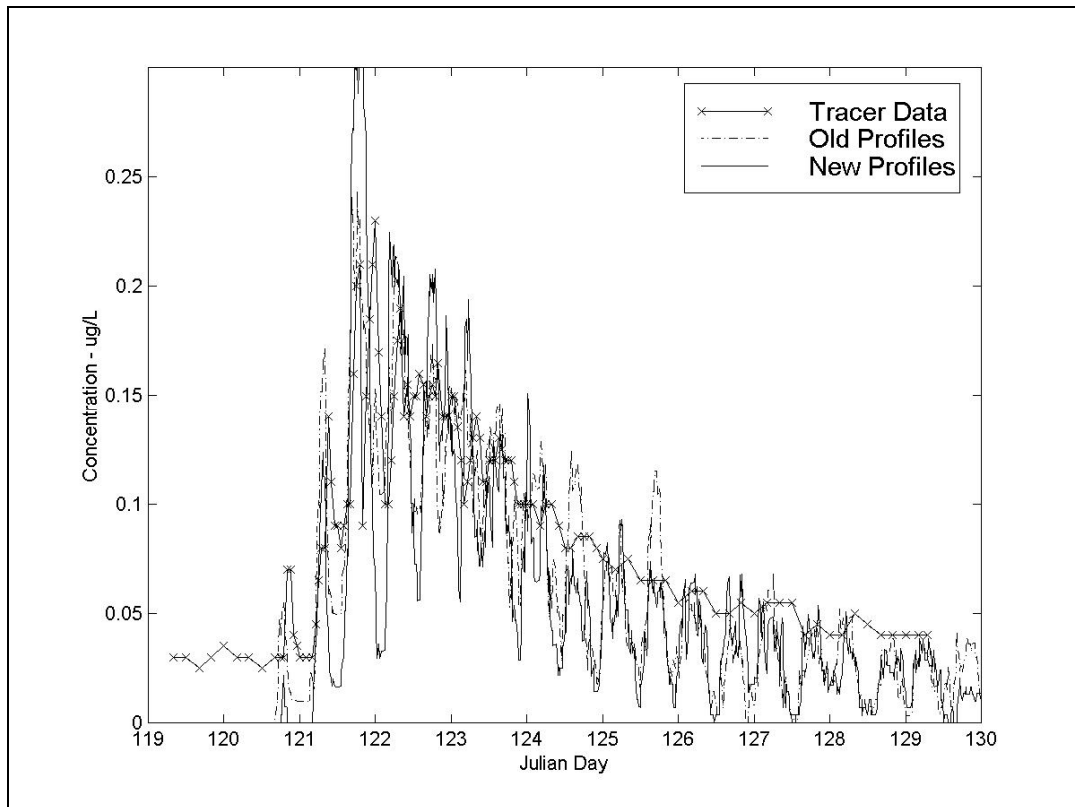


Figure 4-38: PTM and Tracer Comparison on SJR at Mandeville Reach.

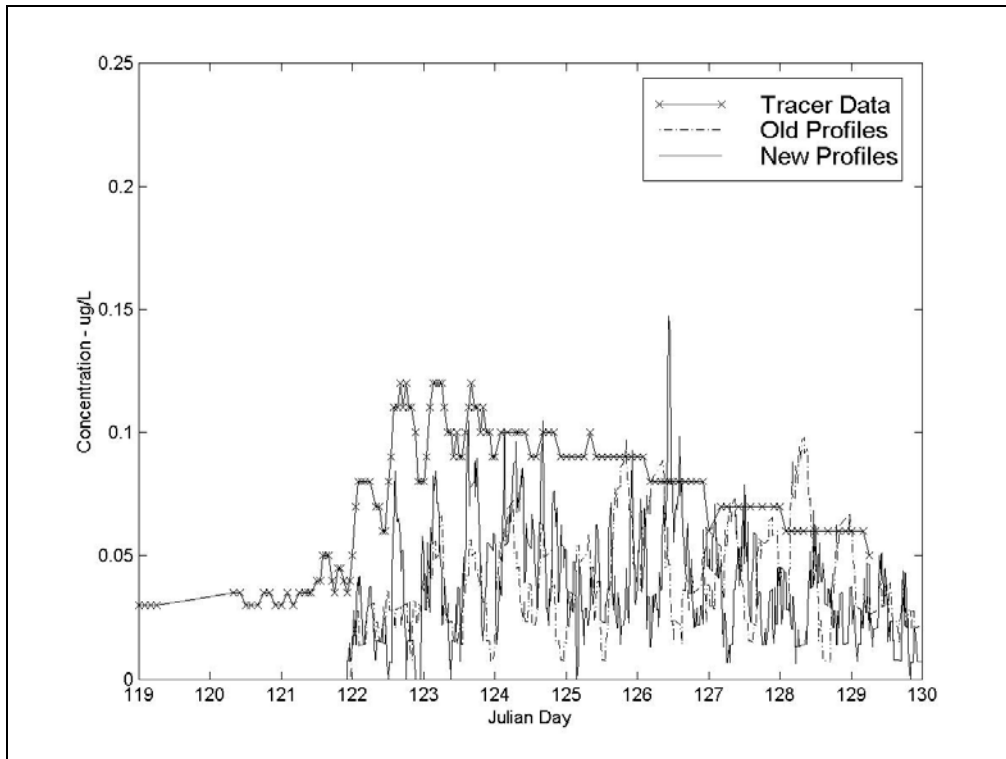


Figure 4-39: PTM and Tracer Comparison on Middle River South of Columbia Cut.

4.5.3 No Dispersion

Investigation of the importance of dispersion to the movement of particles throughout the Delta is now investigated with comparisons to the new velocity profiles discussed earlier. The first condition compared is the case where the system is only subjected to advective forces. The flow in both the vertical and transverse directions are uniform, thus the velocity across the entire channel is equivalent to the mean velocity.

Figure 4-40 displays the tracer study data, the simulated tracer concentration using the new profiles, and the no-dispersion condition at Turner Cut. The arrival time of particles under the no-dispersion case matches fairly well with both the tracer and new profiles. This suggests the dominance of advection in the Sacramento – San Joaquin Delta over the effects of dispersion. However, it is obvious the no-dispersion condition does a poorer job at simulating the tracer concentration than either the original or modified velocity profiles used for representation of dispersion. While the general timing of particles is similar to the previous results, the large oscillations in particle concentration are unrepresentative of the tracer data. The movement of particles with this advection-only situation shows how the particles do not spread longitudinally – they maintain their original distribution and are controlled by the hydrodynamics of the Delta.

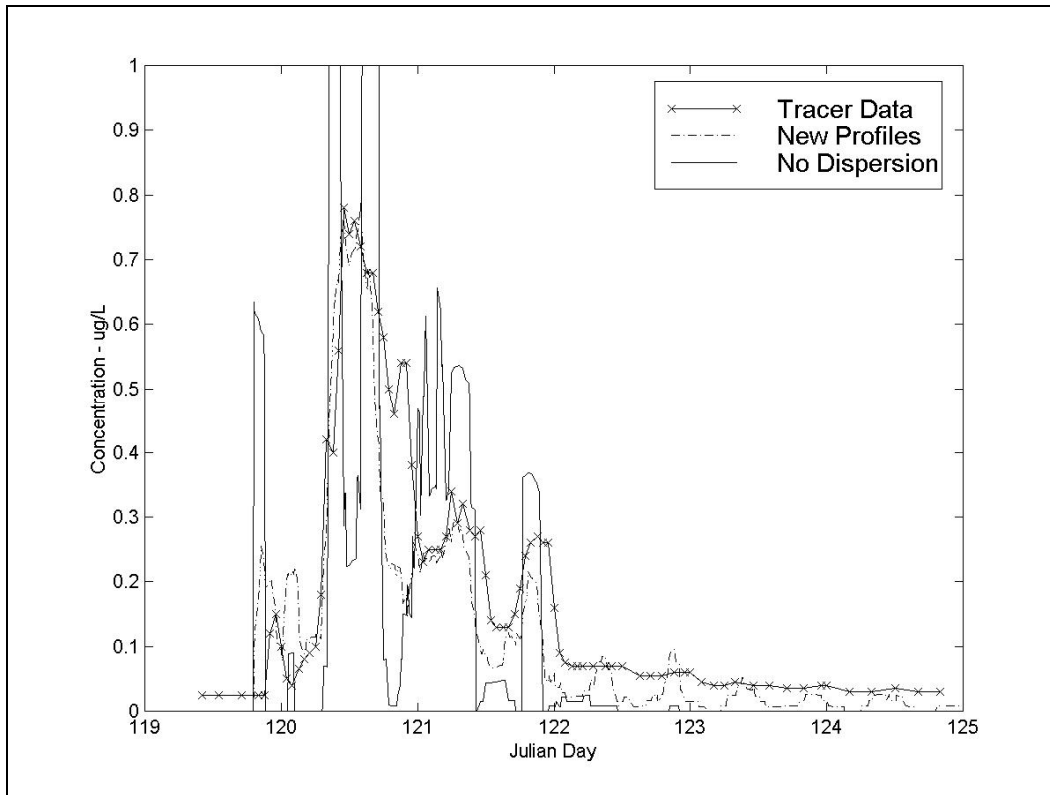


Figure 4-40: PTM and Tracer Comparison with No Dispersion at Turner Cut.

4.5.4 No Vertical Shear

Removal of the vertical velocity profile from the “best fit” PTM simulation shows how particles travel with a uniform vertical profile. All dispersion with this scenario is generated from the transverse velocity profile. Figure 4-41 shows the results of this simulation for Turner Cut. This shows a slight difference between the “best” profiles and the uniform vertical profile. The trend shows the particle arrival time as slightly earlier than the “best” profile results. While the differences are slight, it does not compare well with the tracer data. Without the vertical distribution, dispersion is slightly underestimated.

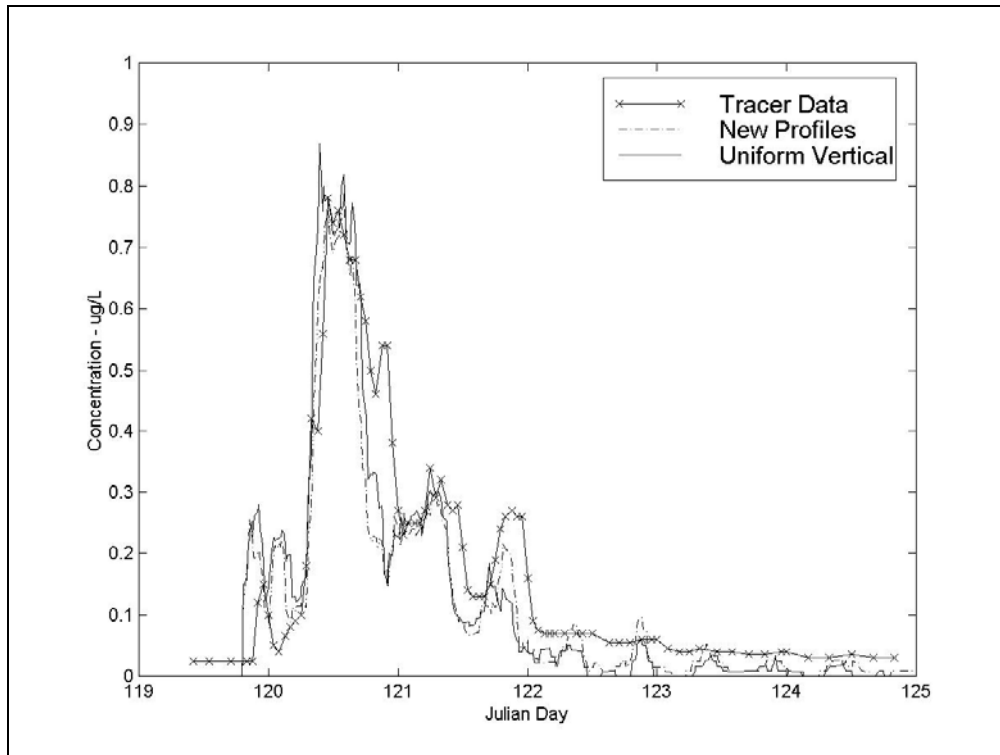


Figure 4-41: PTM and Tracer Comparison with Uniform Vertical Velocity Profile at Turner Cut.

4.5.5 No Transverse Shear

Following a similar examination of a uniform vertical velocity profile, removal of the transverse velocity profile is now presented. The dispersion generated with this condition is only from that produced by the vertical velocity profile. Figure 4-42 shows the PTM results with the tracer data for Turner Cut. This shows the PTM model, without the transverse velocity profiles, predicts a much more advective particle movement than the tracer and “best” fit profiles. This also may be compared to the uniform vertical velocity profile. These show the transverse velocity profile is more important to the dispersion process than the vertical velocity profile. This observation was discussed by Fischer (1979) and supported here with the PTM results.

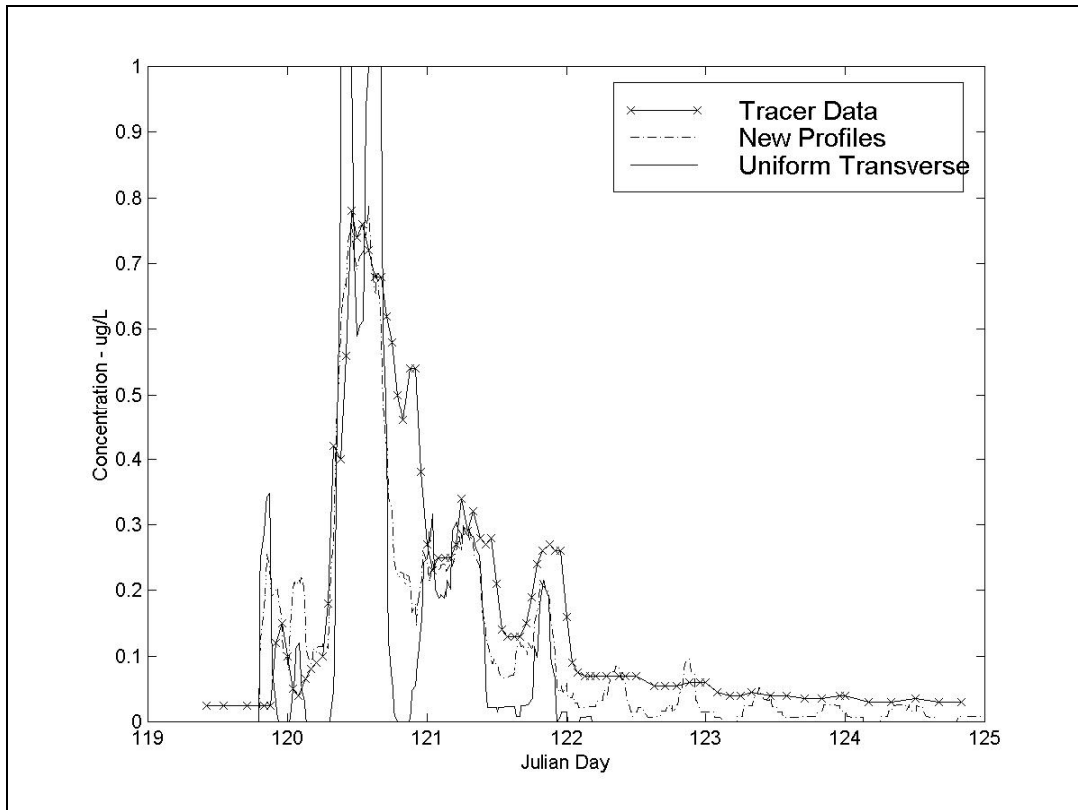


Figure 4-42: PTM and Tracer Comparison with Uniform Transverse Velocity Profile at Turner Cut.

4.6 Conclusions

The following conclusions may be made based upon the previous discussion and analysis:

- ❑ As discussed in the literature, the dispersal cloud is proportional to the square-root of the longitudinal dispersion coefficient. Addition of an oscillating flow condition reduces the dispersion by about one half. These lead to the conclusion that the modeling results are rather insensitive to slight changes in the mechanisms causing dispersion.
- ❑ The existing velocity profiles used in the Particle Tracking Model consistently over-predict the peak velocities found in the ADCP data. The mean velocity is accounted for, but the shear created by the excessive velocity profiles overestimates the dispersion in the system.
- ❑ Modification of the transverse and vertical velocity profile coefficients allow for an improved representation of the velocities found by the ADCP data. Channel irregularity can be attributed to the inconsistencies between the idealized profiles and those shown in the data.
- ❑ Simulation of the tracer study conducted by USBR with the Particle Tracking Model yields fair results with the original profiles. Even though the original profiles overpredict the peak velocities, the movement of particles is rather insensitive to the dispersive

processes.

- ❑ Incorporation of the modified velocity profile coefficients into the Particle Tracking Model results in improved simulation of the tracer study. While the particle movement is rather insensitive to the amount of dispersion in the system, it is nonetheless an important process and cannot be ignored.
- ❑ The “no-dispersion” simulation by PTM shows the importance of including dispersion in the model. The overall dominance of advection in the system is shown by the fairly accurate arrival time of particles corresponding with peak tracer concentrations. The lack of dispersion, however, produces particle distributions that do not correspond to the tracer data.
- ❑ The comparison between the uniform vertical velocity profile and the uniform transverse velocity profile show the relative importance of the transverse profile to the production of dispersion in the Delta.
- ❑ The vertical velocity profile plays a minor role in the development of dispersion in the Delta. Two very different approximations of the vertical velocity profile, uniform and either the original or modified von Karman representations, result in fairly similar simulations of the tracer study. This lessens the concerns about inconsistencies between the von Karman approximation of the vertical velocity profile and the ADCP data.
- ❑ Inspection of the HYDRO and PTM results show the importance of accurate simulation of the hydrodynamics of the Delta prior to the simulation of PTM. If any error exists in HYDRO, it will be carried through to the PTM model results.

4.7 Future Directions

The following suggestions are made based upon the previous discussion and analysis:

- ❑ Incorporate the new geometry files used for the DSM2-HYDRO simulation. These include updated bathymetry data for most of the Delta. More accurate determination of the hydrodynamics of the Delta will improve the simulations of PTM. The process of calibrating these new geometry files has yet to be completed. A similar investigation of the PTM simulation of the 1997 tracer study should be performed once the calibration process is completed.
- ❑ Improve the tracer study to compare the PTM simulations. The number of locations useful for this simulation study was limited to four. The data collection stations should include more stations located throughout the entire Delta. Also, the concentration levels should be high enough as to not become lost to background noise to ensure the collected data are valid.

4.8 References

- Bogle, G. (1997). "Stream Velocity Profiles and Longitudinal Dispersion." *J. Hyd. Eng. ASCE*. 123 (9).
- California Department of Water Resources. (1998). *Temporary Barriers Project: Fishery, Water Quality, and Vegetation Monitoring, 1997*.
- DeLong, L.L., D.B. Thompson, and J.K. Lee. (1995) "FourPt: A model for simulating one-dimensional, unsteady, open-channel flow." Water-Resources Investigations Report 95-XXXX. U.S. Geological Survey.
- Fischer, H.B., E.J. List, R.C.Y. Koh, J. Imberger, N.H. Brooks. (1979). *Mixing in Inland and Coastal Waters*. New York, Academic.
- Oltmann, R. N. (1998). *Measured Flow and Tracer – Dye Data Showing Anthropogenic Effects on the Hydrodynamics of South Sacramento – San Joaquin Delta, California, Spring 1996 and 1997*. United States Geological Survey, Open File Report 98-285.
- RD Instruments. (1996). *ADCP Principles of Operation: A Practical Primer*.
- Wilbur, R. (2000). *Validation of Dispersion Using the Particle Tracking Model in the Sacramento-San Joaquin Delta*. M.S. Thesis. University of California, Davis.

Methodology for Flow and Salinity Estimates in the Sacramento-San Joaquin Delta and Suisun Marsh

**22nd Annual Progress Report
August 2001**

Chapter 5: DSM2 San Joaquin Boundary Extension

Author: Thomas Pate

5 DSM2 San Joaquin Boundary Extension

5.1 Introduction

The purpose of the DWR DSM2 boundary extension is to create a direct dynamic link between the Delta and the state's second longest river, the San Joaquin. Many Delta water supply, water quality, and fishery issues are closely linked to conditions in the San Joaquin River (SJR). Extension of the SJR boundary will provide a tool to investigate how the Delta may respond to different SJR management strategies.

The system domain for this project is the portion of the SJR from near Vernalis to the Mendota Pool (see Figure 5-1). The project was divided into two phases because of substantial gaps in bathymetry data. Phase I is that portion of the domain from the Bear Creek confluence near Stevinson to the current boundary near Vernalis. Phase II is that portion of the domain from Stevinson to Mendota Pool. In general, the SJR boundary extension work reported herein is limited to Phase I.

5.2 Description

The SJR Basin is 290 miles long and averages about 130 miles wide, encompassing approximately 32,000 square miles, or one-fifth of California. The SJR flows west from its headwaters in the Sierra National Forest, then north along the southern Central Valley floor to the Sacramento-San Joaquin Delta.

Within the Phase I boundaries, there are three major eastside tributaries draining portions of the Sierra-Nevada western slope:

- ❑ Stanislaus River
- ❑ Tuolumne River
- ❑ Merced River

These tributaries primarily convey spring snowmelt with some rainfall runoff and agricultural drainage from the lower reaches. The water quality of these sources is generally good.

There are five tributary streams on the westside draining portions of the Diablo Coastal Range eastern slope:

- ❑ Hospital/Ingram Creek
- ❑ Del Puerto Creek
- ❑ Orestimba Creek
- ❑ Mud Slough
- ❑ Salt Slough

Rainfall runoff is relatively sparse along the eastern slope of the coastal range due to a rain shadow effect. These tributaries primarily convey agricultural drainage most of the year with some rainfall runoff during storm events. The water quality of these sources is relatively poor.

The agricultural activities influencing the SJR within the Phase I boundaries can be compartmentalized into two components:

- Eastside Agriculture
- Westside Agriculture

The eastside is fairly well organized and accountable with a small number of irrigation districts and a clearly defined plumbing system. The westside can be characterized as just the opposite.

There are only three identified municipal discharges to the SJR within the Phase I boundaries:

1. Newman Wastewater Treatment Plant
2. Turlock Wastewater Treatment Plant
3. Modesto Wastewater Treatment Plant

There are no significant industrial discharges identified within the Phase I boundaries (Kratzer et al. 1987).

5.3 Model Geometry Development

A set of USGS 7.5-minute topographic maps encompassing the project area was used to discretize the domain into 92 reaches with 93 nodes (Phase I & II). The locations of the nodes generally correspond to a hierarchy of major tributaries, possible point sources of inflow and outflow, or convenient landmarks. The geographic coordinate of each node was manually measured from the maps using the Universal Transverse Mercator, Zone 10 (UTM) reference system. The length of each reach was manually measured from the maps using a digital planimeter. Three values per reach were measured then averaged. The reaches are approximately 1 to 2 miles long.

Bathymetry data for the system domain were obtained from the U.S. Army Corps of Engineers (USACE). The data were transformed from the latitude/longitude coordinate system to the UTM coordinate system using “Corpscon,” public domain software developed by USACE. The transformed bathymetry data and nodal coordinates were then input into DWR’s Cross Section Development Program (CSDP).

CSDP was used to define the system geometry, such as channel alignment and cross sections, for input to DSM2. The model’s river reaches were defined by aligning centerlines to follow the thalweg (low flow channel) that was visually located from the bathymetry data graphically displayed in CSDP. A new function was added to CSDP that calculates the reach length from the aligned centerlines. However, special care is necessary for this function to give sufficient results. The thalweg can be difficult to visually extract from the data and is highly sinuous. The placement of many short centerline segments may be necessary to accurately define a meandering channel alignment. Many short segments were used to describe the channels in

CSDP. As a benchmark, the reach lengths computed by CSDP were compared to the manual planimeter measurements. The total net difference overall between the two methods was approximately 2 feet, with CSDP yielding the greater length.

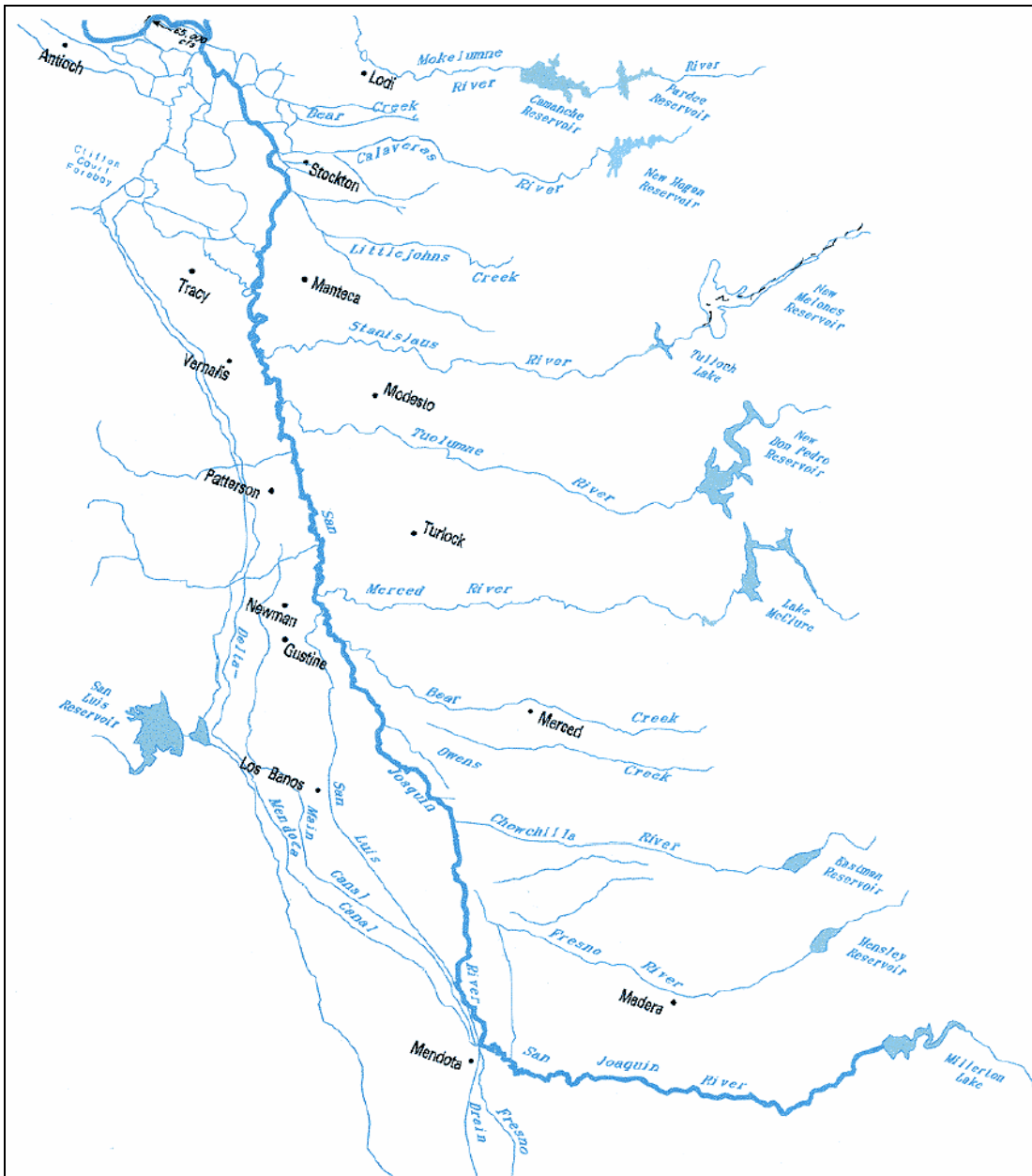


Figure 5-1: San Joaquin River.

Irregular cross sections were developed using CSDP to approximate the river’s existing natural shape. Every channel has at least one representative irregular cross section and some have as many as three. Engineering judgement was used to distinguish a realistic cross section from the bathymetry data displayed near chosen locations. In most cases, the thalweg of the cross section was well defined but the floodplain was not. Digital aerial photos were used to reasonably approximate the shape and extent of the flood plains.

Even with the use of irregular cross sections, DSM2 still requires the definition of two rectangular cross sections per channel segment. These rectangular cross sections are only used if there is not at least one irregular cross section in a given channel segment. Therefore, a homogeneous rectangular cross section width of 500 feet was specified at the upstream and downstream sides of each node with a linear bottom slope between nodes. The slope was calculated using the change in channel elevation from the upstream boundary near Stevinson to Vernalis, approximately 60 feet (msl) to 0 feet (msl), respectively, divided by the number of reaches between those locations. A stage of 12 feet above the bottom elevation was specified for the initial condition.

5.4 Geometry Refinement

A mock planning study was developed for the model's first trial run.. The purpose of this exercise was to test the planning mode input files and new geometry for design flaws. A few select periods with hydrologic conditions representative of dry, normal, and wet scenarios were chosen. The hydrology for the Delta and major SJR tributaries was obtained from the DWR Planning Simulation Model (DWRSIM). Agricultural consumptive use was not readily available for the SJR and was neglected for these preliminary simulations.

The major problem encountered in the first trial run was posed by channels drying up for the dry hydrologic scenario. DSM2 will not allow a discontinuity in the flow regime and model calculations will not proceed if a channel dries up. This error can typically be attributed to large changes in cross sectional area or dramatic changes in bottom elevation between irregular cross sections.

A systematic approach was developed to debug the geometry design. The model was run until a channel segment dried up, then the irregular cross section(s) associated with that channel segment was (were) removed and the model run again. If no irregular cross sections are defined for a given channel segment, then the model will default to the rectangular cross section defined for that channel segment. This process was repeated until the model ran to a successful completion. Approximately 40 percent of the irregular cross sections was removed, most of them consecutive and localized to four general areas. This consecutive and highly localized trend suggested that not all of the cross sections removed were problematic.

The bottom elevation of a default rectangular cross section in one channel segment may not closely match the bottom elevation of an irregular cross section in a neighboring channel. This requires the introduction of a continuous block of rectangular cross sections where the elevations of the upstream and downstream ends of this section approximate the elevations of the neighboring irregular cross sections. Also, a problematic cross section may not cause an error in its own channel segment, but may cause an error in other channel segments in close proximity. In some cases where a channel segment had multiple cross sections, only one cross section was the source of error.

Based on these conclusions, a refinement process was conducted to differentiate potentially good cross sections from the problematic ones. Each problem area was investigated independently of the others. Irregular cross sections were reintroduced and removed in systematic combinations

until only a minimal number of irregulars were necessary to be removed to achieve a completed run. This process reduced the number of likely problematic cross sections to approximately 35 percent.

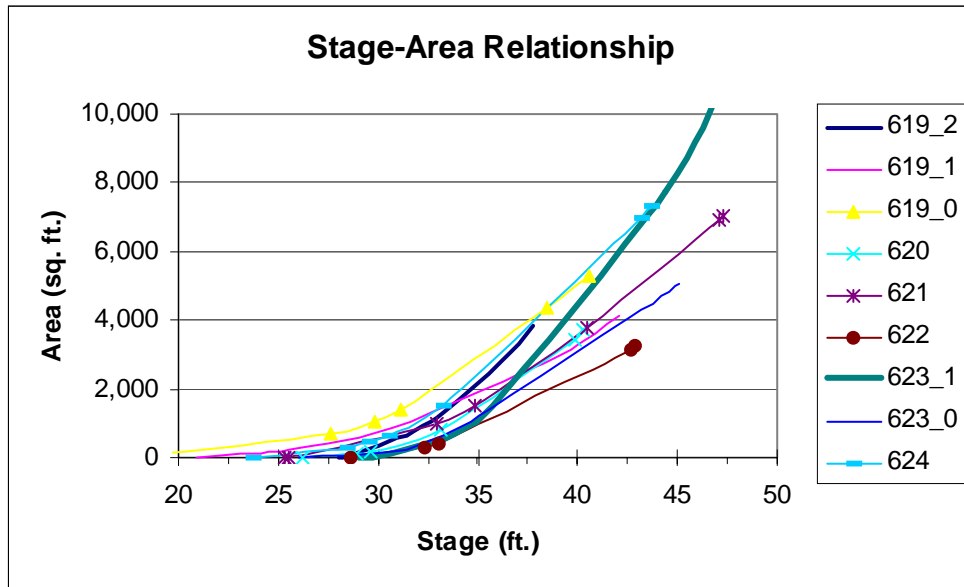


Figure 5-2: Stage-Area Relationship for Channels 619 to 624.

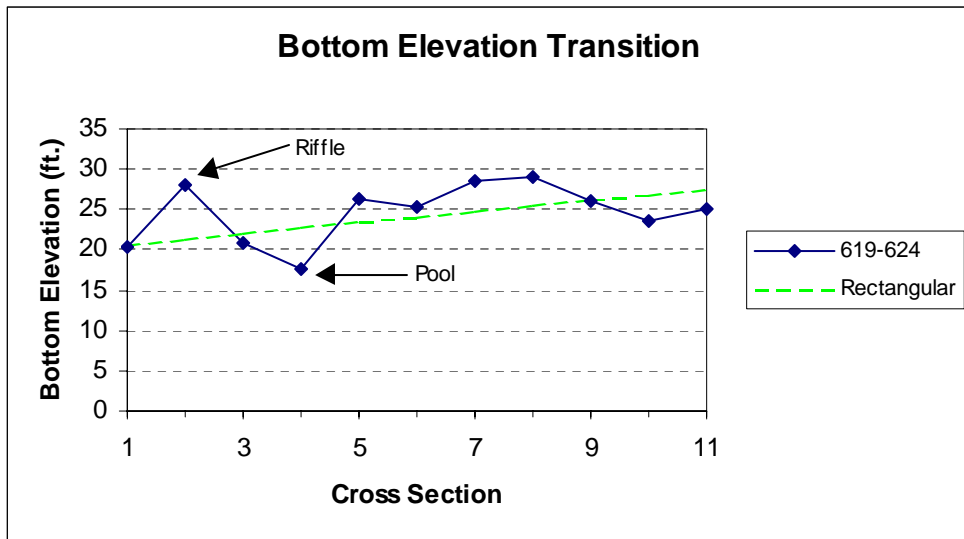


Figure 5-3: Bottom Elevation Transition for the Irregular Cross Sections from Channels 619 to 624.

The next step was to determine which cross section was the likely source of the problem. Two visualization methods were applied. The first method was to plot a family of stage to cross sectional area relationship curves for both the problematic cross section and a few cross sections upstream and downstream of that location (see Figure 5-2). The other method was to sequentially plot the bottom elevations of a problematic cross section and a few neighboring

cross sections (see Figure 5-3). These tools were valuable assets in determining which geometric attribute was most likely causing the problem. In all cases, the bottom elevation transition was found to be the problem. The model generally experienced channel drying with changes in elevation greater than 5 feet between cross sections.

Some of the deep pools and shallow riffles needed to be averaged. The bottom elevations of the corresponding rectangular cross sections were superimposed on a “bottom elevation transition” plot such as shown in Figure 5-3. This provided a reference baseline to a working slope since the model ran successfully when those cross sections were used as substitutes. The bathymetry data were revisited to determine a better location in the channel to draw a representative cross section with a bottom elevation closer to this baseline. In a few cases where a channel had more than one irregular cross section, a surplus section was deleted when relocation failed. After some iteration, the model ran to a successful completion without substitution of rectangular cross sections.

5.5 Historical Study Development

A historical study was developed to calibrate the DSM2 model extension for the HYDRO and QUAL modules. Flow (cfs) and stage (Feet, MSL) were simulated for HYDRO and salinity (EC) for QUAL. The concept of the historical study is to run the model using historical data as the boundary conditions and compare simulated model results to known historical observations.

5.5.1 Development of Boundary Conditions

A mass balance water quality model known as the San Joaquin River Input-Output (SJRIO) model was originally developed by the California State Water Resources Control Board (SWRCB) and University of California, Davis (UCD) staff. SJRIO has been extensively tested and calibrated (Kratzer et al., 1987) and is currently used by Central Valley Regional Water Quality Control Board (CVRWQCB) and the San Joaquin River Management Program Water Quality Subcommittee (SJRMWQS) for water quality predictions. The SJRIO model code, documentation, its developers, and current users were consulted in developing the first-cut boundary conditions for DSM2. The intention was to mimic the source and sink locations and types as closely as possible, and use the assumptions utilized by SJRIO where other data sources could not be located. The following SJRIO model components were considered in the development of DSM2 boundary conditions:

- ❑ SJR at Lander Avenue, the upstream boundary
- ❑ Three eastside tributaries: Stanislaus R., Tuolumne R., Merced R.
- ❑ Five westside tributaries: Hospital/Ingram Cr., Del Puerto Cr., Orestimba Cr., Mud and Salt Sloughs
- ❑ Appropriative and riparian diversions from the SJR and eastside tributaries
- ❑ Surface agricultural discharges, including tail water and operational spills
- ❑ Subsurface agricultural discharges
- ❑ Municipal discharges
- ❑ Natural groundwater accretions or depletions

The evaporation, precipitation, and riparian vegetation water-use components were neglected. SJRIO development, boundary conditions, and assumptions are described in detail by Kratzer et al., 1987.

Research for the best available sources of data was conducted in conjunction with the SJRMP-WQS. In general, there are two types of data: observed or empirical. Six data sources were identified to fulfill the DSM2 boundary data needs and are summarized in Table 5-1.

Table 5-1: Summary of Data Sources for DSM2 Boundary Conditions.

Source	Type	Interval
California Data Exchange Center (CDEC)	Real-Time Monitoring	Hourly
United States Geological Survey (USGS)	Real-Time Monitoring	15 Minute
United States Bureau of Reclamation (USBR)	Historical CVP Operation	Monthly
Local Agencies	Historical Operation	Monthly
CVRWQCB	Historical Grab Sample	Weekly
SJRIO	Empirical Relationship	Variable

These sources are listed in order of desirability due to reliability, time scale interval, and availability. CDEC and USGS are best due to availability at fine time scales.

5.5.1.1 Tributaries

The observed data used to describe the DSM2 tributary boundaries for the calibration period are summarized in Table 5-2. A location map for the USGS and CDEC gauging stations is provided as Figure 5-4.

Table 5-2: Description of Current DSM2 Tributary Boundary Conditions.

Location	Description
Upper SJR	Hourly flow from the DWR SJS gauging station near Stevinson from CDEC and weekly salinity from CVRWQCB grab samples near Stevinson (Lander Avenue).
Merced River (MER)	Hourly flow from the DWR MST gauging station near Stevinson from CDEC and daily salinity from SJRIO.
Tuolumne River (TUO)	Hourly flow from the DWR MOD gauging station at Modesto from CDEC and daily salinity from SJRIO. Flow data has been shifted forward 12 hours to account for gage distance from confluence with SJR.
Stanislaus River (STA)	Hourly flow and salinity from the DWR RIP and USBR RPN gauging stations, respectively, at Ripon from CDEC. Flow data has been shifted forward 12 hours to account for gage distance from confluence with SJR.
Salt Slough (SSL)	15-min flow and hourly salinity from the USGS gauging station 11260000 at Hwy 165 near Stevinson.
Mud Slough (MSL)	Hourly flow and salinity from the USGS gauging station 11262900 near Gustine.
Orestimba Creek (ORE)	15-min flow and salinity from the USGS gauging station 11274538 at River Road near Crows Landing.
Del Puerto Creek (DPC)	15-min flow from the USGS gauging station 11274630 near Patterson. The flow station is located a considerable distance away from SJR confluence allowing drainage to enter ungaged below the station. Some of this ungaged drainage is estimated by SJRIO. Salinity is assumed to be the same as ORE.

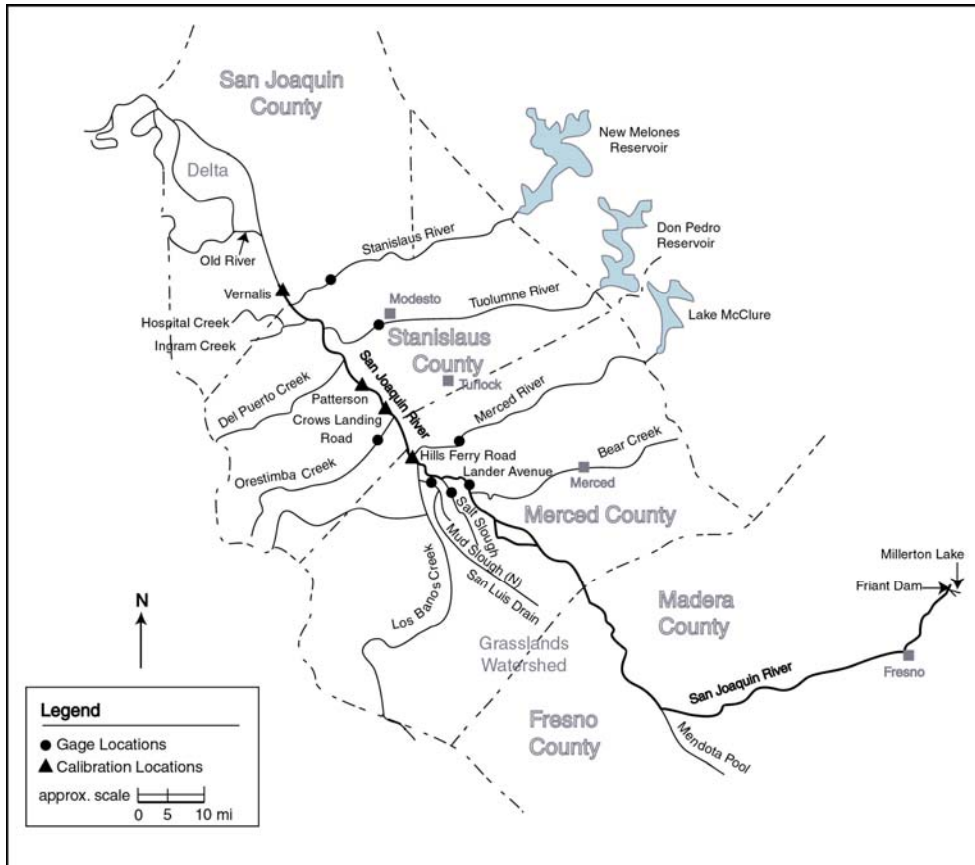


Figure 5-4: Map of Gauging Stations.

Hospital/Ingram Creek (H/I) is an ungaged watershed. Per SJRIO, flow hydrology is calculated as a percentage of ORE based on watershed size, which is approximately 64 percent. H/I salinity is also assumed to be the same as ORE due to geographic similarities.

5.5.1.2 Municipal

The City of Modesto is the only municipality that discharges directly to the SJR. The Modesto Wastewater Treatment Plant (MWWTP) maintains total monthly discharge records. The City of Turlock Wastewater Treatment Plant (TWWTP) discharges indirectly to the SJR and is accounted for later. The City of Newman Wastewater Treatment Plant (NWWTP) uses a system of retention, evaporation, and land disposal. The NWWTP only discharges to the SJR during the rainy season when the disposal site is saturated and unable to assimilate the effluent. NWWTP flow and salinity contributions to the SJR are assumed negligible (Kratzer et al. 1987).

5.5.1.3 Eastside Agriculture

Two large irrigation districts supply water for eastside agricultural (EAG) activities (see Figure 5-5). Modesto Irrigation District (MID) services the area bounded by the STA, SJR, and TUO. The area between the TUO, SJR, and MER is serviced by Turlock Irrigation District (TID). Both of these districts receive irrigation water from offstream storage sources upstream of the gages on the STA and TUO, respectively. Operational spills and agricultural tail-waters from each district are collected and conveyed by canals to point sources on the SJR, TUO, and STA.

MID has approximately 10 canals that combine and discharge to three discrete points and one spreading basin within the study boundaries:

- ❑ Lateral No. 4 (MID#4) spills to the SJR.
- ❑ Lateral No. 5 (MID#5) spills to a slough adjacent to the TUO near the SJR confluence and downstream of the MOD gauging station. This flow was assumed to reach the TUO.
- ❑ Lateral No. 6 (MID#6) spills to the STA above Koetitz Ranch and downstream of the RIP gauging station.
- ❑ Modesto Main Drain (MMAIN) conveys spills from Lateral No. 3 and 7 to Miller Lake.

Miller Lake has the ability to spill into the STA. However, no records of Miller Lake flows into the STA have been found. MMAIN spills are assumed to reach the STA by seepage, thus no time adjustments were made to the data set.

TID has approximately six canals that discharge to six discrete points within the study boundaries:

- ❑ Lateral No. 1 Spill (TID#1) spills to the TUO downstream of the MOD gauging station
- ❑ Lower Lateral No. 2 Spill (TID#2) spills to the SJR
- ❑ Lateral No. 3 Drain (TID#3), a.k.a. Westport Drain, discharges to the SJR
- ❑ Lateral No.5 Drain (TID#5), a.k.a. Carpenter Drain, discharges to the SJR
- ❑ Lateral No. 6 and 7 Spills (TID6&7) combine and spill to the SJR
- ❑ Lower Stevinson Spill (TID_LSTV) spills to the MER downstream of the MST gauging station

These six canals compound drainage from seven other canals in the TID network:

- ❑ TID#3 combines drainage from Lower Laterals (LL) #2.5 and #3
- ❑ TID#5 combines drainage from Lower Lateral Spills (LL) #4, #4.5 and #5.5
- ❑ Lateral Spills (L) #5 and #5.5. The TWWTP also discharges treated wastewater into L#5

This information was used to reconstruct portions of incomplete data sets at some discharge points when possible.

The eastside districts maintain monthly total flow records relatively close to the release points. Flow data were not available for TID#1. Some sparse salinity data were also maintained and used to determine some average “static” salinity values for quality of these sources.

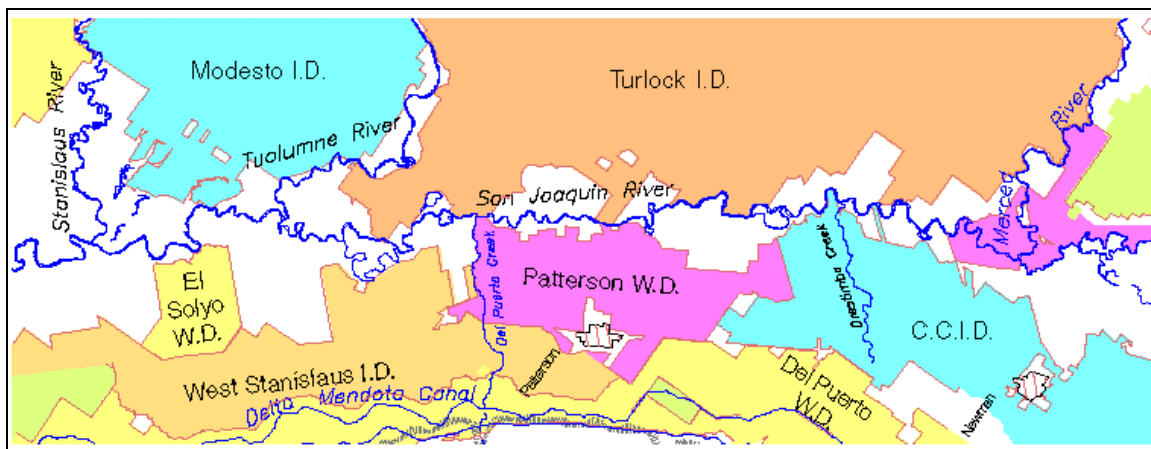


Figure 5-5: Boundaries of Relevant Public Agencies.

5.5.1.4 Westside Agriculture

Currently, five entities supply irrigation water for westside agricultural (WAG) activities (see Figure 5-5):

- ❑ El Solyo Water District (ESWD)
- ❑ West Stanislaus Irrigation District (WSID)
- ❑ Patterson Water District (PWD)
- ❑ Del Puerto Water District (DPWD)
- ❑ Central California Irrigation District (CCID)

There are three sources of water used for irrigation on the westside: SJR diversion, Central Valley Project (CVP) deliveries, and pumped groundwater. The only observed data currently available are CVP deliveries by the USBR and total monthly diversions from the SJR maintained by ESWD, WSID, and PWD. These three districts are referred to as the “BIG3” per SJRIO.

Diversions data were obtained from the BIG3 for the historical simulation period. Other districts' diversions are estimated by river mile using a relationship developed for SJRIO (Kratzer et al. 1987). This formulation is based on applying monthly average usage to maximum allowable diversion ratios of the BIG3 from

$$x_i^{t_a} = \frac{\sum_{i=1}^{12} Q_i^t}{Q_{\max_i}} \Rightarrow \bar{x}^{t_a} = \frac{\sum_{i=1}^3 x_i^{t_a}}{3}, \forall i, t, t_a \in \Omega \quad [\text{Eqn. 5-1}]$$

where:

Q = flow in (AF),
 Q_{\max} = maximum allowable diversion,
 x = annual diversion ratio,
 \bar{x} = average annual 'Big3' diversion ratio,
 t = month,
 t_a = year,
 i = 'Big3' diverters, and
 Ω = time/space domain.

The maximum allocations of the other districts are distributed to assigned river miles by

$$Q_j^{t_a} = \left[\frac{Q_{\max_j}}{12} \right] \bar{x}^{t_a}, \forall j, t_a \in \Omega \quad [\text{Eqn. 5-2}]$$

$$Q_j^t = \left[\sum_{i=1}^3 \frac{Q_i^t}{Q_i^{t_a}} \right] Q_j^{t_a} \lambda_j^t, \forall j, t \in \Omega \quad [\text{Eqn. 5-3}]$$

where:

j = SJRIO river mile, and
 λ = month of use.

The SJRIO river mile to DSM2 node and af to cfs conversion function is

$$\hat{Q}_n^t = \xi \sum_j^{\forall j \in n} Q_j^t, \forall n, t \in \Omega \quad [\text{Eqn. 5-4}]$$

where:

\hat{Q} = flow (cfs),
 n = DSM2 + SJR node, and
 ξ = acre - ft \rightarrow cfs conversion.

In addition to the five appropriative diverters, there are also riparian diverters whose diversion rights precede formal agreements. These diversions are ungaged and estimated by river mile from assumed acreage, crop type, and crop water demand per SJRIO (Kratzer et al. 1987) as

$$Q_i^t = \sum_{j=1}^3 \frac{A_{ij} h_j^t}{12}, \forall i, t \in \Omega \quad [\text{Eqn. 5-5}]$$

$$\hat{Q}_n^t = \xi \sum_i^{\forall i \in n} Q_i^t, \forall n, t \in \Omega \quad [\text{Eqn. 5-6}]$$

where:

A = crop acreage,
 h = water applied to crop (inches),
 i = SJRIO rivermile, and
 j = crop type.

The crops for the riparian users are almonds, corn, and pasture. Cropping patterns are assumed to remain the same throughout the calibration period.

Agricultural return flows are estimated by applying an efficiency factor to all of the sources of irrigation water by river mile. The tail-water typically totals 30 percent of the water supplied per source. The return calculation has four components contributing to tail-water flows per SJRIO (Kratzer et al. 1987): CVP deliveries to appropriative districts, the BIG3 SJR diversions, all other SJR diversions, and groundwater pumped from shallow aquifers. These components are combined to estimate the WAG return flows to the SJR as

$$Q_{R_i}^t = \sum_{j=1}^{10} Q_{CVP_j}^t X_{CVP_j} + \sum_{l=1}^3 Q_{BIG_l}^t X_{BIG_l} + \sum_m^{\forall m \in i} Q_{DIV_m}^t X_{DIV_m} + \sum_{k=1}^{13} (Q_{GW_k}^t Y^t) X_{GW_{ik}}, \forall i, t \in \Omega \quad [\text{Eqn. 5-7}]$$

$$\hat{Q}_{R_n}^t = \xi \sum_i^{\forall i \in n} Q_{R_i}^t, \forall n, t \in \Omega \quad [\text{Eqn. 5-8}]$$

where:

R = drainage return,
 X = return factor (%),
 Y = temporal distribution (%),
 CVP = Central Valley Project deliveries,
 BIG = 'Big3' diversions,
 DIV = other SJR diversions,
 GW = groundwater pumping,
 i = SJRIO river mile,
 j = water/irrigation district,
 k = township,
 l = 'Big3' diverter,
 m = SJR diverter, and
 t_y = similar year type.

USBR maintains records of CVP deliveries to the districts. The CVP component was originally based on 10 appropriate districts; however, DPWD acquired six of the 10 in 1995. Since the simulation period is post-1995, the DPWD deliveries needed to be synthetically redistributed to maintain the original assumption of 10 districts. This was achieved by computing the historical average percent of the total DPWD and other six districts among each individual district from data prior to 1995. The historical average percent was then used to divide up the DPWD deliveries after 1995 into pseudo water districts to mimic the original 10. It is assumed that post-1995 geographical water use remains consistent with pre-1995 usage.

Groundwater pumping is estimated using information from USGS. Annual groundwater pumped for 13 townships along the SJR in the project area for water years 1961 to 1977 was originally based on consumptive use of water and power consumption records (Kratzer et al. 1987). The average of each of the four water year types: critically dry, dry, normal, and wet, are used based on the simulation year type in DSM2 per SJRIO.

As previously mentioned, diversions by the BIG3 are known and all other diversions are estimated. The return factors for each of the four sources per river mile was obtained from SJRIO and Kratzer et al., 1987.

The salinity of the WAG agricultural return flows is estimated using a flow-weighted mass balance for each source contribution to a node defined as

$$C_n^t = \frac{\left[\sum_j^{\forall j \in n} \hat{Q}_{R_{CVP_j}}^t \right] (C_{CVP}^t + C') + \left[\sum_k^{\forall k \in n} \hat{Q}_{R_{SJR_j}}^t \right] (C_{SJR}^t + C') + \left[\sum_l^{\forall l \in n} \hat{Q}_{R_{TRB_{nl}}}^t \right] (C_{TRB}^t + C') + \hat{Q}_{R_{GW_n}}^t C_{GW}}{\left[\sum_j^{\forall j \in n} \hat{Q}_{R_{CVP_j}}^t + \sum_k^{\forall k \in n} \hat{Q}_{R_{SJR_j}}^t + \sum_l^{\forall l \in n} \hat{Q}_{R_{TRB_{nl}}}^t + \hat{Q}_{R_{GW_n}}^t \right]}, \quad [\text{Eqn. 5-9}]$$

$$\forall n, t \in \Omega$$

where:

- C = conservative constituent concentration,
- C' = degradation concentration,
- CVP = Central Valley Project contribution,
- SJR = SJR diversion contribution,
- TRB = eastside tributary diversion contribution,
- GW = groundwater pumping contribution,
- j = water/irrigation district,
- k = SJR diversion, and
- l = eastside tributary diversion.

Each source has a different initial quality. Historical salinity data are available for the STA, SJR, and CVP. The TUO, MER, and GW are assumed to have static EC values of 150, 150, and 1000 umhos/cm, respectively. The initial concentration is increased to account for degradation from agricultural activities. A degradation concentration of 150 umhos/cm was used per SJRIO.

Some salinity data were obtained directly from SJRIO and converted from TDS to EC units using a TDS:EC ratio of 0.64 when necessary.

In addition to these returns, there are also nine tile drains on the westside that discharge directly to the SJR. These subsurface drains carry percolated irrigation water that is characterized by low flow and high salinity. Static annual flow and salinity values for each drain were obtained directly from SJRIO. The basis for these values are described by Kratzer et al., 1987.

5.5.1.5 Groundwater

In the original formulation of SJRIO, groundwater accretions and depletions were calculated using a steady-state, 1-dimensional deterministic model based on the Dupuit-Forchheimer assumptions. Groundwater flows to the SJR were calculated monthly per river mile for water years 1979, 1981, 1982, 1984, and 1985. Flows to the eastside tributaries were calculated monthly for the entire reach below the gauging stations to their confluence with the SJR. The details of the groundwater model are described in Kratzer et al., 1987. The results of the groundwater model are given as monthly and annual flow summaries.

The mean monthly groundwater flows were used to create static annual set of monthly distribution ratios by

$$\alpha^{t_m} = \frac{\bar{Q}^{t_m}}{\sum_{t_m=1}^{12} \bar{Q}^{t_m}}, \forall t_m \in \Omega \quad [\text{Eqn. 5-10}]$$

where:

- α = monthly mean flow distribution,
- \bar{Q} = average flow (AF)
- t_m = month of mean year, and
- i = SJRIO river mile.

The distribution ratios are then used to distribute the annual groundwater flows to the SJR per river mile by

$$\bar{Q}_i^{t_m} = \alpha^{t_m} \bar{Q}_i, \forall t_m, i \in \Omega \quad [\text{Eqn. 5-11}]$$

$$\hat{Q}_n^{t_m} = \xi \sum_i^{\forall i \in n} \bar{Q}_i^{t_m}, \forall t_m, n \in \Omega \quad [\text{Eqn. 5-12}]$$

The same formulation given by equations 5-10, 5-11, and 5-12 is used for the tributaries STA, TUO, and MER, except without the “i” subscript. The result yields a set of mean monthly groundwater flows that vary spatially and monthly but are constant on an annual basis. The current version of SJRIO does not use this formulation.

The salinity values associated with the groundwater were obtained from Kratzer et al., 1987. A static salinity is assigned based on river mile.

The necessary boundary conditions for the Delta portion used for the DSM2 simulations were previously developed by the Delta Modeling Section.

5.5.2 Calibration Procedure

The methodology for hydrodynamic calibration is to systematically vary the model parameters for channel roughness, Manning’s ‘n’, throughout the model domain until the “best” convergence between the model output and the historical data is achieved. For the SJR above Vernalis, water quality calibration can only be achieved through boundary input manipulation. The dispersion coefficient has no effect due to the lack of tidal influence upstream of Vernalis. An initial value of 0.035 was chosen for channel roughness and 0.2 for the dispersion coefficient for all channels upstream of Vernalis. These parameter values for DSM2 channels below Vernalis were consistent with DSM2 Calibration Run #49 from the IEP DSM2 Project Work Team calibration effort (see Chapter 2).

Four calibration stations (see Figure 5-4) were selected within the Phase I domain for comparison benchmarks:

- ❑ SJR near Newman, Hills Ferry Road Bridge (NEW), flow only
- ❑ SJR at Crows Landing Road Bridge (CLB), flow and salinity
- ❑ SJR at Patterson Bridge (SJP), flow only
- ❑ SJR near Vernalis at Airport Road Bridge (VER), flow and salinity

These locations were chosen because reliable gauging stations that are independent of the model results are present there and are listed in succession from upstream to downstream. All four stations provide data for stage and flow, but only two have corresponding salinity data.

From a thorough review of these data sources, a calibration simulation time window was chosen. The period of May, 1997 through September, 1999 was selected due to the most comprehensive availability of data at all boundaries.

Stage, flow, and salinity at the four calibration locations were obtained from the HYDRO and QUAL runs, respectively, for the calibration period. The model output was compared to the observed data using time series and error plots for each location. The mean sum of the squared residuals (MSS) was also computed for all acceptable observed values, as

$$e = \sqrt{\frac{\sum_{i=1}^n (\hat{Y}_i - Y_i)^2}{n}} \quad [\text{Eqn. 5-13}]$$

where:

- e = MSS,
- Y = observed value,
- \hat{Y} = model estimated value, and
- n = accepted values of Y

The MSS calculates the average deviation (error) of the model simulation from the observed data and was used as a benchmark to detect subtle differences between successive model calibration runs.

5.5.3 Pre-Calibration Results

A series of approximately 15 HYDRO preliminary calibration runs have been conducted to date. QUAL was run in conjunction with HYDRO beginning with the 10th run. Refinement of the boundary conditions and assumptions were conducted for each successive pre-calibration run until the point of diminishing return was reached. HYDRO Run14a and QUAL Run14 correspond to the best effort pre-calibration model runs given the best available historical data and derived relationships.

5.5.3.1 HYDRO

In general, the HYDRO results showed good trending with the field observations. As flood waves moved through the system, the model properly simulated the rise and fall of the observed hydrographs at the calibration stations. There are usually two annual characteristic flow regimes that occur on the SJR: a high-flow regime during the winter and spring storm season, and a low-flow regime during the summer and fall. The chosen calibration period contains an extreme flood season (1998) and a moderate (1999) one. The model performance was typically good during the low-flow regime (less than 5,000 cfs). However, the model did not perform as well for the high-flow regime from approximately February 1998 through July 1998. The magnitude and phase of the flood waves were typically missed during this period. The model's estimated flood peaks were over- and underestimated inconsistently between the calibration locations. The model's phase consistently lead the observed flood peaks. This phase shift can be distinguished as abrupt spikes on the residual plots that accompany the calibration results for each calibration station below. The MSS residual at the calibration locations increased in the downstream succession, with the greatest propagation of error occurring at VER.

Modeled stage at NEW was typically a good match to the observed data (see Figure 5-6). The model slightly overestimated for the majority of the simulated period. The difference between the modeled and observed flood peak stage was approximately 0.3 feet and averaged about 1.5 feet throughout the high-flow period. Some divergent behavior was exhibited toward the tail end of the simulation period from approximately March 1999 to the end of the simulation period.

DSM2 overestimated stage at CLB during the low-flow period and underestimated during the high-flow period (see Figure 5-7). The difference between the modeled and observed flood peak stage was approximately 1.5 feet. Divergent behavior was also exhibited at this location during the same period.

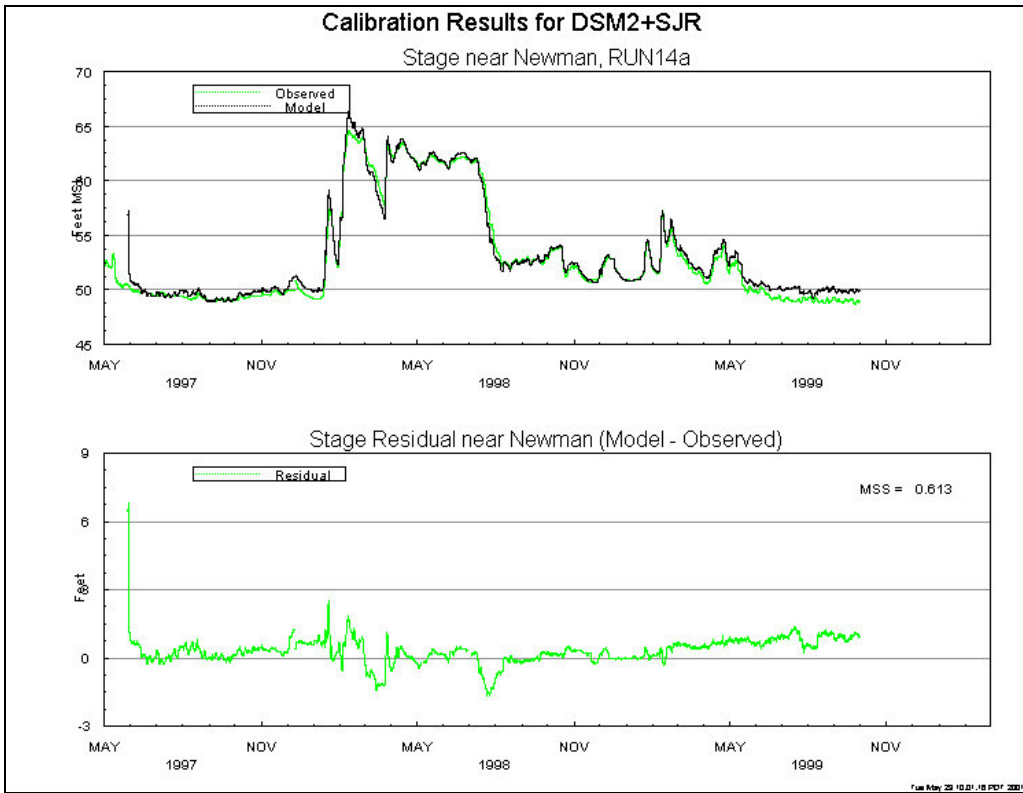


Figure 5-6: DSM2 Pre-Calibration Results for Stage at NEW.

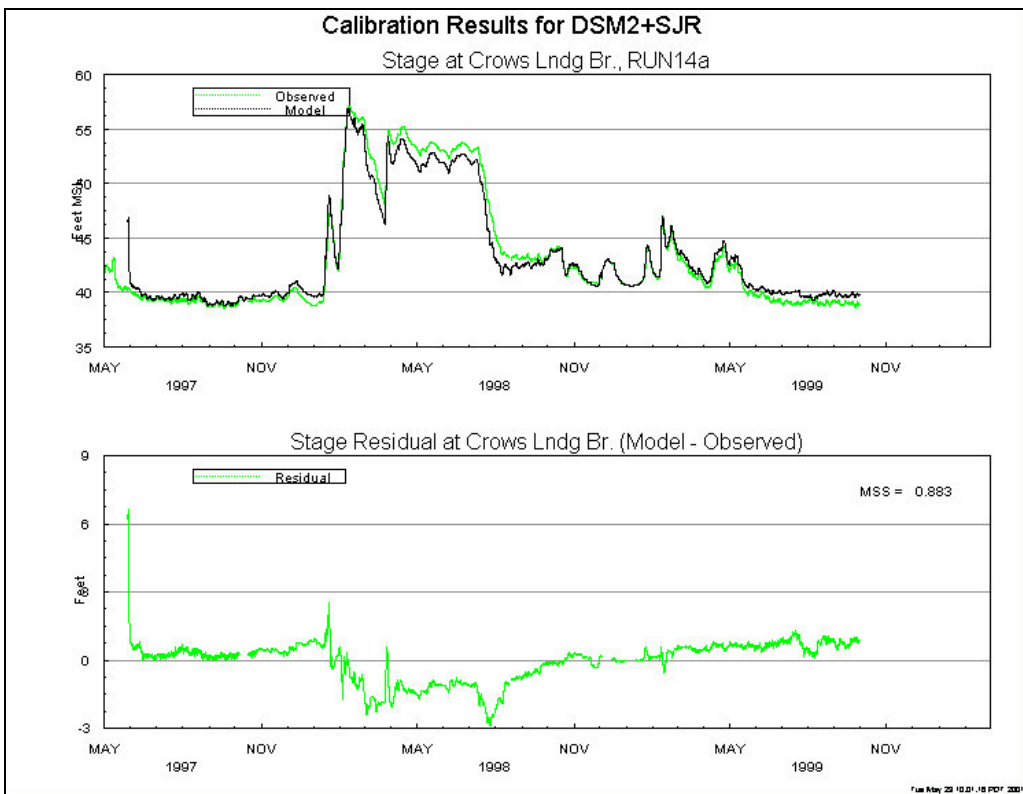


Figure 5-7: DSM2 Pre-Calibration Results for Stage at CLB.

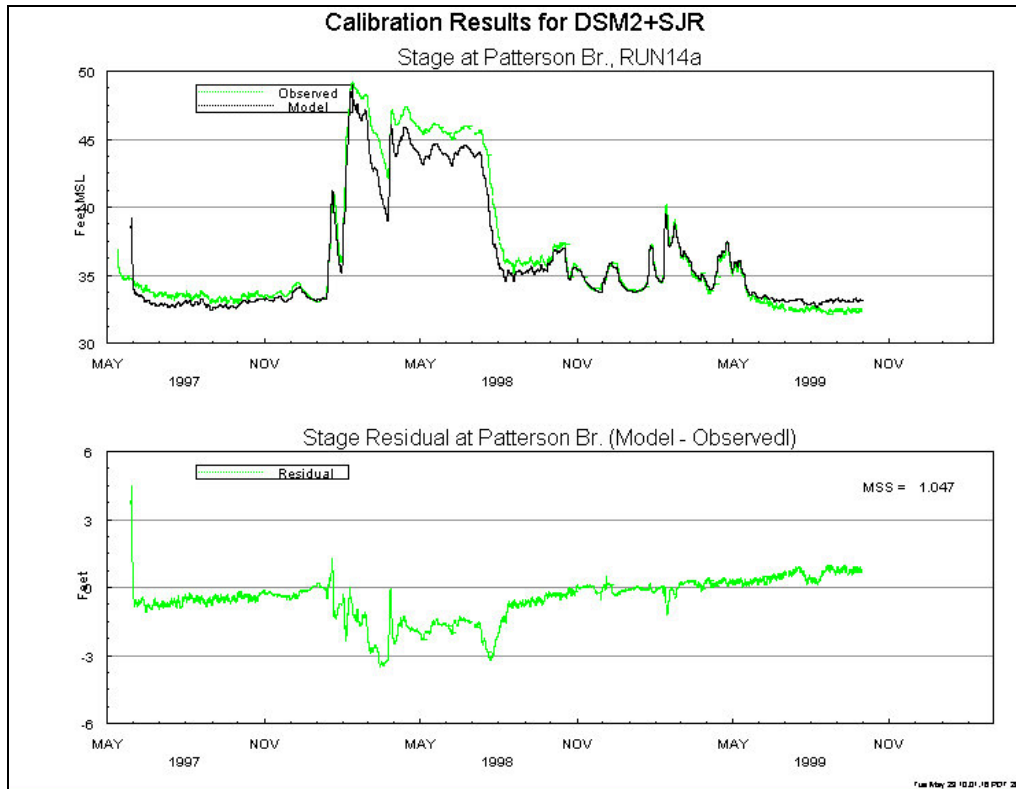


Figure 5-8: DSM2 Pre-Calibration Results for Stage at SJP.

Modeled stage at SJP was underestimated from the beginning of the simulation period through November 1998, and then was overestimated for most of the remaining period (see Figure 5-8). The difference between the modeled and observed flood peak stage was approximately 0.5 feet and averaged about 1.5 feet throughout the high-flow period. Divergent behavior was also exhibited at this location during the same period as at NEW and CLB.

Stage at VER was generally underestimated throughout the majority of the simulation period (see Figure 5-9). The difference between the modeled and observed flood peak stage was approximately 0.5 feet. An average deficiency of about 1.5 feet was exhibited from the beginning of the simulation period through the first low-flow period. As the simulation approached the high-flow period, the model simulation converged toward the observed data. The period from approximately July 1999 to the end of the simulation, the last low-flow period, exhibited an average deficiency of about 0.75 feet with divergent behavior.

In general, DSM2 stage was a good match to the observed data at NEW, CLB, and SJP during the period from November 1998 to March 1999. The front-end and tail-end divergence magnitudes increased in the downstream station progression.

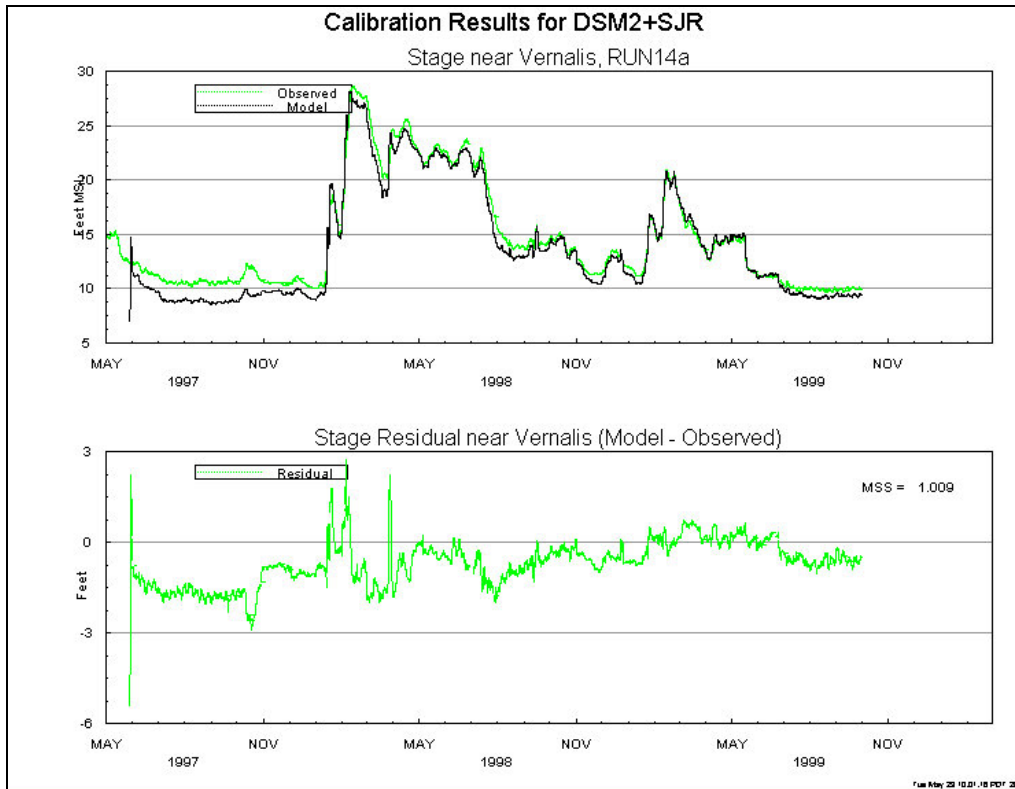


Figure 5-9: DSM2 Pre-Calibration Results for Stage at VER.

Modeled flows at NEW and CLB were an excellent match to the observed flows during the low-flow periods (see Figures 5-10 and 5-11). The model's simulation typically overestimated at NEW and consistently underestimated at CLB. The difference between DSM2 and the observed flood peaks was approximately +2,000 cfs and -3,500 cfs for NEW and CLB, respectively, with DSM2 leading the observed results. The phase shift was approximately eight hours and 15 hours, respectively.

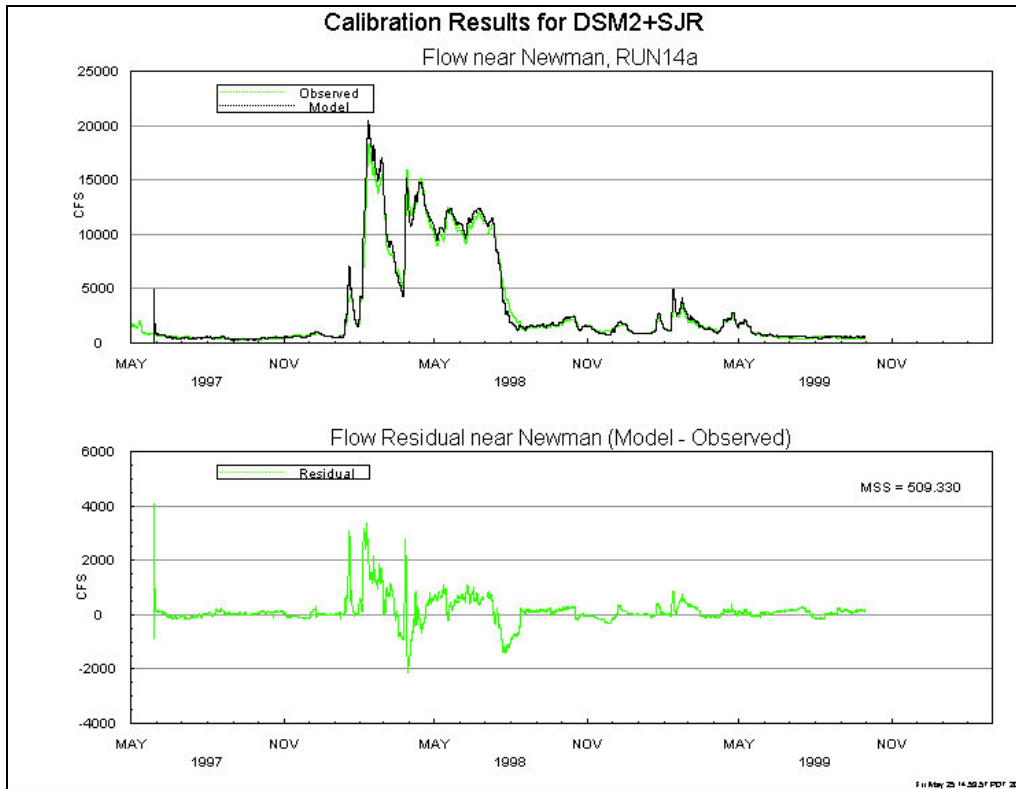


Figure 5-10: DSM2 Pre-Calibration Results for Flow at NEW.

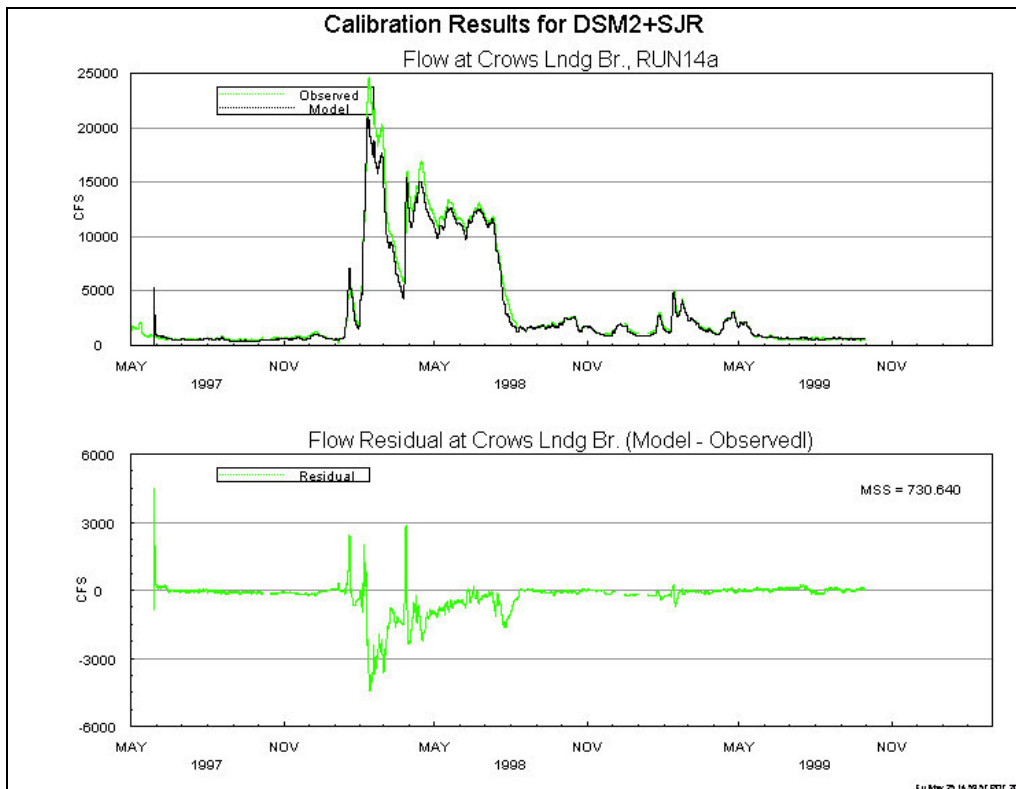


Figure 5-11: DSM2 Pre-Calibration Results for Flow at CLB.

DSM2 generally underestimated the flows during the low-flow period (see Figures 5-12 and 5-13) at SJP and VER. During the high-flow period, flows at SJP and VER were mixed. The magnitude of the flood peak at SJP was overestimated by approximately 2,500 cfs. The largest phase shift at SJP did not occur at flood peak but ranged from 16 to 24 hours at secondary peaks. The magnitude of the flood peak at VER was underestimated by approximately 700 cfs and exhibited a phase shift of approximately 70 hours (see Figure 5-14).

In general, modeled flow was very good at NEW, CLB, and SJP during the period from November 1998 to March 1999. The low-flow regime modeled flow deficit increased with the progression of stations downstream.

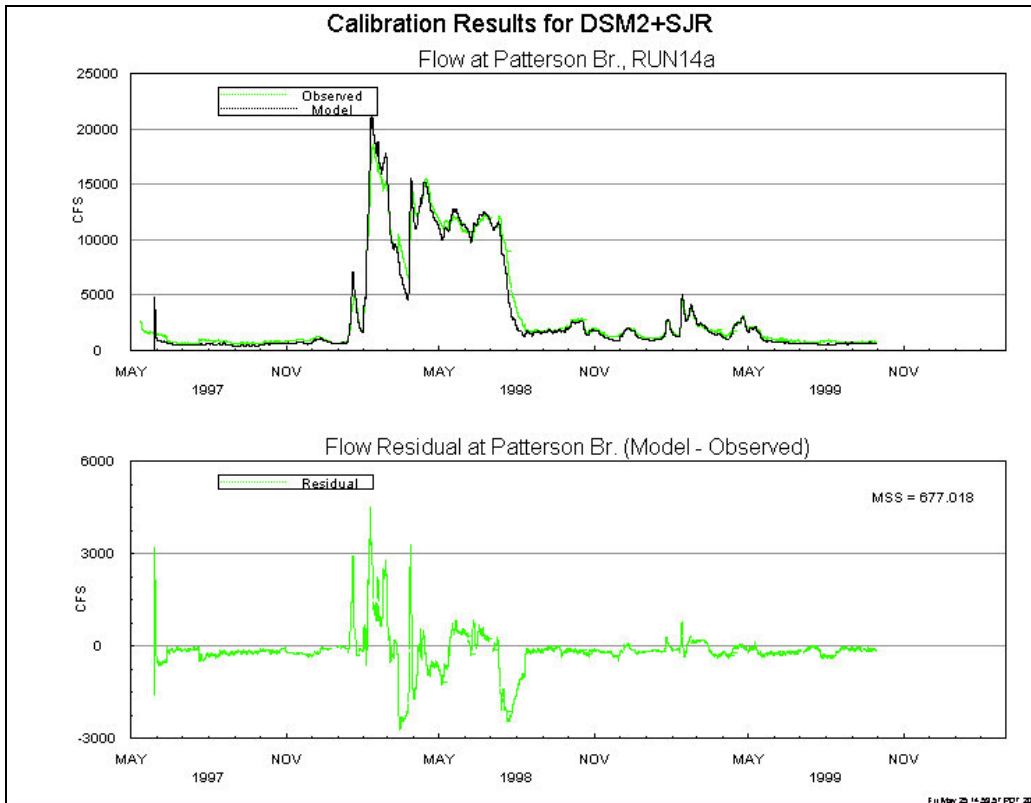


Figure 5-12: DSM2 Pre-Calibration Results for Flow at SJP.

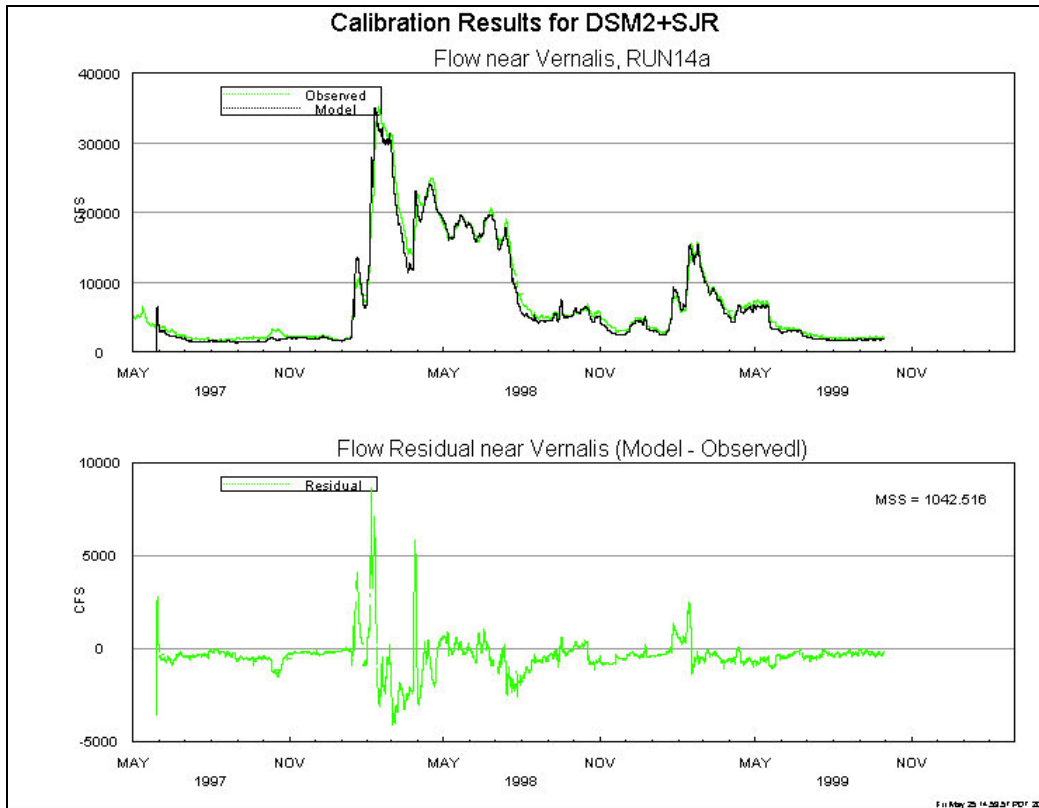


Figure 5-13: DSM2 Pre-Calibration Results for Flow at VER.

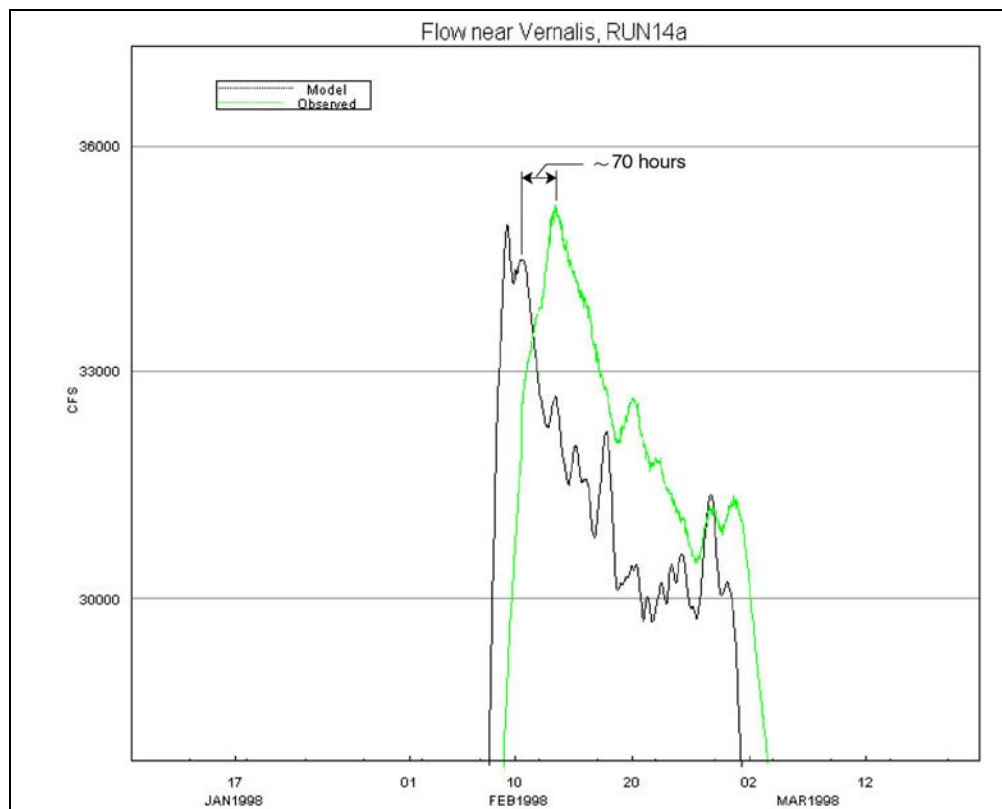


Figure 5-14: Example of Flood Peak Phase Shift at VER.

5.5.3.2 QUAL

In general, the QUAL results showed good trending with the field observations. As poor quality flows moved through the system, the model properly simulated the rise and fall of the observed salinity at the calibration stations. There are usually three annual characteristic salinity regimes that occur on the SJR: a low-salinity regime during the spring prior to the irrigation season; the irrigation season during the summer and fall, which contributes to a moderate-salinity regime due to irrigation tail-water; and a high-salinity regime during the winter storm season that flushes accumulated salts from the land to the river. The model performance was typically good during the low-salinity regime. However, the model did not perform as well for the high-salinity regime.

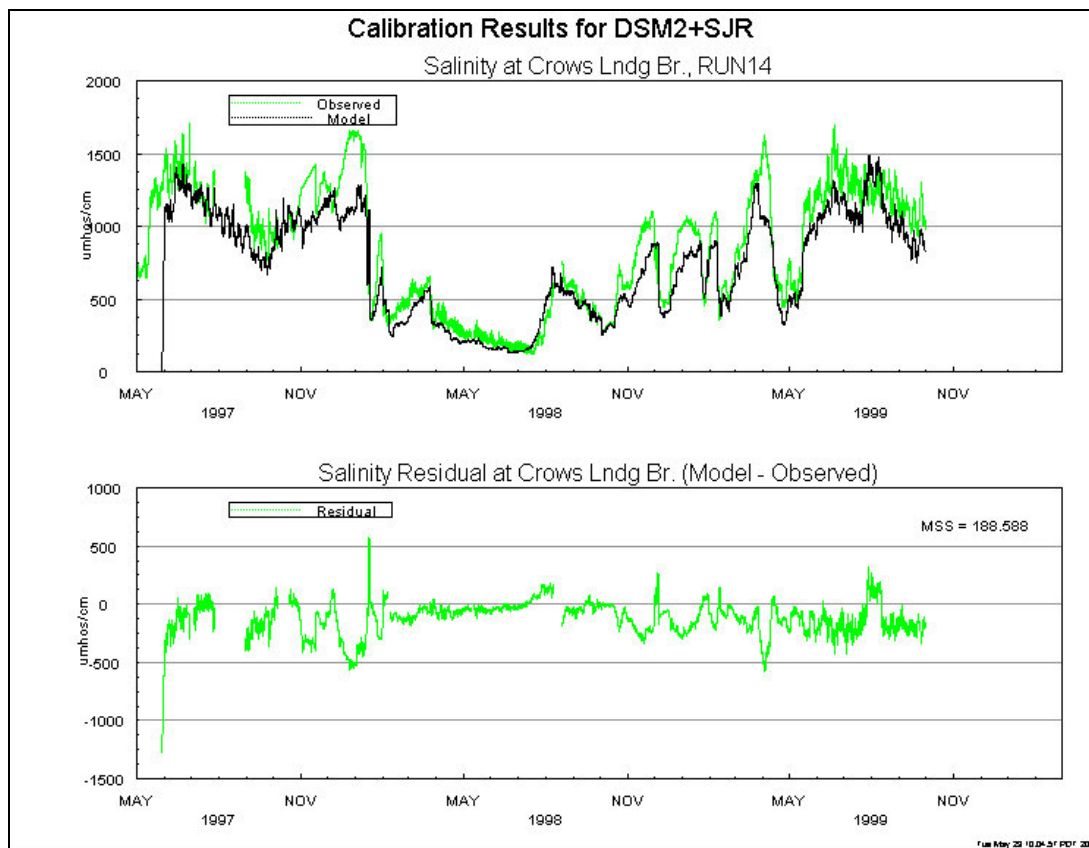


Figure 5-15: DSM2 Pre-Calibration Results for Salinity at CLB.

DSM2 generally under-predicted the salinity at CLB compared to the observed data (see Figure 5-15). The peaks during the high-salinity periods were often missed by an approximate average of 300 umhos/cm. The results were similar at VER (see Figure 5-16) except for the period from January 1998 through October 1998. During this period, the model tended to slightly over-predict the salinity.

As expected, the salinity dramatically decreased from CLB to VER. This is primarily due to contributions from the higher quality Eastside tributaries downstream of CLB, particularly the Stanislaus River.

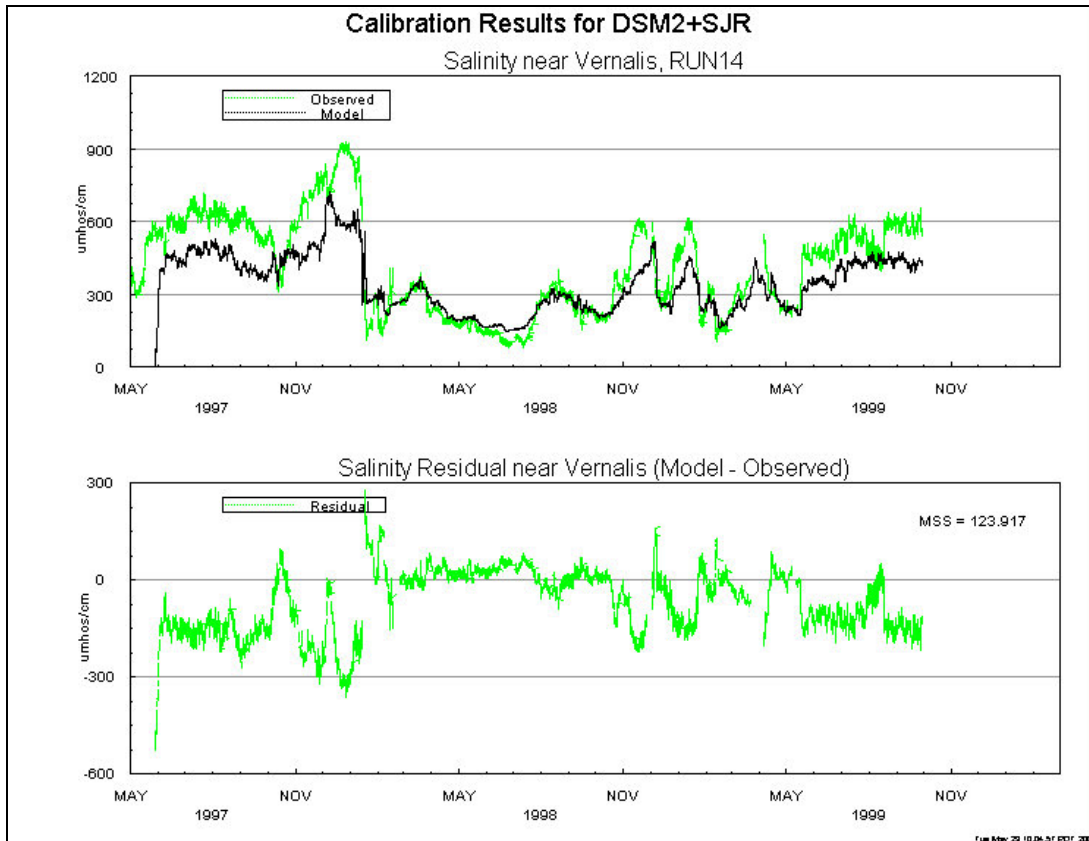


Figure 5-16: DSM2 Pre-Calibration Results for Salinity at VER.

5.5.4 Current Calibration Results

A thorough analysis of the pre-calibration model results compared to the field observations indicated that some information present in the observed data is not being reflected in the boundary conditions outlined previously.

With the exception of the high-flow regime, the simulated flow during the low-flow regime at NEW and CLB are a relatively good match. The corresponding simulated salinity at CLB could be better but the flow is already a good match. Thus, in order to improve the modeled salinity, the representation of the boundary conditions must be improved, which is difficult to do without deviating from some SJRIO assumptions.

In contrast, the low-flow regime at SJP and VER was not as good. The total average simulated flow deficit at VER is approximately 350 cfs during these periods. A closer evaluation of the pre-calibration simulation results shows that 200 of the 350 cfs occurs in the reach between CLB and SJP. The remaining 150 cfs must occur in the reach between SJP and VER. The model consistently under-predicted the salinity by as much as 300 umhos/cm during those periods.

Since there is a significant amount of flow missing, parameterizing Manning's 'n' would be premature at this juncture. The timing of the missing flow coupled with the discrepancy in the salinity leads to the conclusion that the missing water is from a poor quality source such as agriculture tail-water or groundwater base flow.

In order to proceed, a concept termed “add-water” was developed. Constant base flows of 200 cfs and 150 cfs were added to the boundary conditions just upstream of SJP and VER, respectively. HYDRO and QUAL Run18 correspond to the best calibration model run utilizing the add-water concept.

5.5.4.1 HYDRO

Since changes were only introduced downstream of CLB, the HYDRO Run18 results for NEW and CLB are not shown below because they are the same as HYDRO Run14a.

Minor improvement in simulated stage at SJP was achieved between Run14a and Run18 (see Figure 5-19). The MSS value decreased from 1.047 to 1.021 (see Figures 5-8 and 5-17), respectively. More improvement was achieved at VER (see Figure 5-19). The MSS value decreased from 1.009 to 0.731 (see Figures 5-9 and 5-18), respectively. Please note the scale difference of the Y-axis between the two plots in Figure 5-19.

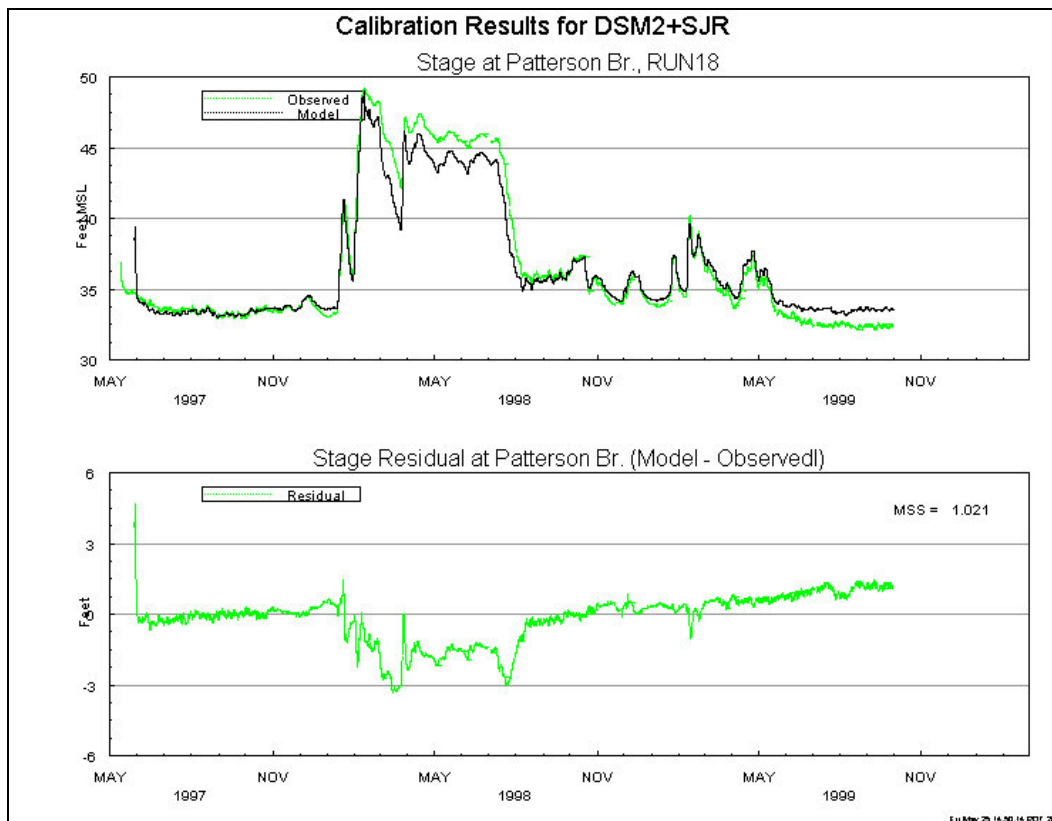


Figure 5-17: DSM2 Calibration Results for Stage at SJP.

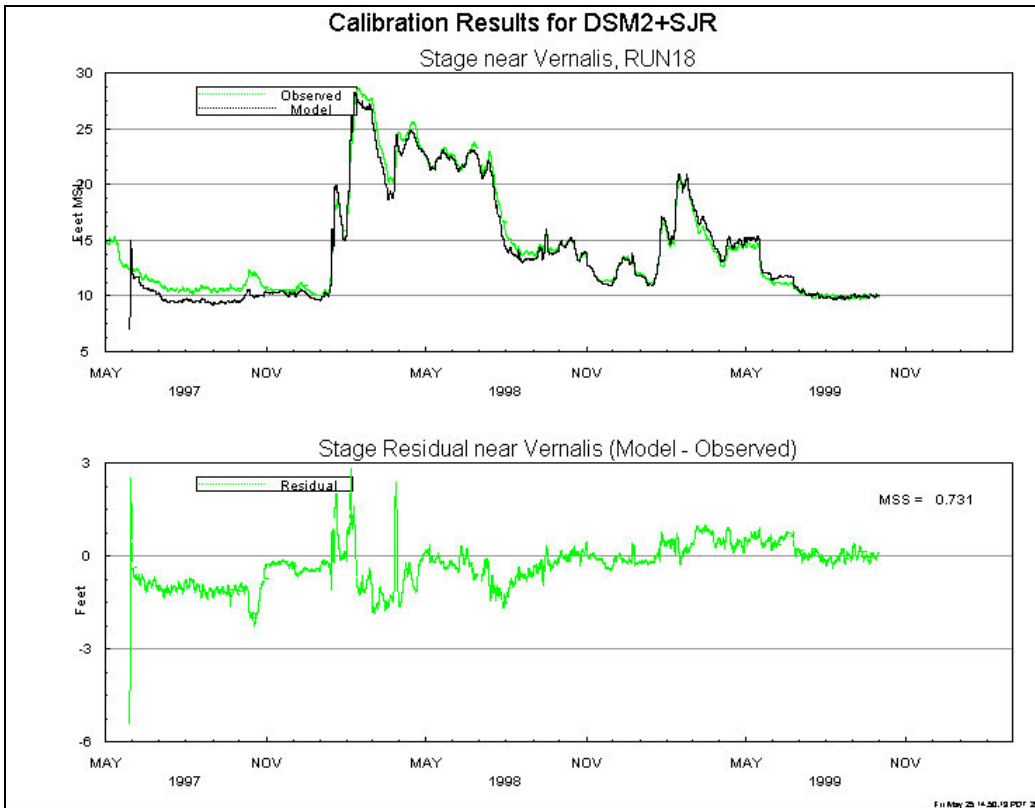


Figure 5-18: DSM2 Calibration Results for Stage at VER.

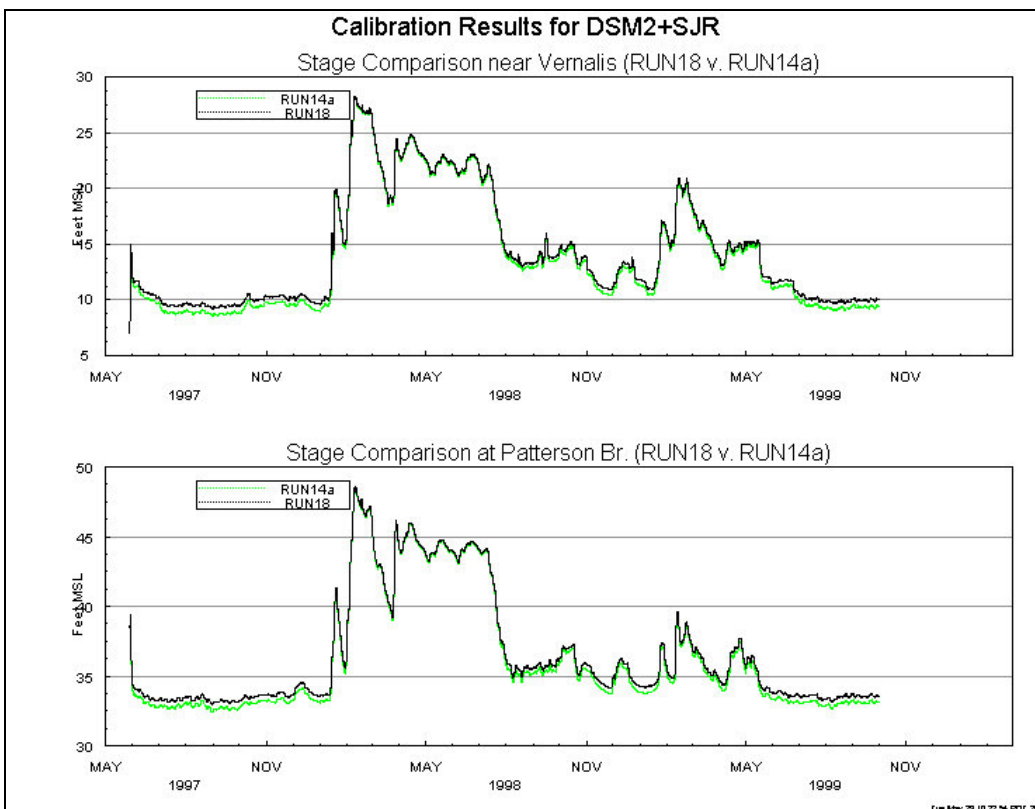


Figure 5-19: Comparison of Pre-Calibration and Calibration Stages at SJP and VER.

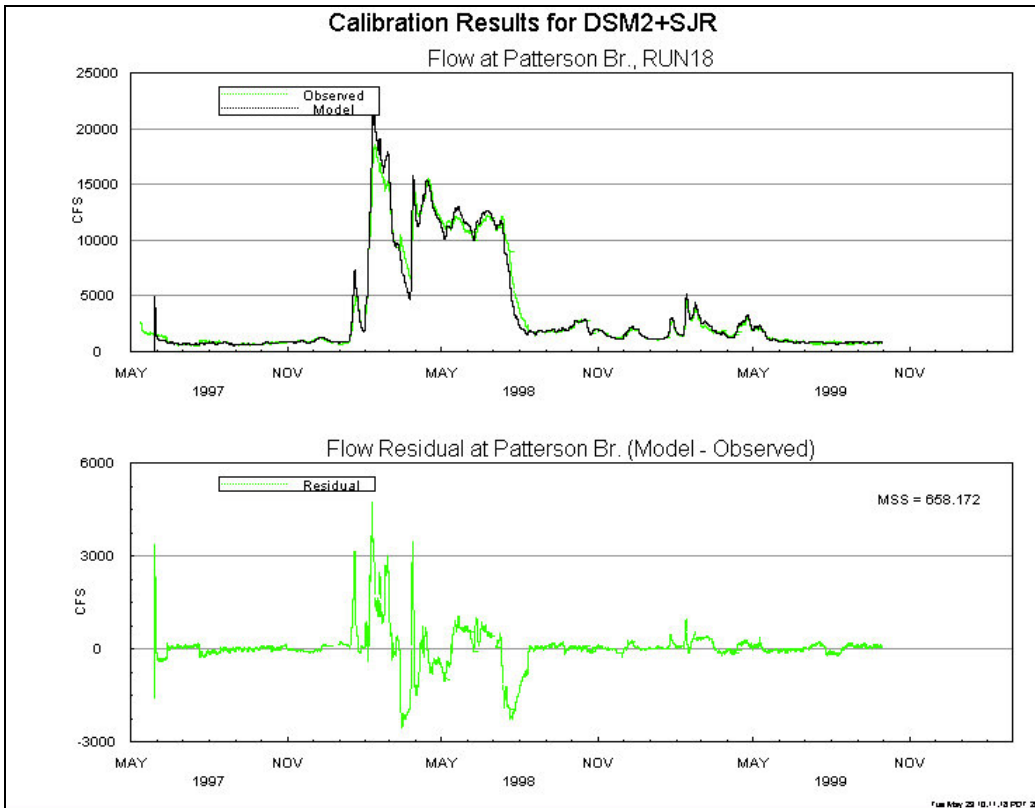


Figure 5-20: DSM2 Calibration Results for Flow at SJP.

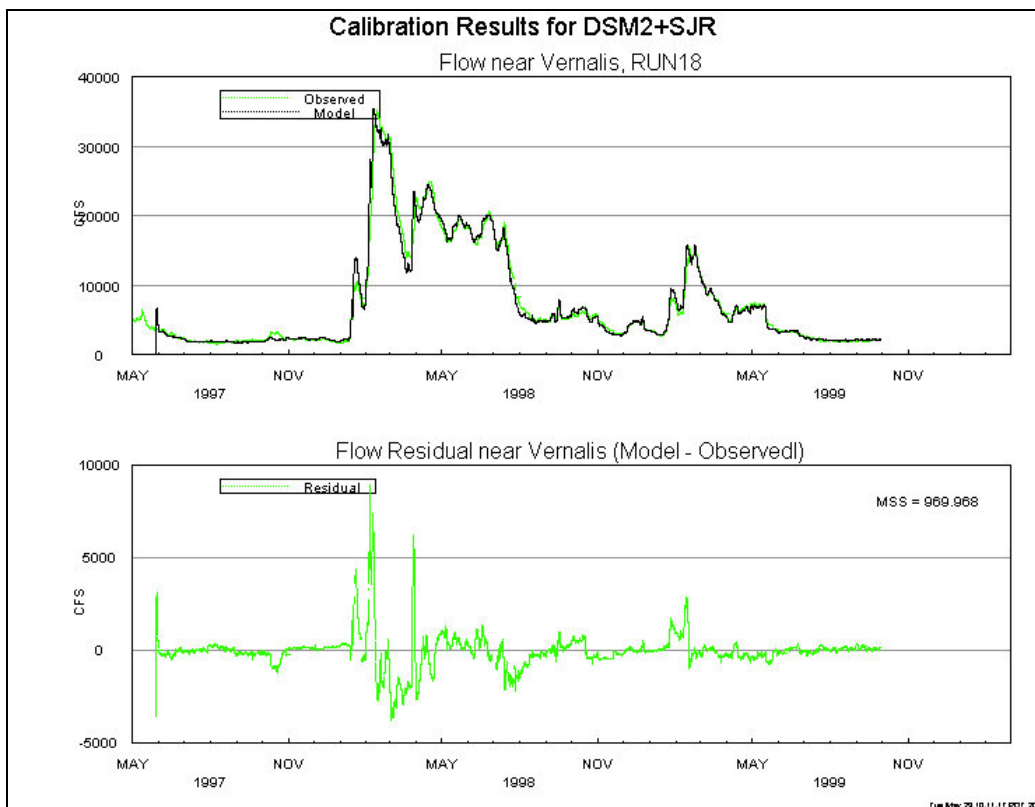


Figure 5-21: DSM2 Calibration Results for Flow at VER.

Significant improvement in simulated flow at SJP was achieved during the low-flow regime between Run14a and Run18 (see Figure 5-22). The MSS value decreased from 677.0 to 658.1 (see Figures 5-12 and 5-20), respectively. Significant improvement was also achieved at VER (see Figure 5-22). The MSS value decreased from 1042.5 to 969.9 (see Figures 5-13 and 5-21), respectively. Please note the scale difference of the Y-axis between the two plots in Figure 5-22.

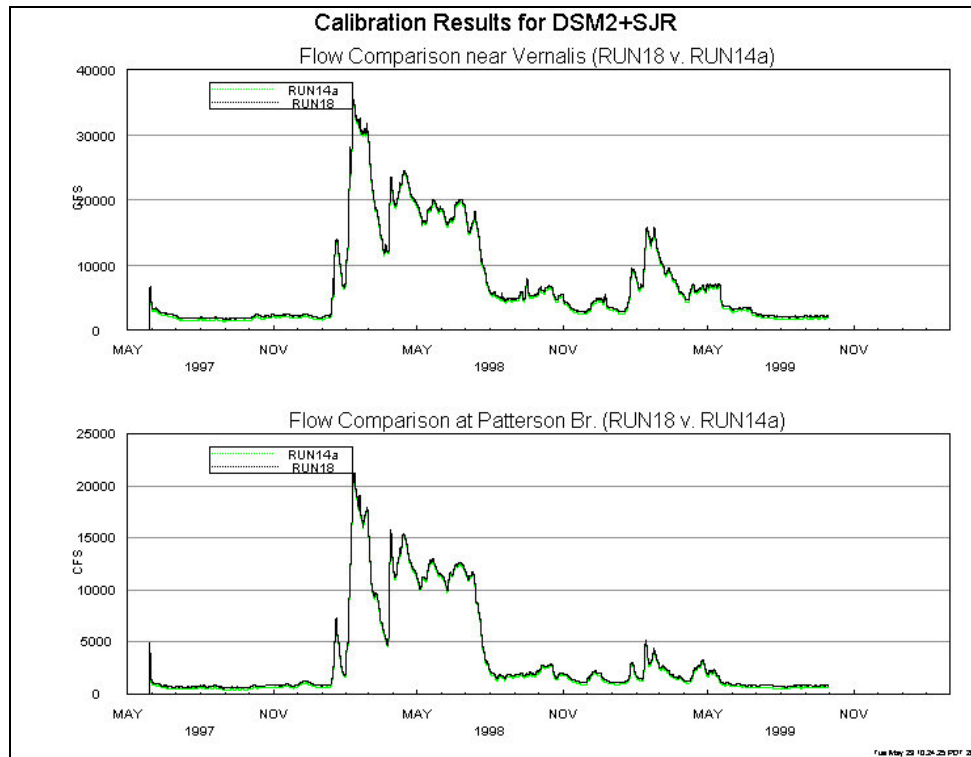


Figure 5-22: Comparison of Pre-Calibration and Calibration Flows at SJP and VER.

5.5.4.2 QUAL

Since changes were only introduced downstream of CLB, the QUAL Run18 results for CLB are not shown below because they are the same as QUAL Run14.

Now that a better flow match was achieved, a reasonable salinity trend needed to be determined to assign to the add-water. Due to the seasonal trend of the flow and salinity deficits, the temporal trend of an agriculture return appeared appropriate, but the magnitude needed to be higher than a typical agriculture return to improve the deficit. After some iteration, a salinity signature was developed with the temporal variability of an agriculture return and a magnitude consisting of a combination of 10% to 30% groundwater and 70% to 90% agriculture tail-water.

This salinity signature produced a significant increase in simulated salinity throughout the calibration period (see Figures 5-23 and 5-24). The MSS value between Run14 and Run18 was 123.9 to 75.7, respectively (a change of approximately 40%). The most significant changes were during the high-salinity regime with little change during the low-salinity regime. This trend is due to dilution of the poor quality add-water by high system flows.

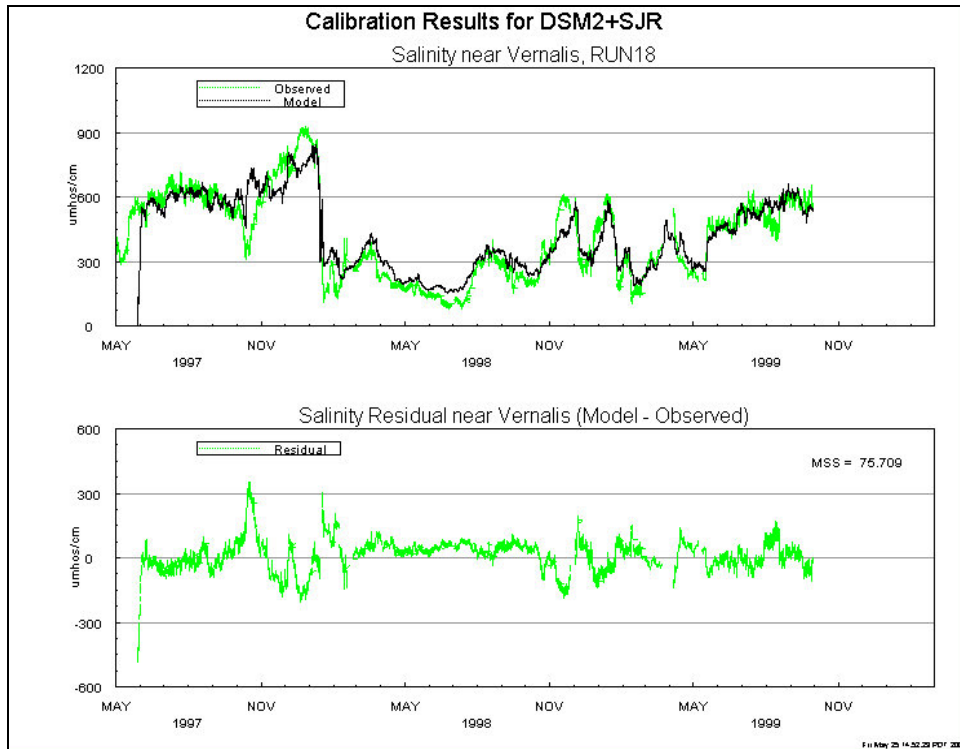


Figure 5-23: DSM2 Calibration Results for Salinity at VER.

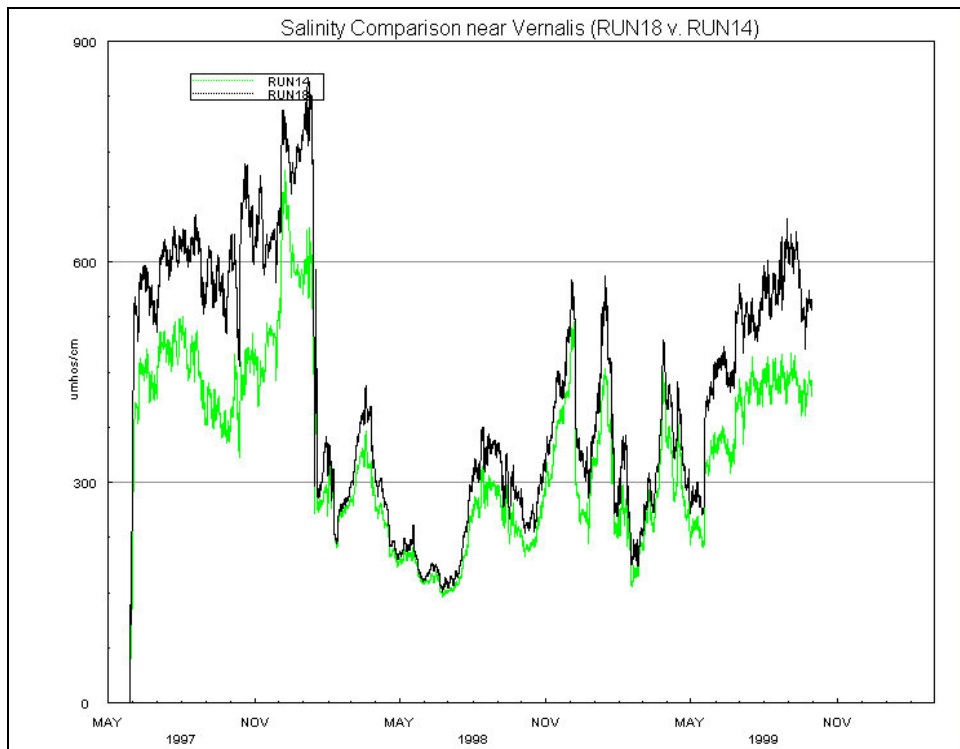


Figure 5-24: Comparison of Pre-Calibration and Calibration Salinities at VER.

5.5.5 Discussion

Some of the inconsistencies between over- and underestimation of stage at the same location during the simulation period such as high and low flow regimes may be explained by scour and deposition phenomenon that occurs in the actual system but is not accounted for by DSM2. These processes can affect the modeling results because the changes in the channel bottom elevation will affect the field stage readings, but the model's channel bottom elevation is fixed and cannot compensate for the higher or lower field reading for the equivalent flow. Possible discrepancies between the field and model's estimated geometry of flood plain representation could also be a factor.

Flow discrepancies between the model and observed values may also be explained by scour and deposition phenomenon. Flows at gauging stations are obtained using developed rating curves that relate the river stage and static geometry to a flow value. These rating curves are not reevaluated as often as the cross section changes. Therefore, if the rating curve is developed for a particular cross section and the geometry of the section changes but the relationship is not updated, then the reported flow will not be accurate. These potentially inaccurate flows are then used as boundary conditions and calibration benchmarks. Possible discrepancies between the field and model's estimated geometry of flood plain representation could also be a factor in flow discrepancies.

Trend discrepancies between stage and flow at the same time and location lend further support to the scour and deposition effects in the simulation results. Sometimes, the stage will over-predict while the flow is under-predicted. Therefore, it may not be reasonable to expect a good match during these extreme flow event periods.

Preliminary investigation of the phase shift has led to suspicion that gage errors may be an important factor. More often than not, gauging stations tend to stop logging or log erroneous data during storm events. Many of the boundary conditions used for this historical study were missing flood peaks and sometimes the entire flood hydrograph. These missing hydrographs and flood peaks had to be estimated using engineering judgement for the most part. Another possible factor could be improper lagging of the eastside tributary flows. Since the gauging stations that provided the Stanislaus and Tuolumne River boundary flows are located approximately 15 miles upstream of their confluence with the SJR, the flows seen at these gages will be seen at the confluences later in time. However, some sensitivity analysis of the lag factor has shown this may not be likely. The rating-curve, geometry, scour, and deposition issues mentioned previously could play a role here as well.

The major weaknesses in the boundary conditions are the westside agriculture and groundwater components borrowed from SJRIO. These relationships were developed almost 20 years ago from a very limited amount of information. The westside agricultural contribution is modeled by static relationships, which are thoroughly documented in Kratzer et al., 1987. Some of the assumptions used to develop these relationships may no longer be representative of the current state of the system. Many water districts have merged, agricultural practices have become more efficient, and land use has changed during that time. The groundwater component is too monotonous to be representative of wet and dry years alike. However, to improve upon the SJRIO assumptions will require a significant amount of time and information to justify changes.

Some new data sources for westside agriculture activities are being developed by the San Joaquin River Management Program Water Quality Subcommittee. Also, the Hospital/Ingram Creek watershed is completely un-gauged and Del Puerto Creek does not have a salinity monitor in conjunction with flow measurement. These tributaries are important contributors of salinity to the SJR.

Some improved boundary condition data will be available in the future due to recent installations of new gauging stations. Salinity monitoring equipment was added at Tuolumne River and SJR near the Stevinson locations. The flow and salinity station at the Merced River location was rehabilitated. New salinity monitoring is proposed for the SJP and SJR at Maze Road locations. These additions will create more salinity calibration locations.

5.5.6 Conclusions

- ❑ The add-water concept can be used effectively to calibrate the DSM2 model. A longer historical simulation period is needed to refine the general assumptions to improve the add-water parameters.
- ❑ The current state of the DSM2 model is an effective tool for studies concerned with low-flow regime issues. Typically, the primary focus of studies in the SJR is during flow periods, so it is not critical for an excellent calibration match during high-flow periods at this time.
- ❑ There are some weaknesses in the boundary conditions that need improvements. The recent installation of some new stations will improve future simulations as new data become available.
- ❑ The empirical relationships inherited from SJRIO need to be replaced with observed data or the derivations updated.

5.6 Future Directions

- ❑ Develop an isolated SJR model (without the Delta) using the nonreflective Martinez stage boundary,
- ❑ Incorporate improved boundary conditions,
- ❑ Conduct a long-term historical validation,
- ❑ Plan study development and linking with CALSIM II,
- ❑ Extend model grid to the Eastside tributary reservoirs, and
- ❑ Extend Phase II to the Mendota Pool.

5.7 References

Kratzer, C.R., P.J. Pickett, E.A. Rashmawi, C.L. Cross, and K.D. Bergeron. (1987). *An Input-Output Model of the San Joaquin River from the Lander Avenue Bridge to the Airport Way Bridge*. Technical Committee Report No. W.Q. 85-1. California State Water Resources Control Board.

Methodology for Flow and Salinity Estimates in the Sacramento-San Joaquin Delta and Suisun Marsh

**22nd Annual Progress Report
August 2001**

Chapter 6: Dissolved Oxygen and Temperature Modeling Using DSM2

Author: Hari Rajbhandari

6 Dissolved Oxygen and Temperature Modeling Using DSM2

6.1 Introduction

Low dissolved oxygen (DO) levels are of concern in the San Joaquin River (SJR) in the vicinity of Stockton because they frequently fall below the U.S. Environmental Protection Agency (EPA) standard of 5 mg/l for aquatic health and the Regional Water Quality Control Board standard of 6 mg/l for upstream migration of fall-run Chinook salmon. The Total Maximum Daily Load (TMDL) Stakeholder process was created for this portion of the SJR to meet the water quality standards established by the Federal Clean Water Act. This chapter focuses on the Section's work to characterize the spatial and temporal distributions of DO and related water quality variables in the river by enhancing DSM2-QUAL (QUAL). This enhanced version of QUAL can be used to identify the principal factors that may contribute to low DO levels in this reach of the SJR.

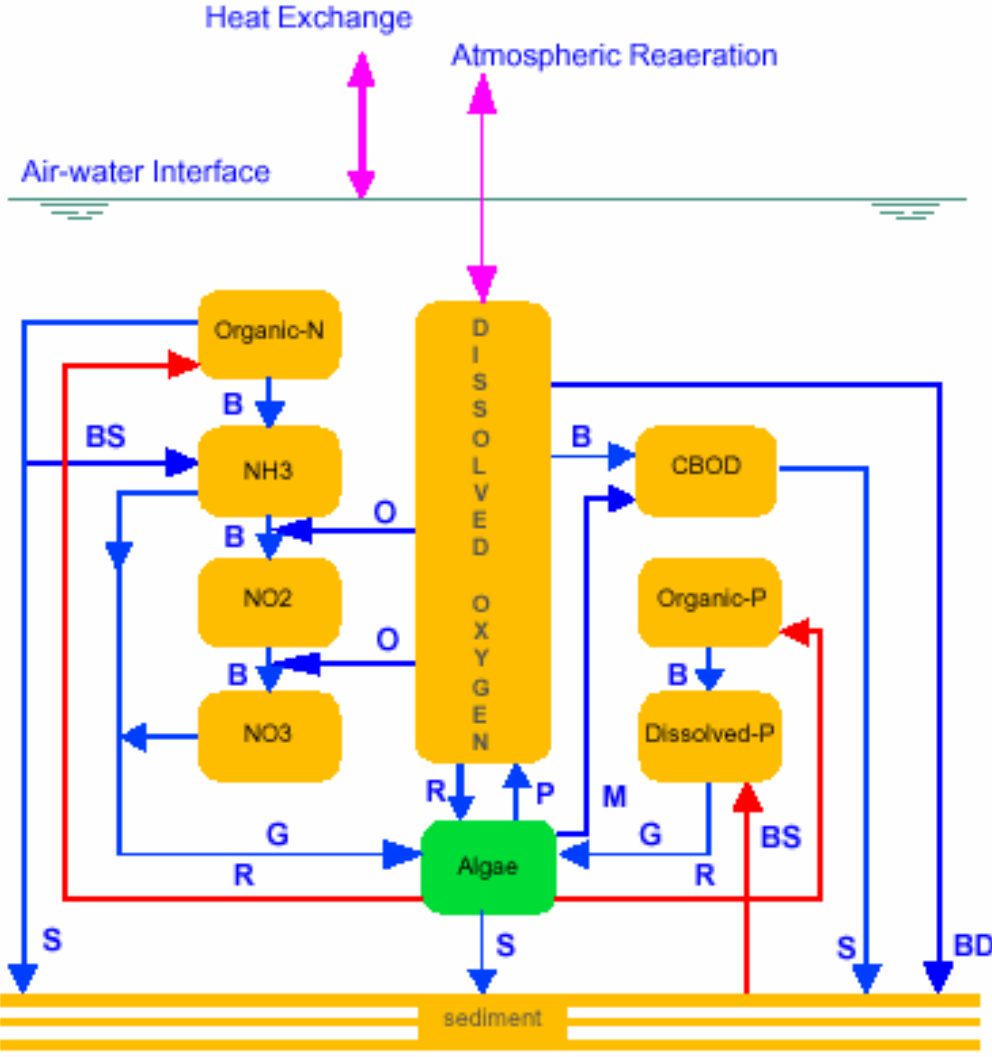
Using a dynamic flow field obtained from the hydrodynamic model DSM2-HYDRO (HYDRO), QUAL performs advective and dispersive steps of mass transport including net transfer of energy at the air-water interface. Changes are accounted for in mass of constituents due to decay, growth, and biochemical transformation. Calibration and validation of the model were performed using field observation of DO, temperature, and nutrients over two three-month periods representing different hydrologic conditions.

The extension of the DSM2 grid to the region upstream of Vernalis (see Chapter 5) is expected to enhance model prediction of DO levels. However, the DSM2 with SJR extension was not available at the time of this study. Through evaluations of different hypotheses, QUAL can aid in developing potential management strategies to address water quality degradation in the San Joaquin River near Stockton.

6.2 Model Input

Simulation of DO requires information on water temperature, BOD, chlorophyll, organic nitrogen, ammonia nitrogen, nitrite nitrogen, nitrate nitrogen, organic phosphorus, dissolved phosphorus (ortho-phosphate), and EC in the Delta. In order to simulate DO, a group of related variables has to be simulated at the same time. Interaction among water quality variables in DSM2 is shown in Figure 6-1. The rates of mass transfer (shown by the arrows) are functions of temperature. It is important that temperature simulation be included in DO simulation. The sources and sinks of DO are indicated in the figure. Further information on DSM2 kinetics is given in reference (Rajbhandari 1998), also available at the Delta Modeling web site <http://modeling.water.ca.gov/delta/repts>.

Interaction among Water Quality Constituents



TRANSFORMATION PROCESSES:

- B = Bacterial Decay
- G = Growth
- R = Respiration
- P = Photosynthesis
- S = Settling
- BD = Benthic Demand
- BS = Benthic Source
- O = Oxidation
- M = Mortality

Note: Rates of mass transfer shown by are functions of temperature.

Figure 6-1: Interaction among Water Quality Constituents.

Available data collected at hourly intervals for DO, temperature, and EC provide boundary information needed by DSM2. At most stations in the Delta, only grab samples are available. Usually, these data are collected at biweekly or monthly intervals, which were used as approximations for initial condition input. Since continuous data were not available at Vernalis (RSAN112), hourly values of DO, EC, and temperature available from the nearby station at Mossdale (RSAN087) were used to approximate these quantities for the boundary inflow at

Vernalis. Since the flows at Vernalis are primarily unidirectional, and the hydraulic residence time is relatively short, this assumption is less critical. Data on effluent flows from the City of Stockton's Regional Wastewater Control Facility (RWCF) were obtained from the Stockton Municipal Utilities District. Nutrient data at Vernalis were approximated from the San Joaquin River TMDL measurements sampled at weekly intervals in 1999. The nutrient data at Freeport on the Sacramento River were approximated from the latest publication of the U.S. Geological Survey report (USGS 1997) and chlorophyll data were approximated from DWR (1999). An estimate of flows and water quality of agricultural drainage returns at internal Delta locations was based on DWR studies. Climate data representing air temperature, wetbulb temperature, wind speed, cloud cover, and atmospheric pressure (source: National Climatic Data Center) provided DSM2 input for simulation of water temperature.

6.3 Calibration

The process of calibration for DO is data intensive, and a narrowing of data gaps through additional field measurements is recommended. DSM2 calibration for EC is discussed in chapter 2. Based primarily on availability of data, the period of August through October of 1998 was chosen for calibration (Rajbhandari 2000). During this period, the flows in the SJR at Vernalis ranged from about 5,000 to 7,000 cubic feet per second (cfs). Combined export ranged from about 4,000 to 13,000 cfs. The historical record of tide at Martinez was used for the hydrodynamic simulation of the Delta using DSM2.

Reaction kinetics represented in DSM2 were expanded to include algae mortality and corresponding increases in BOD. This enhancement of phytoplankton-DO dynamics helped the process of calibration by including a mechanism that accounts for the oxygen consumption by volatile suspended solids (VSS) observed in the San Joaquin River. The process of calibration began with the calibration of water temperature. Evaporation coefficients were adjusted until there was reasonable agreement between simulated and measured temperature as discussed below. During DO calibration, the following parameters were adjusted: algae (growth, respiration, settling, and mortality rates), nitrogen (organic nitrogen decay and oxidation rates of ammonia and nitrite), and sediment oxygen demand. Calibrated coefficients are within the range suggested in the literature (Bowie et al 1985, Brown and Barnwell 1987, Thomann and Mueller 1987, Jones and Stokes 1998).

Figure 6-2 is presented to show the comparison of simulated water temperature with field data at the continuous monitoring station at SJR near Rough and Ready Island (RRI). DSM2 seems to overestimate the observed data by less than 1 degree C. The plots seemed to agree better in the cooler period since DSM2 results were within 0.5 degree °C of measured DO during October and the latter part of September.

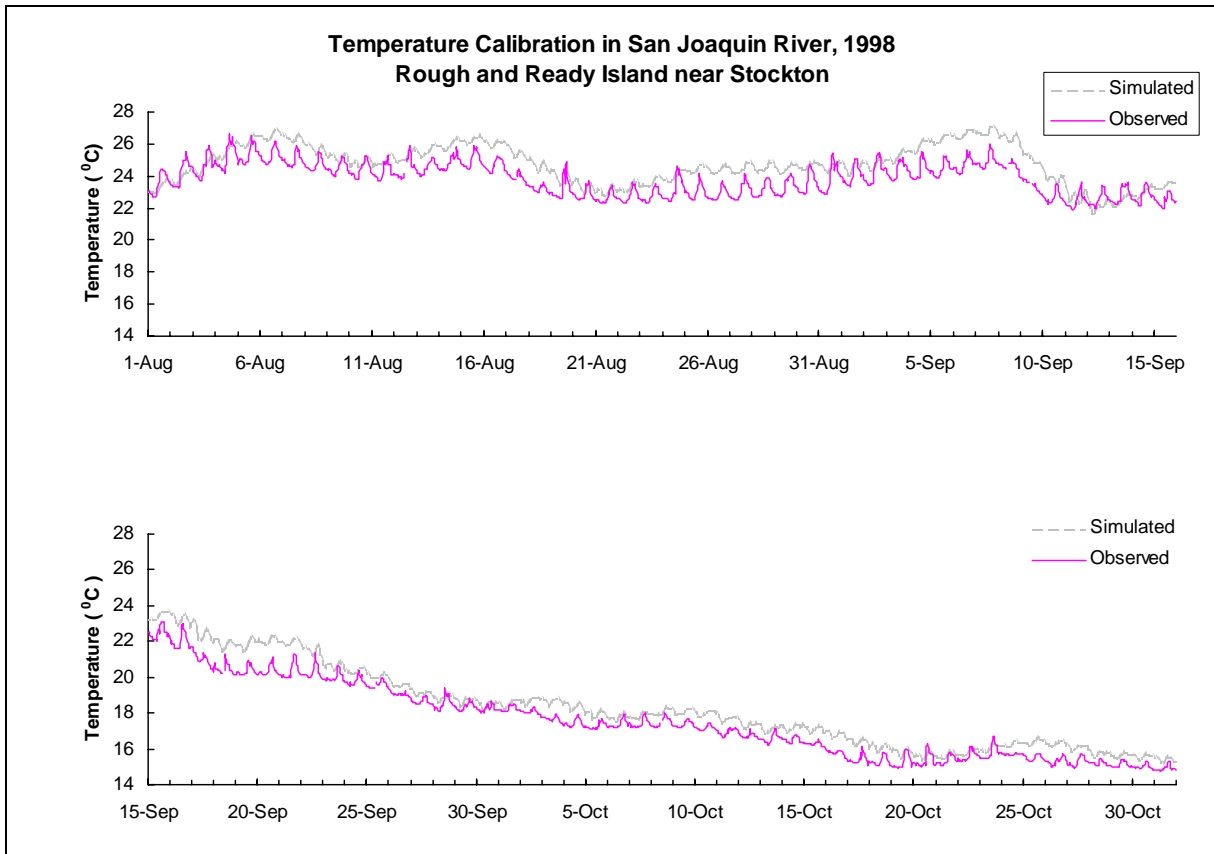


Figure 6-2: Temperature Calibration in the San Joaquin River, at Rough and Ready Island near Stockton, 1998.

Figure 6-3 presents the comparison of model results and field observations in the San Joaquin River near RRI. In general, the differences between model and field DO were within 1 mg/l, and the highs and lows appear to be in phase. During the middle of August and September, the differences between model and field observations are somewhat higher, at times as high as 1.5 mg/l. Also, the model could not capture the large diurnal range that occurred during the period between the middle of August and the middle of September. There is a possibility that this may have been partially due to DO stratification that tends to occasionally occur in the water column, which cannot be directly accounted for by the 1-dimensional model.

Based on the above, the model was considered calibrated for this reach of the SJR. Figure 6-4 illustrates how QUAL results compare with field measurements when averaged over a day. In evaluating planning alternatives, flow and salinity comparisons were traditionally based on either daily or monthly averaged model output. This mode of analysis made it easier to quantify the impact of different alternatives.

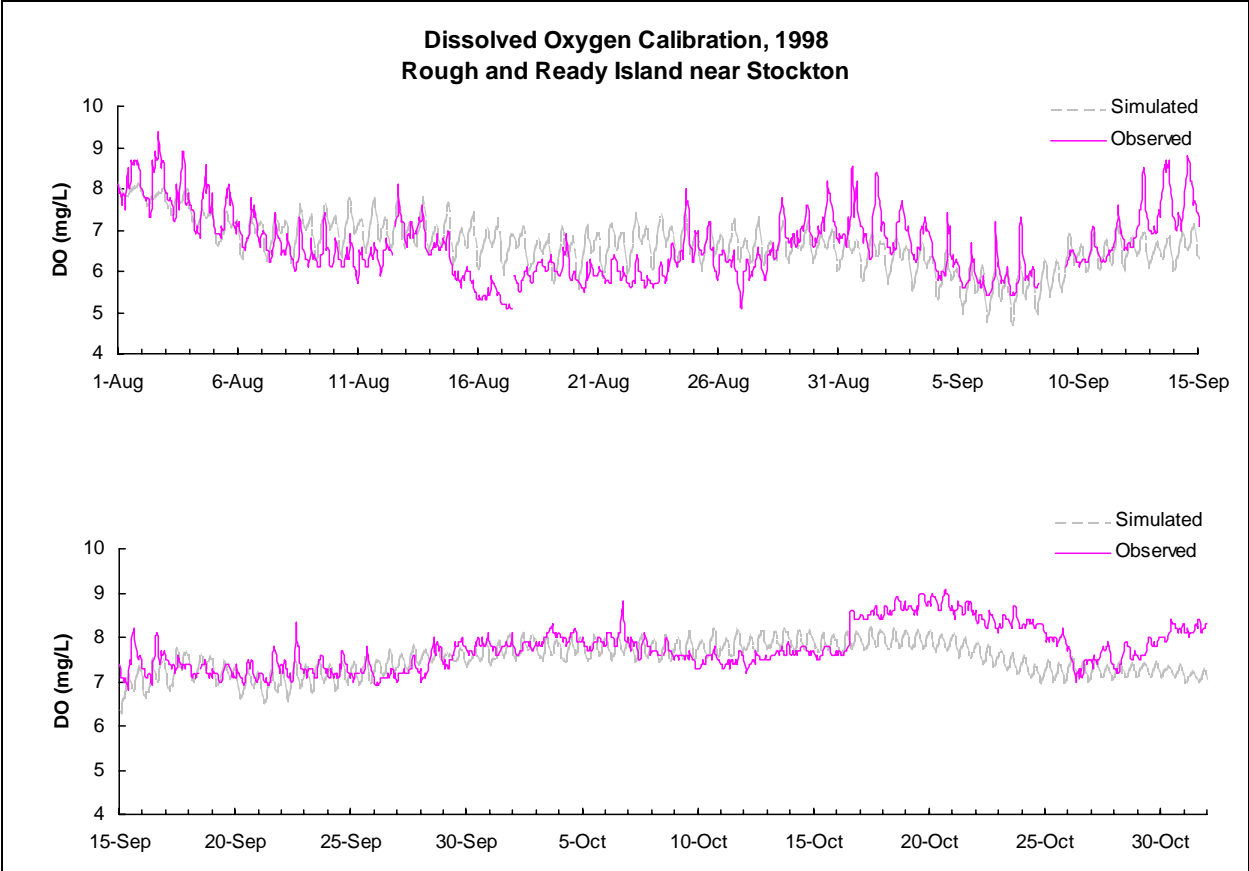


Figure 6-3: Dissolved Oxygen Calibration, Rough and Ready Island near Stockton, 1998.

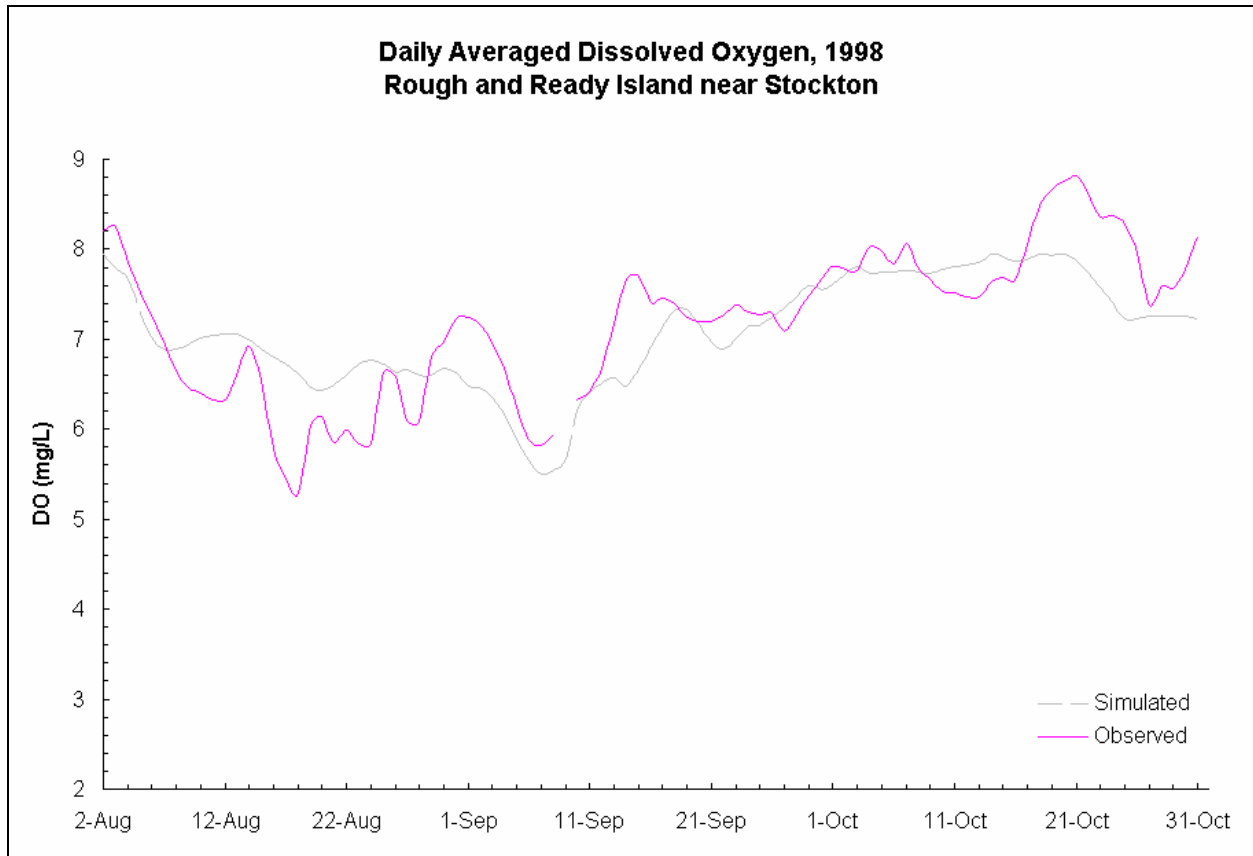


Figure 6-4: Daily Averaged Dissolved Oxygen, at Rough and Ready Island near Stockton, 1998.

6.4 Validation

Model validation was done for the period from July through September 1999, when the flows in the San Joaquin River at Vernalis were around 2,000 cfs, which is considerably lower than the San Joaquin River flows from the calibration period. The rate coefficients adopted during calibration were kept the same during this simulation. Within the region of interest, the first 15 days are considered the “warm up” period and the simulated results for both water temperature and DO should be ignored during this period.

Figure 6-5 is presented to show how DSM2 results compare with the measured water temperature at San Joaquin River near RRI. The comparison seems favorable with the differences being mostly within 1 degree C. Figure 6-6 shows the comparison of simulated and observed DO during this period. There seems to be an agreement in the general trend of the simulated results with field data. Most of the time, the differences are within 1 mg/l. However, during the middle week of July and the first weeks of August and September, the differences are about 1-1.5 mg/l. Beginning on Sept. 23, measured data were missing for the following 25 hours after which DO levels continued to fall, reaching to a low 1.7 mg/l on September 30. This indicates a strong possibility of instrument errors during the last week of September. As for the calibration period, Figure 6-7 is presented to illustrate how DSM2 results compare with field measurements when averaged over a day.

Additionally, model results were compared with field data at San Joaquin River near Fourteen Mile Slough (Figure 6-8), and near Columbia Cut (Figure 6-9) located downstream of Rough and Ready Island. Since field data were available only as grab samples on a weekly basis, model results are shown as the daily maximum and minimum DO enveloping the field data.

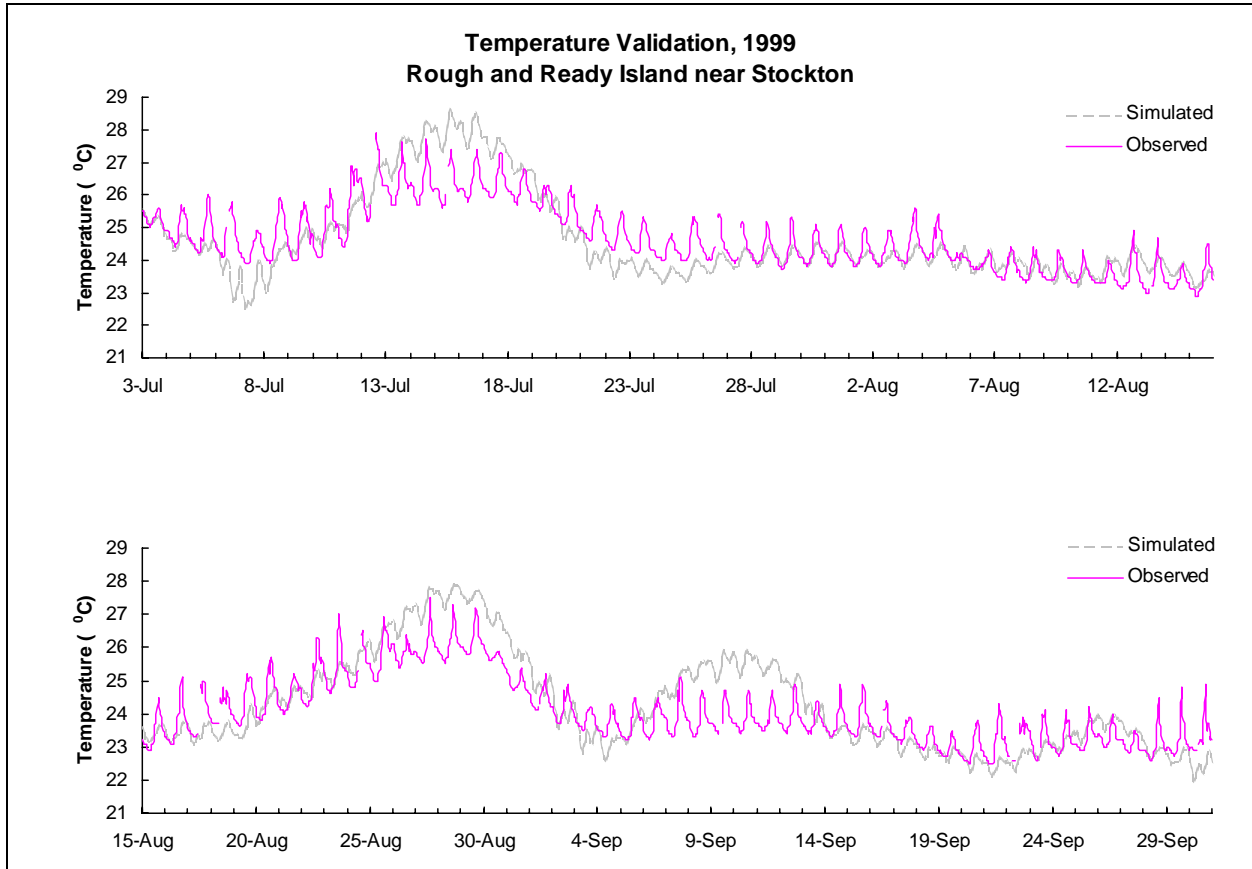
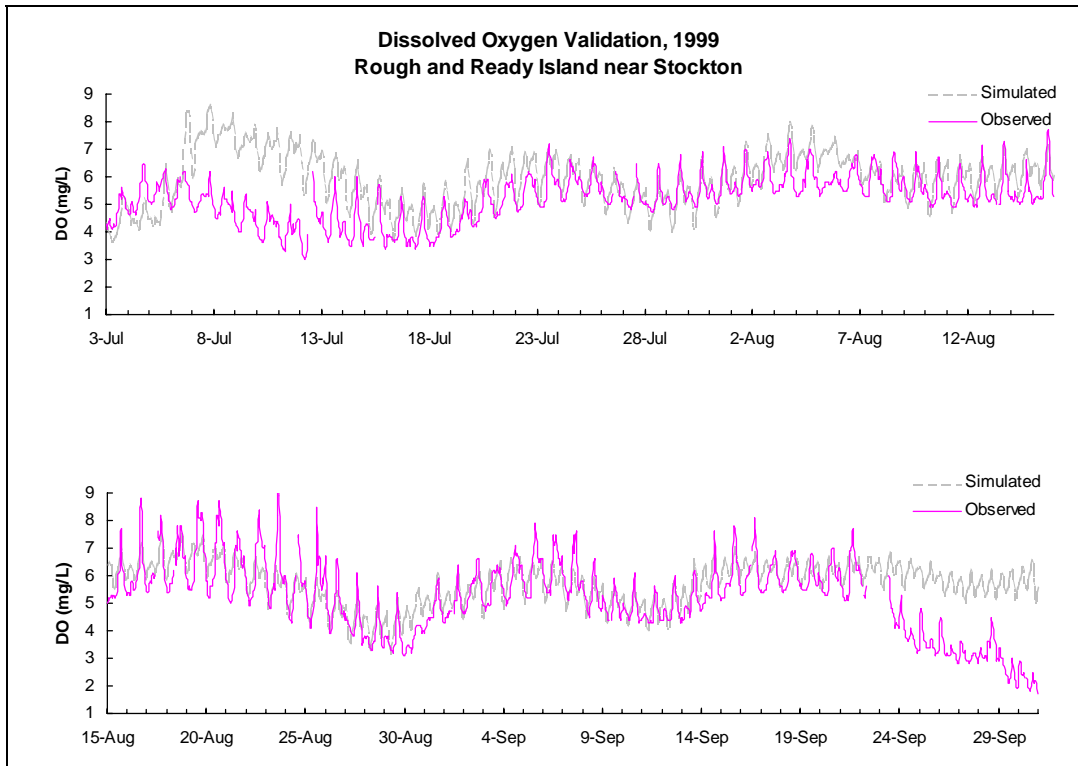
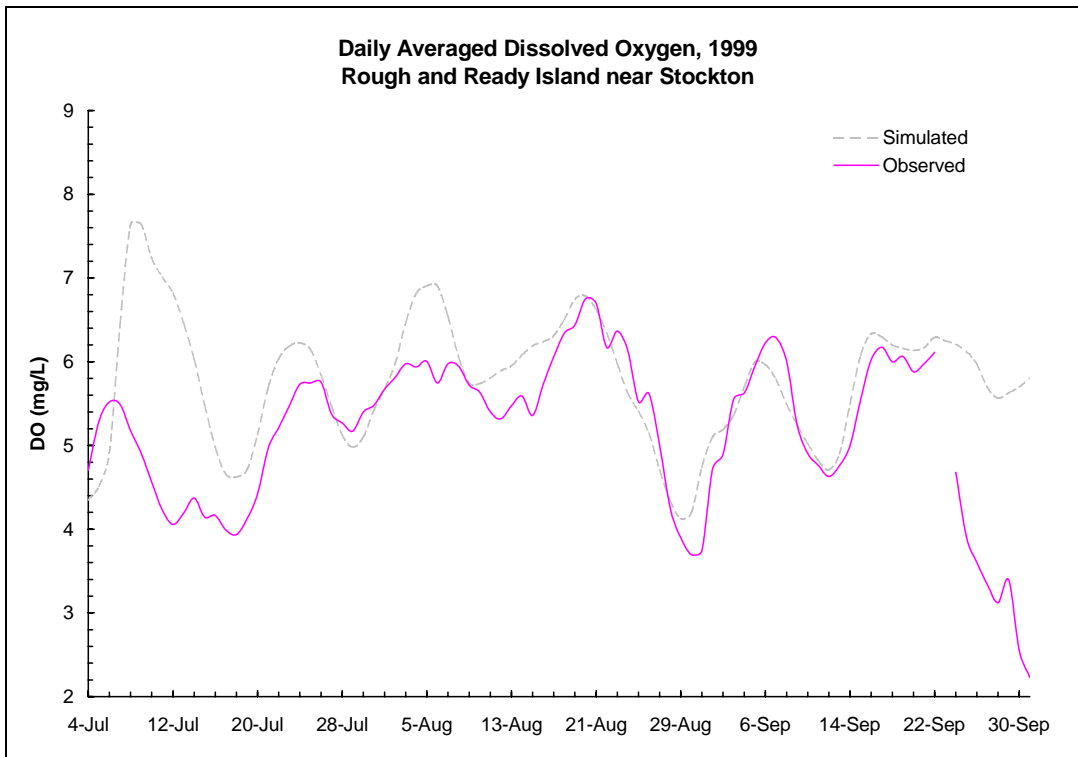


Figure 6-5: Temperature Validation, at Rough and Ready Island near Stockton, 1999.



**Figure 6-6: Dissolved Oxygen Validation,
at Rough and Ready Island near Stockton, 1999.**



**Figure 6-7: Daily Averaged Dissolved Oxygen,
at Rough and Ready Island near Stockton, 1999.**

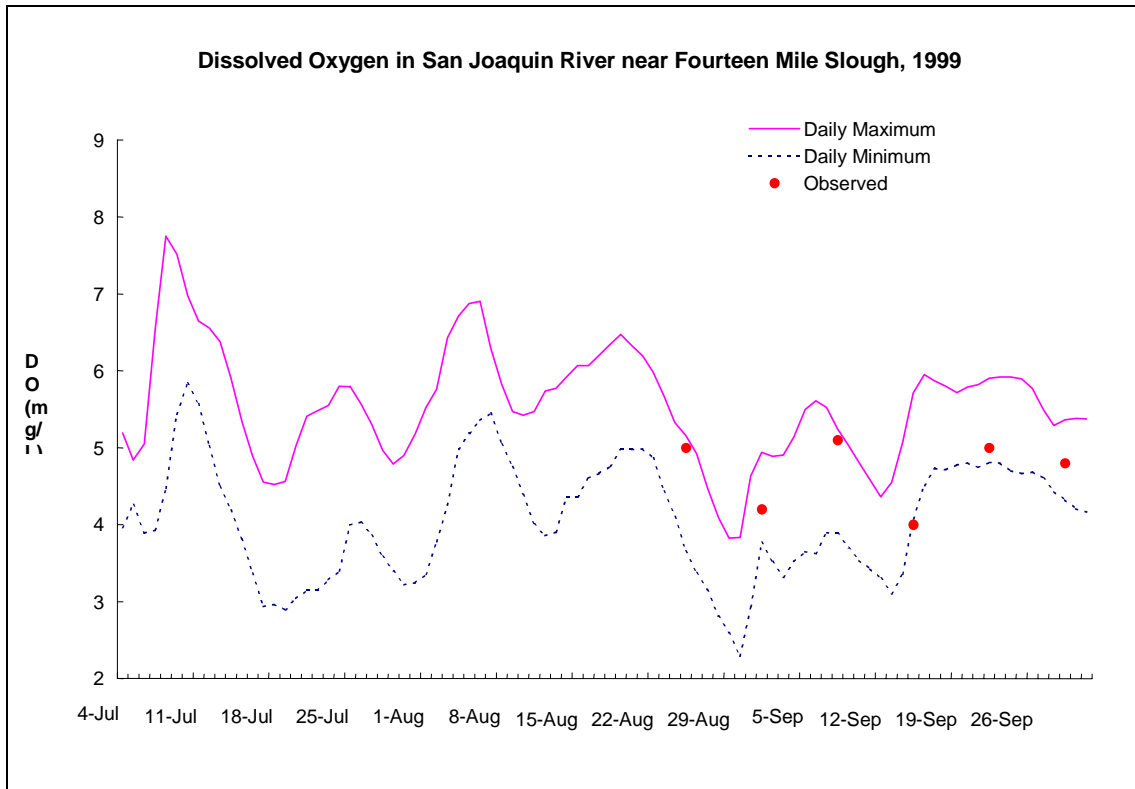


Figure 6-8: Dissolved Oxygen in the San Joaquin River near Fourteen Mile Slough, 1999.

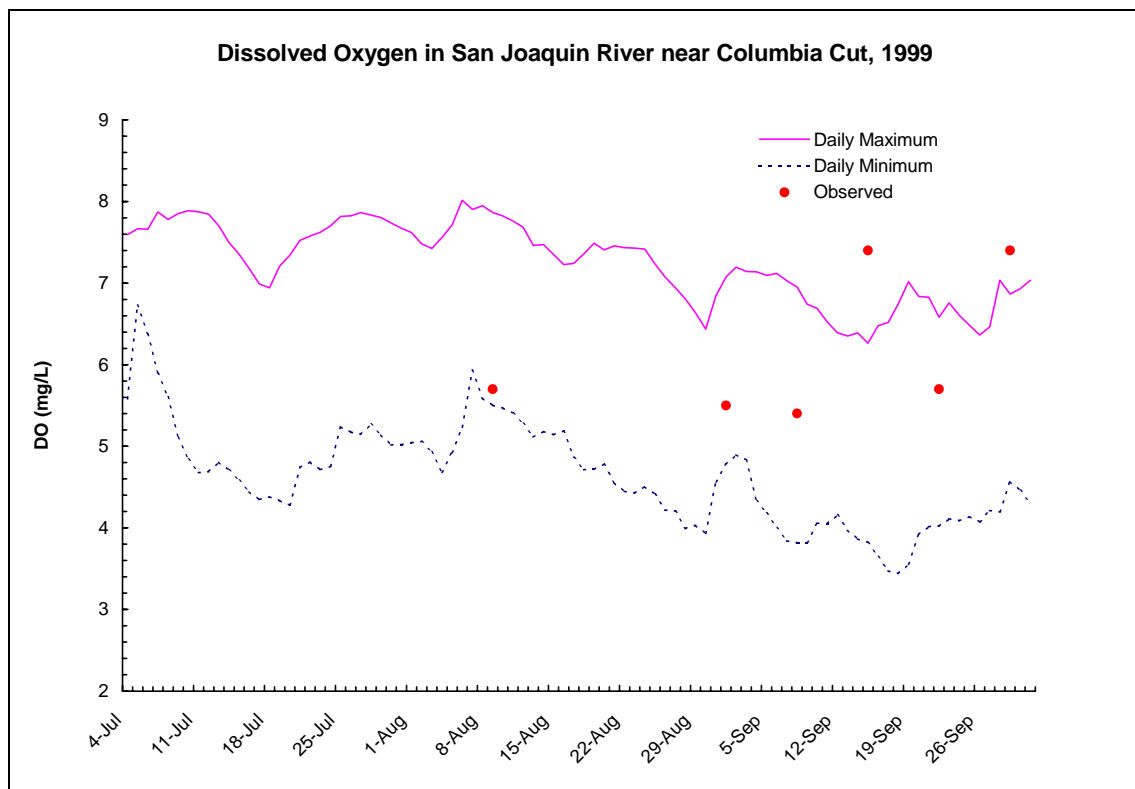


Figure 6-9: Dissolved Oxygen in the San Joaquin River near Columbia Cut, 1999.

6.5 Conclusions

A combination of several important factors contributes to low DO levels in the San Joaquin River near Stockton. Calibration of DO requires an extensive database of field measurements. However, for lack of such a database, a number of approximations and assumptions had to be made. Ideally, a calibration period of 1 to 3 years would be more appropriate. However, blocks of data were missing over different periods of time. Thus, the three-month period of August through October 1998, with mostly continuous data, was chosen. Also, because hourly time series data were available only at the Rough and Ready Island in the region of interest, calibration was primarily based on comparisons in that location. DO and water temperatures were within the range of grab sample values at nearby stations with data during the period. Considering these data limitations, the current calibration and validation results are encouraging.

6.6 References

- Bowie, G.L., W.B. Mills, D.B. Porcella, C.L. Campbell, J.R. Pagenkopt, G.L. Rupp, K.M. Johnson, P.W.H. Chan, and S.A. Gherini. (1985). *Rates, Constants and Kinetics Formulations in Surface Water Quality Modeling*, 2nd Ed. US EPA. Athens, Georgia. EPA 600/3-85/040.
- Brown, L.C. and T.O. Barnwell. (1987). *The Enhanced Stream Water Quality Models QUAL2E and QUAL2E-UNCAS; Documentation and Users Manual*. US EPA. Athens, Georgia. EPA 600/3-87/007.
- Jones & Stokes Associates. (1998). "Potential Solutions for Achieving the San Joaquin River Dissolved Objectives". Report to De Cuir & Somach, Sacramento, CA and City of Stockton, Stockton, CA. June, 1998.
- Rajbhandari, H.L. (2000). "Chapter 9: Dissolved Oxygen Modeling using DSM2 QUAL". *Methodology for Flow and Salinity Estimates in the Sacramento-San Joaquin Delta and Suisun Marsh. 21st Annual Progress Report to the State Water Resources Control Board*. California Department of Water Resources. Sacramento, CA.
- Rajbhandari, H.L. (1998). "Chapter 3: DSM2 Quality". *Methodology for Flow and Salinity Estimates in the Sacramento-San Joaquin Delta and Suisun Marsh. 21st Annual Progress Report to the State Water Resources Control Board*. California Department of Water Resources. Sacramento, CA.
- Thomann, R. V., and Mueller, J. A. (1987). *"Principles of Surface Water Quality Modeling and Control."* Harper and Row, New York.
- US Geological Survey. (1997). "Water Resources Data, California, Water Year 1997." Vol. 4.
- California Department of Water Resources. (1995). "Water Quality Conditions in the Sacramento-San Joaquin Delta during 1988." Div. of Local Assistance.

Methodology for Flow and Salinity Estimates in the Sacramento-San Joaquin Delta and Suisun Marsh

**22nd Annual Progress Report
August 2001**

Chapter 7: Integration of CALSIM and Artificial Neural Networks Models for Sacramento-San Joaquin Delta Flow-Salinity Relationships

Authors: Ryan Wilbur and Armin Munevar

7 Integration of CALSIM and Artificial Neural Network Models for Sacramento-San Joaquin Delta Flow-Salinity Relationships

7.1 Introduction

Determination of flow-salinity relationships in the Sacramento-San Joaquin Delta is critical to both project and ecosystem management. Project managers and planners require estimates of the flows required at specific peripheral locations in the Delta to satisfy salinity targets for municipal, industrial, agricultural, and environment uses at various interior locations. Likewise, ecosystem managers often want to control salinity at specific locations in the Delta to manage plant, fish, and bird species. DWR's Delta Simulation Model 2 (DSM2) is a 1-dimensional hydrodynamic and water quality model capable of simulating flow, stage, and water quality throughout the Delta. DSM2 requires input flows for the rivers that feed the Delta at the boundaries. DWR's CALSIM Model is a statewide planning model covering the entire State Water Project and Central Valley Project and is used for analysis of various structural and nonstructural alternatives. The upstream reservoir operations, as modeled in CALSIM, are often dependent on Delta salinity standards. Salinity in the Delta cannot be modeled accurately by the simple mass balance routing and coarse timestep used in CALSIM. Likewise, the upstream reservoirs and operational constraints cannot be modeled in DSM2. An Artificial Neural Network (ANN) has been developed (Sandhu et al. 1999) that attempts to faithfully mimic the flow-salinity relationships as modeled in DSM2, but provide a rapid transformation of this information into a form usable by the statewide CALSIM model. The ANN is implemented in CALSIM to constrain the operations of the upstream reservoirs and the Delta export pumps in order to satisfy particular salinity requirements.

7.2 Background

Prior attempts to develop flow-salinity relationships for statewide planning models were based primarily on operator experience or historical measurements. The first attempt to implement Delta outflow requirements for particular salinity targets was the Minimum Delta Outflow (MDO) curves and was primarily based upon operator experience. Curves were developed that specified required Delta outflow given a level of export, salinity target, and Delta Cross Channel gate position. The required Delta outflow increased in a nonlinear fashion as the export level increased. The MDO procedure was used in the first statewide planning models developed by DWR.

Contra Costa Water District's G-model (Denton and Sullivan 1993) relates salinity at various locations in the Delta to the net Delta outflow, as well as the prior history of net Delta outflow. The use of antecedent outflow conditions was a significant step in the development of flow-salinity relationships. The G-model is based on historical observations of flow and salinity in the Delta and uses an equation similar in form to the advection-dispersion equation for salinity

transport. The parameters required for the solution of this equation, however, are determined by field measurements at the locations of interest. The equation may be solved for a required Delta outflow given a particular outflow history (G value) and desired salinity. The G-model is used in this form to estimate flow-salinity relationships in the current CALSIM model.

The MDO curves were developed to demonstrate that, at different levels of pumping, a nonlinear relationship of Delta outflow exists for the same salinity target. However, the curves did not account for antecedent conditions in the Delta. The G-model improved upon the prior model by including the antecedent outflow condition, but did not aggregate the flow patterns within the Delta. In reality, cross-channel gate operation, export levels, Sacramento River and San Joaquin River inflows, and channel depletions all affect the salinity regime in a slightly different way. For example, for a Delta outflow of 20,000 cfs, the export level could be 10,000 cfs with inflows of 30,000 cfs, or exports of 5,000 cfs with inflows of 25,000 cfs. The resulting salinity is the same in both cases when computed by the G-model, since the dependent flow parameter (Delta outflow) remains unchanged at 20,000 cfs. Similarly, a change in the cross-channel gate position would not affect the resulting salinity in the prior models since the Delta outflow is not affected.

The ANN developed by DWR (Sandhu et al. 1999) attempts to statistically correlate the salinity results from a particular DSM2 model run to the various peripheral flows and gate operations. The ANN is “trained” on DSM2 results that may represent historical or future conditions. For example, a reconfiguration of the Delta channels to improve conveyance may significantly affect the hydrodynamics of the system. In such a case, the MDO curves and G-model may not represent the new flow-salinity relationships since they are based on historical measurements or experience. The ANN, however, would be able to represent this new configuration by being retrained on DSM2 model results that included the new configuration. Thus, by accounting for the major flow and operational parameters as independent parameters rather than aggregated Delta outflow, and the ability to better represent future modified conditions in the Delta, the ANN is a significant improvement over the existing models.

The current ANN predicts salinity at various locations in the Delta using the following parameters as input: Sacramento River inflow, San Joaquin River inflow, Delta Cross Channel gate position, and total exports and diversions. Sacramento River inflow includes Sacramento River flow, Yolo Bypass flow, and combined flow from the Mokelumne, Cosumnes, and Calaveras rivers (East Side Streams). Total exports and diversions include State Water Project (SWP) Banks Pumping Plant, Central Valley Project (CVP) Tracy Pumping Plant, North Bay Aqueduct exports, Contra Costa Water District diversions, and net channel depletions. A total of 148 days of values of each of these parameters is included in the correlation, representing an estimate of the length of “memory” in the Delta.

7.3 Implementation of Artificial Neural Networks in CALSIM

7.3.1 Flow-Salinity Relationship

Implementation of Delta salinity standards in CALSIM, based on the ANN, requires a basic understanding of the flow-salinity relationship. In theory, the flow-salinity relationship is a multi-dimensional plot with all the previously listed flow parameters affecting salinity.

However, several of the parameters are either known or can be estimated in the CALSIM simulation. For example, Delta Cross Channel gate position is dictated by current Delta standards (SWRCB 1995); Yolo Bypass, channel depletions, and East Side Stream flows are input data in the current CALSIM version; the San Joaquin River system is operated independently of the Delta in CALSIM; and North Bay exports and Contra Costa Water District diversions can be estimated based upon demand. The major independent (and unknown) flow parameters that have a significant influence on salinity are Sacramento River flow and combined project exports (CVP Tracy and SWP Banks Pumping Plants). Sacramento River flow (Q_{SAC}) and combined project exports (Q_{EXP}) are the two decision variables used by CALSIM's LP solver to impose the ANN restrictions (discussed later in Section 7.3.2: *Operational Constraints*). The flow-salinity relationship at a location in the Delta can be found by computing the salinity values resulting from all possible combinations of these two parameters. An example salinity surface developed by this method is shown in Figure 7-1 for the Emmaton water quality location.

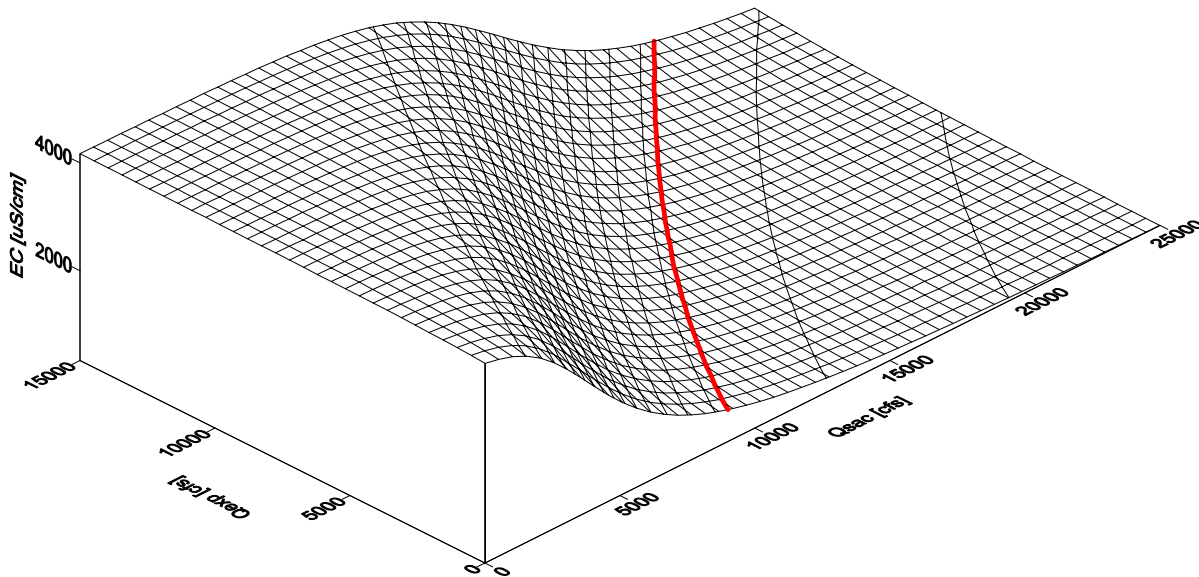


Figure 7-1: Salinity Surface Plot: Emmaton (Ex: October 1976) (uS/cm).

Development of a contour plot of this surface (Figure 7-2 – lines of equal EC) indicates that the relationship between Sacramento River flow and combined project exports at a constant EC is well behaved and approximately linear. A similar plot for Old River at Rock Slough in October 1976 is shown in Figure 7-3.

The combined project export – Sacramento River flow relationship represents the upper limit of potential flow combinations for the current period; any point to the right of this curve is considered a feasible operation in that it results in an equal or lower salinity than the given standard.

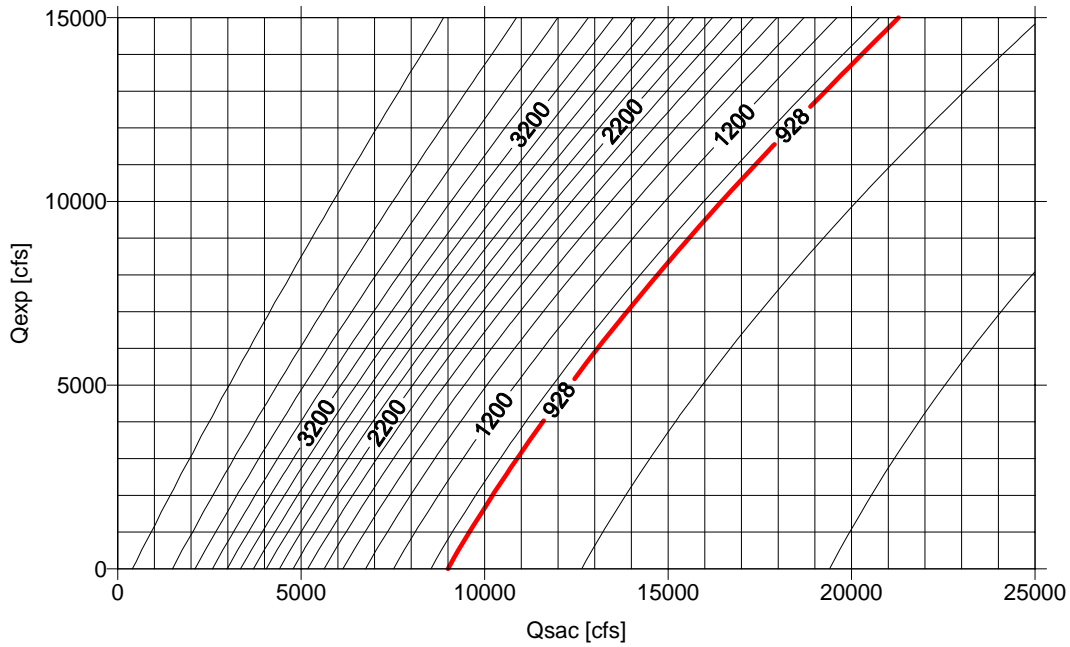


Figure 7-2: Salinity Contour Plot: Emmaton (Ex: October 1976) (uS/cm).

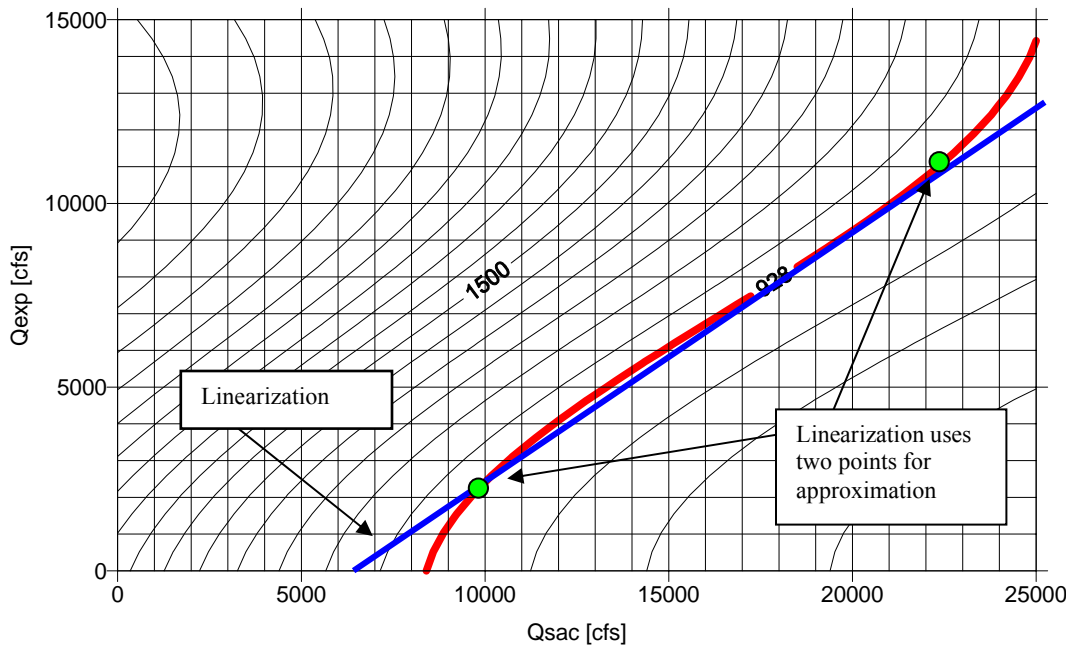


Figure 7-3: Salinity Contour Plot with Linearization: Old River at Rock Slough (Ex: October 1976) (uS/cm).

7.3.2 Operational Constraints

CALSIM utilizes a linear programming solver for determining routing of water throughout the statewide network and therefore requires all constraints to be in a linear form. This necessitates approximation of the ANN combined project export – Sacramento River flow relationship such

that a linear constraint may be formulated. The constraint that represents the approximated linear relationship between flows for a given salinity target is:

$$Q_{EXP} \leq m Q_{SAC} + b \quad \text{[Eqn. 7-1]}$$

where m and b are the slope and intercept, respectively. The slope and intercept are based on a prior month's Sacramento River inflow, San Joaquin River flow, total exports, and Delta CrossChannel gate operation, and on the current month computations of the Delta Cross Channel gate, Yolo Bypass, channel depletions, East Side Streams, San Joaquin River, and North Bay and Contra Costa diversions.

The method used to linearize (as is shown in Figure 7-3) the ANN representation uses two points from the combined project export – Sacramento River flow plot: exports at 2,000 and 11,000 cfs. These two points were selected because they represent the probable range of exports and avoid the extreme areas where the relationship may deviate from linear and there is less confidence in the ANN. The current CALSIM-ANN studies of 73 years of simulation have approximately four months each above the 11,000 cfs and below 2,000 cfs export level. The slope and intercept of Equation 7-1 are determined from these two points. The Sacramento River flows corresponding to these two export levels are found using the ANN. The greatest inconsistencies between the linearized and original ANN curve are due to the nonlinearity at low and high exports. At high export levels, the linearized form will require more Sacramento River flow than the original ANN. Conversely, the linearized form will require less water at low export levels.

The linear constraint (Equation 7-1) is normally directly implemented in CALSIM as a limitation on project operations such that the salinity target is met. However, three cases exist that affect how Equation 7-1 is implemented. The solution field under which Equation 7-1 is valid is within a range of exports up to 15,000 cfs and a range of Sacramento River flow up to 25,000 cfs.

7.3.2.1 Case 1: Basic Implementation

Under the basic implementation, there exists a combination of combined project exports and Sacramento River flow within the valid solution field. The slope and intercept are determined in CALSIM by calling the ANN subroutine with the prior month's parameter values as well as the current month values for the known parameters. The constraint (Equation 7-1) is activated in CALSIM and project operations are adjusted accordingly. In general, the Sacramento River flow is increased by upstream reservoir releases in order to support exports for South of Delta demand and storage targets.

7.3.2.2 Case 2: Salinity Standard Has No Possible Control on Project Operations

The second case arises from the possibility that, for the given salinity standard, Equation 7-1 has no controlling effect on exports or Sacramento River flow. Determining the salinity at maximum exports and minimum Sacramento River flow performs a check for this case. If the resulting salinity is less than the target, project operations are considered to have no controlling effect on Delta salinity. Under this scenario, the slope is set to zero and the intercept is set to 999,999. This results in Equation 7-1 having no impact on the solution ($Q_{EXP} \leq 999,999$). The Sacramento River flow and the Delta exports are unrestricted according to the ANN requirements.

7.3.2.3 Case 3: No Project Operations Will Meet Salinity Standard

The third case exists when Equation 7-1 cannot be met for any combination of combined project exports and Sacramento River flow. This case is determined by predicting the salinity when the Delta exports are reduced to zero and Sacramento River flow is set to 25,000 cfs. If the resulting salinity is greater than the target, project operations are considered to be unable to satisfy the current salinity standard. To prevent the ANN requirements from releasing large volumes of water from storage while not meeting the salinity requirements, caps are placed on the required Sacramento River (25,000 cfs) and on the combined project exports (1,500 cfs). Also, the requirement of satisfying Equation 7-1 is relaxed.

7.3.3 Modeled Locations

The current CALSIM-ANN integration allows the simulation of flow-salinity relationships at three locations: (1) Emmaton, (2) Jersey Point, and (3) Contra Costa Canal Pumping Plant #1 (CCC PP#1). The Emmaton and Jersey Point standards are modeled directly at their respective locations in the Delta. However, the CCC station salinity standard is translated into an equivalent salinity standard at Old River at Rock Slough due to difficulties in accurately representing water quality by DSM2 in this slough. The current transformation of the standard is:

$$\text{Old River at Rock Slough EC} = (\text{CCC PP\#1 Chloride} + 23.6)/0.268 \quad (\text{uS/cm}) \quad [\text{Eqn. 7-2}]$$

The CCC PP#1 salinity standard in the current Water Quality Control Plan (SWRCB 1995) specifies the number of days each year that the chloride concentration will be lower than 150 mg/l. The number of days required for this standard is based on the water year type (Wet = 240 days; Above Normal = 190; Below Normal = 175; Dry = 165; Critical = 155). A maximum chloride standard of 250 mg/l applies at all times. Buffers are applied to each of these standards due to the fact that CALSIM uses a monthly time step. These buffers are conservative in nature, such that the 250 mg/l field standard becomes 225 mg/l in CALSIM and the 150 mg/l standard becomes 130 mg/l. The model determines the timing of the 130 mg/l Contra Costa Canal standard by waiting until the last possible month before it requires this stricter standard to be satisfied. The model determines the number of days on which the 130 mg/l standard needs to be met based on water year type. During all months, beginning in February, the code will test the previous month's actual salinity concentration for meeting the 130mg/L standard. If the stricter standard is satisfied, 30 days credit is applied toward meeting the standard. This continues until the number of days required to meet the lower standard equals the number of days left in the year. When this occurs, the 130 mg/l standard applies for the remainder of the year.

7.3.4 Partial Month Standards

Occasionally, salinity requirements change within a month or are specified for time periods less than a full month. This may occur due to the actual written standards (Emmaton and Jersey Point) or due to the implementation procedure (Contra Costa Canal). This causes difficulty in simulating these standards in CALSIM because it uses a monthly time step. To compensate for this difference in time step, partial month standards are averaged according to an exponential function (Figure 7-4) that attempts to mimic the flow-salinity relationship shown in the G-model development (Denton and Sullivan 1993). A monthly average standard is developed by integrating the function and weighting the areas under the curve for the higher and lower

standards according to their respective number of days. In general, the average standard is weighted more towards the lower standard since the required flow increases exponentially with a unit reduction in the salinity standard. For example, if 15 days remain to meet the Contra Costa Canal 130 mg/l standard (with the remaining 16 days standard at 225 mg/l) the area under the curve between 0 and 15 days is 5.68 and the area between 15 and 31 is 0.52. The salinity standard averaging is calculated as $(130 \times 5.68 + 225 \times 0.52) / (5.68 + 0.52)$, which results in a monthly standard of 138 mg/l. If a salinity standard is specified for less than a full month and no other standard exists for the remainder of the month, then the highest salinity standard is selected as the target for the remainder of the month.

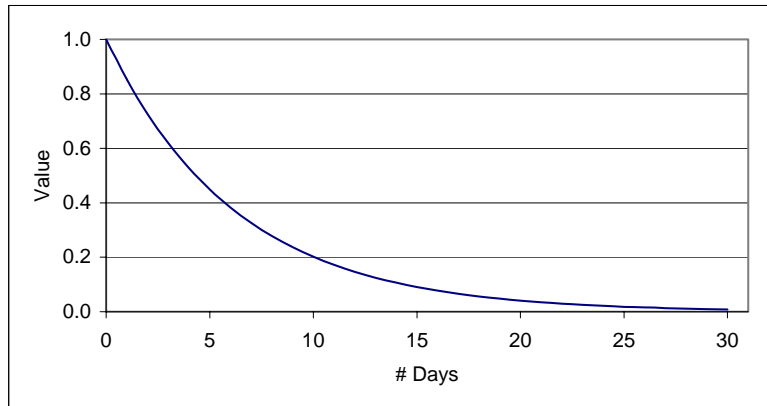


Figure 7-4: Exponential Averaging Function for Partial Month Salinity Standards.

7.4 Limitations

As with all attempts to capture the flow-salinity relationship in the Delta, there are limitations to the Artificial Neural Network implementation in CALSIM. First, it needs to be noted that CALSIM implements an *approximation* to the true ANN by linearizing the combined project export – Sacramento River flow relationship at a given salinity target. At the Emmaton and Jersey Point locations, this relationship is fairly linear such that the approximation does not introduce significant error. For most periods at the Old River at Rock Slough station, the relationship remains fairly linear. However, there exist several months for which the combined project export – Sacramento River flow relationship is linear in the mid-range of flows, but nonlinear at the extremes. At these extremes, the current CALSIM implementation will deviate from the true ANN solution and errors in implementing ANN into CALSIM will occur. It remains unclear whether the nonlinear relationship at the extremes is due to the actual salinity dynamics of the Delta or to inherent errors in the “training” of the ANN from DSM2 results.

Another possible limitation is directly linked to the ability of the ANN to faithfully capture the dynamics of the Delta under conditions other than those under which it was trained. Presumably, the ANN does not require retraining when export or inflow patterns or magnitudes change. However, it is possible that the ANN will exhibit errors in flow regimes beyond those in which it was trained. In addition, change in operation of the Delta Cross Channel gate requires a new training of the ANNs. A clearer picture of the robustness of the ANN and magnitude of errors

will be developed when the “full circle” (DSM2-ANN-CALSIM-DSM2) analysis is performed with the newly calibrated DSM2 model.

7.5 Recommendations

The current implementation of the ANN in the CALSIM statewide planning model represents a major improvement in determining salinity standard water costs and impacts to the projects. In addition, the flow-salinity relationships are dynamically represented by taking into account numerous peripheral flows and operations as well as antecedent conditions. The ability of the ANN to be retrained when the configuration of the Delta has changed represents a significant enhancement over prior models. However, the robustness of the ANN and the capability of the DSM2 model to predict salinity at the locations of interest needs to be measured. It is recommended that once the new DSM2 calibration is complete, a full circle analysis of the CALSIM-ANN implementation should be performed in which errors are quantified in each step of the process.

The CALSIM implementation of the ANN has been rigorously tested. CALSIM, like any other planning model, would require iteration of the entire network solution in order to solve the nonlinear export-flow-salinity relationship that exists at extreme export levels at specific locations. The iteration of the entire network is unacceptable for the solution and use of CALSIM as a planning tool. The linearization of this relationship within the mid-range of exports represents the best attempt to capture the system dynamics within the range of expected operations of the export facilities. Further investigation may provide insight into whether the nonlinearities at the export extremes, only present at the Old River at Rock Slough location, are real or are a result of the ANN training.

7.6 References

- Denton, R. and G. Sullivan. (1993). *Antecedent Flow-Salinity Relations: Application to Delta Planning Models*. Contra Costa Water District.
- Sandhu, Nicky. (1995). “Chapter 7: Artificial Neural Networks and Their Applications.” *Methodology for flow and salinity estimates in the Sacramento-San Joaquin Delta and Suisun Marsh. 16th Annual Progress Report to the State Water Resources Control Board*. California Department of Water Resources. Sacramento, CA.
- Sandhu, N., D. Wilson, and R. Finch. (1999). *Modeling Flow-Salinity Relationships in the Sacramento – San Joaquin Delta Using Artificial Neural Networks*. Technical Information Record OSP-99-1. California Department of Water Resources. Sacramento, CA.
- State Water Resources Control Board. (1995). *Water quality control plan for the San Francisco Bay/Sacramento-San Joaquin Delta Estuary*.

Methodology for Flow and Salinity Estimates in the Sacramento-San Joaquin Delta and Suisun Marsh

**22nd Annual Progress Report
August 2001**

Chapter 8: *An Initial Assessment of Delta Carriage Water Requirements Using a New CALSIM Flow-Salinity Routine*

Authors: Paul Hutton and Sanjaya Seneviratne

8 An Initial Assessment of Delta Carriage Water Requirements Using a New CALSIM Flow-Salinity Routine

[Editor's Note: Chapter 8 was originally circulated as a technical memorandum. The memo was reformatted to be consistent with the Annual Progress Report, but its content remains unchanged. The CALSIM flow-salinity routine has been modified subsequent to circulation of the memorandum, resulting in water supply impacts that are lower than those presented in Figure 8-5. The modification corrects a model bias towards over-estimation of Old River at Rock Slough salinity, which is discussed in Section 8.3.2. At the time that this editor's note was prepared, carriage water estimates had not been updated to reflect the refined flow-salinity routine. But as noted in the discussion (Section 8.6), it is anticipated that other factors will need to be considered in the next update of carriage water estimates, including (but not necessarily limited to) input from the Bay-Delta Modeling Forum Carriage Water Review Team and progress in the modeling of CVPIA b(2) and EWA operations.]

8.1 Introduction

The purpose of this study is to report (1) the water supply impacts associated with a new CALSIM flow-salinity routine for modeling Delta standards and (2) the range of carriage water costs as computed by the new CALSIM routine.

Properly accounting for Delta standards is essential for effective planning and management of CVP and SWP facilities and has a major impact on reservoir releases and Delta export pumping. Key standards include:

- ❑ M&I and agricultural water quality standards
- ❑ Delta outflow (X2) standards
- ❑ Maximum percent of Delta inflow diverted (E/I ratio)

In order to properly simulate Delta standards in a CVP-SWP system planning model such as CALSIM, hydrology, hydraulics and flow-salinity relationships must be accurately specified. This study focuses on the specification of flow-salinity relationships in CALSIM.

Carriage water is closely interrelated with Delta flow-salinity relationships. While the concept of quantifying carriage water is controversial, it is necessary to determine the true costs of meeting Delta standards and transferring water across the Delta. In the State Water Resources Control Board's Notice of Resumption of Public Hearing for Phase 8 of the Bay-Delta Water Rights Hearing dated April 19, 2000, the State Board identified as a key issue the determination of the amount of carriage water when water is exported from the Delta. The Bay Delta Modeling Forum created a review team to develop a recommendation to the State Board on the methodology for calculating carriage water. Staffs from the department and Contra Costa Water District are working with this review team to undertake technical analyses on carriage water.

The study presented in this report summarizes work to date conducted by DWR Modeling Support staff.

Carriage water calculation is also important for estimating the water supply benefits or costs of alternate Delta operations and configurations. For example, the following types of operations or facilities may incur water supply benefits through carriage water savings: more frequent Delta Cross Channel opening, construction and operation of through-Delta or isolated Delta facilities, strategic levee restorations for wetland enhancement, and construction and operation of in-Delta storage facilities. Tradeoffs for these types of projects would likely exist between water supply benefits and water quality benefits. Conversely, more frequent DCC closings and strategic levee failures may impact water supply through higher carriage water costs.

8.2 Background

8.2.1 Carriage Water Definitions

The term “carriage water” has different meanings to different people under different circumstances. The following definitions are introduced to clarify its concept:

Carriage Water Cost to Meet Delta Water Quality Standards. Carriage water may be defined as the extra water necessary to carry a unit of water across the Delta for export while maintaining all agricultural and M&I water quality standards in the Delta. This “traditional” carriage water definition evolved from the D-1485 regulatory environment and applies to conditions when water quality standards are in danger of being violated.

Carriage Water Cost to Prevent Water Quality Degradation. Carriage water may also be defined as the extra water necessary to carry a unit of water across the Delta for export while maintaining water quality at a specified location. This definition, also referred to as a “marginal export cost”, is similar to the traditional definition but is independent of prescribed water quality standards.

Carriage Water Cost to Meet Delta Water Quality and Ecological Standards. The “traditional” carriage water definition may be expanded to include the extra water necessary to carry a unit of water across the Delta for export while maintaining ecological standards such as export-to-inflow (E/I) ratio, X2 position, and minimum Delta outflow. This carriage water definition, which is most appropriate for quantifying potential water transfer costs under the D-1641 regulatory environment, is employed in this study to estimate carriage water requirements.

8.2.2 Previous Efforts to Model Delta Flow-Salinity Relationships

The ability to quantify Delta flow-salinity relationships is critical to CVP-SWP project operations and management. The physics of Delta flow-salinity relationships is highly complex and is a function of several variables, including, but not limited to, the time history of Delta hydrology, water facilities and agricultural operations, channel geometry, tidal action, wind, and barometric pressure. DWR's Delta Simulation Model 2 (DSM2), a 1-dimensional hydrodynamic and water quality model, simulates most of the complex interactions described above and is

therefore able to accurately predict Delta flow-salinity relationships. However, the computation time necessary to conduct a DSM2 simulation prohibits direct implementation in CALSIM.

The first attempt to model Delta water quality standards in DWRSIM was through a mass balance routine called Minimum Delta Outflow, or MDO (DWR 1987, 1991). The MDO routine calculated required Delta outflow given a level of export, a salinity target, and a Delta Cross Channel gate position. The required Delta outflow increased in a nonlinear fashion as the export level increased. The MDO routine was criticized for its steady-state net flow assumptions and poor validation with observed data and was replaced with Contra Costa Water District's G-model in 1995.

The G-model (Denton and Sullivan 1993) relates salinity at various locations in the Delta to the time history of net Delta outflow. The use of antecedent outflow conditions was a significant improvement in the development of flow-salinity relationships. The G-model is based on historical observations of flow and salinity in the Delta and uses an equation similar in form to the advection-dispersion equation for salinity transport. The parameters required for the solution of this equation, however, are determined by field measurements at the locations of interest. The equation may be solved for a required Delta outflow given a particular outflow history (G value) and desired salinity. While the G-model is in the current version of CALSIM, its basic formulation limits its use in CVP-SWP system planning. The model has a single, independent variable – an antecedent Delta outflow term – and is therefore insensitive to the relationship between water quality and Delta inflows, exports and gate operations for a constant Delta outflow. Because it does not explicitly model the relationship between Delta exports and water quality, the G-model formulation cannot be used to estimate carriage water requirements.

8.3 A New CALSIM Routine to Estimate Delta Flow-Salinity Relationships

DWR has adopted artificial neural network technology to simulate flow-salinity relationships and carriage water in the Delta. The ANN routine was developed and recently implemented in a CALSIM beta version (DWR 1999, 2000). The ANN routine will be an integral part of the next major release of CALSIM, i.e. CALSIM2. This routine statistically correlates DSM2 model-generated salinity at key locations to the time histories of Delta exports, DCC operations, and major Delta inflows. Accounting for these individual flow and operation components is essential for estimating carriage water requirements.

8.3.1 Formulation and Implementation

The ANN routine implemented in CALSIM is calibrated or “trained” on a DSM2 simulation of CALSIM Study 898. This study represents current Delta facilities, operations, and channel configuration. However, the ANN routine is capable of being retrained to account for alternate Delta facility, operation and channel configurations. This robust feature is useful for modeling the interrelationship between Delta conditions and Delta flow-salinity relationships. Delta reconfigurations, such as channel improvements for through-Delta conveyance or levee modifications for wetland enhancement, could significantly affect overall system

hydrodynamics. The ANN routine could simulate the resulting flow-salinity regimes by first being retrained on a DSM2 simulation that includes the new Delta configurations.

The current ANN flow-salinity module predicts electrical conductivity at three locations for the purpose of modeling Delta water quality standards: Old River at Rock Slough, San Joaquin River at Jersey Point, and Sacramento River at Emmaton. Salinity is estimated based on a time history of the following variables: Sacramento River inflow, San Joaquin River inflow, DCC gate position, and several Delta export and diversion variables. The Sacramento River inflow term combines flows from the Sacramento River at Freeport, the Yolo Bypass, and the Mokelumne, Cosumnes, and Calaveras rivers. San Joaquin River inflow is the flow measured at Vernalis. DCC gate position is assumed to be fully open or fully closed. Delta exports and diversions include SWP exports at Banks and the North Bay Aqueduct, CVP exports at Tracy, Contra Costa Water District diversions at Rock Slough and Los Vaqueros, and Delta agricultural net channel depletions. The time history for each variable spans 148 days, representing an estimate of the length of water quality “memory” in the Delta.

CALSIM utilizes a linear programming solver to route water throughout the CVP-SWP network, and therefore requires all constraints to be in a linear form. This framework necessitates approximating the ANN flow-salinity relationships such that a linear constraint may be formulated. CALSIM dynamically approximates the relationship between Sacramento River flow and Banks/Tracy exports (both CALSIM decision variables) at each time step as a linear function. This linear approximation is illustrated in Figure 8-1. CALSIM implementation is described in detail elsewhere (DWR 2000).

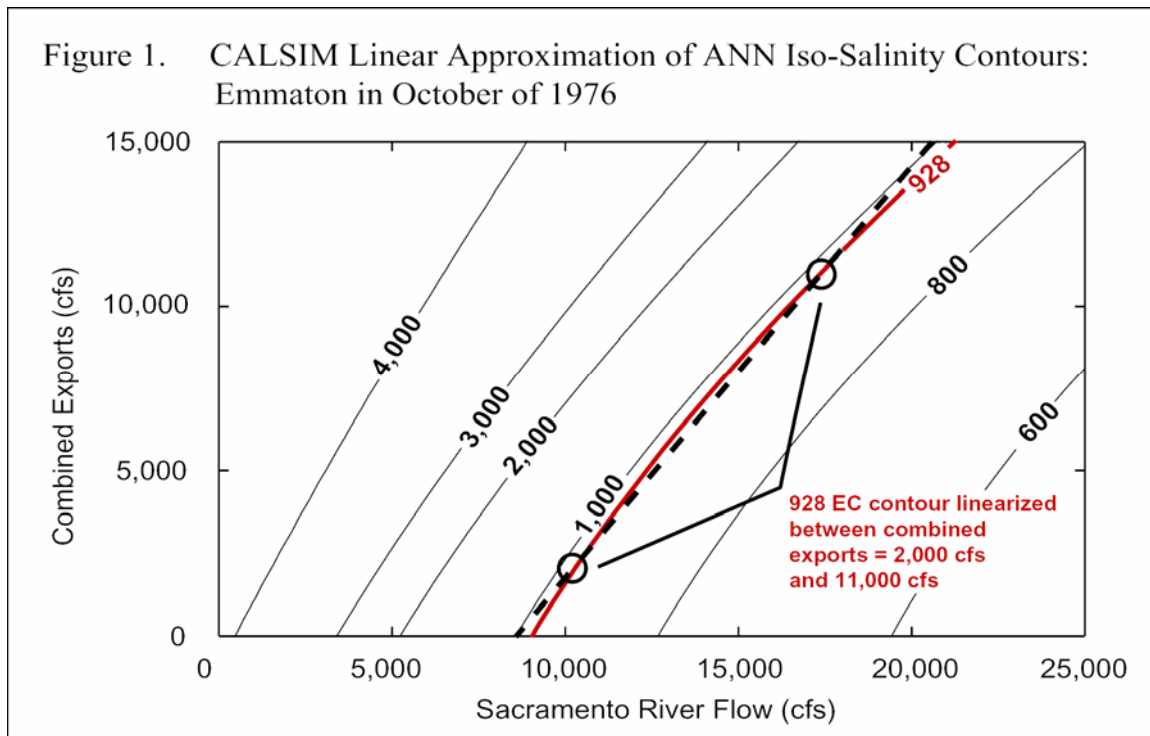


Figure 8-1: CALSIM Linear Approximation of ANN Iso-Salinity Contours: Emmaton in October of 1976.

8.3.2 Validation

A “full-circle” analysis was conducted to confirm that the ANN replicates DSM2 model results. The analysis consists of the steps outlined below and presented schematically in Figure 8-2.

1. Train the ANN module on an appropriate set of DSM2 simulations and implement in CALSIM.
2. Conduct a CALSIM simulation. Evaluate water quality results at key standard locations, i.e. Rock Slough, Jersey Point, and Emmaton.
3. Conduct a DSM2 simulation assuming Delta inflows, exports, and operations from the CALSIM output generated in Step 2. Evaluate water quality results at key standard locations, i.e. Rock Slough, Jersey Point, and Emmaton.
4. Compare water quality results from Steps 2 and 3. If the results compare favorably, the ANN module is validated. If the results are not favorable, retrain the ANN module.

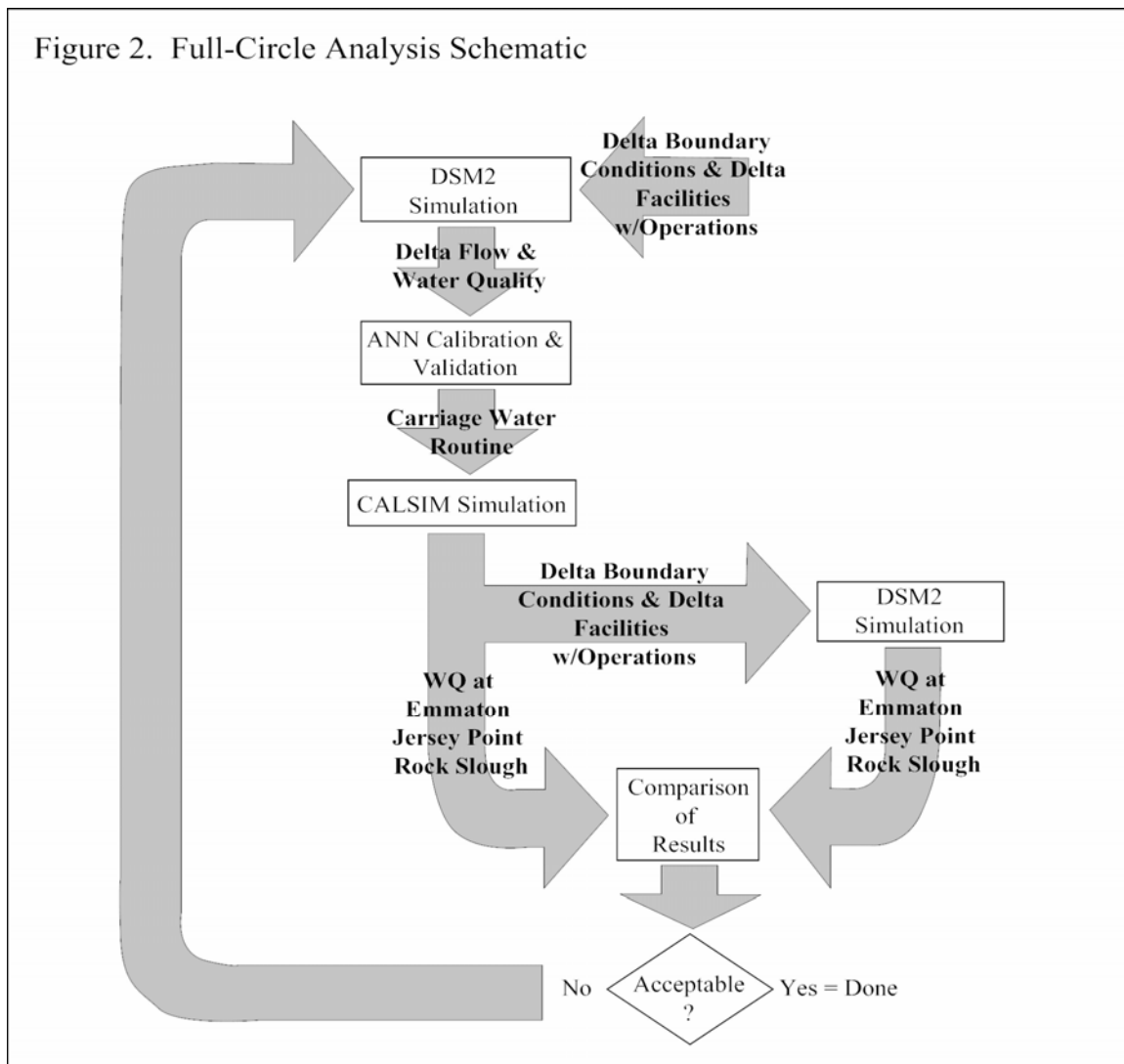


Figure 8-2: Full-Circle Analysis Schematic.

Figure 3. Full-Circle Analysis Time Series Results: Water Years 1976 -91

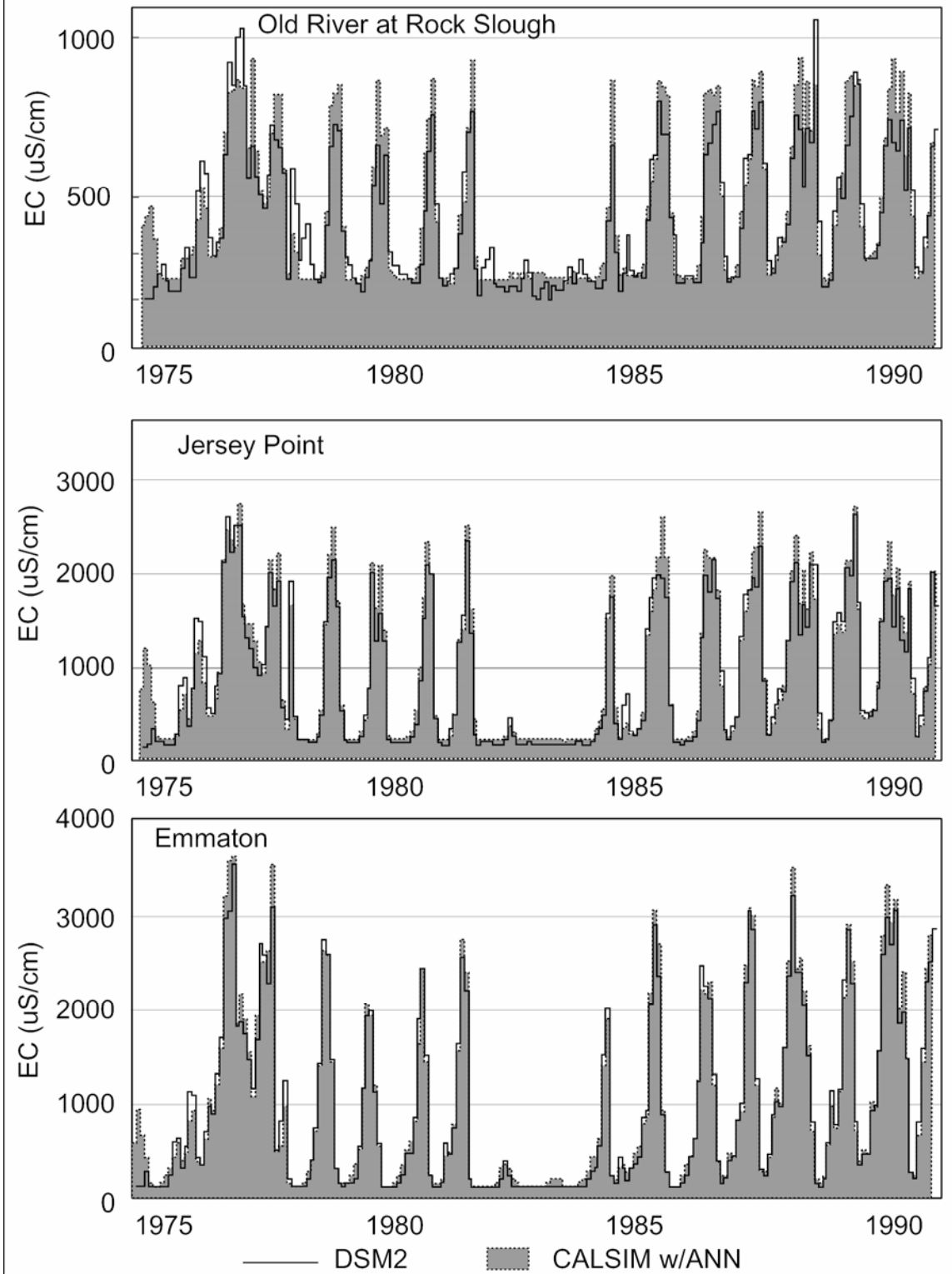


Figure 8-3: Full-Circle Analysis Time Series Results: Water Years 1976 – 1991.

Figure 4. Full-Circle Analysis Scatter Results: Water Years 1976 - 91.

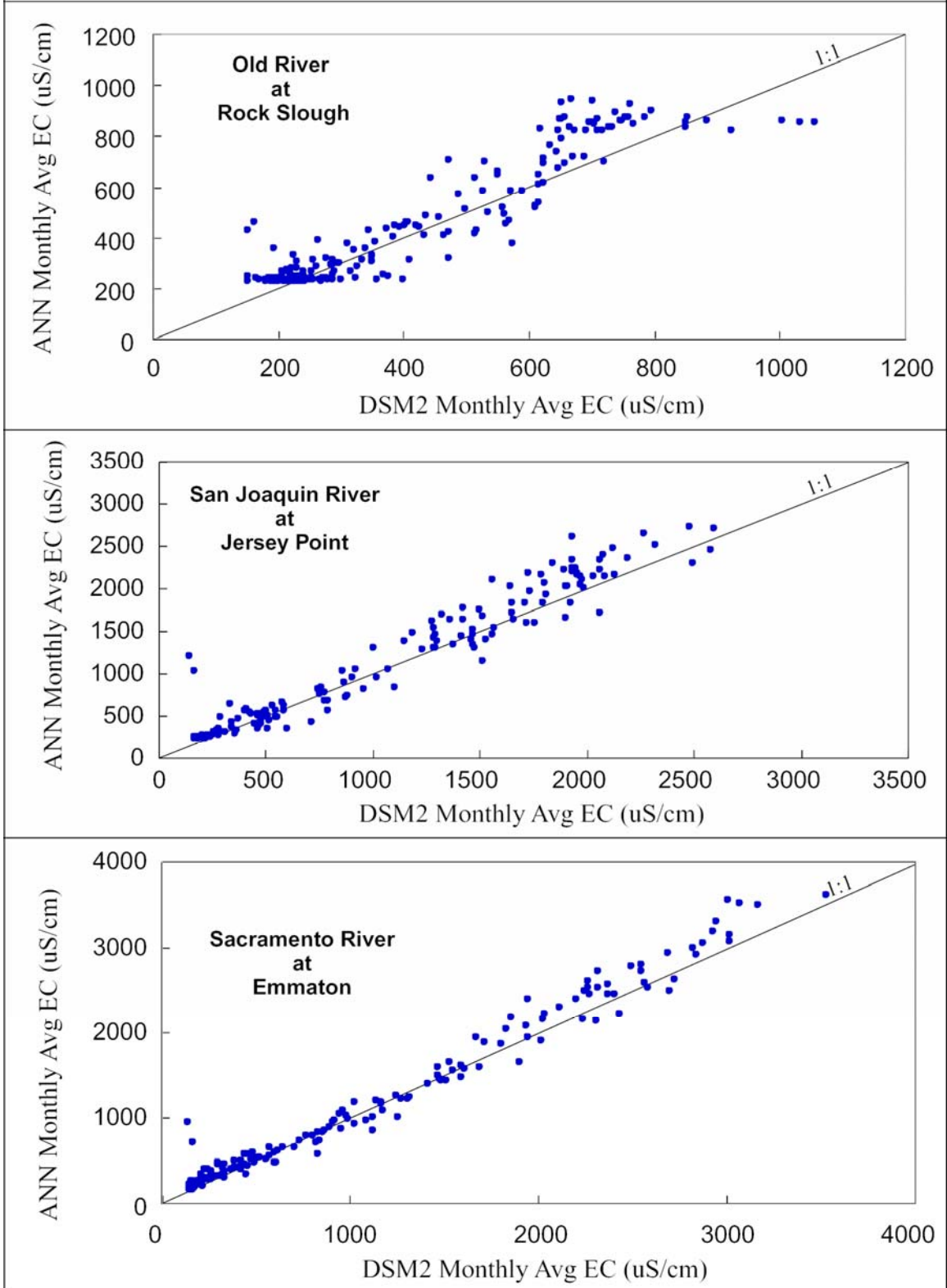


Figure 8-4: Full-Circle Analysis Scatter Results: Water Years 1976 – 1991.

Full-circle validation results for this study are presented in Figure 8-3 as time series plots and in Figure 8-4 as scatter plots. The figures show favorable comparisons between DSM2 and CALSIM water quality estimates at Rock Slough, Jersey Point, and Emmaton. The figures reveal a systematic ANN bias toward over-estimation at Rock Slough.

8.3.3 Impact on CALSIM Water Supply Estimates

A CALSIM base study (Study 898) was run with the G-model and with the ANN module to evaluate water supply impacts associated with the new flow-salinity routine. The ANN module generally requires more water than the G-model to meet Delta water quality standards and therefore results in lower dry-year and 73-year average CVP-SWP deliveries. For the 1928-to-1934 and 1987-to-1992 dry periods, the ANN model shows average annual delivery reductions of 430 and 350 TAF, respectively. Over the 73-year period, the ANN model shows an average annual delivery reduction of 30 TAF. Figure 8-5 displays the ANN water supply impacts.

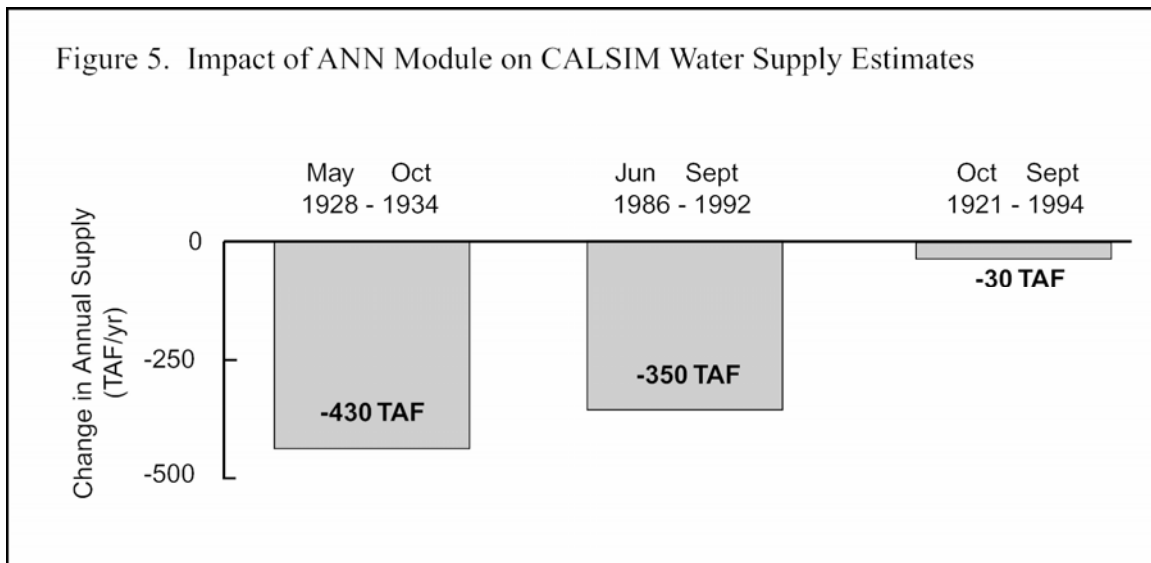


Figure 8-5: Impact of ANN Module on CALSIM Water Supply Estimates.

The difference in the CALSIM base study water supply required to meet Delta standards can be explained by simulating the resulting Delta inflows and operations in DSM2. Figure 8-6 shows a 1976-91 time series comparison of DSM2-predicted water quality with the applicable water quality standards at Old River at Rock Slough, Jersey Point, and Emmaton. The figure shows that the G-model CALSIM operation systematically gives higher Delta salinity than the ANN CALSIM operation. As a result, the G-model CALSIM operation frequently violates water quality standards. At Rock Slough, the G-model operation exceeds the standard in 37 months (18% of the time) while the ANN operation exceeds the standard in only three months. At Jersey Point, the G-model operation exceeds the standard in 18 months (9% of the time) while the ANN operation exceeds the standard in only two months. Finally, at Emmaton, the G-model operation exceeds the standard in 10 months (5% of the time) while the ANN operation does not exceed the standard.

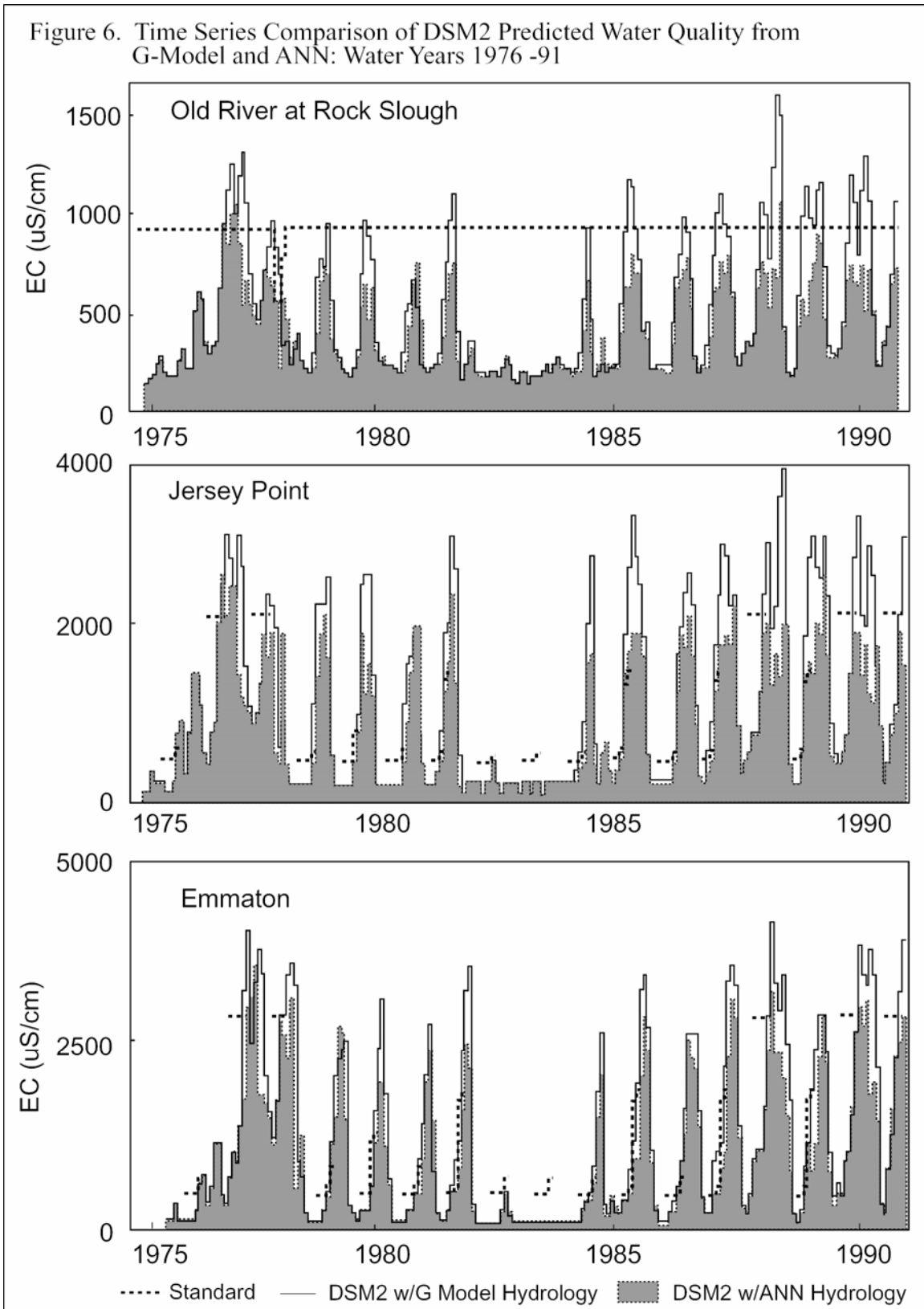


Figure 8-6: Time Series Comparison of DSM2 Predicted Water Quality from G-Model and ANN: Water Years 1976 – 1991.

8.4 Methodology for Estimating Carriage Water Requirements

A CALSIM study was designed to estimate a range of carriage water costs for each month of the year under a variety of water year types. The study defines carriage water as the additional volume of water necessary to transfer water across the Delta while maintaining water quality and ecological standards. Carriage water was released in the Sacramento River to accommodate water transfers from the Sacramento River Region to an unspecified South-of-Delta location. Water transfers from the San Joaquin River Region were not considered in this study. The initial study design considered water transfers of 30 TAF (500 cfs) and 60 TAF (1000 cfs).

8.4.1 Study Assumptions

CALSIM study assumptions are outlined below:

1. An artificial neural network (ANN) representation of the Delta was employed in CALSIM. The ANN was trained on data generated by the new production version of DSM2, which was recently calibrated by the IEP DSM2 Project Work Team.
2. The base CALSIM study is Study 898. Study 898 assumes 1995-level hydrology and demand levels and SWRCB Decision 1641 Delta standards.
3. Water transfers are independent of each other and have no impact on upstream or downstream system operations. A “position analysis” was employed to ensure the independence of each transfer. The Delta component was de-coupled from the upstream and downstream components of CALSIM.
4. The simulated transfer must meet all Delta constraints.
5. A Banks Pumping Plant capacity of 10,300 cfs was assumed. Water transfers that were constrained by this capacity were dropped from the analysis.
6. Downstream conveyance capacity constraints were not enforced.
7. Carriage water was not quantified in April and May, as pumping restrictions severely limit opportunities to transfer water in these months.
8. Extraordinarily high water requirements were not included in the carriage water estimates. In two months of the 30 TAF study (October 1947, October 1961), project operations could not meet the Rock Slough salinity standard and Sacramento River flow was constrained to 25,000 cfs. In these studies, water transfers did not trigger high water requirements to meet the Roe Island X2 standard.

8.4.2 Study Mechanics

A CALSIM “position analysis” was conducted to ensure the independence of each transfer and required the following steps:

1. Run base CALSIM Study 898.
2. Use output from Study 898 as initial conditions for the position analysis.
3. Simulate a 12-month period, beginning with a single water transfer in October 1921.
4. At the end of the 12-month period, reset all Delta conditions to the base condition in October 1992 (Study 898).
5. Simulate another 12-month period, beginning with a single water transfer in October 1922.
6. Repeat Steps 4 and 5 for the entire hydrologic period (water years 1922-94).
7. Repeat Steps 2 through 6 for other months.

8. Repeat Steps 2 through 6 for additional water transfer scenarios.

CALSIM was run 20 times (10 months x 2 transfer scenarios) in accordance with the steps outlined above.

8.5 Results

Tables 8-1 and 8-2 show 73-year average carriage water requirements by month and year type for transfers of 30 TAF (500 cfs) and 60 TAF (1000 cfs), respectively. Carriage water requirements are shown as percentages. Figures 8-7 and 8-8 show the same information graphically. Carriage water requirements are presented as average monthly flows rather than as percentages in the figures. The figures differentiate between salinity-based carriage water requirements and other carriage water requirements.

Table 8-1: Carriage Water Requirements for a 30-TAF Transfer by Month and Water Year Type (values in percent of transfer).

Table 1. Carriage Water Requirements for a 30 TAF Transfer by Month and Water Year Type (values in percent of transfer)										
Year Type	Oct	Nov	Dec	Jan	Feb	Mar	Jun	Jul	Aug	Sep
Wet	23	-	-	-	-	-	78	-	4	-
Above / Below Normal	50	19	-	-	-	-	153	63	42	61
Dry / Critical	68	45	18	6	44	101	78	38	39	53

Table 8-2: Carriage Water Requirements for a 60-TAF Transfer by Month and Water Year Type (values in percent of transfer).

Table 2. Carriage Water Requirements for a 60 TAF Transfer by Month and Water Year Type (values in percent of transfer)										
Year Type	Oct	Nov	Dec	Jan	Feb	Mar	Jun	Jul	Aug	Sep
Wet	16	-	-	-	-	-	74	-	-	-
Above / Below Normal	51	20	-	-	-	-	153	64	42	57
Dry / Critical	66	47	18	7	52	107	84	40	39	52

Figure 7. Average Sacramento Flow Required for a 30 TAF Transfer by Month and Water Year Type

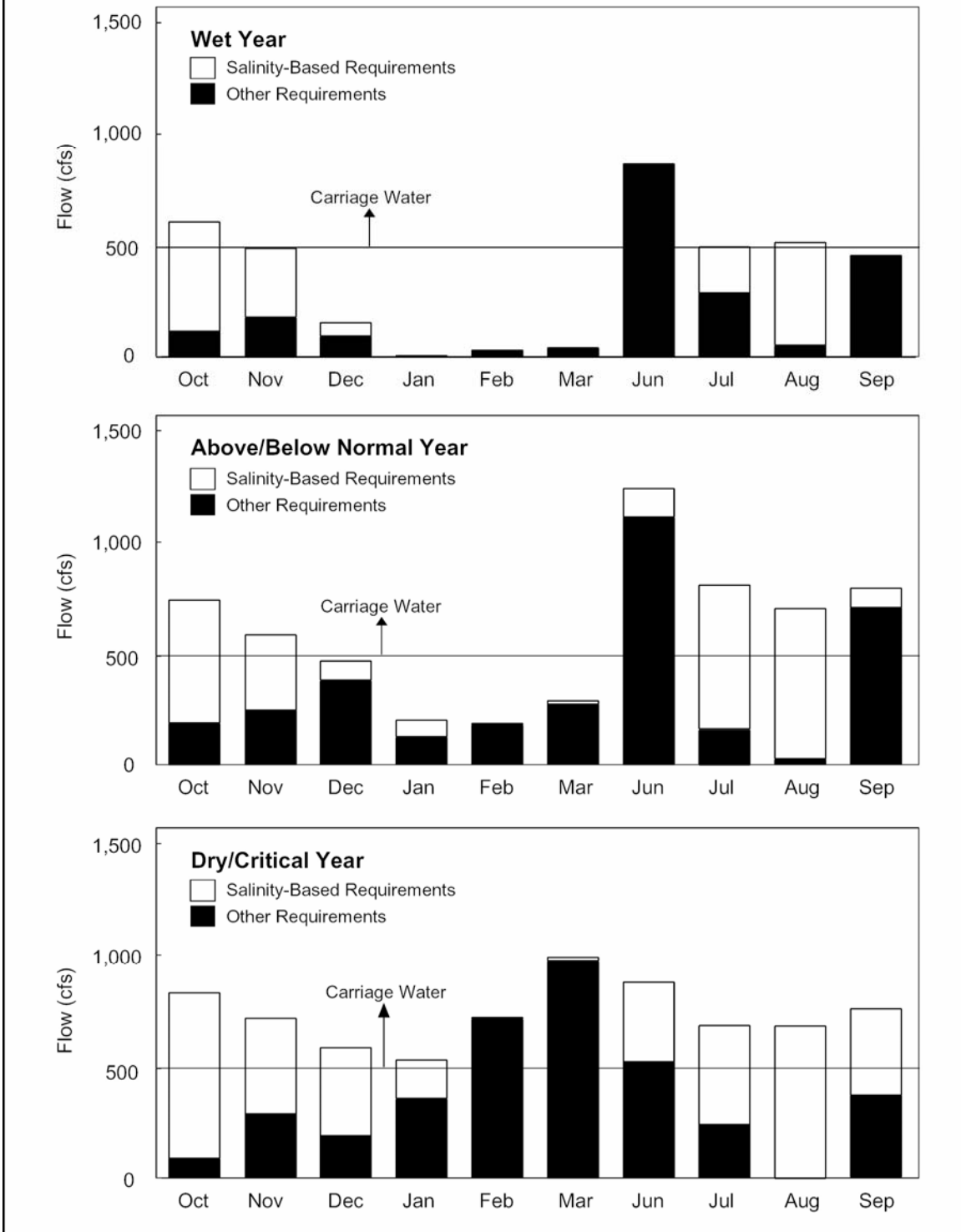


Figure 8-7: Average Sacramento Flow Required for a 30-TAF Transfer by Month and Water Year Type.

Figure 8. Average Sacramento Flow Requirement for a 60 TAF Transfer by Month and Water Year Type

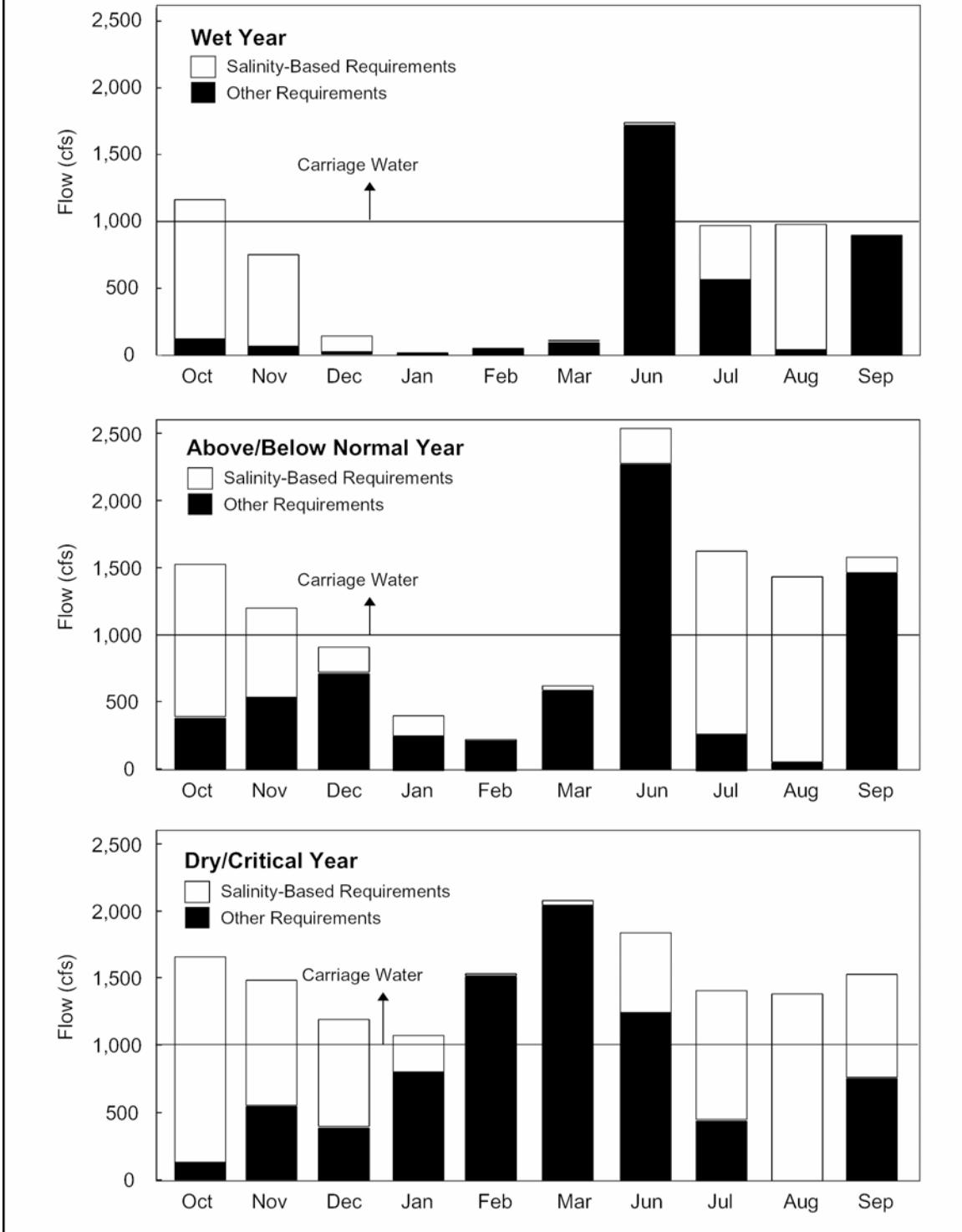


Figure 8-8: Average Sacramento Flow Requirement for a 60-TAF Transfer by Month and Water Year Type.

Key explanations and observations are provided below:

1. A 10 percent carriage water requirement suggests that, to export an additional 1,000 cfs from the South Delta, 1,100 cfs must be released upstream to meet Delta standards.
2. Several periods show no average carriage water requirement. In these months, the 73-year average upstream release required to export an additional 1,000 cfs from the south Delta vary up to 1000 cfs. Under certain hydrologic regimes, additional pumping draws water from the Sacramento River without significant salt intrusion, thus improving water quality in the south Delta.
3. Water year types are aggregated into three groups – wet, above/below normal, and dry/critical – to increase statistical sample sizes.
4. Carriage water requirements are sensitive to water year type, particularly those requirements associated with meeting salinity standards. In wet years, average carriage water requirements are at or near zero except during the months of October and June. In above/below normal water years, average carriage water requirements are typical in summer and fall months. In dry/critical water years, average carriage water requirements exist in all months.
5. The month of June is of special significance, showing high 73-year average carriage water requirements, regardless of water year type. The E/I ratio of 0.35 often controls in June, requiring 2.86 units of additional inflow for every additional unit of export ($1/0.35$). This additional inflow increases Delta outflow by 1.86 units ($2.86 - 1$) and results in a 186% carriage water requirement. Average carriage water requirements are significantly higher in June of above/below normal water years than in dry/critical water years. This is because the E/I ratio usually controls in June of above/below normal water years but rarely controls in June of dry/critical water years.
6. The month of October is also of special significance, showing a significant 73-year average carriage water requirement in all water year types. The CCC PP #1 salinity standard is often controlling in October. Table 8-2 shows an average carriage water requirement in the range of 20 to 70%.
7. The CCC PP #1 salinity standard often controls in November, December, and January of dry/critical water years and results in average carriage water costs of 10 to 50%. Meeting the E/I ratio in November of above/below normal water years typically requires carriage water of 20%.
8. February and March show 73-year average carriage water requirements of 40 to 110% in dry/critical water years to meet E/I standards.
9. Minimum outflow and Jersey Point salinity standards typically control in July and August, and result in average carriage water costs in the range of 40 to 60% in above/below normal years and approximately 40% in dry/critical water years. Average July carriage water requirements are significantly higher in above/below normal water years than in dry/critical

water years. This is because the Jersey Point salinity standard is more stringent in above/below normal water years.

- The month of September shows 73-year average carriage water requirements in the range of 50 to 60% in all but wet water years. The E/I ratio controls more frequently in above/below water years and the CCC PP #1 salinity standard controls more frequently in dry/critical water years.

Differences in 73-year average carriage water requirements (on a percent basis) between the 30-TAF transfer and the 60-TAF transfer are not significant. See Figure 8-9 for a comparison.

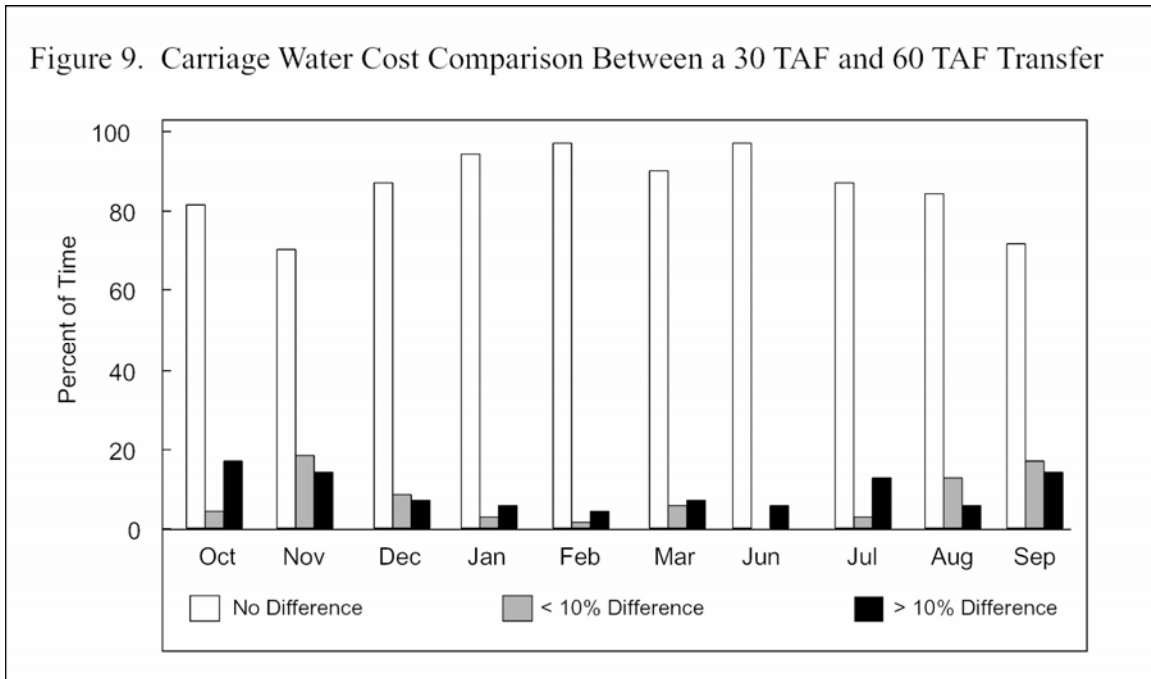


Figure 8-9: Carriage Water Cost Comparison Between a 30-TAF and 60-TAF Transfer.

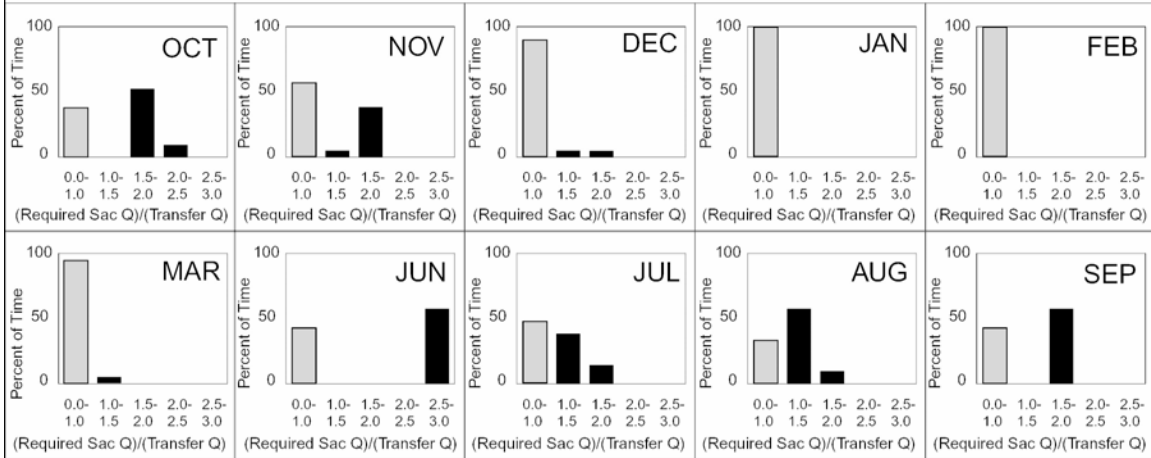
Carriage water is sometimes required in months subsequent to the transfer month. Table 8-3 illustrates this “lag” carriage water effect over the 73-year hydrologic sequence when 60 TAF (1000 cfs) is transferred in September. In many years, particularly during dry/critical water years, carriage water is required in September to meet outflow or salinity standards. However, even with this additional release of water, additional pumping results in Delta water quality degradation and triggers the CCC PP #1 salinity standard in October. Additional water must be released in October to meet the standard; and this additional carriage water is assessed to the September transfer. While this lag effect can be significant for a particular transfer, it is small over a 73-year average.

Table 8-3: Required Sacramento Flow for September Water Transfers (60 TAF) Over the 73-year Hydrologic Sequence.

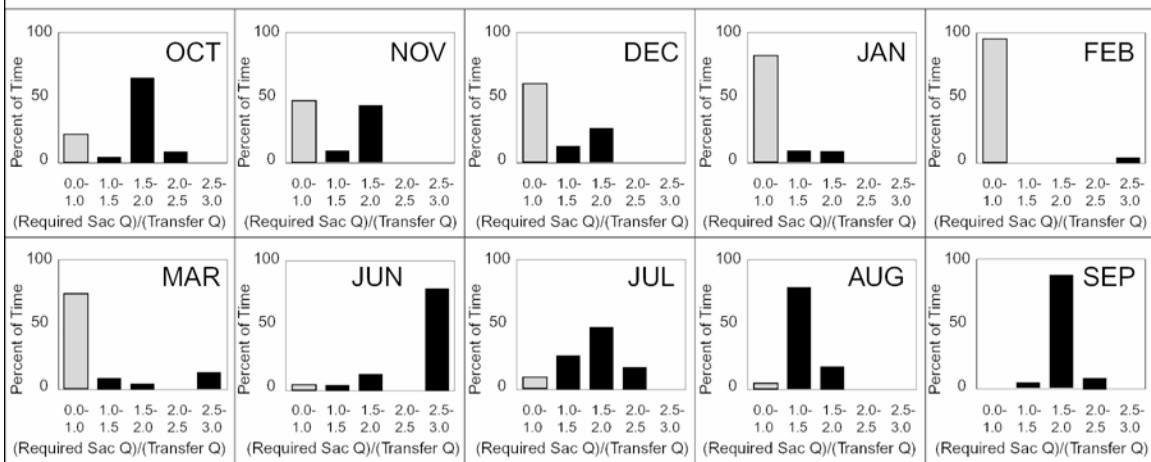
Table 3. Required Sacramento Flow for September Water Transfers (60 TAF) Over the 73-year Hydrologic Sequence											
Year	Type	Required Sac Flow (cfs)		Year	Type	Required Sac Flow (cfs)		Year	Type	Required Sac Flow (cfs)	
		Sep	Oct			Sep	Oct			Sep	Oct
1922	AN	1538	0	1951	AN	1538	0	1981	D	1124	810
1923	BN	1538	0	1952	W	0	0	1982	W	0	0
1924	C	1000	703	1953	W	1538	0	1983	W	0	0
1925	D	1538	0	1954	AN	1538	0	1984	W	1538	0
1926	D	1000	0	1955	D	1459	0	1985	D	1432	0
1927	W	1538	0	1956	W	1538	0	1986	W	1538	0
1928	AN	1538	0	1957	AN	1538	0	1987	D	1000	789
1929	C	1448	0	1958	W	0	0	1988	C	1478	0
1930	D	1130	444	1959	BN	1538	0	1989	D	1538	0
1931	C	1402	0	1960	D	1538	0	1990	C	1451	0
1932	D	1534	0	1961	D	1043	476	1991	C	1504	0
1933	C	1456	0	1962	BN	1538	0	1992	C	1473	0
1934	C	1440	0	1963	W	1538	0				
1935	BN	1000	1028	1964	D	1000	0				
1936	BN	1538	0	1965	W	1538	0				
1937	BN	1260	329	1966	BN	1410	0				
1938	W	0	0	1967	W	0	0				
1939	D	1000	983	1968	BN	1086	615				
1940	AN	1538	0	1969	W	0	0				
1941	W	1538	0	1970	W	1538	0				
1942	W	1538	0	1971	W	1164	0				
1943	W	1538	0	1972	BN	1538	0				
1944	D	1000	1072	1973	AN	1538	0				
1945	BN	1133	644	1974	W	0	0				
1946	BN	1538	0	1975	W	796	0				
1947	D	1000	0	1976	C	1000	913				
1948	BN	1538	0	1977	C	1342	0				
1949	D	1538	0	1978	AN	1538	0				
1950	BN	1538	0	1979	BN	1538	0				
1951	AN	1538	0	1980	AN	1538	0				

Figure 10. Distribution of Sacramento River Flow Required to Transfer 30 TAF by Month and Water Year Type (values in percent of time)

Wet Years



Above Normal / Below Normal Years



Dry / Critical Years

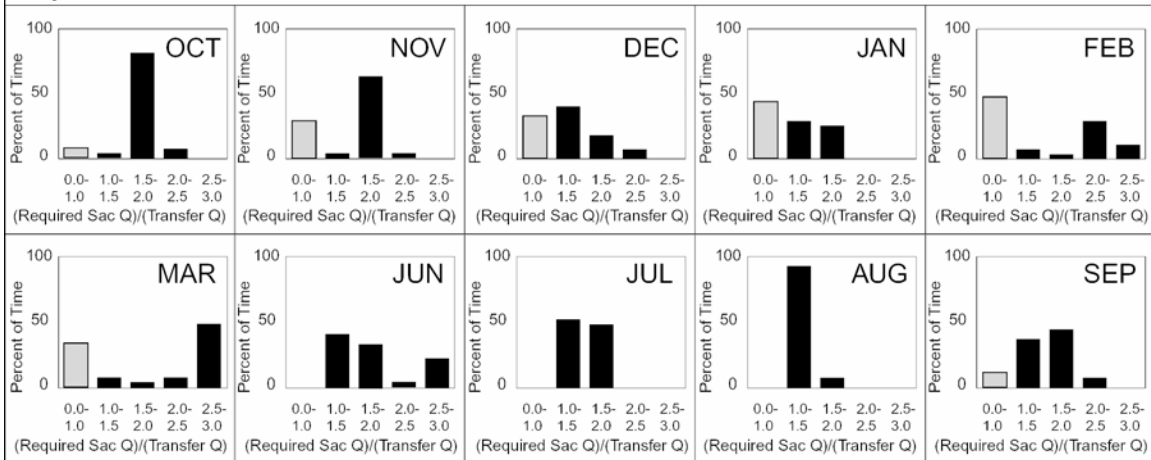
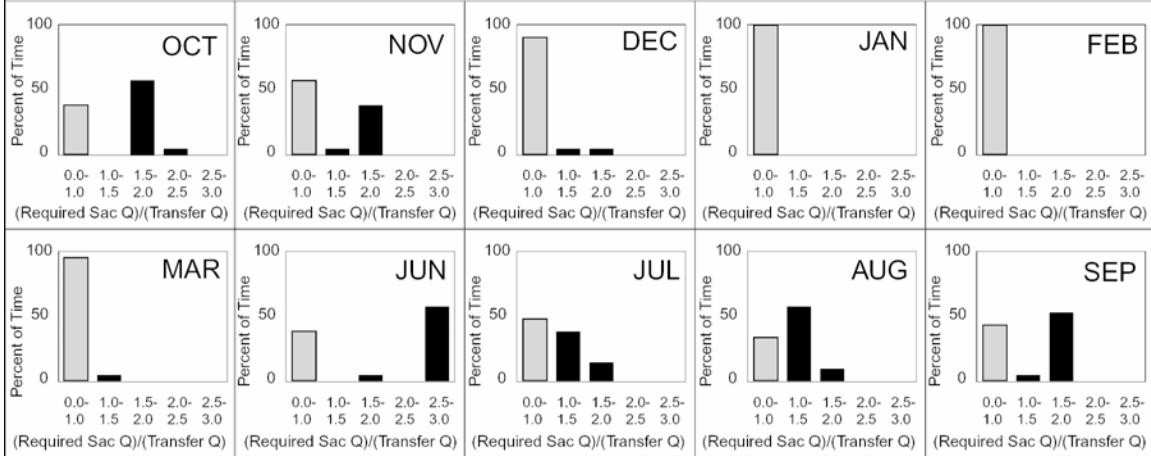


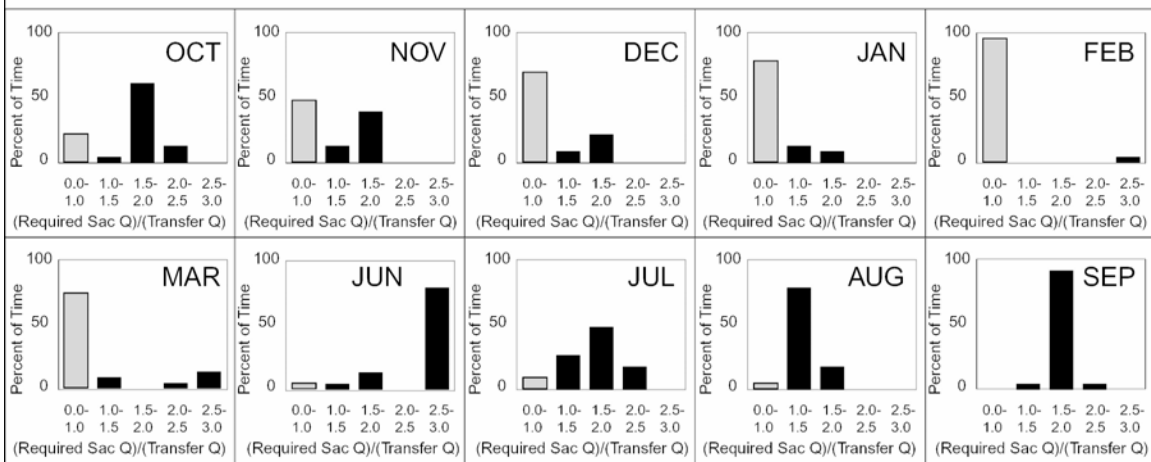
Figure 8-10: Distribution of Sacramento River Flow Required to Transfer 30 TAF by Month and Water Year Type.

Figure 11. Distribution of Sacramento River Flow Required to Transfer 60 TAF by Month and Water Year Type (values in percent of time)

Wet Years



Above Normal / Below Normal Years



Dry / Critical Years

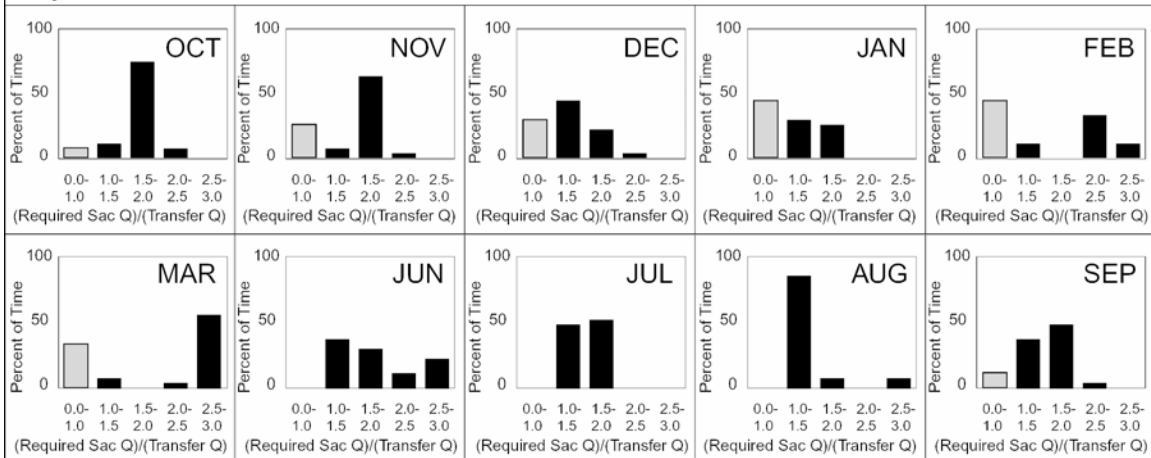


Figure 8-11: Distribution of Sacramento River Flow Required to Transfer 60 TAF by Month and Water Year Type.

Carriage water requirements can vary widely from year to year, depending on the particular monthly hydrology and Delta operation. Figures 8-10 and 8-11 show the carriage water requirement frequency by month and year type for transfers of 30 TAF (500 cfs) and 60 TAF (1000 cfs), respectively. Carriage water requirements are shown in these figures as the ratio of required Sacramento River flow to transfer flow. Consider a 60-TAF (1000 cfs) transfer in September of wet years. While Table 8-2 shows no average carriage water requirement for such a transfer, Table 3 reveals a Sacramento River flow requirement of 1,538 cfs in 11 of 21 wet years over the 73-year hydrologic sequence. The additional wet year flow is needed to meet the E/I standard. In other words, even though a 60-TAF transfer in September of wet years has no carriage water requirement on average, such a transfer would have a 54% carriage water requirement roughly half the time.

8.6 Discussion

8.6.1 Significance of Results

This study shows that ANN technology provides a fast and accurate method of approximating the flow-salinity relationships in DSM2, and therefore is a good candidate for modeling Delta salinity standards in CALSIM. The ANN approach will be adopted in CALSIM 2. Adopting ANN will have some impact on CALSIM base study water supply.

This study, which is the first to quantify Sacramento River water transfer costs over a long-term hydrologic sequence, supports DWR's typical carriage water assessments of 10 to 30%. As expected, the study shows carriage water costs to be fairly sensitive to water year type. Carriage water costs associated with meeting salinity standards are particularly sensitive to water year type. Over the long-term period, carriage water costs are small in wet water years and large in dry/critical water years. Carriage water costs in above/below normal water years are typical in summer and fall months. June uniquely shows high carriage water costs to meet E/I requirements, regardless of water year type. The department or other interested parties may wish to consider alternate statistical approaches to presenting carriage water results.

8.6.2 Using DSM2 to Quantify Carriage Water Costs

Tables such as those provided in Tables 8-1 and 8-2 should provide an appropriate level of detail for many planning-level carriage water estimates, including those needed for the State Board's Term 91 computations. However, it is noteworthy that DSM2 could be used to obtain a refined estimate of carriage water costs associated with a specific water transfer. In a practical application, the following steps could be followed to estimate carriage water costs for a specific water transfer:

1. Utilize the carriage water table to arrive at a reconnaissance-level carriage water estimate.
2. Update the carriage water estimate 2 to 3 weeks before the water transfer is to take place through a DSM2 forecast simulation.
3. Estimate the realized carriage water requirement after the water transfer has taken place through a DSM2 postcast simulation.

8.6.3 Negotiations with BDMF

The findings of this report have been shared with the BDMF Carriage Water Review Team. It is the intent of this team to reach a settlement among interested parties regarding the calculation of carriage water. If the team members do not reach a consensus, this report will provide the department with information on which to base its individual testimony regarding carriage water requirements.

8.6.4 Future Refinements

The carriage water estimates provided in this report will be updated as new information and model enhancements become available. In particular, carriage water estimates will be updated to include input from the BDMF Carriage Water Review Team and to reflect progress in baseline modeling of CVPIA b(2) and EWA operations.

8.7 References

- California Department of Water Resources. (1987). Summary of SWRCB Phase I Testimony by Mike Ford on Export-Outflow Relationships. Exhibits DWR-260 through DWR-264. July.
- California Department of Water Resources. (1991). Implementation of Delta Water Quality Standards in DWRSIM. Unpublished memorandum report, May.
- California Department of Water Resources. (2000). Integration of CALSIM and Artificial Neural Network Models for Sacramento-San Joaquin Delta Flow-Salinity Relationships. Unpublished memorandum report, December.
- Denton, R. and G. Sullivan. (1993). *Antecedent Flow-Salinity Relations: Application to Delta Planning Models*. Contra Costa Water District.
- Sandhu, N., D. Wilson, and R. Finch. (1999). *Modeling Flow-Salinity Relationships in the Sacramento-San Joaquin Delta Using Artificial Neural Networks*. Technical Information Record OSP-99-1. California Department of Water Resources. Sacramento, CA.

Methodology for Flow and Salinity Estimates in the Sacramento-San Joaquin Delta and Suisun Marsh

**22nd Annual Progress Report
August 2001**

Chapter 9: Use of Repeating Tides in Planning Runs

Author: Parviz Nader-Tehrani

9 Use of Repeating Tides in Planning Runs

9.1 Introduction

The Delta Modeling Section has traditionally utilized a “19-year mean tide” (at Martinez) in all DSM2 planning runs. The hydrology used in a traditional planning run has been monthly varying. The main argument for using a 19-year mean tide has been a reduction in CPU time and disk-space requirements, since a one tidal day HYDRO simulation was used for the entire month of QUAL simulation. The main disadvantage of using a 19-year mean tide (as opposed to a non-repeating or “real” tide) is the absence of spring/neap effects. The arrival of faster computers with larger disk-space is making the use of a real tide more practical. In fact, the Delta Modeling Section plans to use a real tide in planning runs in the near future (See Chapter 10).

During the past DSM2 calibration/validation effort (see Chapter 2), actual Martinez stage was used in the simulations. It has always been assumed that a 19-year mean tide would provide water quality results that are on average close to those corresponding to a real tide. However, this had never been proven.

Recent tests revealed results that were inconsistent with the intuitive assumptions. These tests showed that the predicted salinity results using a 19-year mean tide were consistently higher than those using the real tide. However, the first calibrated version of DSM2 (1997) on average had a tendency to underestimate salinity in the Delta. Thus, results using a 19-year mean tide were in fact closer to the field data. The predicted salinity in the Delta using the latest calibrated version of DSM2 approaches much closer to the field data compared to the 1997 version. So, it became apparent that using a 19-year mean tide with the latest calibrated version of DSM2 may overestimate the salinity in the Delta. In fact, a test run confirmed this hypothesis.

9.2 Design Repeating Tide

A modified repeating tide was generated. The goal was for the model results using this repeating tide to be very close to those using a real tide. To accomplish this, stage values for the 19-year mean tide were modified in such a way that the average value was kept the same, but the amplitude was reduced. The following equation illustrates how this was implemented:

$$Z^*(t) = Z_{avg} + (1-R) \times [Z(t) - Z_{avg}] \quad [\text{Eqn. 9-1}]$$

Where:

- $Z^*(t)$ = time-series for stage at Martinez for the proposed repeating tide,
- $Z(t)$ = time-series for stage at Martinez representing the 19-year mean tide,
- Z_{avg} = average stage based on the 19-year mean tide, and
- R = Reduction rate in amplitude (Used as a calibration parameter).

The reduction in amplitude implies a less powerful tide, and thus a reduction in salinity intrusion is expected. The magnitude of the reduction in amplitude was considered as a calibration parameter. A series of test runs were completed with varying degrees of reduction in amplitude of the tidal stage (R). These test runs covered January 1992 through September 1999.

9.3 Results

Test runs revealed that a 10% reduction in amplitude leads to the closest match with the model results using the real tide. Figure 9-1 shows a comparison of the 19-year mean tide versus the proposed repeating tide. Figures 9-2 through 9-4 show a three-way comparison of EC predictions at three key locations in the Delta using the proposed repeating tide, and those using the 19-year mean tide versus the ones using the real tide.

Figure 9-1: 19-Year Mean Tide and Adjustment

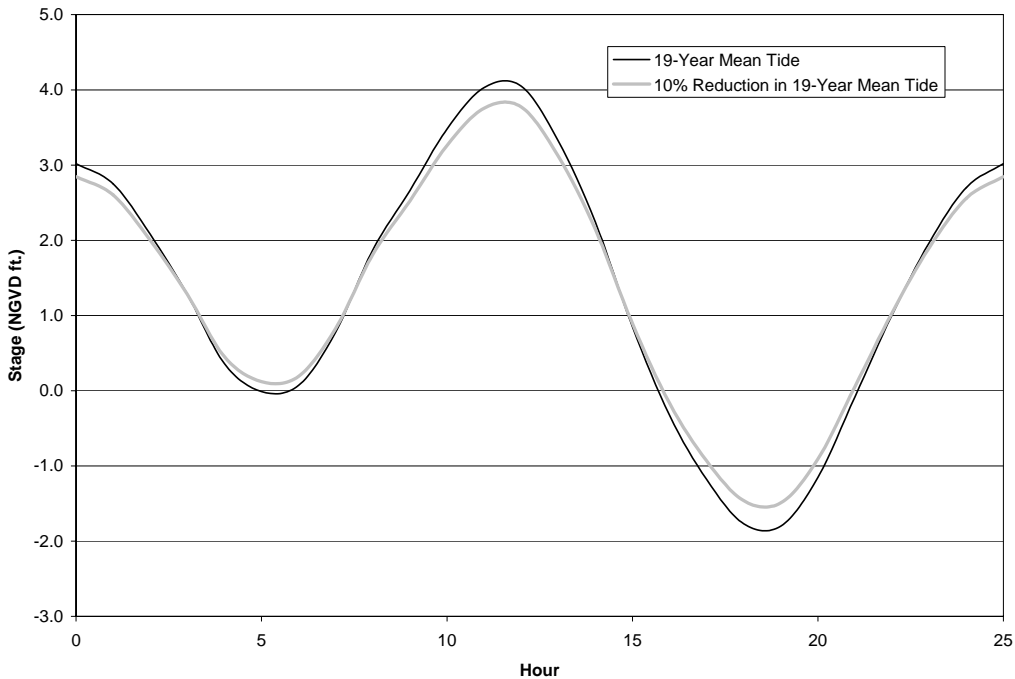


Figure 9-1: 19-Year Mean Tide and Adjustment.

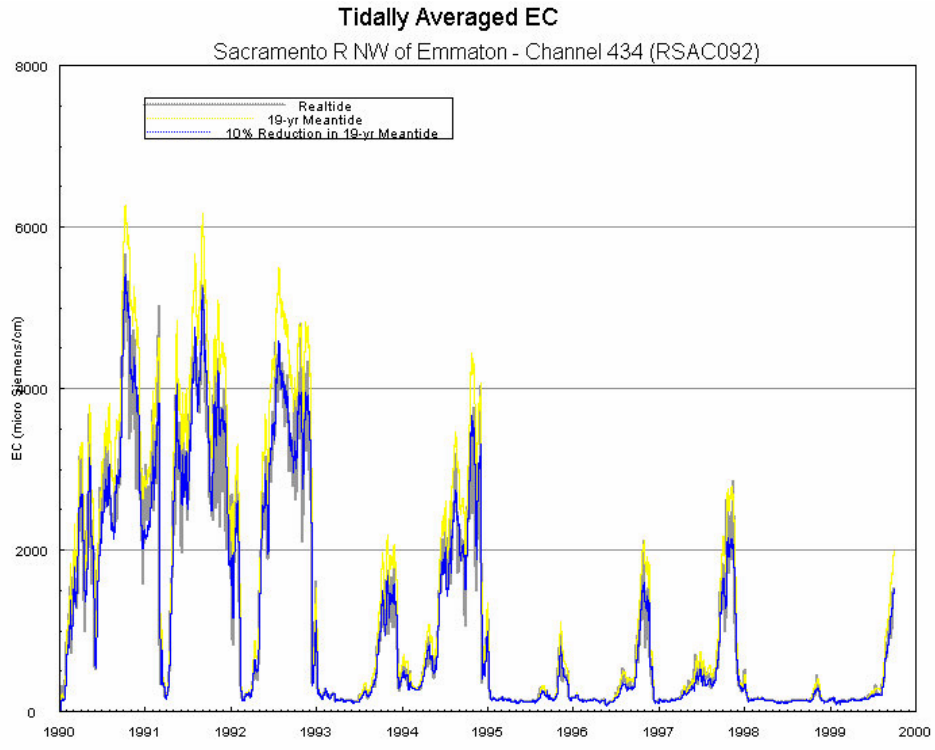


Figure 9-2: Comparison of EC for the Sacramento River at Emmaton.

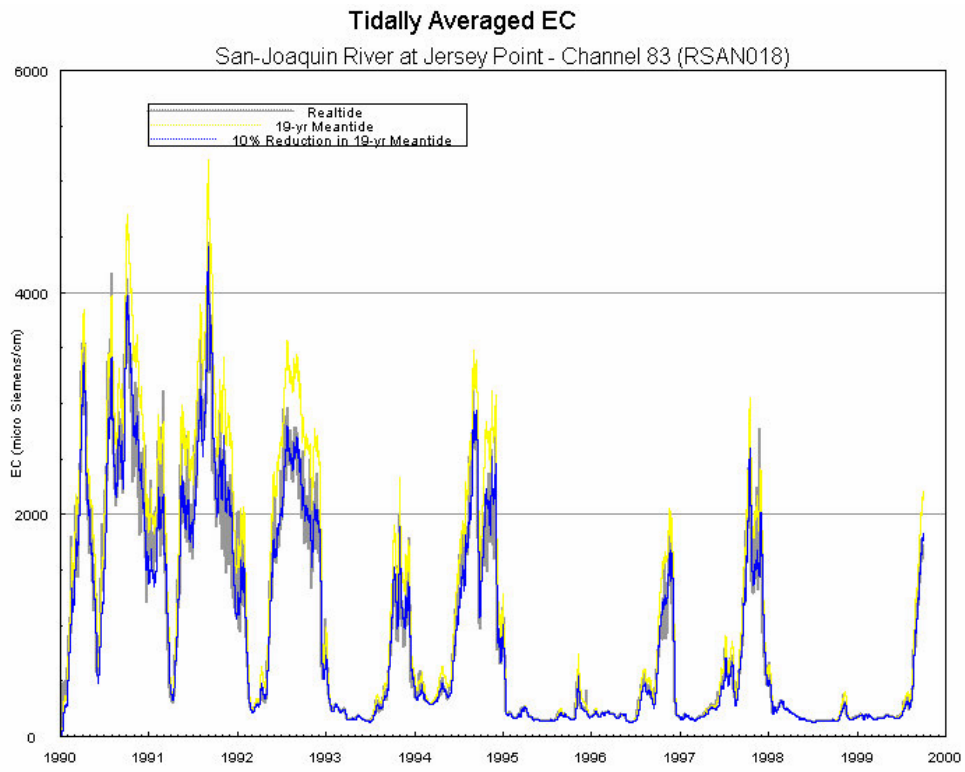


Figure 9-3: Comparison of EC for the San Joaquin River at Jersey Point.

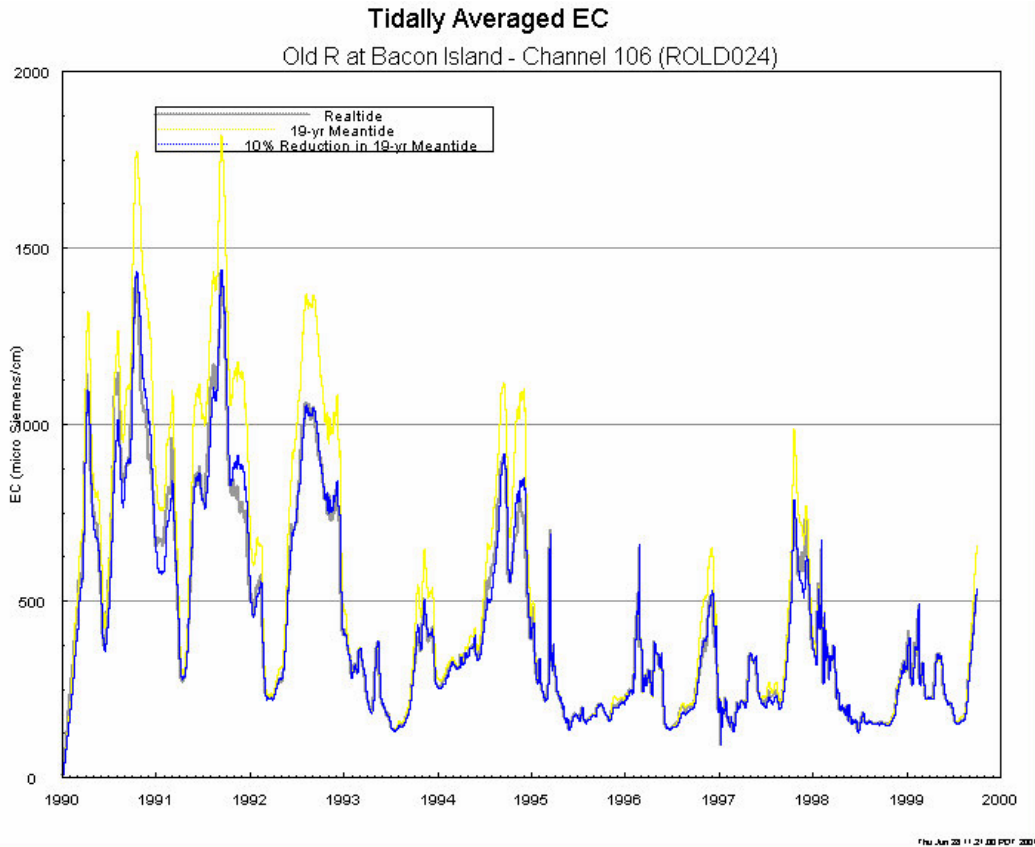


Figure 9-4: Comparison of EC for the Old River at Bacon Island.

9.4 Recommendations

It is recommended that all future DSM2 planning runs using repeating tides utilize the above proposed tide. This can be considered a short term solution until the methodology for using a real tide in planning runs is in place.

As for the terminology, it is recommended that this proposed tide be called a “Design Repeating Tide”, as it is no longer a 19-year mean tide.

Methodology for Flow and Salinity Estimates in the Sacramento-San Joaquin Delta and Suisun Marsh

**22nd Annual Progress Report
August 2001**

Chapter 10: Planning Tide at the Martinez Boundary

Author: Eli Ateljevich

10 Planning Tide at the Martinez Boundary

10.1 Introduction

The variety of study most frequently conducted by the Delta Modeling Section is the *planning study*. A planning study is a simulation in which a hydrologic input from a water project simulation model (CALSIM) is applied to the Delta to determine specific impacts on water levels, flows and quality. Because planning studies are needed to simulate the impact of a new policy or new facility under a variety of hydrologic conditions, these studies tend to cover large time periods. Currently, DSM2 planning studies simulate 16 years of monthly operations.

The computational burden of such a long simulation has forced modelers to make simplifications. The most important of these is the *repeating tide*. Instead of employing a 16-year-long stage boundary condition at Martinez that includes the spring and neap tides, planning models have employed a single 25-hour-long design tide¹, repeated many times over. After approximately a half dozen 25-hour cycles, the tide reaches a dynamic equilibrium with the inflow and pumping boundary conditions, which are held constant over a month. Once the equilibrium is achieved, the cyclical (25-hour) equilibrium flow regime is repeated over the entire month without the need for further hydrodynamic calculations.

Computational power has improved, and the Delta Modeling Section has begun to experiment with more realistic tidal boundary conditions. This chapter describes the construction of a new 1968-to-1999 planning tide (Martinez stage at a 15-minute time step) for this purpose. The goals for the new tide are realism, simplicity, and consistency. Higher accuracy filling of historical records is discussed elsewhere (Ateljevich 2000). The method presented here comprises two components: (1) an astronomical model to generate accurate harmonic components and spring-neap variation, and (2) a filtration of the San Francisco NOAA tidal station data to estimate long period fluctuations due to barometric changes and nonlinear tidal interactions. The model relating San Francisco to Martinez is based on residuals from a preliminary harmonic analysis, rather than the entire tide.

The tidal stage boundary and tidal salinity boundary must be estimated by methods that are consistent. Tidal salinity estimation is discussed in Chapter 9.

10.2 Available Data

The IEP database, <http://www iep.water.ca.gov/dss/>, has water level observations that list a number of stage stations in the estuary going back to about 1986 to 1988 (including Martinez). Before this time, consistent data are available only at the NOAA station in San Francisco. For the sake of consistency, it was decided to use only San Francisco data to help generate the 1968-1999 planning tide, rather than to weave data in and out from stations with limited availability.

¹ Some say “19-year mean tide”.

10.3 Tidal Composition

Ateljevich (2000) gives a qualitative description of tidal observations between San Francisco and Suisun Bay. Over this stretch of the estuary, tides are predominantly astronomical. This is particularly true at San Francisco – Munk and Cartwright (1966) cited San Francisco as an example of a particularly well-behaved harmonic tidal station. Martinez, being farther upstream, is slightly distorted compared to San Francisco. The tide is less sinusoidal, contains evidence of friction, and is occasionally influenced by very high values of Delta outflow. Since these shallow water phenomena are generated mostly between San Francisco and Martinez, the San Francisco tide is not much help in estimating them.

Fortunately, however, the most important deviations from a harmonic prediction are not distortion, but rather long period (4 day – 1 month) fluctuations due to barometric events and long wave non-linear interactions between tidal constituents. Figure 10-1 shows the tide at San Francisco and Martinez after the application of a low-pass tidal filter to remove diurnal, semi-diurnal and higher frequencies. The magnitude of low frequency fluctuations is up to several feet. Note that the tides at San Francisco and Martinez are also very similar in character at these frequencies. It is this similarity that we hope to harness.

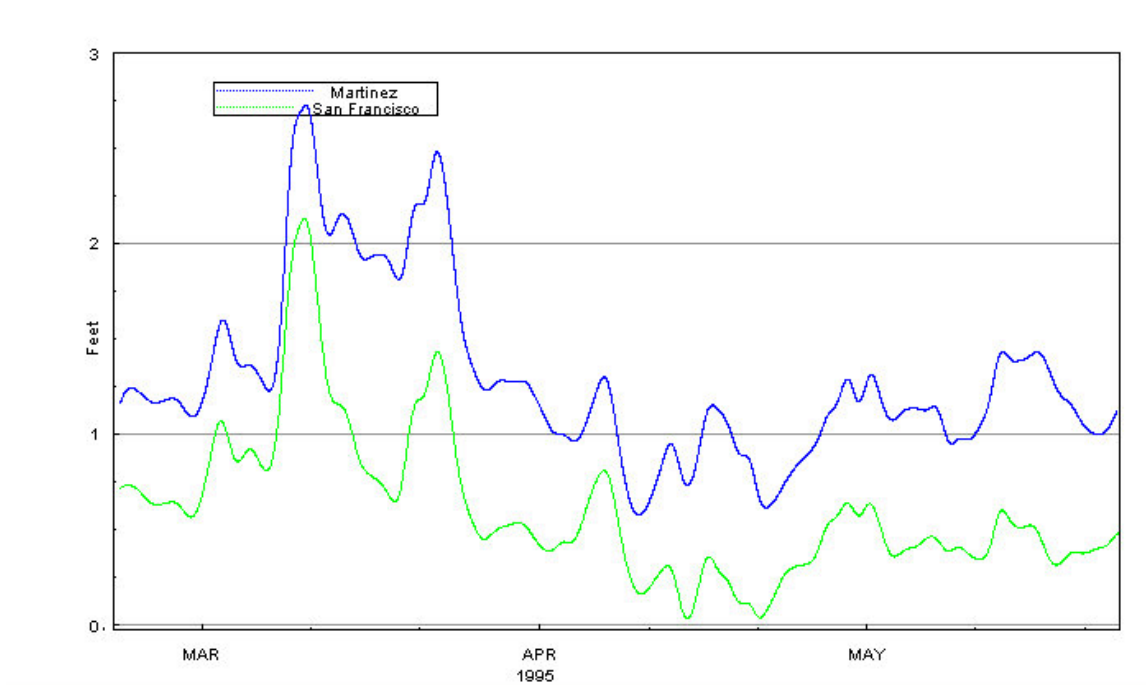


Figure 10-1: Stage After Application of a Low Pass Tidal Filter.

10.4 Astronomical Estimation

As in Ateljevich (2000), the model relating Martinez to San Francisco concentrates on the tidal residue – the portion of the tide that remains after removal of the main harmonic components. The formation of these residuals requires a harmonic estimate at both stations. The harmonic model is taken to be of the form:

$$z_{astro}(t) = \sum_{i=1}^N f_i a_i \cos(\omega_i t + \phi_i + u_i) \quad [\text{Eqn. 10-1}]$$

where $z(t)$ is the water surface height, at time t , ω_i are known frequencies associated with astronomical motion, a_i and ϕ_i are amplitude and local phase, and f_i and u_i are slowly varying amplitude and phase adjustments, as tabulated by the National Ocean Service (see Schureman 1941). The nodal adjustments are taken to be constant over each calendar year. Nodal adjustments are required for intermediate-sized (2- to 19-year) tidal records in order to compensate for the effects of satellite frequencies – clusters of frequencies so close to the “main” tidal frequencies that they cannot be resolved without an extremely long record. Tidal constituents (N) are selected as follows:

- Candidates are chosen from the standard NOS tabulation of common constituents. These are submitted for inclusion according to their magnitude in the tidal (gravity) potential, on the assumption that magnitude in the ocean tide is roughly proportional to magnitude in the tidal potential.
- Constituents with amplitudes less than a threshold (say, 0.01 feet) are dropped.

In the context of the residual model described in the next section, it turns out to be beneficial for the astronomical models for San Francisco and Martinez to be derived from the same time period. Since this limits us to the period for which Martinez observations are available, we will not be doing the best we possibly could at San Francisco. Specifically, by confining ourselves to a 10- to 15-year record, we forgo the opportunity to estimate constituents that resolve over a 19-year nodal cycle. Recall, however, that San Francisco plays only an auxiliary role in this process. Our goal is to generate similar residuals at San Francisco as at Martinez, rather than to eliminate error at San Francisco altogether.

10.5 Residual Tide

As mentioned in the previous section, the main model between stations is based on astronomical residuals. After experimentation with several model sizes, it was decided that the following rudimentary linear model is appropriate for relating Martinez residual tide to that at San Francisco:

$$z'_{mz}(t) = 0.50 [z'_{sf}(t-1) + z'_{sf}(t-2)] \quad [\text{Eqn. 10-2}]$$

where the primes indicate residuals from the harmonic model and time is in hours. The number 0.5 was obtained through ordinary least squares (OLS). OLS is asymptotically efficient for

estimating this model. Regression statistics such as R^2 are not appropriate due to time correlation of the errors, thus R^2 is not reported here.

10.6 Reconstruction

After the residual at Martinez is estimated using Equation 10-2, the tide must be reconstructed:

$$z_{mz}(t) = z_{astro}(t) + z'_{mz}(t) \quad [\text{Eqn. 10-3}]$$

In order to avoid large, wasteful errors simply from interpolation, it is recommended that the astronomical estimate be at a time step no coarser than 15 minutes and that the residual $z'(t)$ be interpolated from one hour to the finer time step *before* being added to the astronomical estimate. As long as these recommendations are followed, the actual interpolation method (linear, spline) is not particularly important. The author used a fourth order shape-preserving spline due to Huynh (1993).

10.7 Implementation and Discussion

The residual model described above was embedded in a VPlotter session (see Sandhu 2000) and used to prepare a 1968-to-1999 tide. The top plot of Figure 10-2 shows the Martinez tide residuals for the planning tide (with the aid of the San Francisco station) and for the astronomical model. The rms error is reduced 50%, from approximately 0.3 to 0.2 feet, and the number of excursions to a magnitude of 0.5 feet or more has been reduced dramatically. The bottom plot is the tidal average (through use of a Godin filter) of these same residuals. From this plot, it is clear that long wave variation is now confined to a very small band of about ± 0.15 feet, confirming that critical long-period variation has been properly estimated and the error statistics are now dominated by distortion and non-linear shallow water effects.

Compared to the best historical filling algorithms, the method is accurate, simple and computationally inexpensive. However, there is at least one caveat that applies to the approach. Long-period variation is still not predicted from physical principles. The long-wave component must be regarded as the realization of a seasonal random process.

Why is this important? Because, at least in theory, the barometric events that affect ocean water levels are related to storms affecting the major rivers. This presents no difficulty when the planning study is conducted using historical hydrology. However, under contrived alternate hydrology, any correlation between mountain hydrology and ocean events will not be preserved. This shortcoming becomes relevant only during major storms, because the correlation is small. For instance, the sample correlation between combined rainfall at two precipitation gages in the American River basin and San Francisco ocean heights (or changes in ocean heights) is less than 0.05. Any scheme sophisticated enough to relate storms to pressure and then pressure to ocean levels would not meet the simplicity requirements for this project.

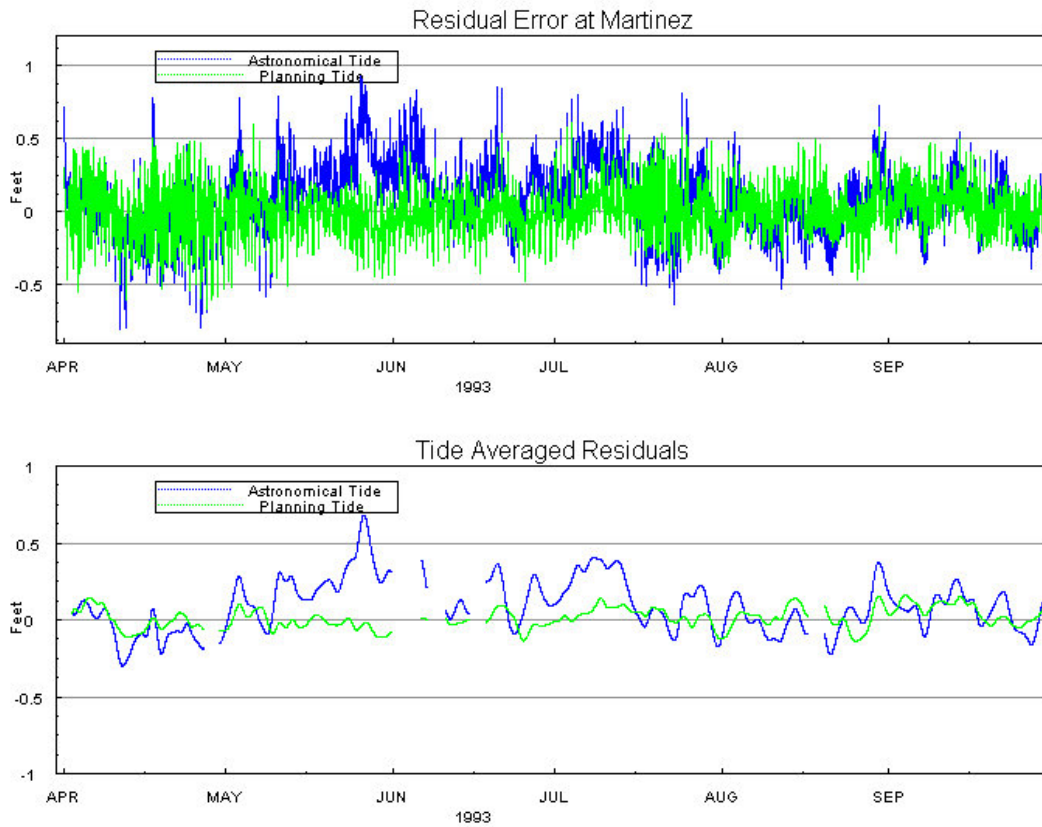


Figure 10-2: Comparison of the Planning and Astronomical Residual Tides in 1993.

10.8 References

- Ateljevich, E. (2000). "Chapter 8: Filling In and Forecasting DSM2 Tidal Boundary Stage." *Methodology for Flow and Salinity Estimates in the Sacramento-San Joaquin Delta and Suisun Marsh. 21st Annual Progress Report to the State Water Resources Control Board.* California Department of Water Resources. Sacramento, CA.
- Huynh, H.T. (1993). "Accurate Monotone Cubic Interpolation." *SIAM J. Numer. Analysis.* 30(1), pp 57-100.
- Godin, G. (1972). *The Analysis of Tides.* University of Toronto Press.
- Sandhu, N. (2000). "Chapter 4: VPlotter." *Methodology for Flow and Salinity Estimates in the Sacramento-San Joaquin Delta and Suisun Marsh. 21st Annual Progress Report to the State Water Resources Control Board.* California Department of Water Resources. Sacramento, CA.
- Schureman, P. (1941). *Manual of Harmonic Analysis and Prediction of Tides.* Special Publication No. 98. U.S. Coast and Geodetic Survey.

Zetler, Bernard D. (1982). *Computer Applications to Tides in the National Ocean Survey, Supplement to Manual of Harmonic Analysis and Prediction of Tides*. (Special Publication No. 98). National Ocean Survey (NOAA).

Methodology for Flow and Salinity Estimates in the Sacramento-San Joaquin Delta and Suisun Marsh

**22nd Annual Progress Report
August 2001**

Chapter 11: Improving Salinity Estimates at the Martinez Boundary

Author: Eli Ateljevich

11 Improving Salinity Estimates at the Martinez Boundary

11.1 Introduction

Empirical modeling plays an important role both in planning studies and in real-time modeling. Both of these modeling applications involve simulations over periods for which there is no observed data at the ocean boundary, as there is with historical runs. Without a stream of recorded data, Martinez is not a “boundary” for salinity in a simple physical sense. Rather, the location marks a compromise between the appropriateness of a 1-dimensional approximation (which is better upstream) and independence from the mechanics of the Delta (which is better downstream). At Martinez, salinity can be modeled empirically using aggregate boundary quantities such as Net Delta Outflow (NDO), without considering hydrodynamics within the model domain¹. Since the quantities required for the estimate are available prior to the DSM2 run, the estimates can be computed off-line ahead of time and used in DSM2 just like any other boundary condition.

Under current practice, the boundary empirical estimate is carried out as a preprocessing step to a planning run. Artificial neural networks (ANNs) estimate tidally averaged salinity as a function of the time history of Net Delta Outflow^{2,3}. A tidal component is then added to the daily average estimate, constructed using *Kristof coefficients*. These are a series of 25 hourly coefficients arranged in a tidal pattern that are multiplied by daily averaged salinity to produce a scaled tidal fluctuation. The tidal fluctuation is synchronized with the Martinez design (“19-year mean”) tide used for stage, so that the hydrodynamic (DSM2-HYDRO) and transport (DSM2-QUAL) parts of the simulation are realistically phased.

Several developments in Delta modeling practice have motivated the development of a better boundary salinity estimator. One is the real-time modeling program. Real-time modeling combines recent historical information with short-term projections and hypothetical operational decisions (see Chapter 12 for more information about real-time modeling). The empirical boundary estimate used for the hypothetical part of the run must agree with the earlier historical data. This is accomplished with a combination of better absolute accuracy and data assimilation. Another impetus for improving the boundary salinity model comes from planning studies. Planning studies traditionally have been conducted using a simplified 25-hour synthetic stage and salinity boundary. The computational limitations requiring this simplification have ceased to be relevant, and the Section is endeavoring to produce a more sophisticated planning simulation based on realistic tides for both stage and salinity.

¹ A reported exception are some activities in Suisun Marsh.

² See http://modeling.water.ca.gov/delta/studies/CalFed/models/mtz_ec_boundary/boundary.html.

³ In practice, a salinity surrogate such as EC is used, and the choice of surrogate is currently under review.

Because of the contrived nature of a planning scenario, the requirement for boundary estimates is not absolute accuracy, but rather realism. To be realistic, the salinity estimate must be consistent with Net Delta Outflow (NDO). In addition, the tidal fluctuation in salinity must be an appropriate counterpart to the tidal flows and water levels at the boundary – as much as possible, we want to avoid patterned aberrations. Repetitive, patterned error is more damaging than white noise to a water quality simulation – the system is damped and effectively smoothes out any mistake that does not repeat itself. Similarly, stage and empirical salinity must remain correctly in phase with one another over an entire 19-year lunar nodal cycle.

This report introduces an improved method of salinity estimation at the Martinez boundary. The model was designed to accommodate both real-time and planning applications. However, the real-time data assimilation component will not be discussed. The basis of the method is G-model and the work of Denton (1993). G-model was originally designed to predict daily-averaged salinity (EC). It is modified here with one major additional assumption: to derive tidal (15-minute) salinity estimates. The proposed model is not, however, a disaggregation of a daily-averaged model. In fact, heuristic arguments are presented here to suggest that the current brand of daily-averaged salinity estimate is a poor basis for any tidally disaggregated model.

11.2 G-model Basics

G-model is a conceptual-empirical model of salinity transport along the main stem of the Sacramento River. Details of the model may be found in Denton (1993) and in documents supplied to DWR and Delta modeling community by Dr. Gregory Gartrell and Dr. Richard Denton of Contra Costa Water District. The parametric form of the G-model is based on a successive steady-state argument. The development begins with the steady-state solution to a simple, 1-dimensional advective-diffusion problem in a steady current in an infinitely long channel with a downstream ocean and an upstream river boundary condition. The solution may be written as an exponential longitudinal salinity profile as follows (Denton, 1993):

$$s(x) = s_b + (s_o - s_b) \exp(-\tilde{\alpha} q_{\text{steady}} x) \quad [\text{Eqn. 0-1}]$$

where

$s(x)$ is salinity or a surrogate over longitudinal distance (x),

s_b is the ambient salinity that exists in upstream fresh water,

s_o is the ocean salinity at the downstream boundary,

q_{steady} is the steady, uniform flow rate, and

$\tilde{\alpha}$ is a dispersion parameter.

The most rudimentary successive steady state approximation would be to substitute time-varying $q_{\text{out}}(t)$ for q_{steady} in Equation 0-1. This substitution would be justified if the differential system was fast compared to the rate of change of $q_{\text{out}}(t)$. This is not the case in the Delta during dynamic periods, so the authors substituted *antecedent outflow* $g(t)$ instead, where:

$$\dot{g}(t) = \frac{g(q_{\text{out}} - g)}{\beta} \quad [\text{Eqn. 0-2}]$$

where

$g(t)$ is antecedent outflow,

$q_{\text{out}}(t)$ is net delta outflow, and

β is a parameter that determines how slowly the system reacts to changes in delta outflow.

Antecedent outflow converges to q_{steady} under steady conditions, and changes much more slowly than $q_{\text{out}}(t)$ does under dynamic circumstances. Empirically, $g(t)$ produces good transient results, although the author is not aware of any formal connection between the solution of the original time-varying transport equations and the solution of the steady-state form with the antecedent flow substitution.

After antecedent outflow is substituted in Equation 0-1, and considering a fixed point x , the standard form of G-model is as follows:

$$s(t) = s_b + (s_o - s_b) \exp(-\alpha g^n(t)) \quad [\text{Eqn. 0-3}]$$

where

$s(t)$ is salinity (or a surrogate such as EC),

s_o and s_b respectively represent ocean and river salinity (or upper and lower bounds),

α is the result of consolidating upstream distance into the dispersion parameter, and

n is an additional empirical shape parameter close to unity, used to compensate for imperfections in the antecedent outflow and exponential profile assumptions.

One difficulty with the use of *antecedent outflow* is finding an initial condition for Equation 0-2, the differential relationship between $g(t)$ and $q_{\text{out}}(t)$. Because $g(t)$ is a contrived quantity, it does not have a natural initial condition. To get around this problem, the original G-model tools use $g(0) = q_{\text{out}}(0)$. This analogy between antecedent outflow and actual outflow is a good approximation near the end of long periods of steady Net Delta Outflow. It is particularly useful in planning models, where the circumstances are synthetic, there is no field salinity to be matched, and the duration of the simulation is so long that salinity initial conditions influence only a small fraction of the model period.

In historical studies where an initial salinity is available and short-term accuracy is desired, we can use Equation 0-3 to convert $s(0)$ directly to $g(0)$ instead of using a flow. Equation 0-3 represents a functional, rather than differential, relationship between salinity and $g(t)$, so we can translate $s(0)$ into an initial condition without any assumptions of the equilibrium of the system. This choice of initial conditions dramatically improves the short-term performance of

G-model. In real-time applications, recent data are assimilated into the empirical model by means of a recursive filter, which more or less trivializes the initial condition.

In the conversion to a tidal model, a G-like model is integrated over steps smaller than one day, and there are a few special steps required to do this. First, Net Delta Outflow is interpolated to smaller time steps using a spline, although its interpretation is still as a daily average (just with a moving window over smaller time steps). The differential model for antecedent outflow is integrated with a standard second-order trapezoidal method. Note that for standard applications of G-model to estimate daily-averaged salinity, there is no reason to interpolate NDO or integrate the standard G-model at time steps smaller than a day.

Finally, the original authors of G-model have proposed corrections to Net Delta Outflow to account for both Delta filling and draining and better island consumptive use estimates. Only the Net Delta Outflow correction was used in the work presented here. This correction is of the form:

$$q_{\text{corrected}}(t) = q_{\text{ndo}}(t) - A\Delta z(t) \quad [\text{Eqn. 0-4}]$$

where A is a coefficient that represents the storage area filled by an incremental change in (tidally filtered) water surface height $\Delta z(t)$ or an estimate of $\Delta z(t)$ (see Section 11.6). The value of A currently being used is equivalent to $A = 40,000 \text{ ft}^2$ for daily increments of water surface height.

11.3 Tidal Model

The tidal extension of G-model is based on the following simplification of tidal dynamics:

Tidally-varying salinity is the result of a uniform, harmonic advection acting on the exponential salinity profile from G-model.

This advection is illustrated in Figure 11-1. Between time t_0 and t_1 , the salinity profile is shifted upstream (to the right) by a flood tide. Later, between t_1 and t_2 , the salinity profile moves back downstream with the ebb tide. To emphasize the role of advection, the profile has been drawn the same each time step. Figure 11-2 shows the full model, with independent changes in the G-model and advection components: the profile changes shape as it oscillates before the observer.

The interaction of the tide and the concentration profile is significant from the point of view of an observer. Imagine that t_0 represents a “centered” (or median) period during the tidal day and that the profiles t_1 and t_2 represent the tidal excursion in either direction. Due to the convex shape of the concentration profile, salinity at the point of the observer will achieve a greater extreme during flood than at ebb (dots have been placed on the plot to show the peaks in both directions). This lopsided tidal effect favoring the flood is regularly observed at Martinez and nearby stations. It is shown in Figure 11-3 during a period in 1998 with low-moderate salinity. In periods of high salinity, the salinity gradient is more linear over the length of the tidal excursion, and the phenomenon is less important.

It was asserted earlier that the temporal mean salinity is not an appropriate basis for a tidal model. The reason for this is tied to the lopsided tidal fluctuation just described. The tide does not attain its mean salinity when the displacement of the profile is at its tidally “centered” position. Instead, the mean salinity is biased above the centered value, and is attained sometime when the profile is upstream of the centered position. Just how far upstream depends on the curvature of the concentration profile, which, in turn, is dependent on flow regime and difficult to correct. Since the mean salinity and mean displacement do not coincide, schemes that begin with a mean estimate of salinity and then add a tidal fluctuation centered on this estimate tend to show common shortcomings. They fail to realistically capture the lopsided shape of the tidal fluctuation, and they grow increasingly inaccurate as concentrations decrease.

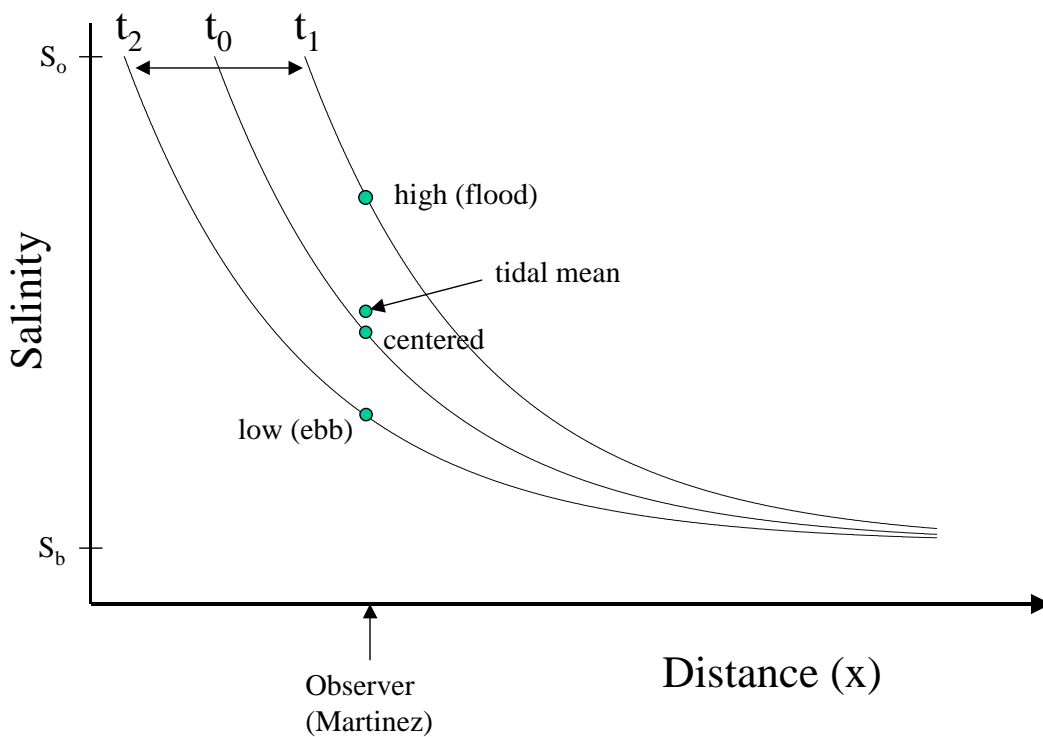


Figure 11-1: Advection of a Concentration Profile Back and Forth of an Observer.

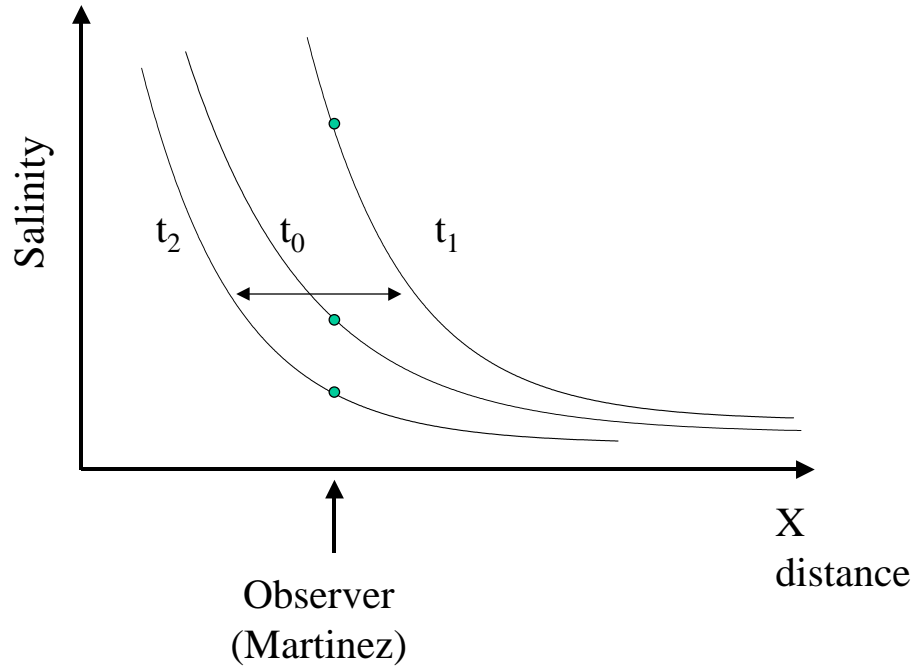


Figure 11-2: Advection of a Changing Concentration Profile.

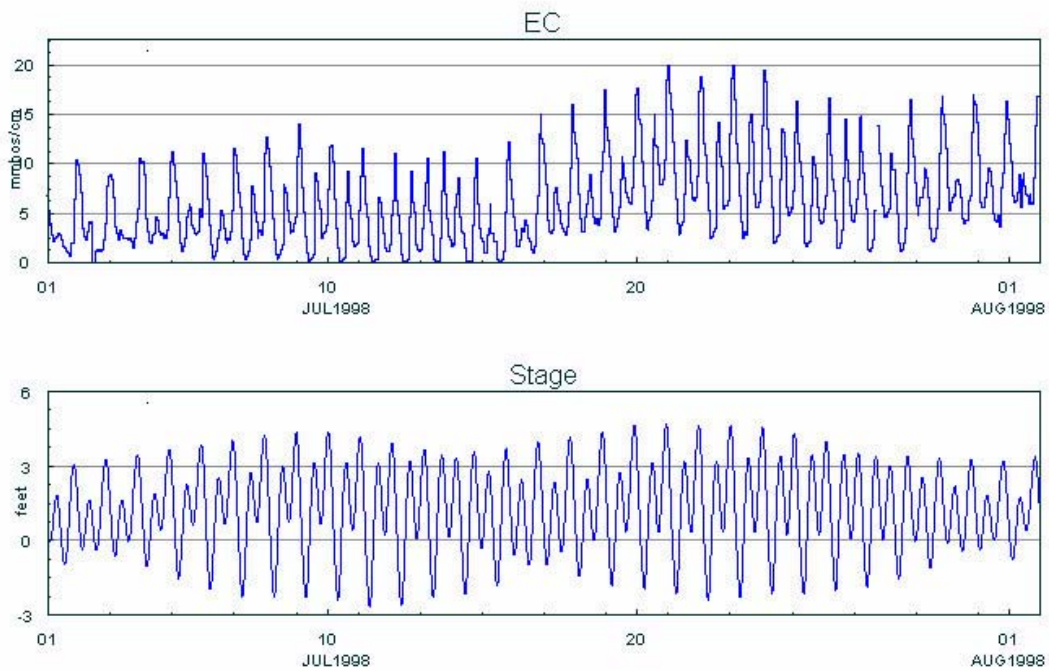


Figure 11-3: Comparing the Shape of the Stage and EC Tidal Fluctuation.

11.4 Mathematical Formulation

The conceptual model thus described can be written symbolically as follows:

$$s(t) = s_b + (s_o - s_b) \exp(-\tilde{\alpha} g^n(t) x(t)) \quad [\text{Eqn. 0-5}]$$

where the terms are as before and

$s(t)$ is (tidally varying) salinity,

$\tilde{\alpha}$ is the decay parameter of Equation 0-1 before distance was bundled into it for G-model (the longitudinal salinity profile is not used explicitly in G-model), and

$x(t)$ is a harmonic position, reflecting displacement of the profile.

Rearranging Equation 0-5, we obtain:

$$\ln\left(\frac{s(t) - s_b}{s_o - s_b}\right) = -\tilde{\alpha} g^n(t) x(t) \quad [\text{Eqn. 0-6}]$$

We can further write $x(t) = x_0 + x'(t)$ as a centered position x_0 and harmonic perturbation $x'(t)$, and combine the scalar product $-\tilde{\alpha} x_0$ into a coefficient β_1 :

$$\ln\left(\frac{s(t) - s_b}{s_o - s_b}\right) = \beta_1 g^n(t) + x'(t) g^n(t) \quad [\text{Eqn. 0-7}]$$

Comparing the model to the original G-model, it is clear that in the centered position $x'(t) = x_0$, the tidal model and G-model share the same parametric form, with β_1 analogous to the G-model parameter $-\alpha$. The only difference is that: β_1 will be chosen to fit the tidal model (i.e., it represents salinity when the concentration profile is tidally centered), whereas α is chosen to estimate daily-averaged values.

Next, we must model $x'(t)$, the component that reflects tidal displacement of the concentration profile. Because the local flow processes are dominated by linear terms, we will assume that $x'(t)$ is composed mostly of the same harmonic constituents as the stage. However, we opted not to fit an independent harmonic tide for the tidal displacement because tidal constituents would be resolved much less precisely for tidal displacement than for stage. The stage signal is directly observable, relatively noise free, and more perfectly harmonic in character. In contrast, tidal displacement is not directly observable – it is an intermediate term in our nonlinear model whose ultimate output (EC or salinity) is particularly noisy.

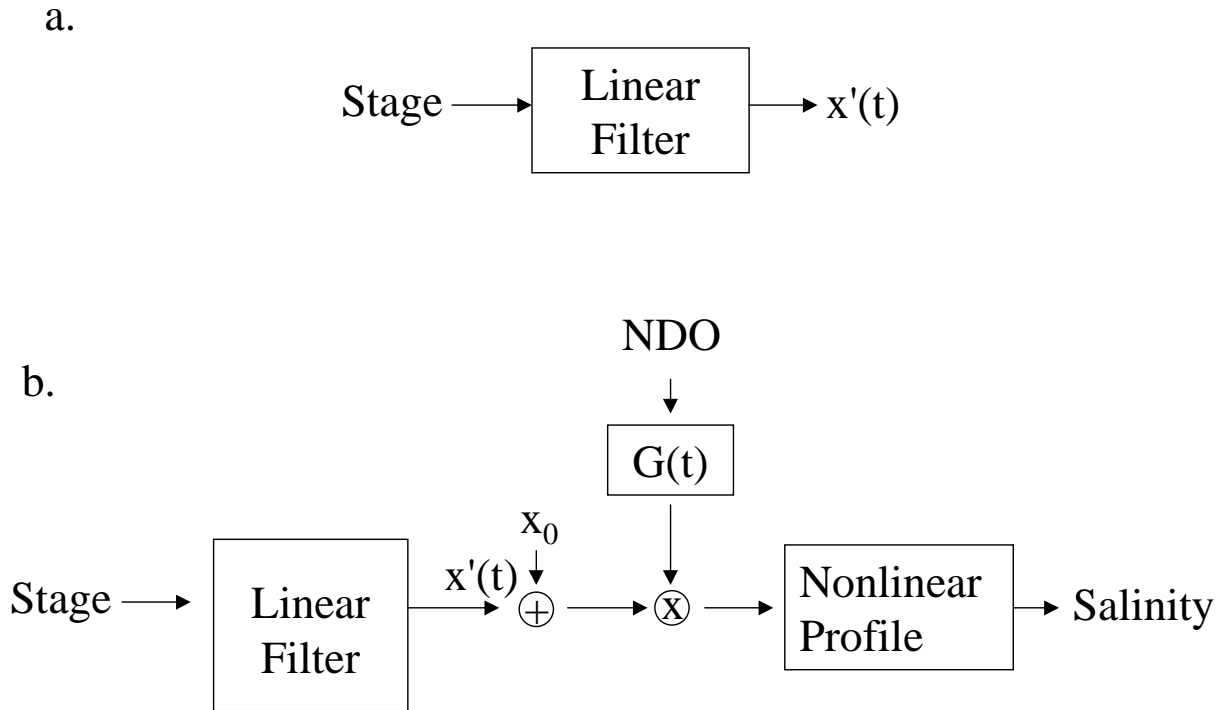


Figure 11-4: Models of Tidal Displacement. a) The Displacement Model as a Linear Filtration of Stage. b) The Displacement Model as Embedded in the Full Salinity Model.

A better way to control the relationship between stage and displacement of the salinity profile is to model $x'(t)$ as a linear filtration of stage. This solution allows stage to be estimated at whatever level of refinement is possible, and for the details to be inherited by the salinity model at whatever level is appropriate. The description here is based on the rudimentary system depicted in Figure 11-4a, a linear filter which takes stage as input and tidal displacement as output. We must bear in mind, however, that this an abstraction – the filter is embedded in a larger nonlinear model (Figure 11-4b), and since our only observations are salinity or EC, we will be grappling with the full non-linear model for estimation purposes.

Linear filters (such as the one represented schematically in Figure 11-4a) are very general and ubiquitous analysis tools for describing input-output systems. A familiar example in the water resources field is the “hydrograph”, which relates rainfall to runoff using a convolution filter. In the present case, we will also use a convolution filter modeling displacement on lagged values of stage:

$$x'(t) = \sum_{k=0}^{n_k-1} a_k z(t + k_0 \Delta t - k \Delta t) \quad [\text{Eqn. 0-8}]$$

where

a_k are the filter coefficients

$z(t)$ is a band-limited estimate of the tide,

n_k is the length of the convolution kernel (number of lagged input values used),

Δt is a spacing between lagged values (for instance we may take every third hourly value), and

k_0 is an offset of the filter allowing a shift in the first hour used.

Although the convolution sum of lagged values is a bonafide and familiar representation of a linear system, it is not particularly useful for discussing the system's effect on tides. Instead, we are interested in the frequency response, or “transfer function,” of the system – the gain or phase shift at various frequencies in the spectrum. For instance, in converting stage to tidal displacement, we might want to know whether the diurnal species are damped or shifted more or less compared to the semidiurnal species. These, incidentally, are the only types of effects that a linear filter can have – it cannot give rise to new frequencies that are not present in the input. For more on the spectral characteristics of linear filters, the reader is referred to any standard linear systems texts; Oppenheim and Willsky (1996) is recommended.

In the present case, the physical processes are consistent with a fairly simple transfer function. The linear filter used here is one that varies very slowly with frequency – enough that waves from different species (long waves, diurnal, semidiurnal, etc.) can be treated differently, but not so much to allow great variation in the treatment of waves within a species (e.g. M2 and S2). The simplicity in the transfer function will be achieved by choosing the convolution filter from the same family proposed by Munk and Cartwright (1966).

Munk and Cartwright (1966) was a landmark paper in tidal literature, which treated the oceanic tide as a filtration of gravitational tidal potential⁴. The authors posited a “credo of smoothness” for the transfer function of their model, much like the one suggested in the previous paragraph for the relationship between stage and the position of the salinity profile. They showed that a rudimentary family of smooth transfer functions could be generated using convolution filters with evenly (and fairly widely) spaced weights.

The filter proposed here is based on a “credo of even more smoothness”. Munk and Cartwright imposed smoothness within tidal bands, but used separate filters for long wave, diurnal and semidiurnal species. In the present model, smoothness is imposed across the entire important part of the spectrum, from long wave to semidiurnal. Because this broadness of the transfer function is associated with smaller time steps in the time domain, the filter spacing $\Delta t = 3$ hours was selected instead of the $\Delta t = 48$ hours adopted by Munk and Cartwright for their application.⁵ The actual “wiggleness” of the frequency response is determined by the number of terms the convolution kernel n_k ; longer filters admit more detail. In the present case $n_k = 7$ equally spaced

⁴ Gravitational potential is a fairly complicated function of the spherical geometry between (mainly) the sun, moon, and earth. It is a theoretical value used as the input or forcing of the filter. Oceanic tide is the output.

⁵ See the original paper for the arguments relating filter spacing to the domain of the of the transfer function.

components was thought to be the most detail that could be justified based on the data and the postulated simplicity of the system.

Finally, the input series $z(t)$ must be band limited. The filter is not designed for high frequencies (terdiurnal and higher species), but does have a frequency response at these frequencies and will exhibit unwanted behavior if the input includes them. This undesirable behavior can be avoided by excluding high frequencies from the stage estimate (z). If an observed stage signal is used as input – which is not particularly recommended – it should be low-pass filtered with a sharp cutoff frequency under 3 cycles/day. If the semidiurnal limitation suggested here proves too strict, the filter domain can be extended to terdiurnal species by taking $\Delta t = 2$ days.

With the filter in place, the full salinity model can now be written:

$$\ln\left(\frac{s(t) - s_b}{s_o - s_b}\right) = \beta_1 g^n(t) + g(t) \sum_{k=0}^{n_k-1} a_k z(t + k_0 \Delta t - k \Delta t) \quad [\text{Eqn. 0-9}]$$

Notice that the shaping exponent n has been dropped from the tidal term. This allows for slight deviation from a perfectly exponential profile, and was found to yield a better fit over a variety of flow regimes.

11.5 Estimation

The model (Equation 0-9) has thus far been described deterministically and mechanically. In order to estimate the parameters of the model from field data, however, we must consider the uncertainty due to model imperfections and generally noisy data. A naïve least squares approach is not appropriate for this fit, and the results it gives are poor.

No standard statistical model applies to the full tidal model. However, if we assume that we know $g(t)$, Equation 0-9 can be estimated conditional on $g(t)$ from a wide family of appropriate models. Therefore, the approach used to estimate the tidal model iterated informally between the following two steps:

- An outer step to fit the G-model parameter β from Equation 0-2 and the Net Delta Outflow correction A from Equation 0-4, and the parameter.
- An inner iteration for all the remaining parameters relating salinity or EC to $g(t)$ using a statistical model and Generalized Estimating Equations. This fitting procedure is statistically consistent conditional on a single set of G-model parameters from the previous step (these guarantees of consistency do not necessarily apply to the iterative process when the outer step is included).

There is little of a technical nature to describe about the outer procedure. The G-model fit in the outer step was mostly qualitative – although some refinement was carried out based on squared

residual error from the inner iteration. The main qualitative criterion for adjusting β was to match the response-time salinity data to long-period (three week or more) variations in outflow observed in the field data. The main criterion for assessing the Delta outflow correction was correctness of the shape of the tidal envelope over two-week cycles. These two goals are somewhat conflicting, a point that will be taken up again during the discussion of results. The parameter s_b was fixed at a value of 200 $\mu\text{mhos/cm}$ based on physical arguments, and the parameter s_o was nominally set at 32,000 $\mu\text{mhos/cm}$ (it is effectively corrected in the next step, anyway). The shaping factor n was taken to be 0.7.

The inner procedure is based on a more formal statistical model. Assume that an adequate guess for the G-model parameters is available and $g(t)$ has been pre-calculated. We will introduce the random component into our formula by means of expectations:

$$\ln \left[E \frac{s(t) - s_b}{s_o - s_b} \right] = \beta_0 + \beta_1 g^n(t) + g(t) \sum_{k=0}^{n_k-1} a_k z(t + k_0 \Delta t - k \Delta t) \quad [\text{Eqn. 0-10}]$$

In Equation 0-10, the expected value is internal to the logarithm. By applying the expectation to a term linear in $s(t)$, we avoid bias due to the log transformation, and can cast the expression conveniently as a Generalized Linear Model (GLM). The difference $s_o - s_b$ can also be removed successively from both the expectation and the log, in which case it just becomes an additive scalar that can be absorbed or corrected by the intercept term β_0 . This is the reason that the initial choice of s_o was described before as “nominal”.

Given that the products of $g(t)$ with the lags of $z(t)$ are pre-calculated, Equation 0-10 is in the

form of a GLM, with log link function, response variable $y = \frac{s(t) - s_b}{s_o - s_b}$ or $y = s(t) - s_b$ as

convenient and linear parameters β_0, β_1, a_k ($k = 0 \dots n_k$). The log function is a natural link of the Gamma family of distributions, which have skew, sign, and mean-variance relationship that are appropriate for the physical circumstances. The choice of a Gamma distribution is more general and robust than, say, a Gaussian distribution. To add further robustness, the Gamma family for the GLM was converted to a robust family using the Splus function for this purpose.

The fit can be improved further if we bear in mind that the model errors are time-correlated. We can account for this with minimal variation in approach by using Generalized Estimating Equations (Liang and Zeger 1986), which are an extension of GLM that allows a correction for patterned, correlated error. Generalized Estimating Equations (GEE) allow a “working covariance” model for the covariance, and one popular choice is the AR1 time-correlated model. GEE gives consistent coefficients for the linear parameters even if the working covariance model is only approximate. The AR1 model is, of course, only approximate, but it is better than the naïve assumption of white noise. In fact, the YAGS (Yet Another GEE Solver) software performing the fit estimated the residual autocorrelation parameter as high as 0.909, which indicates that the errors are far from “white”.

Table 11-1 lists the calculated coefficients for the model, fit to data spanning from August 20, 1991 to September 5, 1992. Examples in the tide literature using similar filter design (the “response” method) indicate that the coefficients vary considerably more in the time domain than in the frequency domain, so the convolution weights should not be over-interpreted. The robust standard error estimates are constructed to account for model failures: the “naïve” standard error estimates, which do not take these into account, tend to be just less than half the robust values. The z-score statistic is based on the asymptotic (normal) distribution of the coefficient estimates and can be interpreted in pretty much the same way a t-statistic is in regression. Several of the coefficients (β_0 , a_1 , and a_2) are not significant according to this statistic, but they were retained in order to maintain the evenly spaced pattern of the filter and interpretation of the model.

Table 11-1: Coefficient Estimates, Standard Error, and Z-Scores (GEE).

<i>Component</i>	<i>Coefficient</i>	<i>Robust std. Error</i>	<i>Robust z-score</i>
β_0	1.37E-02	3.58E-02	0.3821742
β_1	-6.43E-05	6.74E-06	-9.5344983
a_0	1.59E-04	1.91E-05	8.3407955
a_1	-1.28E-05	1.50E-05	-0.8485398
a_2	6.96E-06	2.40E-05	0.2898766
a_3	4.83E-05	1.34E-05	3.6016491
a_4	-7.67E-05	1.63E-05	-4.7145223
a_5	6.93E-05	8.77E-06	7.8985614
a_6	-3.85E-05	1.42E-05	-2.7054738

It is perhaps more relevant (and stable) to view the transfer function in the frequency domain when the filter components a_k ($k = 0 \dots n_k$) are interpreted literally as a linear filter on $z(t)$. Figure 11-5 shows the transfer function under the GEE/YAGS estimate, including both gain (magnitude amplification) and phase shift.⁶ For comparison, the corresponding fit for GLM is shown in Figure 11-6. The GEE/YAGS estimate spans a greater range, but the differences are modest near the important frequencies of $1c/d$ and $2c/d$. The main trend in either case is greater attenuation of higher frequencies than of lower frequencies. There is an apparent phase shift induced by the filter that varies linearly with frequency. This, however, is just the artifact of using a 3-hour initial offset ($k_0 = -1$) for the filter. Three hours comprise a greater proportion of a shorter (say, 12-hour) period than it does of a longer (say, 25-hour) period constituent. So, in terms of degrees or cycles, the offset causes a greater shift in high frequency, short period waves. When the transfer function is adjusted to remove this offset (not pictured), the phase response is otherwise quite flat.

⁶ Magnitudes are small because the filter output is normally multiplied $g(t)$ to produce salinity estimates and this multiplication is not represented here.

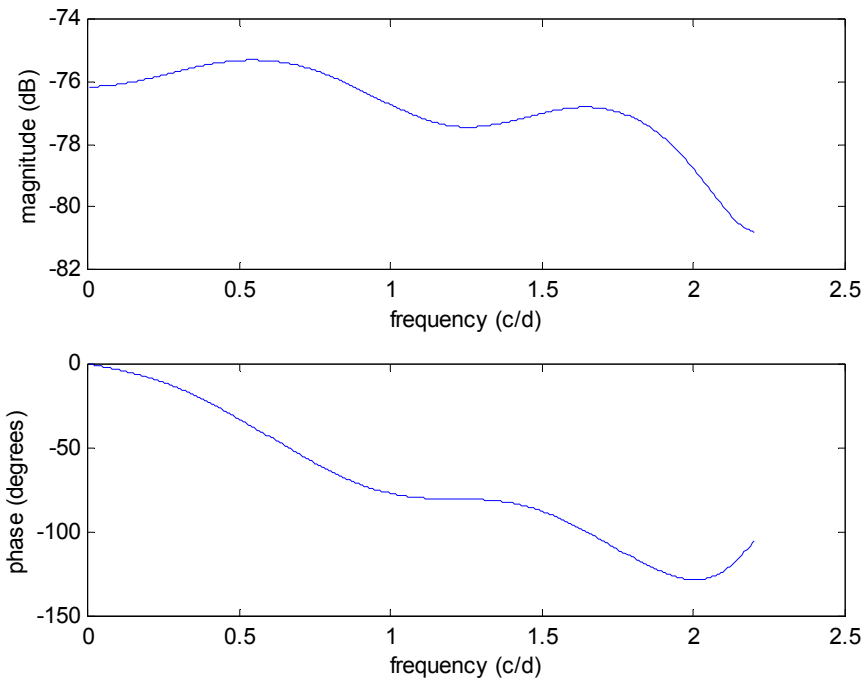


Figure 11-5: Transfer Function Characteristics of the Filter Relating Concentration Profile Displacement $x'(t)$ to Water Surface Height. Estimate Using GEE with Robust Gamma Distribution and Log Link.

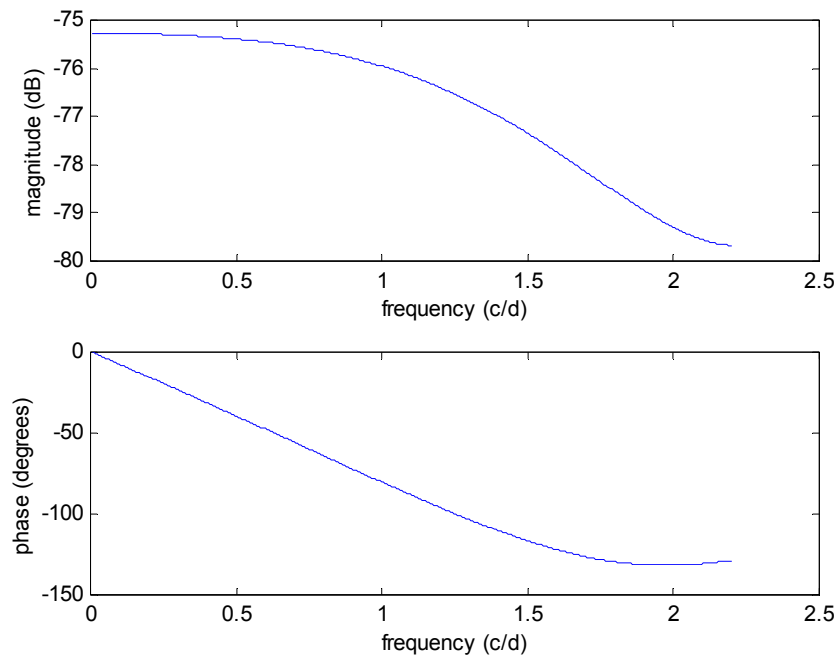


Figure 11-6: Transfer Function Characteristics of the Filter Relating Concentration Profile Displacement $x'(t)$ to Water Surface Height. Estimate Using GLM with Robust Gamma Distribution and Log Link.

11.6 Validation and Discussion

The coefficients were estimated from the period August 20, 1991 to September 5, 1992. The fit model was then applied over a validation period spanning the two calendar years 1993 to 1994. The results and residuals are pictured in Figure 11-7. Little detail is apparent from this plot, but we can see the ability of the model to pick up the main trend and the tidal envelope. Root mean squared error over the validation period is 2,828 $\mu\text{mhos/cm}$. When rms error is applied to the daily average salinity, the result is 1,863 $\mu\text{mhos/cm}$. This is lower than cross-validation rms error of the best daily-averaged (i.e., standard) G-model that the author was able to fit (2020 $\mu\text{mhos/cm}$), illustrating that it is advantageous to account for mechanics at finer time scales even if the output is to be time-averaged.

To illustrate the tidal component of the model, a shorter subset of the test data during a period with fairly constant average salinity is pictured in Figure 11-8. Several features are worth noting. First, under moderate dynamics, the residuals show little diurnal or semidiurnal fluctuation, indicating that the tidal model, even when it fails, does not produce patterned error that would bias a planning run. Around May 1 each year, for instance, there is a period when salinity is overestimated for several days. Despite this error, the tidal fluctuation is reasonable.

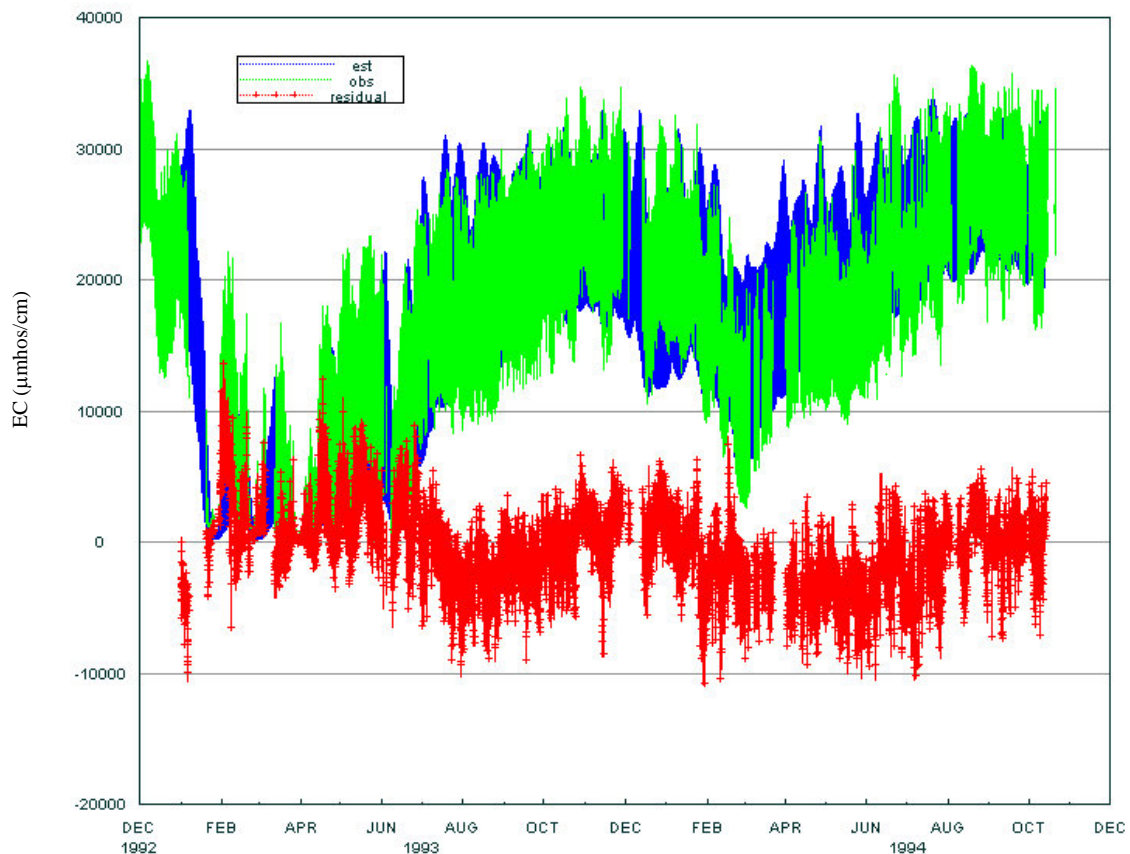


Figure 11-7: Validation Estimates for the Years 1993-1994

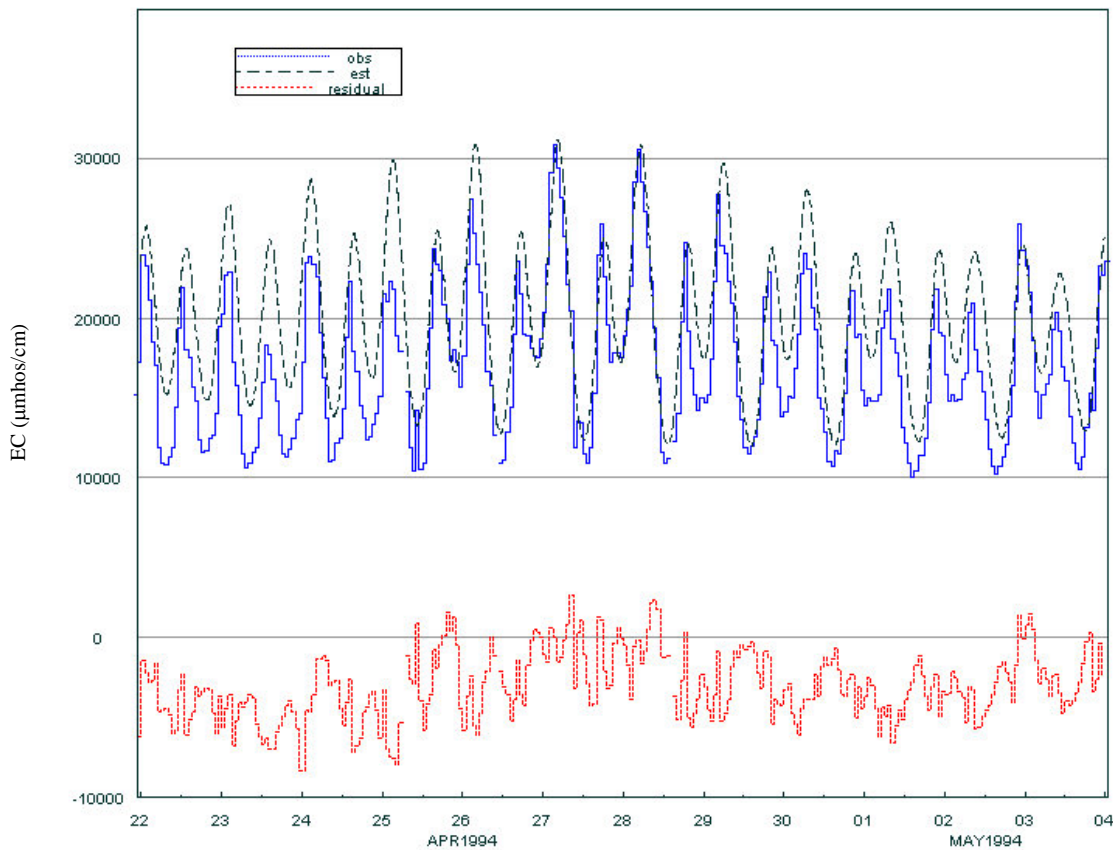


Figure 11-8: Model Performance Over a Two-Week Period.

In contrast, the error on the left hand side of Figure 11-8 (and to some extent the far right) represents the most vexing problem in the analysis. To see the problem, note the shape of the tidal envelope over a 14-day cycle. The estimate, mimicking stage, has a fairly symmetric envelope top and bottom. During the neap tide at the left side of the plot, the envelope is curved toward the center as in the center of an hourglass. Field salinity, on the other hand, does not exhibit a symmetric envelope. The upper envelope is curved as expected, but the lower envelope is flat over the entire spring-neap cycle at about 10,000 $\mu\text{mhos/cm}$ – the middle part of the hourglass has been pressed down. This phenomenon is common whenever salinity is high enough to expect a tidal shape.

Analysis by Denton attributes these anomalies in salinity over the spring-neap cycle to the draining of the Delta. There is a non-linear interaction between tidal constituents that tends to produce high water levels and salinity when tidal energy is high, and low water levels and salinity when tidal energy is low. The resulting 14-day fluctuation in (tidally averaged) water levels is known as the “filling and draining” of the Delta. The storage correction to Net Delta Outflow is intended to compensate for this cycle – evacuated storage is considered to augment Net Delta Outflow. Denton reported G-model results in which this correction dramatically improves the performance of the standard G-model. A similar correction was used here, but the correction has proven to be problematic both practically and conceptually.

Astronomical stage estimates contain a classic spring-neap cycle, but this is just a linear superposition of waves – its tidal average is zero. The planning tides described in Chapter 12 augment astronomical tides with low-frequency components modeled on San Francisco. These low-frequency component estimates also provide good surrogates for use in the filling and draining correction (Equation 0-4). See Chapter 12 for a more complete discussion of the low-frequency Martinez and San Francisco tides.

The limitation of this method is that historical San Francisco stage data must be available. This is true over most of the century (planning runs), but not for the future (real-time runs). When San Francisco estimates are not available, tidal energy can be used to predict filling and draining. Figure 11-9 shows the correspondence between filling and draining (low-passed observed tide) and predicted tide energy (low-passed squared astronomical tide). Periods of very high tidal energy often coincide with high values of stage, but the relationship is mild and often overwhelmed by other factors during less powerful spring-neap cycles. Occasionally, the filling fails to occur even during times of high tidal energy. An example of this is shown in the plot around July 12, 1993. Even during periods where the relationship holds well qualitatively, the fluctuations are not an adequate basis for a numerical prediction.⁷

Barometric pressure is usually assumed to be an important contributing physical factor determining water levels, but it is somewhat collinear with tidal energy and only explains a tiny fraction (about 6%) of the remaining squared error in tidal height when added to a model based on tidal energy. Perhaps this is fortunate, because pressure is not available for prediction anyway.

In addition to these practical difficulties, there are two conceptual problems with the filling and draining correction. The first is that it gives rise to two conflicting time scales. For the draining correction to have any effect at all on salinity, the 14-day fluctuations must be allowed to register rather strongly in $g(t)$. This, in turn, means that the parameter β must be small enough to allow response at this time scale. The problem is that a small value of β is not particularly consistent with changes in Net Delta Outflow at longer time scales. Even though great care was taken to avoid compromising accuracy at these longer time scales in order to accommodate filling and draining, a slight tendency for the estimate to respond too quickly to changes in flow regime is still apparent in Figure 11-7.

⁷ Richard Oltmann and Michael Simpson of the USGS have also studied this phenomenon. Their plots and text at <http://sfbay.wr.usgs.gov/access/delta/tidalflow/tidalcycle.html> include both stage and flow observations at Jersey Point. They concluded that at this location filling and draining coincide well with the spring-neap cycle; however, their plots also include irregularities and exceptions of the types described here.

The second conceptual problem is the question of causality: is it the draining of the Delta that causes salinity to fall or is it reduced tidal energy and dispersion? The discussion so far borrows the G-model premise that outflow determines salinity – filling and draining merely provide a correction to outflow. In contrast, one preliminary DSM2 study⁸ suggests that in DSM2, the most important mechanism is tidal energy and dispersion and that the spring-neap phenomena can be reproduced even if low-frequency water levels are held artificially flat. The issue is probably best settled by analysis of observed data, since neither model was calibrated in a way that ensures that one transport mechanism was not traded off in favor of the other.

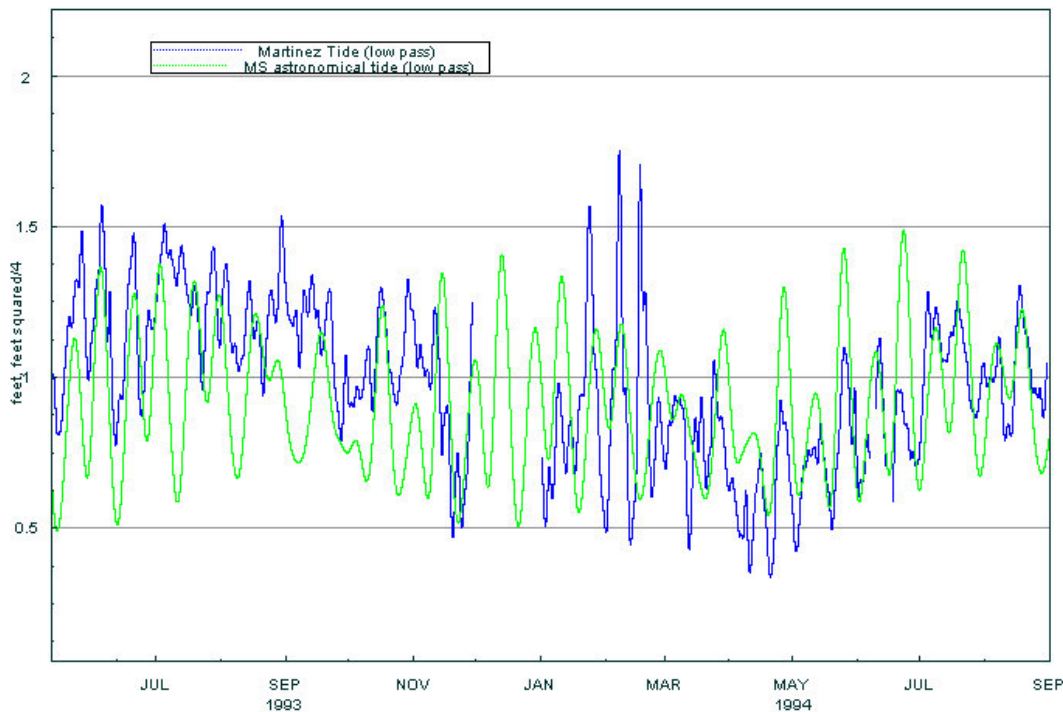


Figure 11-9: Comparing Low-Passed Martinez Stage (Filling and Draining) to Low-Passed Square Tide (a Measure of Tidal Energy).

11.7 References

Denton, R. and G. Sullivan. (1993). *Antecedent Flow-Salinity Relations: Applications to Delta Planning Models*. Contra Costa Water District.

Liang, K.-Y. and S.L. Zeger. (1986). *Longitudinal Data Analysis Using Generalized Linear Models*. *Biometrika*, **73**. pp.13-22.

⁸ The study, over August – October 1994, compared a simulation using historical Martinez EC and stage to a simulation using historical EC but with stage that had been high passed to remove low frequency fluctuations (below 0.5 cycles per day). The two runs gave nearly identical results at interior stations and both exhibited lower salinity during periods of reduced tidal energy.

Munk, W.H. and D.E. Cartwright. (1966). *Tidal Spectroscopy and Prediction*, Phil. Trans. Roy. Soc. (London), Ser. A **259**, pp. 533-81.

Oppenheim, A.V. and A. S. Willsky. (1996). *Signals and Systems*, Prentice Hall.

Methodology for Flow and Salinity Estimates in the Sacramento-San Joaquin Delta and Suisun Marsh

**22nd Annual Progress Report
August 2001**

Chapter 12: DSM2 Real-Time Forecasting System

Author: Michael Mierzwa

12 DSM2 Real-Time Forecasting System

12.1 Introduction

For several years, the Delta Simulation Model 2 (DSM2) has been used by DWR's Operations and Maintenance Environmental Compliance Section as a decision support tool. Real-time field data were combined with several different alternative forecast flow regimes and barrier configurations throughout the Delta through use of a series of pre-processing scripts. Observed tidal data from Martinez were combined with astronomical tidal data when running DSM2-HYDRO. DSM2-QUAL and/or DSM2-PTM then used the hydrodynamics modeled by HYDRO to explore a series of "what if" questions related to the alternative flow regimes and/or barrier configurations.

These DSM2 "Real-Tide" studies were performed on an *ad hoc* basis. Typically, DSM2 was used to answer short-term questions in a short amount of time. For example, project operators or biologists have relied on these studies to answer some of the following questions (the principal DSM2 module(s) used to answer these questions is(are) listed in parenthesis).

- ❑ How will south Delta stage change based on the operation of the South Delta Temporary Barriers? (HYDRO)
- ❑ What impact does the timing of the Clifton Court Forebay gates have on South Delta stage? (HYDRO)
- ❑ Will there be a carriage water cost associated with a water transfer? (HYDRO & QUAL)
- ❑ What impact will closing or opening the Delta Cross Channel have on Central Delta salinity? (QUAL)
- ❑ Will changing upstream reservoir releases exceed Central Delta water quality standards? (QUAL)
- ❑ Will reducing exports change the location of X2? (QUAL)
- ❑ Can opening the flap gates on the South Delta Temporary Barriers increase fish survival? (PTM)

These and many other questions are often the focus of multi-agency and multi-disciplinary meetings charged with the responsibility to find solutions to water-related problems associated with the Delta. Unfortunately, the solution to one water supply, quality, or environmental need may aggravate another water supply, quality, or environmental need. While DSM2 Real-Tide studies have allowed several alternatives to be explored within the framework of the same initial conditions, the scripts used to pre-process the alternatives for each of the three DSM2 modules

were difficult to use under the short time constraints. Thus, time that could have been spent creating alternative scenarios that could better address a host of questions was instead spent on creating a single base case scenario.

In response to these needs, the following groups within DWR have worked to create a new set of scripts and procedures designed around the existing DSM2 Real-Tide simulations.

- ❑ Division of Operations and Maintenance Project Operations Planning Branch
- ❑ Environmental Services Office Suisun Marsh Planning Section
- ❑ Environmental Services Office Interagency Information System Services Section
- ❑ Office of SWP Planning Temporary Barriers Project and Land Management Section
- ❑ Office of SWP Planning Delta Modeling Section

DSM2-HYDRO, QUAL, and PTM have not been changed, but the steps involved in linking the DSM2 modules have been simplified to such an extent that the new DSM2 application is now called the “DSM2 Real-Time Forecasting System”.

This chapter will cover the development and use of the DSM2 Real-Time Forecasting System. Its focus will not be on the technical theory behind the tools used in this system, but instead on the use of these tools as a comprehensive modeling system. A more detailed explanation dealing with the technical improvements related to filling in and forecasting DSM2 stage at Martinez was covered by Ateljevich (2000a). More detailed descriptions of the technical issues related to both the initial water quality conditions used by QUAL were also described by Ateljevich (2000b). The method used to fill in missing periods of EC at the downstream Martinez boundary is discussed in Chapter 11.

Complete step-by-step guides designed to lead numerical modelers through every step involved in a DSM2 forecast are also available at <http://modeling.water.ca.gov/delta/real-time/>. This on-line document was designed to be flexible enough so that it could be easily updated and used by numerical modelers in order to ensure quality in their forecast runs. It was also designed on the theory that a modeler familiar with the DSM2 Real-Time Forecast System could easily navigate through short checklists (available at <http://modeling.water.ca.gov/delta/real-time/real-time.html>), while new users or the end users of the system (typically decision makers) could follow links to pages covering greater detail to answer any specific questions they might have. This report will not attempt to recreate this documentation.

12.2 Background

As discussed above, various groups within DWR have been combining real-time field observations with forecast Delta operations in DSM2 in order to forecast hydrodynamic, water quality, and particle fate within the Delta on an *ad hoc* basis for several years. In November 1999, an interagency recommendation was made to close the Delta Cross Channel gates in order to protect out-migrating juvenile salmon smolts.¹ The closure of the Delta Cross Channel gates roughly corresponded with the neap tide. Water quality levels in the Delta were already

¹ In November the Delta Cross Channel gates may either be opened or closed.

approaching several of the water quality standards, and by early December 1999, the Rock Slough Chloride standard was violated.

In mid December 1999, it was recommended by the CALFED Ops Data Assessment Team (DAT) to operate the Delta Cross Channel gates on a tidal basis in order to offer some protection to any remaining out-migrating salmon, while allowing some fresher Sacramento River water to pass through the Delta Cross Channel in order to improve Central Delta water quality conditions. Due to the need to make a quick decision, DSM2 was used to forecast water quality in the Central Delta based on this proposed operation of the Delta Cross Channel gates. Planned upstream inflows and South Delta export rates were input into DSM2. However, due to large periods of missing boundary stage data, the DSM2 simulations were not finished in time to aid in the decision regarding the operation of the Delta Cross Channel gates.

While reviewing the December 1999 decisions, the Bay Delta Modeling Forum (BDMF) requested that this late November - December period be modeled by DSM2 and the subject of a special BDMF workshop². Several other alternative scenarios were investigated by DSM2 at this same time in an attempt to model what other options could have been implemented in order to protect Central Delta water quality. The results of these DSM2 simulations were presented at this BDMF workshop in February 2000, where it was agreed by DWR that the use of DSM2 should be improved in order to provide decision makers with a variety of alternative forecasts in a timely fashion.

A DWR project work team consisting of members from the groups listed in the introduction began working on solving both the technical and institutional problems involved in creating a DSM2 Real-Time Forecasting System. The Division of Operations and Maintenance Project Operations Planning Branch agreed to provide forecast information (including the information necessary to construct several alternatives) in addition to funding part of the development of the system. The Office of SWP Planning (OSP) Delta Modeling and Environmental Services Office (ESO) Interagency Information System Services Sections both took the lead in developing the tools necessary to address many of the technical problems associated with both the pre-processing and running of DSM2. The ESO Suisun Marsh Planning Section developed a visual way to quickly share the modeling results to a wide range of decision-makers. The Division of Operations and Maintenance Operations Planning Branch and the OSP Temporary Barriers Project and Land Management Section represented two of the end users of the system.

A prototype of the DSM2 Real-Time Forecast System was in intermittent use by DWR Operations and Maintenance by the fall of 2000. In conjunction with the IEP and CALFED funded Delta Cross Channel investigations in the Fall of 2000, DSM2 was used to forecast the impact of several different Delta Cross Channel gate operations well in advance of the actual operations. The primary concern at the time was “what impact would tidal operations of the Delta Cross Channel have on Central Delta water quality?”. Based on these DSM2 forecasts, which did not show a marked increase in Central Delta salinity, the IEP / CALFED investigations continued without any major changes.

² The focus of Bay Delta Modeling Forum workshop in February 2000 was to review the ability of the various models used by the San Francisco Bay-Delta community to be used as Real-Time decision tools. DSM2 was just one of the models presented in the workshop.

Although work on improving the DSM2 Real-Time Forecast System continues, the system is currently in use by Operations and Maintenance, the Suisun Marsh Planning Section, and the Delta Modeling Section.

12.3 Real-Time Modeling Forecast Processes

Any real-time modeling forecast system can be described as having five essential processes that follow a simple flow chart (see Figure 12-1). The raw data and model results are represented by trapezoids in the flow chart. The remaining three processes include pre-processing the data, running the model, and post-processing the results. These middle three processes will need to be repeated for each alternative scenario that is run. However, since each alternative should focus on a single permutation, the time spent constructing and reviewing the alternatives typically will be no longer than the time spent preparing the base case scenario. More detailed discussions of how these general steps are integrated into DSM2 are discussed below.

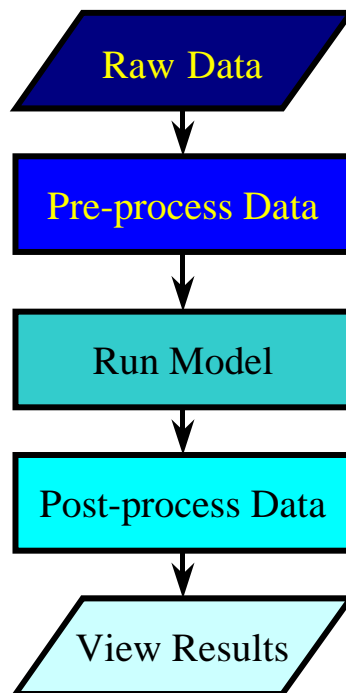


Figure 12-1: Flow Chart of a Numerical Modeling Forecast System.

12.3.1 Raw Data

Real-time raw data is often of highly variable quality and a host of problems arise simply in collecting and storing this data. If the forecast system is used on a regular basis, the questions frequently asked of the model will be known in advance and the decision of what data to actually use can be standardized or automated. This will save time in collecting the raw data. Both observed field data and forecast inflows must be collected. DWR Operations and Maintenance provide the forecast inflows.

The observed hydrodynamic and water quality data are retrieved from the IEP Data Storage System (DSS) database, located at <http://www iep. water. ca. gov/ dss/>. This is accomplished by using VPlotter, which was developed by the Section in order to automate DSS data retrieval and allow users to quickly plot any DSS data (Sandhu 2000). The user only needs to set a time window (a period of interest) in which to download all the data. Before saving the raw data to a local DSS file, the quality of the data can first be checked by graphing the raw data for the time window selected. A screen shot of the VPlotter graphical user interface (GUI) being used to retrieve raw data is shown in Figure 12-2. A more detailed description of how to actually go through and retrieve raw DSS data using VPlotter is available at <http:// modeling. water. ca. gov/ delta/ real- time/ retriever. html>.

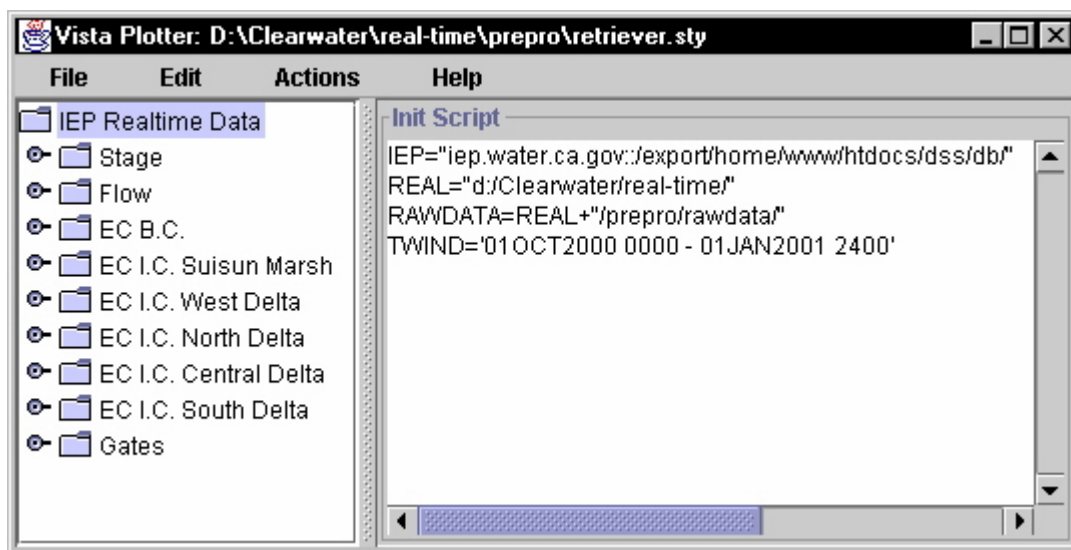


Figure 12-2: VPlotter DSS Data Retrieval GUI.

12.3.2 Pre-processing

Obviously, raw data can not be used without first undergoing a screening procedure. In the case of real-time data, such a pre-processing step often represents the first time that a human has actually spent time looking at the data, thus the time spent preparing the data for a model run is often greater than what would be done in a planning model or in a historical simulation. Judgement must be used to filter out unacceptable data as well as to resolve any problems that arise from missing data.

As discussed above, when raw IEP DSS data are locally downloaded, it can first be graphically viewed as part of a quality control procedure. The raw data retriever process described above was designed to look at and retrieve several different DSS paths for the same location. An example of the VPlotter GUI doing this for the Sacramento River is shown below in Figure 12-3. Each DSS path represents either data collected by a different agency or a different time step. Predetermined standard paths to use in a real-time forecast are listed in Tables 12-1, 12-2, and 12-3 below. Any time the raw data in one of these standard paths is either missing large amounts of data or otherwise can not be cleaned up, one of the other alternate DSS paths for the same location can be used, instead. Any changes made to this list of standard paths will be reflected in the on-line documentation, <http:// modeling. water. ca. gov/ delta/ real- time/ faq. html#ForePaths>.

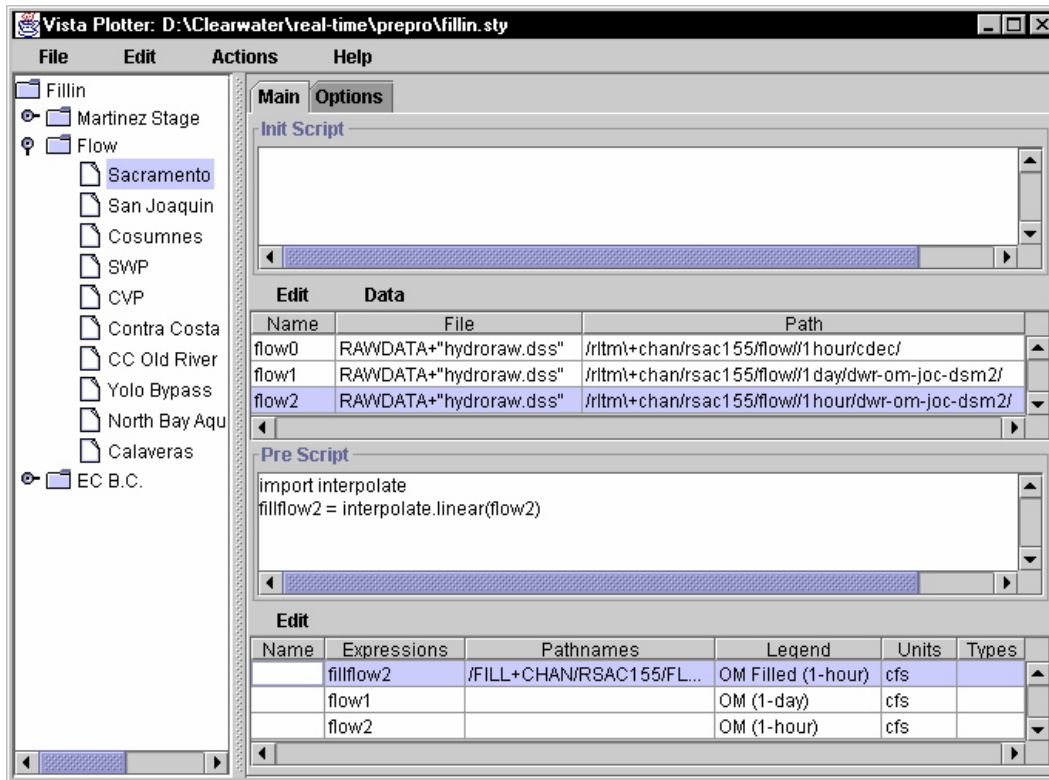


Figure 12-3: Retrieving Multiple Time Series for Same Location.

Table 12-1: Standard IEP DSS Hydrodynamic DSM2 Real-Time Inputs.

Input	Type ³	IEP DSS Path
Calaveras River	Flow	/RLTM+CHAN/RCAL009/FLOW//1HOUR/DWR-OM-JOC-DSM2/
Contra Costa Canal (Rock Slough)	Diversion	/RLTM+CHAN/RCAL009/FLOW//1HOUR/DWR-OM-JOC-DSM2/
Contra Costa Old River (Los Vaqueros)	Export	/RLTM+CHAN/ROLD034/FLOW-EXPORT//1DAY/DWR-OM-JOC-DSM2/
Cosumnes	Flow	/RLTM+CHAN/RCSM075/FLOW//1HOUR/DWR-OM-JOC-DSM2/
Central Valley Project	Export	/RLTM+CHAN/CHDMC004/FLOW-EXPORT//1DAY/DWR-OM-JOC/
Mallard Island	Stage	/RLTM+CHAN/RSAC075/STAGE//1HOUR/CDEC/
Martinez	Stage	/RLTM+CHAN/RSAC054/STAGE//1HOUR/CDEC/
Mokelumne River	Flow	/RLTM+CHAN/RMKL070/FLOW//1HOUR/DWR-OM-JOC-DSM2/
North Bay Aqueduct	Export	/RLTM+CHAN/SLBAR003/FLOW-EXPORT//1DAY/DWR-OM-JOC/
Sacramento River	Flow	/RLTM+CHAN/RSAC155/FLOW//1HOUR/DWR-OM-JOC-DSM2/
San Joaquin River	Flow	/RLTM+CHAN/RSAN112/FLOW//1HOUR/DWR-OM-JOC-DSM2/
S.F. Golden Gate	Stage	/RLTM+CHAN/SHWSF001/STAGE//1HOUR/NOAA/
State Water Project	Export	/RLTM+CHAN/CHSWP003/EXPORT//1DAY/DWR-OM-JOC/
Yolo Bypass	Flow	/RLTM+CHAN/BYOLO040/FLOW//1HOUR/DWR-OM-JOC-DSM2/

³ Types of hydrodynamic inputs include flow, export/diversion, and stage.

Table 12-2: Standard IEP DSS Water Quality DSM2 Real-Time Boundary Inputs.

Input	Type	IEP DSS Path
Mallard Island	EC	/RLTM+CHAN/RSAC075/EC//1HOUR/DWR-OM-JOC-DSM2/
Martinez	EC	/RLTM+CHAN/RSAC054/EC//1HOUR/CDEC/
Sacramento	EC	/RLTM+CHAN/RSAC142/EC//1HOUR/CDEC/
San Joaquin	EC	/RLTM+CHAN/RSAN112/EC//1HOUR/DWR-OM-JOC-DSM2/

Table 12-3: Standard IEP DSS Water Quality DSM2 Real-Time Initial Condition Inputs.

Input	Type	IEP DSS Path
Antioch	EC	/RLTM+CHAN/RSAN007/EC//1HOUR/CDEC/
Bacon Island	EC	/RLTM+CHAN/ROLD024/EC//1HOUR/DWR-OM-JOC-DSM2/
Beldon's Landing	EC	/RLTM+CHAN/SLMZU011/EC//1HOUR/DWR-OM-JOC-DSM2/
Cache Slough	EC	/HIST+CHAN/SLCCH016/EC//1HOUR/USBR-CVO/
Collinsville	EC	/RLTM+CHAN/RSAC081/EC//1HOUR/DWR-OM-JOC-DSM2/
Central Valley Project	EC	/RLTM+CHAN/CHDMC004/EC//1HOUR/DWR-OM-JOC-DSM2/
Emmaton	EC	/RLTM+CHAN/RSAC092/EC//1HOUR/DWR-OM-JOC-DSM2/
Farrar Park (Dutch Slough)	EC	/HIST+CHAN/SLDUT009/EC//1HOUR/USBR-CVO/
Goodyear Slough	EC	/RLTM+CHAN/SLGYR003/EC//1HOUR/DWR-OM-JOC-DSM2/
Green's Landing	EC	/HIST+CHAN/RSAC139/EC//1HOUR/USBR-CVO/
Holland Cut	EC	/RLTM+CHAN/ROLD014/EC//1HOUR/DWR-OM-JOC-DSM2/
Jersey Point	EC	/RLTM+CHAN/RSAN018/EC//1HOUR/DWR-OM-JOC-DSM2/
Middle River @ Hwy. 4	EC	/HIST+CHAN/RMID023/EC//1HOUR/USBR-CVO/
Middle River @ Tracy Blvd.	EC	/RLTM+CHAN/RMID027/EC//1HOUR/CDEC/
Piper Slough @ Bethel Island	EC	/RLTM+CHAN/SLPPR003/EC//1HOUR/DWR-OM-JOC-DSM2/
Pittsburg	EC	/RLTM+CHAN/RSAC077/EC//1HOUR/USBR-CVO/
Prisoner's Point	EC	/RLTM+CHAN/RSAN037/EC//1HOUR/CDEC/
Port Chicago	EC	/RLTM+CHAN/RSAC064/EC//1HOUR/DWR-OM-JOC-DSM2/
Rio Vista	EC	/RLTM+CHAN/RSAC101/EC//1HOUR/CDEC/
Rock Slough	EC	/RLTM+CHAN/CHCCC006/EC//1HOUR/DWR-OM-JOC-DSM2/
San Andreas Landing	EC	/HIST+CHAN/RSAN032/EC//1HOUR/USBR-CVO/
Staten Island	EC	/HIST+CHAN/RSMKL008/EC//1HOUR/USBR-CVO/
Sunrise Club	EC	/RLTM+CHAN/SLCBN002/EC//1HOUR/DWR-OM-JOC-DSM2/
Volanti	EC	/RLTM+CHAN/SLSUS012/EC//1HOUR/DWR-OM-JOC-DSM2/

Separate procedures have been developed to pre-process stage, flow, and water quality data. These procedures are described in detail below.

12.3.2.1 Stage

Correctly characterizing stage at Martinez is critical when attempting any DSM2 simulation. Ateljevich (2000a) discussed the theory behind filling in and forecasting stage at Martinez. Using Jython, a script that replicates the Python scripting language but is written in Java in order to directly incorporate existing Java code, Ateljevich designed an automated three-step tool in VPlotter to quickly characterize stage at Martinez. A step-by-step detailed description of how to use this tool can be found at <http://modeling.water.ca.gov/delta/real-time/fillin.html#3.1>.

The first step uses Jython scripts within a standard VPlotter session to calculate the residual differences between observed stage at three locations, and each location's calculated astronomical stage. These residuals are then used in a vector autoregressive model to fill in missing residual values and forecast the Martinez residual. This is the most time-intensive step involved in pre-processing stage, and typically takes under 5 minutes to fill in and forecast up to two months of tidal data at Martinez.

The quality of the forecast is reviewed in the second step by comparing the newly created filled-in and forecast Martinez stage with the observed values. After verifying that the new stage characterization represents a good fit with the historical data and appears to follow a spring-neap cycle, the new data are saved to a working input file. A final check is made to verify that the correct data were saved in the working input file in the third step by once again graphing the forecast stage data with the observed values. An example of the Martinez stage fill-in verification is shown below in Figure 12-4.

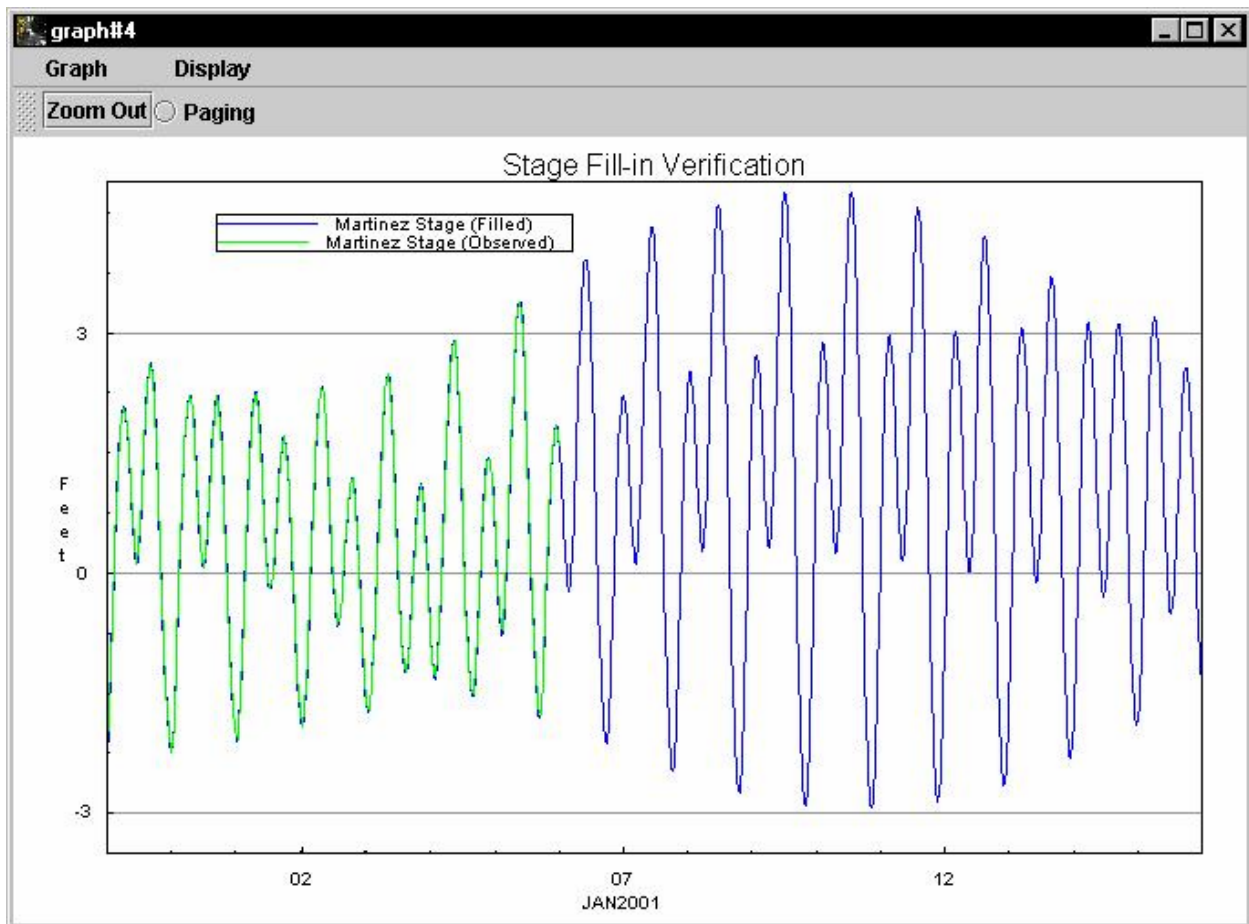


Figure 12-4: Martinez Stage Verification.

12.3.2.2 Flow

Historical and forecast rim inflows and export/diversion flows are pre-processed in different ways. The basic concepts behind pre-processing both the historical and forecast flow data are described below. The process for filling in historical flow values is described in detail at

<http://modeling.water.ca.gov/delta/real-time/fillin.html#3.2>. The process for creating forecast flow data is described in detail at <http://modeling.water.ca.gov/delta/real-time/foreform.html>.

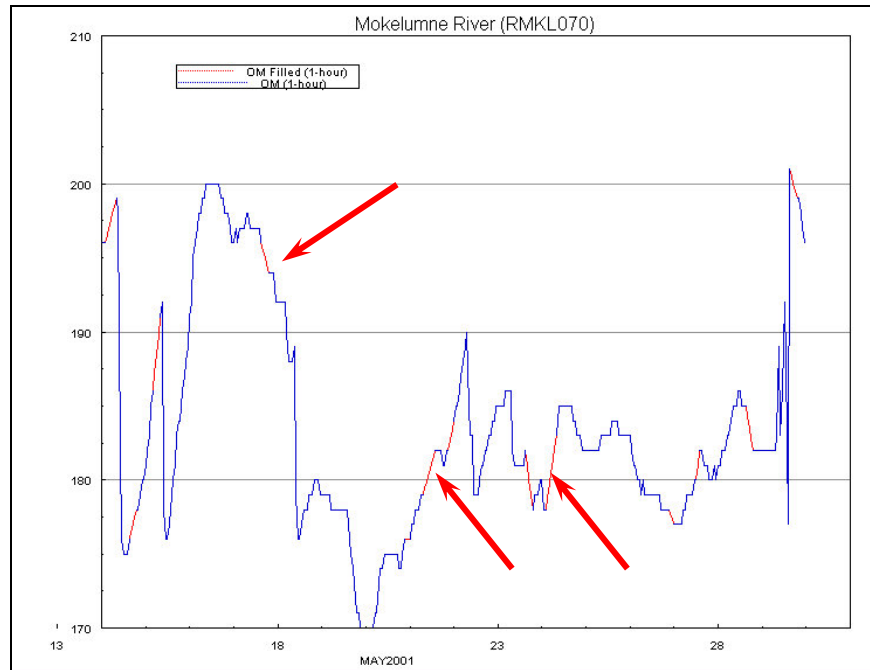


Figure 12-5: Example of Filling in Historical Flow Data (Without Tidal Influence).

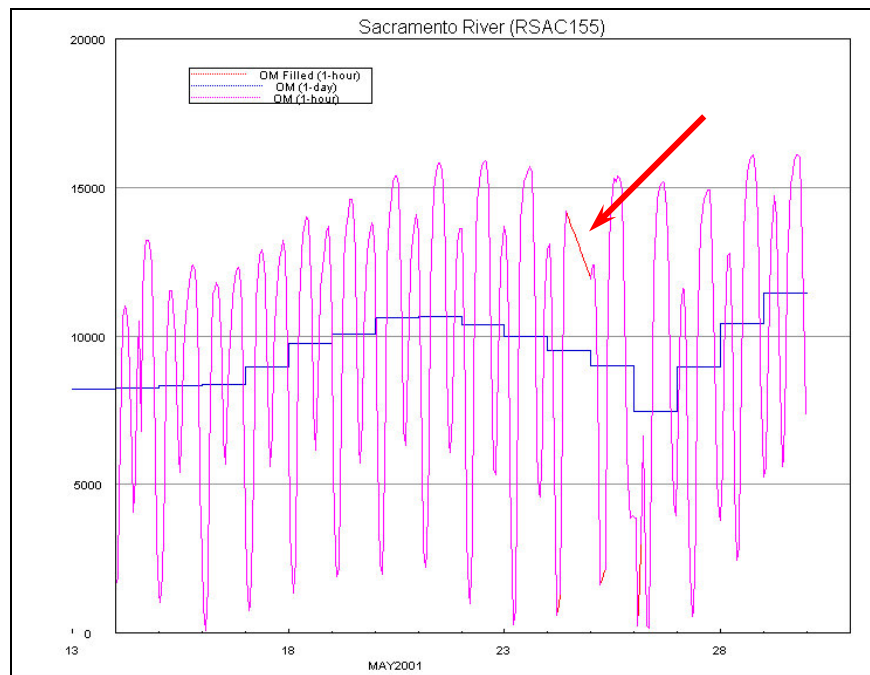


Figure 12-6: Example of Filling in Historical Flow Data (With Tidal Influence).

The historical raw flow data are read in using the same VPlotter script that was used when filling in and forecasting Martinez stage. Missing historical flow data are filled in using a simple linear regression, as is shown above in Figures 12-5 and 12-6. This approach is ideal for filling in

flows that are only missing data in short time periods (on the order of a few hours) and flows that do not have a strong tidal influence, as is shown in Figure 12-5 for the Mokelumne River. However, when the tidal influence is strong, a simple linear regression is not adequate to capture the flood-ebb tides within the missing data, as is shown in Figure 12-6 for the Sacramento River.

Though a linear regression can not capture the flood-ebb tidal cycle that is present on the Sacramento River, during periods of high flow (over 25,000 cfs) this tidal signal will not be present. The use of linear regression to fill in missing data in periods of high flow will be adequate to characterize the flow on the Sacramento River. It has been suggested that a system of priorities similar to other DSM2 applications be used. This could be done by filling in missing hourly data with the daily average data (which also could be missing in some cases) or data from other providers. Moving from an hourly time series to a daily average may, in some cases, result in a jump that is not that much different from the discontinuity between the tidally influenced hourly data and the linear regression fill in values. Moving from data provided by one agency to another may avoid some of these issues, but it is important to remember that the first priority data used by VPlotter were originally found to be of higher quality than the sources at the same location. In fact, some data providers regularly shift their data to reflect time changes associated with daylight savings time. DSM2 does not account for the shift to and from daylight savings time, so if necessary, additional pre-processing steps have to be added when data that is out of phase with the model and other data are being used. The process for making these changes has been outlined in the on-line user's documentation. However, it is important to remember that the goal of pre-processing the historical flow data is to provide a compromise between using appropriate model inputs and being able to produce a series of simulations in a short time frame. Since DSM2 is being used only as a trend analysis tool in this application, it is actually recommended to avoid mixing data from different DSS sources.

Forecast flow data representing both the planned operations of the State Water Project and Central Valley Project and possible alternative operations are created by project operators and decision makers. These forecasts are converted from a MS Excel spreadsheet into DSS for use in DSM2 through a series of MS Access GUIs. This system is referred to as the MS Access Forecast Form (see Figure 12-7 below for the opening page of the form).

As with the Vplotter scripts, the MS Access Forecast Form was designed to quickly convert forecast rimflow, export and diversion, and Net Delta Outflow Index information into a format that can be used in DSM2. The forecast data are reported as daily averages. Again, detailed instructions of how to use the form to create both base forecasts and to alter the raw forecast data in order to create alternative scenarios are available on-line at <http://modeling.water.ca.gov/delta/real-time/foreform.html>. In addition to creating the necessary flow data to run forecasts, the same form can be used to update the operation of the South Delta Barriers, including the Old River at the head of the San Joaquin River, Middle River, Grant Line Canal, and Old River near the Delta Mendota Canal intake barriers. The forecast gate operations use minute-based time steps; thus, complex tidal operations can be created using the MS Access Forecast Form.

Figure 12-7: MS Access Forecast Form.

To keep track of different scenarios, a YYYYMMDD-XXS naming convention has been adopted. The first part of the name (YYYYMMDD) marks the start date of the forecast, t_i , the second part (XX) identifies the length of the forecast, and the third part (S) represents the actual scenario. By using this scenario naming convention, it is necessary to change only the main input file for each DSM2 module (HYDRO, QUAL, and PTM). Furthermore, unique naming conventions prevent old forecast data from accidentally being used.

12.3.2.3 Water Quality

Filling in and forecasting Martinez EC requires a complete forecast of the NDO Index. A more detailed description behind the theory of this process is discussed in Chapter 11. Detailed instructions how to use VPlotter to fill in and forecast Martinez EC are located at <http://modeling.water.ca.gov/delta/real-time/ecdata.html>. The basic process is similar to how Martinez stage is filled in and forecast, in that a series of three quick steps are used. First, observed stage, EC, and NDOI are taken from the raw and forecast data. Next this raw data are graphed for visual inspection, as is shown below in Figure 12-8. If the data are judged to represent a good fit to the observed Martinez EC and generally show an appropriate forecast response, the filled-in data are saved to a local data file for use by DSM2. Finally, the data are again plotted in a verification step in order to ensure that the correct data will be used during DSM2 simulations.

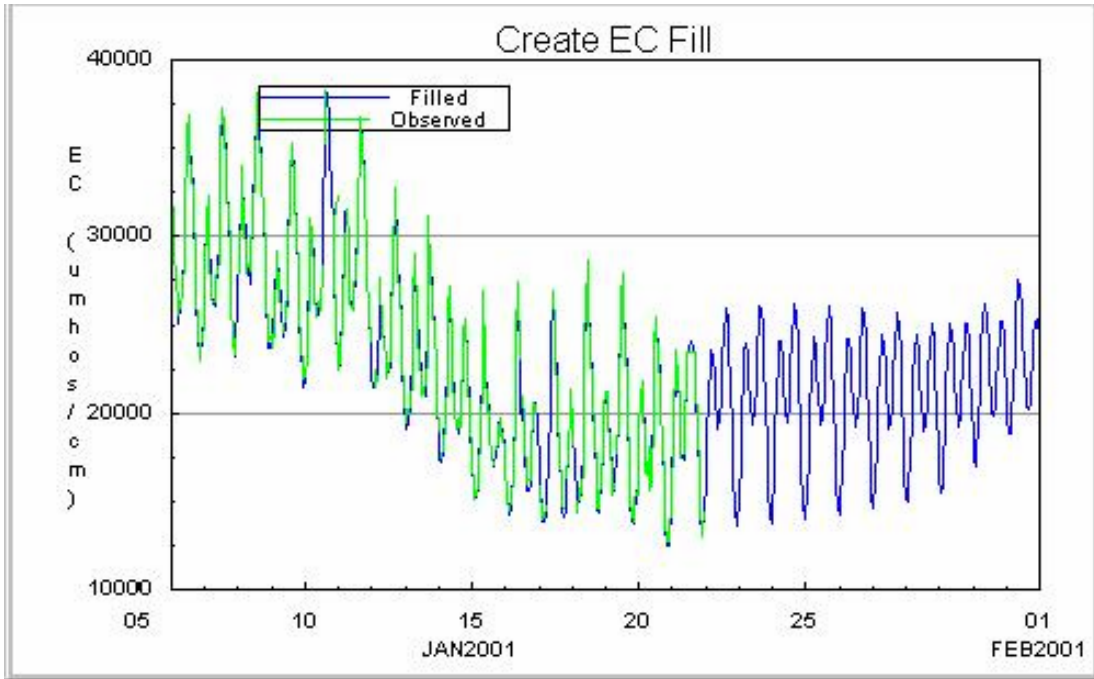


Figure 12-8: Martinez EC Verification.

Missing EC data for both the Sacramento and San Joaquin rivers are filled in using the same linear regressions that were used to fill in missing flow data. The EC for these two locations does not show a response to the flood-ebb tidal signal that was shown to influence the Sacramento River flow during periods of low flow. The EC values for the other major DSM2 rim boundaries are held at fixed concentrations because there are no regular time series data for these locations.

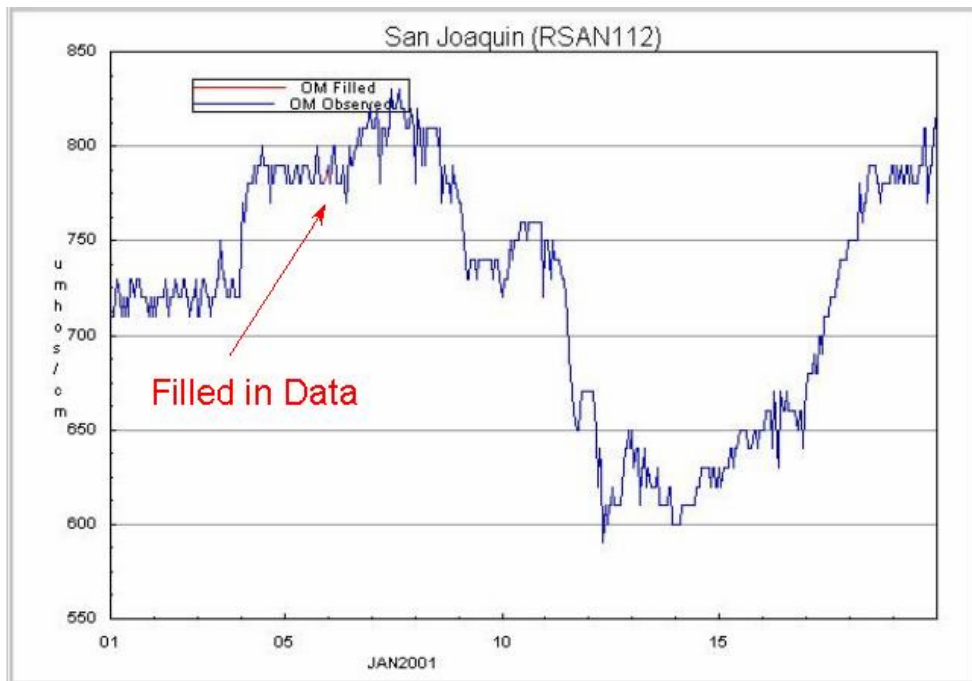


Figure 12-9: Filling in Rim Boundary EC.

Table 12-3 is used to generate the initial salinity conditions within the Delta in a process commonly referred to as “warm start”. A detailed explanation of the theory behind water quality warm start can be found in Ateljevich (2000b). The process of creating warm start initial water quality conditions for the DSM2 Real-Time Forecast System is relatively simple. Two Jython scripts are used to take advantage of QUAL’s multi-constituent capabilities to create initial conditions for the forecast QUAL simulations. These scripts take between 10 and 20 minutes to run. Since only historical data are used, the initial conditions created for the base forecast can be used for all the alternative scenarios. A more detailed explanation of how to actually run these scripts is located at <http://modeling.water.ca.gov/delta/real-time/warmstart.html>.

12.3.3 Running DSM2

The shortest process of the DSM2 Real-Time Forecasting System is actually running DSM2-HYDRO, QUAL, and PTM. Two Jython scripts were created to run HYDRO and QUAL. PTM is run through use of a batch file. However, before running any of the DSM2 modules, a few of the input files need to be updated. Complete instructions describing which input files need to be updated and how to actually run the scripts and batch file for HYDRO, QUAL, and PTM are located at <http://modeling.water.ca.gov/delta/real-time/running.html>.

DSM2 needs to be run once for each scenario. Editing the input files and running HYDRO and QUAL for a single 60-day simulation typically takes less than 20 minutes. Depending on what is being modeled with PTM, a 60-day simulation will take between 20 minutes and 4 hours to run.

12.3.4 Post-processing

To ensure quality in the forecasts, a few VPlotter scripts similar to the script that retrieves raw data are used to visually compare model output with (1) the model input and (2) any observed real-time field data. The observed real-time field data is taken from the IEP DSS database. Two examples comparing model results to the observed real-time data are shown in Figures 12-10 and 12-11. Though there are no observed data during the forecast periods, it is still useful to look at the model results into the forecast period. This is shown in Figure 12-11, in which both the instantaneous and tidally filtered stages at Antioch are displayed for the entire simulation period.

Part of the post-processing procedure is to check the model results in locations near the area of interest for each study. For example, if a forecast was designed to investigate the operations of the South Delta Temporary Barriers, then DSM2 results in the South Delta should be the focus of any comparisons. Unfortunately, the number of real-time telemetered flow and stage locations in the Delta is limited, thus it is impossible to always use recent field data to check the quality of forecast results. In the cases where there are no nearby field data, it is still useful to use the post-processing scripts to examine the model results before publishing the results. The main question that should be asked of any location is “do these model results make sense?”.

It is equally important to compare alternate scenario results to the base case while checking the quality of the forecast. Again using the South Delta Temporary Barrier example, if an alternate scenario involved the removal or installation of a barrier, there should be some difference in the hydrodynamic results between this alternative and the base cases. If this difference does not

appear shortly after the planned alternative operation when looking at the results, there is an error in either the base case or alternative scenario.

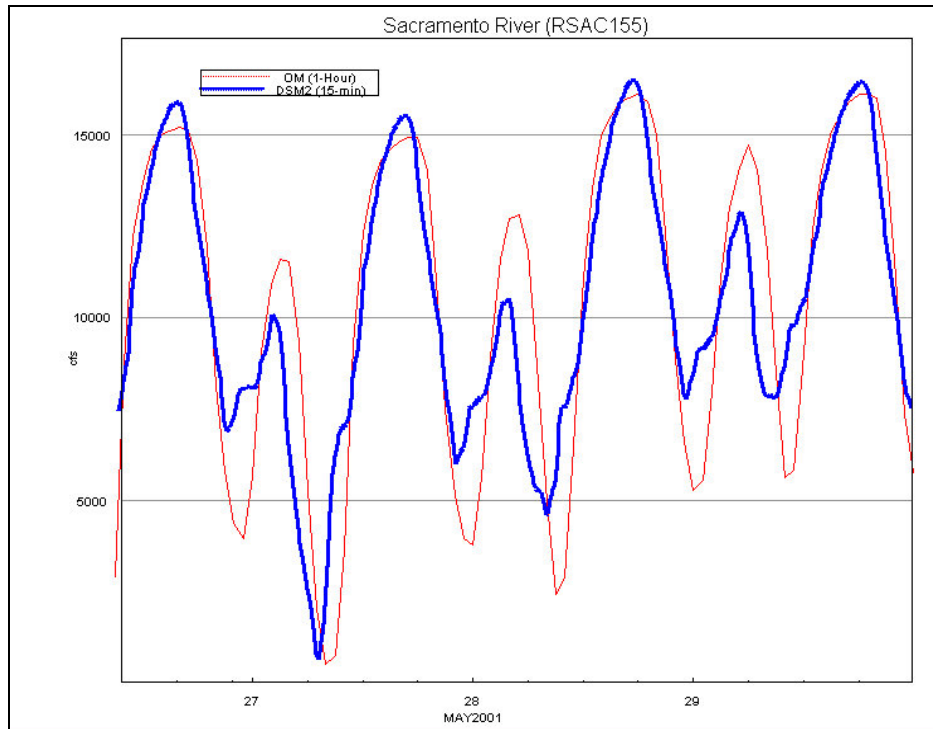


Figure 12-10: Comparison of Modeled Flow versus Observed Flow at Freeport.

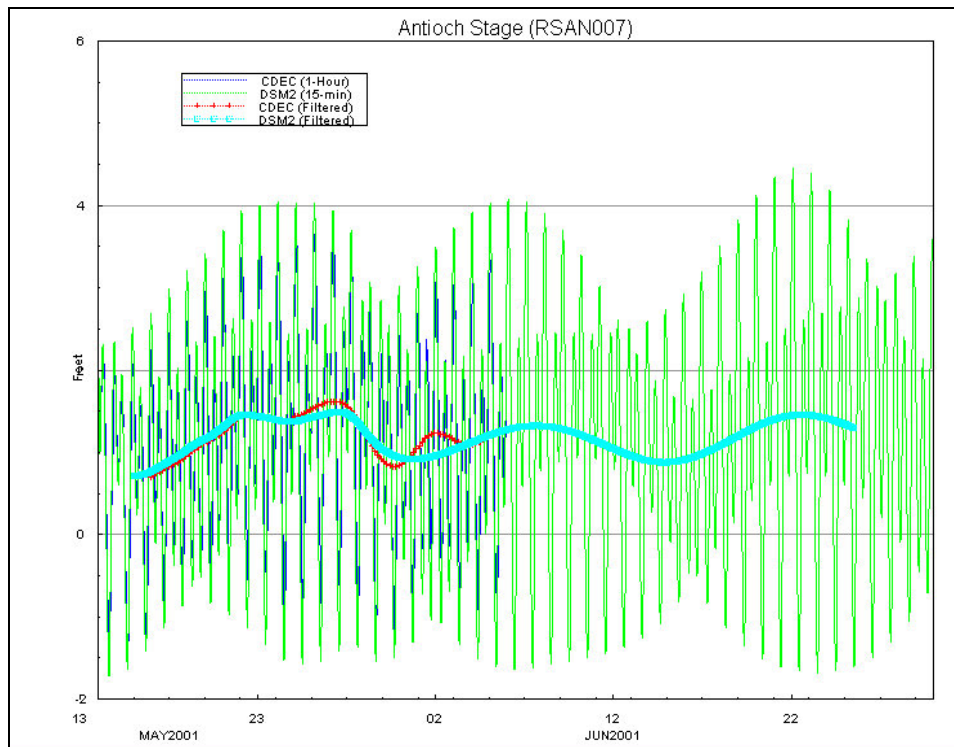


Figure 12-11: Comparison of Modeled Stage versus Observed Stage at Antioch.

When there are either large differences between the simulated results and the field results, or there are unexpected patterns between the base case and alternative scenarios, it is the job of the modeler to review his/her input files. A common mistake (such as forgetting to change an environment variable that is used to point to the most recent forecast data in the DSM2 input files) can quickly be corrected, and the DSM2 forecast simulations should be rerun. While the pre-processing tools described above are easy to use, in the case of a barrier configuration, it is possible that an incorrect time was entered while preparing the forecast. Mistakes similar to these require that the raw data be pre-processed again a second time. Since the preprocessing steps were designed with speed in mind, it is recommended that the entire processing procedure be started over again.

Finally, one way to prevent accidentally pointing to old forecast data is to archive previous forecast input and output data, then delete all of the locally saved raw and processed data files. It is recommended that old forecasts be burned to a CD-ROM. If an end user wishes to revisit an older forecast, the results will be available on-line (as will be discussed below) or he/she can access this information from the CD-ROM.

12.3.5 On-line Output

The last and most visible step involved in the DSM2 Real-Time Forecast System focuses on efficiently presenting the results of the model in a format that is both easily accessible to all the end users and in a way that permits a wide range of end users to be able to interpret the results. One of the scripts used to view the model results in the post-processing step discussed above is also used to convert the model results to a series of images. These images are then stored on an IEP web site dedicated to presenting DSM2 forecast results. This site is located at <http://www.iep.water.ca.gov/cgi-bin/dsm2pwt/realtime/realtime.pl>.

An example of the entry Web page where results can be viewed is shown below in Figure 12-12. At the time of this writing, all of the on-line results pages were still being worked on, as end users (including both operators and biologists) are currently providing input into what would be a more useful way to select forecasts, alternative scenarios, and view these results. The underlying design philosophy behind the continuing development of any forecast output display is that any end user should be able to navigate through the forecast results easily. HYDRO and QUAL results are shown together and can be accessed through an interactive map of the Delta, as is shown in Figure 12-13. PTM results can be viewed either through a series of static plots based on a map of the Delta or through a series of animations. Users must select which two scenarios they wish to view.



DWR Division of Operations and Maintenance Operations Control Office

DSM2 Real Time Forecast Results

Use this site to access DSM2 Real Time model results. Select a forecast date to view a two week forecast beginning on that date. Results are plotted 1 week before and two weeks after the forecast date. For each forecast, up to 6 scenarios may have been run. Plots have been made to compare each scenario to each other scenario. Please be aware that plots may have different Y axis scales.

Particle Tracking Model results will soon be available for every run. Sample output is available in two formats: [static plots](#) and [animation](#)

Available Hydro and Qual Forecast Results YYYY-MM-DD

2001-05-29 ▲
2001-05-21
2001-04-30
2001-02-06
2001-01-18
2000-10-12 ▼

Display Available Scenarios

Notes

**You are using Internet Explorer.
This site works better with Netscape.
If you have problems viewing any images on
this site, disable Automatic Image Resizing.**

**If you have a slow connection, use the [old
Real Time site](#), which does not include
forecast input plots. This site requires you to
load 1.3MB of images.**

Figure 12-12: DSM2 Real-Time Forecast Results Web Page.

**Real Time Forecast Results for
2001-05-29, Scenario A vs Scenario B**

DWR Operations and Maintenance
Operations Control Office

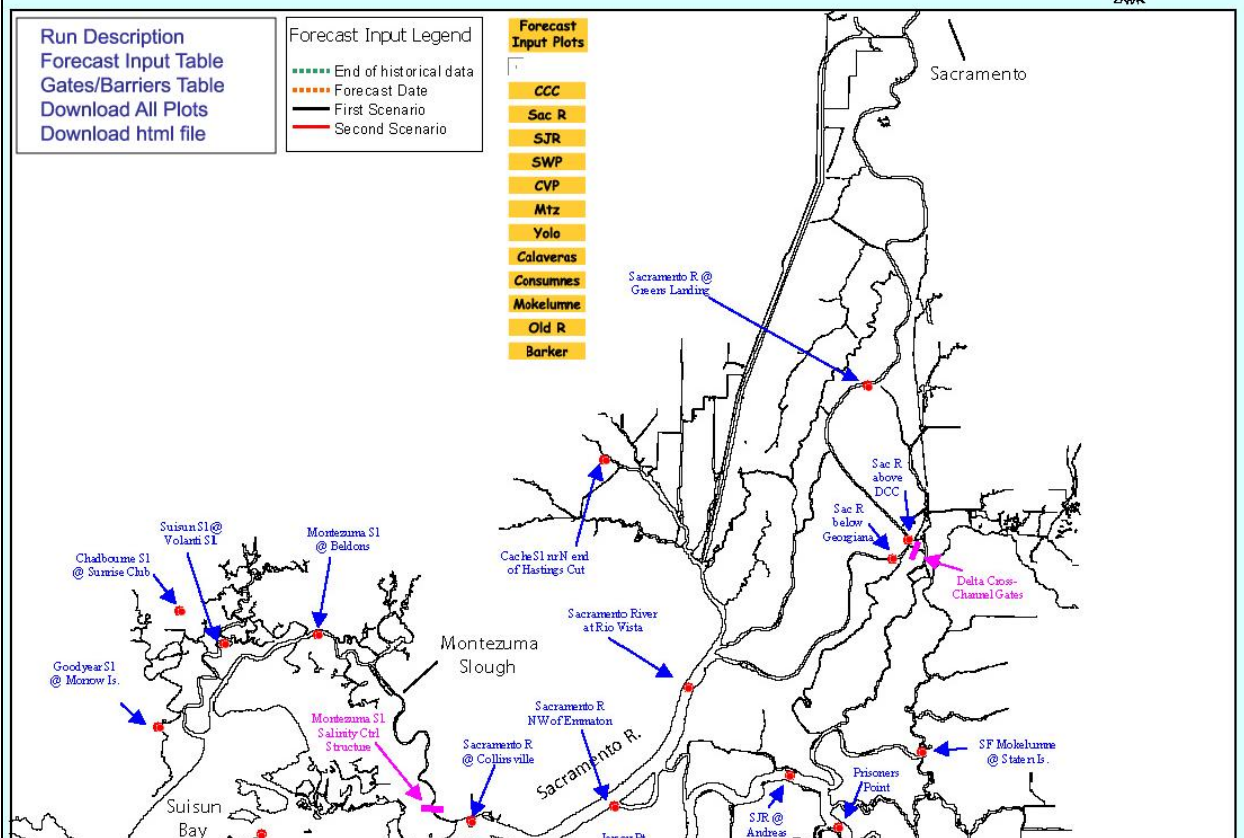


Figure 12-13: Interactive Delta Map to View HYDRO and QUAL Forecast Results.

The interactive map displaying HYDRO and QUAL results can be used to plot time series information about the inputs, as is shown below in Figure 12-14. Both the historical and forecast input data are shown on the same time series. In the example shown in Figure 12-14, there was no difference in the San Joaquin River flow between scenarios A and B. However, if there is a difference in the inputs between two scenarios, these differences will be displayed on these plots.

The same interactive map can be used to view instantaneous or tidally filtered flow, instantaneous or tidally filtered stage, and/or instantaneous or tidally filtered EC. By moving the cursor over a single location, the user can select which of the above time series plots to view as is shown below in Figure 12-15. All results from both scenarios and any observed field results will be plotted on the same time series.

Real Time Forecast Results for 2001-05-29, Scenario A vs Scenario B

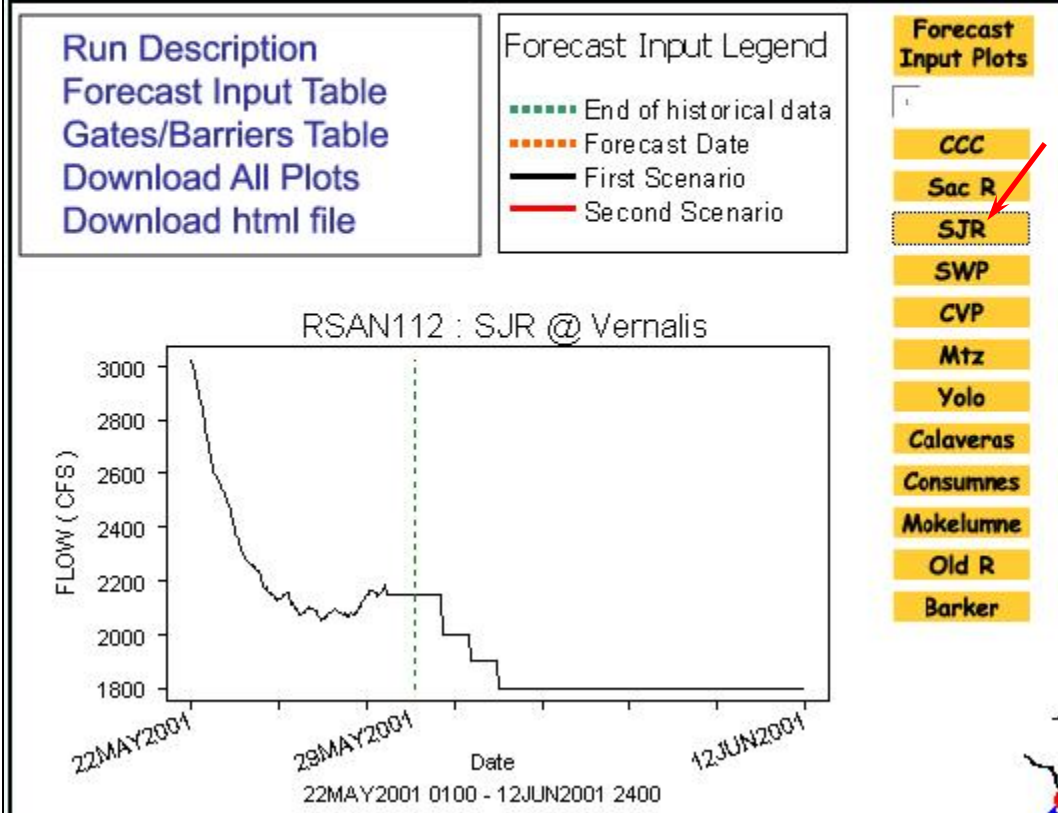


Figure 12-14: Viewing Forecast Input Results on Interactive Delta Map.

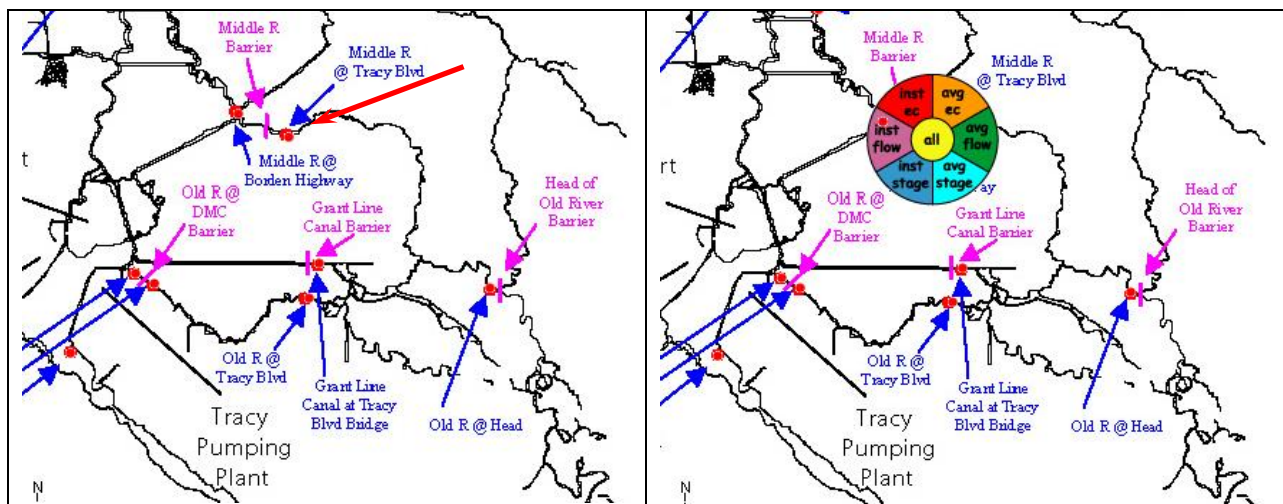


Figure 12-15: Selecting HYDRO and QUAL Results from Interactive Delta Map.

An example of the static PTM forecast results is shown below in Figure 12-16. When post-processing the PTM results, a static PTM plot can be printed once a day. Typically, these static PTM plots are created once every three to five days. The bars on the map represent injection locations. Each bar shows the particle fate for only particles released from that location.

For example, the bar highlighted in Figure 12-16 represents a particle injection location on the San Joaquin River. For this particular forecast, particles were injected into the Delta on June 1, 2001. The static plot shown displays the fate of all of these particles on June 29, 2001. As displayed in the bar, roughly one-third of the particles released on June 1, 2001 at this location ended up in the Central Valley Project, roughly one-third ended up being removed from the Delta via agricultural diversions, and the last one-third of the original particles released were still in the Delta.

For the first few days after the initial release, the majority of the bars will show most of the particles as still being within the Delta. As the particles move in the Delta, they will be exposed to both agricultural diversions and any other export/diversion activities under way. The particles that are listed as passing Chipps Island are considered to have left the Delta. Over time, the number of particles remaining in the Delta will decrease. A summary of the hydrologic information for a particular day shown is located in the upper left corner. Similarly, solid red bars are used to represent the placement of the South Delta barriers. If the barriers are not in place for a particular day, then no bars will appear on the static plot.

A static screenshot of the PTM dual animator is shown in Figure 12-17. The PTM dual animator can be used to (1) observe the spatial distribution and movement of particles in the Delta and (2) compare the overall particle fate at the specified locations. Though the fate locations shown in Figure 12-17 were standardized for the DSM2 Real-Time Forecasting System, the number of particles animated and the locations reported can be changed.

RESULTS 29 DAYS AFTER INITIAL INJECTION

RESULTS FOR JUN-29-2001

24 HR INJECTION ON JUN-01-2001

HYDROLOGY:

SACRAMENTO RIVER = 11300 CFS
 YOLO BYPASS = 700 CFS
 SAN JOAQUIN RIVER = 1800 CFS
 CONSUMNES RIVER = 60 CFS
 MOKELUMNE RIVER = 150 CFS
 CALAVERAS RIVER = 150 CFS
 BANKS PUMPING PLANT = 374 CFS
 TRACEY PUMPING PLANT = 2200 CFS
 NORTH BAY AQUADUCT = 30 CFS
 CCC AT ROCK SLOUGH = 115 CFS
 CCC AT OLD RIVER = 115 CFS

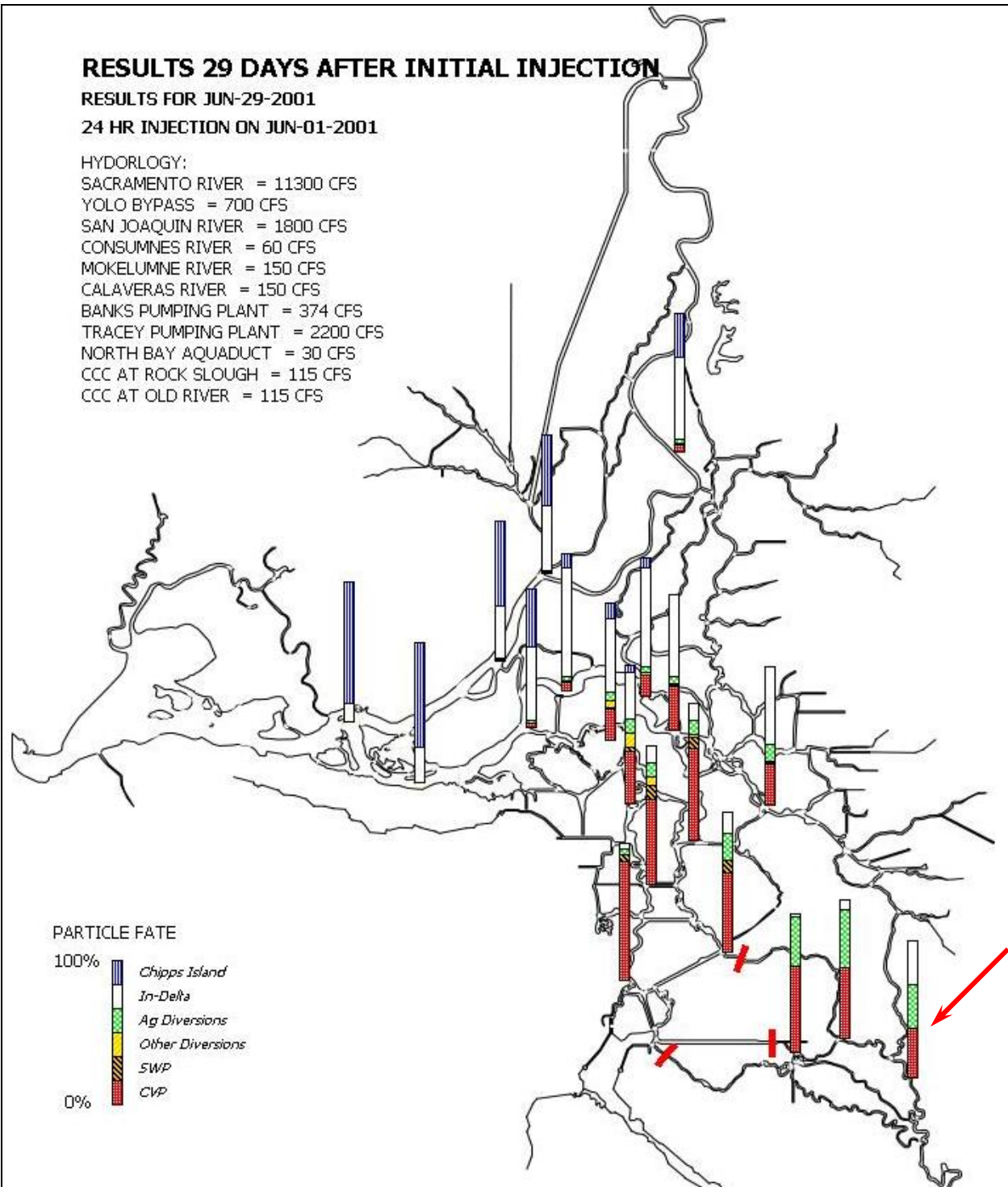


Figure 12-16: Static PTM Forecast Results.

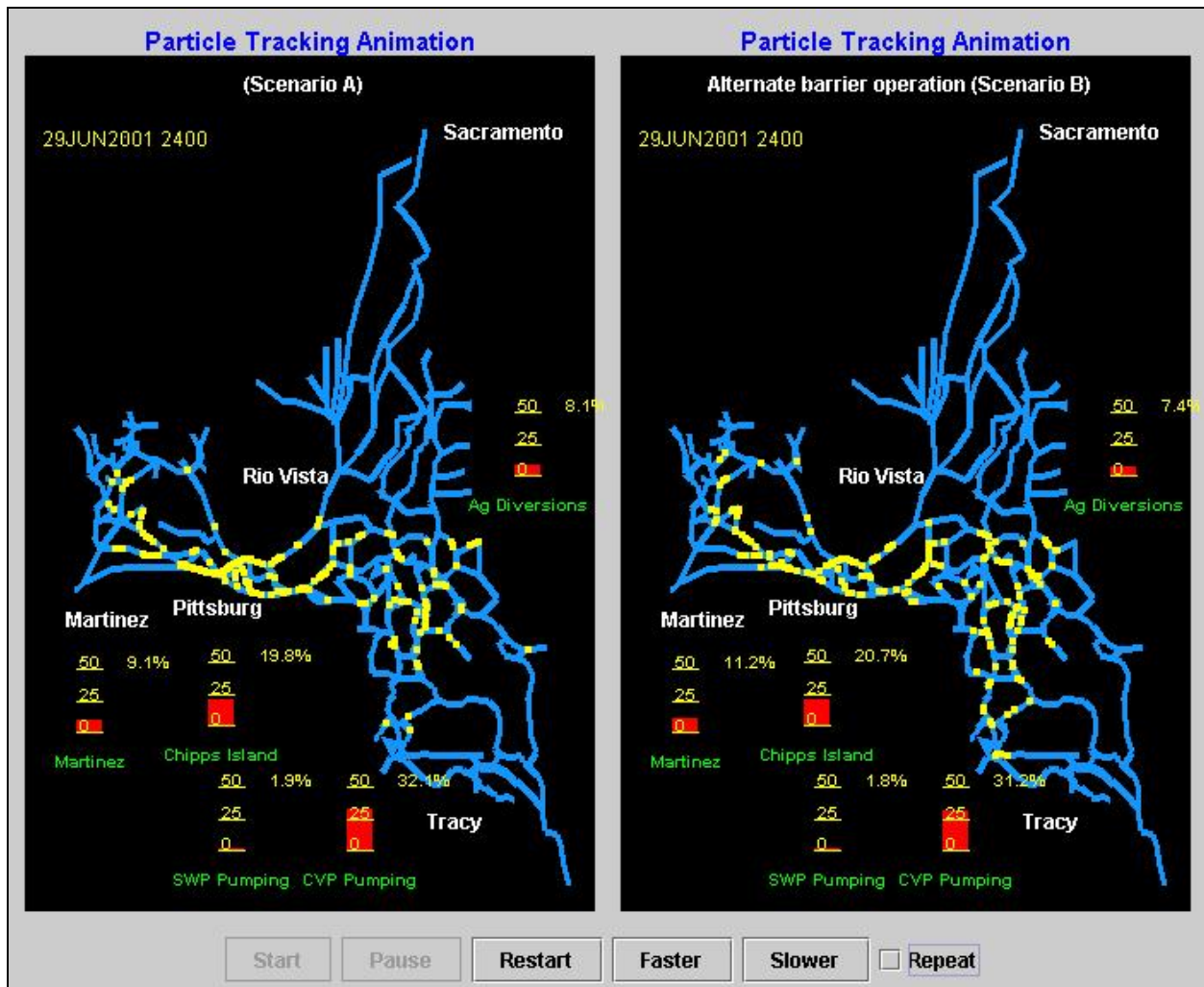



Figure 12-17: PTM Dual Animator.

12.4 Running Alternative Scenarios

The usefulness of DSM2 forecasts in decision support is not limited to running just a single base case scenario, but is also valuable in using the model to investigate the response to several alternative scenarios. The Web page results discussed above allow users to compare any two scenarios at the same time. For HYDRO and QUAL, these scenarios can be selected from a general menu where brief run descriptions of the results are also shown (see Figure 12-18).

Since any proposed operation will take place in the future, the same initial conditions that were developed for the base case can be reused for any alternative simulation. Though the pre-processing steps involved in calculating the warm start conditions or generating the historical flow values and gate operations will not need to be repeated, other steps that include both filling in and forecasting Martinez EC data will need to be repeated. Currently, there is no way to forecast Martinez stage based on planned changes in NDO, thus the base stage forecast will be used for all alternative scenarios. The MS Access Forecast Form can quickly create the input data for alternative flow regimes and gate operations. The steps involved in actually creating alternative scenario inputs using the MS Access Forecast Form are described at

<http://modeling.water.ca.gov/delta/real-time/foreform.html>. Currently, the MS Access Forecast Form can not create alternative operations for: (1) the Clifton Court Forebay Gates, (2) the Delta Cross Channel Gates, and (3) the Montezuma Slough Salinity Control Gate. Presently, the model input for each of these three structures is created by hand.



DWR Operations and Maintenance Realtime Forecast Results for 2001-05-29
Operations Control Office

Run Description	Run Results																																										
<p>Summary of real time forecast run(s) for : 2001-05-29</p> <p>historical period: May 14-28, 2001 forecast period: May 29 - June 29, 2001</p> <p>Highlights of run(s):</p> <p>Run A: Base run (all ag barriers oper. normally)</p> <p>Run B: With middle, GLC, and middle river barriers tied open.</p> <p>Gates Information:</p> <p>DCC: closed from May 14-24, 2001 open from May 25-28, 2001 closed from May 29 and beyond</p> <p>CCFBG: operate to priority 3.</p> <p>Comments: Forecast run through June 29, however, hydro results are shown only through June 13, 2001 since we only want to look out two weeks. It's possible to view results further than two weeks out.</p>	<p>For each forecast, up to 6 scenarios may have been run. Plots have been made to compare each scenario to each other scenario, or to show results for individual scenarios. The following table lists all possible comparisons of scenarios. Each element of the table will appear either as a button if plots are available, or as plain text if plots are not available. Click on a button to view plots for this comparison. For example, if you want to view plots of scenario A vs Scenario B, first check to make sure that element "AB" appears as a button, then click on the button "AB" in the table. Buttons may also appear in the Scenario column if individual scenario plots are available.</p> <table border="1"> <thead> <tr> <th>Scenario</th> <th>B</th> <th>C</th> <th>D</th> <th>E</th> <th>F</th> </tr> </thead> <tbody> <tr> <td>A</td> <td>AB</td> <td>AC</td> <td>AD</td> <td>AE</td> <td>AF</td> </tr> <tr> <td>B</td> <td></td> <td>BC</td> <td>BD</td> <td>BE</td> <td>BF</td> </tr> <tr> <td>C</td> <td></td> <td></td> <td>CD</td> <td>CE</td> <td>CF</td> </tr> <tr> <td>D</td> <td></td> <td></td> <td></td> <td>DE</td> <td>DF</td> </tr> <tr> <td>E</td> <td></td> <td></td> <td></td> <td></td> <td>EF</td> </tr> <tr> <td>F</td> <td></td> <td></td> <td></td> <td></td> <td></td> </tr> </tbody> </table>	Scenario	B	C	D	E	F	A	AB	AC	AD	AE	AF	B		BC	BD	BE	BF	C			CD	CE	CF	D				DE	DF	E					EF	F					
Scenario	B	C	D	E	F																																						
A	AB	AC	AD	AE	AF																																						
B		BC	BD	BE	BF																																						
C			CD	CE	CF																																						
D				DE	DF																																						
E					EF																																						
F																																											

Figure 12-18: Comparing Scenarios When Using On-line Results.

When creating alternative scenarios, it is recommended that only one operational parameter be changed at a time. For example, if several hypotheses are to be tested in DSM2, including changes in the export levels, operation of the Delta Cross Channel, and inflows of the major tributaries, separate scenarios should be created to test the impact of each of these proposed operations. This type of scenario extends into the timing of operations as well. The Delta is highly sensitive to both the operation of barriers/gates and to the levels of inflows and exports. Delaying the installation/removal of a barrier or altering inflows/exports for just one week can make the difference between having a significant impact on stage or water quality versus seeing

no immediate response in the Delta. The MS Access Forecast Form minimizes the effort involved in creating a “delayed” scenario.

While the DSM2 Real-Time Forecast System is robust enough to create alternative scenarios, the primary concern focuses back on the amount of information end users need and how much of that information can be presented in a timely fashion. Although there is no fixed limit to the number of alternative scenarios that can be produced in short order, the current on-line results are limited to displaying up to six different scenarios (including the base). Obviously, DSM2 can be used to run more than six scenarios; however, there is a practical limit to providing decision makers with too many alternatives to discuss in a short meeting.

12.5 Conclusions

Although the DSM2 Real-Time Forecasting System described here is currently in use by various DWR groups, it is still being developed. The majority of the current work is related to both improving the visualization of the model results and establishing a more reliable institutional framework that can support weekly forecast runs.

Collecting real-time raw data will continue to be a critical task. Issues related to phase shifts due to the change from Pacific Standard Time (PST) to Pacific Daylight Time (PDT) need to be resolved between the various agencies that collect field data and the end users of their data. Furthermore, raw field data were shown to serve as a valuable quality assurance/quality control tool. When post-processing model results, the ability to go back and look at the performance of the model at locations away from the boundary locations is important.

It is possible to reduce the amount of time required by the modeler to pre-process the raw data by reducing the number of visual confirmations involved in both downloading the raw data and later confirming that filled-in data look appropriate. However, due to the importance of the decisions that are being made based on these DSM2 results and the tenuous nature of raw data, the quality of completely automated modeling results could not be achieved without relying on frequent checks of both the raw and processed data. Since the “what if” questions that are asked of the DSM2 Real-Time Forecasting System are done during the forecast period, the historical data only need be screened once. Furthermore, if forecasts are run at frequent intervals, the extent of the historical data that have not been screened will decrease as the frequency of pre-processing the raw data increases.

It is important to think of this forecasting tool not as a series of scripts and computer models, but instead to recognize that it is, in fact, a true systems engineering process. The time involved in actually running DSM2 is minimal compared to all of the other work involved. Essentially, there are three main parties that must interact:

- ❑ Providers of the raw data,
- ❑ Users of the raw data/providers of the model results, and
- ❑ Users of the model results/decision-makers.

The breakdown of one process will have a direct impact on the functioning of all the other processes. Furthermore, as the various providers/users work together on a more frequent basis,

the system itself can change to meet the immediate needs of the final end users, the decision-makers. In other words, the system needs to remain flexible enough to answer all of the questions originally proposed in the introduction.

Regular forecasts force the users of the raw data (modelers) to constantly keep in touch with the raw data providers. Should a real-time telemetered monitoring station cease reporting data, or if a station starts to report data that is obviously wrong, the amount of data that is lost during this down period would be less if the data are being regularly examined. It is the responsibility of the data providers to educate the modelers on how the data are obtained from the field and how they are stored. Similarly, it is the job of the modelers to clearly prioritize their data needs.

Model results themselves are another form of unprocessed data. By regularly attending decision making meetings, numerical modelers can not only provide better insight into the assumptions that were made during the forecast, but they also can get a better understanding of the needs of the decision makers. Though the results of the models should be presented in a way that the modeler who processed the raw data and ran the model need not be present, new questions will be asked of both the model data and the model itself. Modelers are responsible for educating decision makers about what their models can do. And, decision-makers need to not only communicate their questions clearly, but they should feel free to consider more than one planned alternative at a time.

Realistically, the timing of changes in gate operations or the hourly flows at the rim boundaries will never be exactly what was modeled. So, the model results should not be considered absolute. DSM2 is a decision analysis tool and is most useful when it is viewed as a trend analysis tool. By asking several “what if” operational questions and running them all based on the same initial conditions, the different modeled responses to these proposed operations can be compared to one another.

12.6 Future Directions

The DSM2 Real-Time Forecasting System is a work in progress. Some of the work currently in progress was discussed above in addition to some of the future needs of this forecasting tool. The following is a short list of this continued effort.

- ❑ Improving the MS Access Form to allow modelers to enter in the operational status of the Clifton Court Forebay Gates, the Delta Cross Channel Gates, and of the Montezuma Slough Salinity Control Gate.
- ❑ Incorporating into the MS Access Form the ability to quickly compute forecast changes to the Net Delta Outflow Index. This will allow the existing pre-processing scripts to quickly compute the EC at Martinez for all alternative simulations.
- ❑ Make use of (if available) any new real-time stage, flow, or EC monitoring stations for Quality Assurance/Quality Control. When new real-time data become available, the pre- and post-processing scripts will be updated to incorporate this data.

- ❑ Continuing to develop user friendly tools to widely distribute forecast results.
- ❑ Performing weekly base case forecasts (and adding additional scenarios to the base forecast when necessary).
- ❑ Continue to maintain and update the on-line documentation, <http://modeling.water.ca.gov/delta/real-time/>. A specific “Frequently Asked Questions” section is being developed to assist model users any time there is a problem with a simulation. This documentation has already been used to convert the tools designed for this application of DSM2 to other DSM2 applications. In the future, parts of this documentation can be used for DSM2 training.
- ❑ Encourage additional groups outside DWR to both use the forecast results (in addition to encouraging greater use of DSM2 outside DWR). This includes having DSM2 modelers working closer with both data providers and decision-makers.
- ❑ Changing how DSM2 simulations affect the Clifton Court Forebay Gates. Currently, DSM2 models all the gates as being either opened or closed. There are five gates at the entrance to the forebay, each of which operates independently from the rest. Improving DSM2’s treatment of the gates will allow the model to be used for sensitivity studies for periods when one or more of the gates is under repair or otherwise not functioning.
- ❑ Develop more appropriate estimates for the Delta Island Consumptive Use (DICU). Currently, the Delta Modeling Section updates the historical DICU data once a year, and no work has been done to come up with forecast DICU data. One plan would be to create several consumptive use “bookends” that represent high and low levels of agricultural diversions and/or returns. Sensitivity studies could then be used to estimate better forecast DICU data.

12.7 References

- Ateljevich, E. (2000a). “Chapter 8: Filling In and Forecasting DSM2 Tidal Boundary Stage.” *Methodology for Flow and Salinity Estimates in the Sacramento-San Joaquin Delta and Suisun Marsh. 21st Annual Progress Report to the State Water Resources Control Board.* California Department of Water Resources. Sacramento, CA.
- Ateljevich, E. (2000b). “Chapter 11: DSM2-QUAL Initialization.” *Methodology for Flow and Salinity Estimates in the Sacramento-San Joaquin Delta and Suisun Marsh. 21st Annual Progress Report to the State Water Resources Control Board.* California Department of Water Resources. Sacramento, CA.
- Sandhu, Nicky. (2000). “Chapter 4: VPlotter.” *Methodology for Flow and Salinity Estimates in the Sacramento-San Joaquin Delta and Suisun Marsh. 21st Annual Progress Report to the State Water Resources Control Board.* California Department of Water Resources. Sacramento, CA.

LIST OF ACRONYMS & ABBREVIATIONS

ADCP - Acoustic Doppler Current Profiler	DSM2 - Delta Simulation Model 2
ANN - Artificial Neural Network	DSS - Data Storage System
AR1 - First Order Autoregressive Model	DWR - Department of Water Resources
BDMF - Bay Delta Modeling Forum	DWRSIM - DWR Planning Simulation Model
BIG3 - SJRIO's name for ESWD, PWD, & WSID	E/I - Export-to-Inflow
BOD – Biochemical Oxygen Demand	EAG - Eastside Agriculture
CALFED - State (CAL) and federal (FED) agencies participating in the Bay-Delta Accord	EC - Electrical Conductivity
CALSIM - California Water Resources Simulation Model	EPA - U.S. Environmental Protection Agency
CCC - Contra Costa Canal	ESO - Environmental Services Office
CCC PP #1 - Contra Costa Canal Pumping Plant #1	ESWD - El Soyo Water District
CCID - Central California Irrigation District	EWA – CVP-IA Environmental Water Account
CDEC - California Data Exchange Center	GEE - Generalized Estimating Equations
CLB - SJR at Crows Landing Road Bridge	GLM - Generalized Linear Model
CPU - Central Processing Unit	GUI - Graphical User Interface
CSDP - Cross Section Development Plan	GW – Groundwater Pumping Contribution in SJRIO
CVP - Central Valley Project	H/I - Hospital/Ingram Creek
CVPIA - Central Valley Project Improvement Act	IEP - Interagency Ecological Program
CVRWQCB - Central Valley Regional Water Quality Control Board	IEP-PWT – IEP DSM2 Recalibration Project Work Team
DAT - Data Assessment Team	ISI - Integrated Storage Investigation
DBP - Disinfection By-product	LP - Linear Programming
DCC - Delta Cross Channel	LSTV - Lower Stevinson Spill
DICU - Delta Island Consumptive Use	M&I - Municipal and Industrial
DMC - Delta Mendota Canal	MDO - Minimum Delta Outflow
DO - Dissolved Oxygen	MER - Merced River
DOC - Dissolved Organic Carbon	MID - Modesto Irrigation District
DPWD - Del Puerto Water District	MMAIN - Modesto Main Drain
DSM1 - Delta Simulation Model 1	MOD - CDEC Gauge Station on Tuolumne River at Modesto
	MSS - Sum of the Squared Residuals
	MST - CDEC Gauge Station on Merced River near Stevinson

MWQI - Municipal Water Quality Investigations
MWWTP - Modesto Wastewater Treatment Plant
NDO - Net Delta Outflow
NDOI - Net Delta Outflow Index
NEW - SJR near Newman, Hills Ferry Road Bridge
NOAA - National Oceanic and Atmospheric Administration
NOS - National Ocean Service
NWWTP - Newman Wastewater Treatment Plant
OLS - Ordinary Least Scales
ORE - Orestimba Creek
OSP - Office of SWP Planning
PDT - Pacific Daylight Time
PST - Pacific Standard Time
PTM - Particle Tracking Model
PWD - Patterson Water District
PWT - Project Work Team (see IEP-PWT)
RD - Reclamation District
RIP – CDEC Gauge Station on Stanislaus River at Ripon
RRI - Rough and Ready Island
RWCF - Regional Wastewater Control Facility
SJP - SJR at Patterson Bridge
SJR - San Joaquin River
SJRIO - San Joaquin River Input-Output
SJRMP-WQS - San Joaquin River Management Program - Water Quality Subcommittee
STA - Stanislaus River
SWP - State Water Project
SWRCB - State Water Resources Control Board
TDS - Total Dissolved Solids
TID - Turlock Irrigation District
TMDL - Total Maximum Daily Load
TTHM - Total Trihalomethane

TUO - Tuolumne River
TWWTP - Turlock Wastewater Treatment Plant
UCD - University of California, Davis
USACE - U.S. Army Corp of Engineers
USBR - U.S. Bureau of Reclamation
USGS - U.S. Geological Survey
UTM - Universal Transverse Mercator
UVA - Ultraviolet Light Absorbance
UVM - Ultrasonic Velocity Meter
VAMP - Vernalis Adaptive Management Plan
VER - SJR near Vernalis at Airport Road Bridge
VSS - Volatile Suspended Solids
WAG - Westside Agriculture
WSID - West Stanislaus Irrigation District
WT – Rhodamine WT, Red Tracer Dye Used In Flow Studies
YAGS - Yet Another GEE Solver